

POLSKIE TOWARZYSTWO MIKROBIOLOGÓW
POLISH SOCIETY OF MICROBIOLOGISTS

Polish Journal of Microbiology

2021

CONTENTS

MINIREVIEWS

The pathogenesis of <i>Aspergillus fumigatus</i> , host defense mechanisms, and the development of AFMP4 antigen as a vaccine GU X., HUA Y.-H., ZHANG Y.-D., BAO D., LV J., HU H.-F.	3
Epidemiology and pathogenesis of <i>Staphylococcus</i> bloodstream infections in humans: a review LISOWSKA-LYSIAK K., LAUTERBACH R., MIĘDZOBRODZKI J., KOSECKA-STROJEK M.	13
Microbiota: a missing link in the pathogenesis of chronic lung inflammatory diseases MAGRYŚ A.	25

ORIGINAL PAPERS

Effects of different ambient temperatures on caecal microbial composition in broilers YANG Y., LI X., CAO Z., QIAO Y., LIN Q., LIU J., ZHAO Z., AN Q., ZHANG C., ZHANG H., PAN H.	33
The effects of different modes of delivery on the structure and predicted function of intestinal microbiota in neonates and early infants PAN K., ZHANG C., TIAN J.	45
Antibiotic and disinfectant resistance in tap water strains – insight into the resistance of environmental bacteria SIEDLECKA A., WOLF-BACA M.J., PIEKARSKA K.	57
Chemotaxis toward crude oil by an oil-degrading <i>Pseudomonas aeruginosa</i> 6-1B strain LIANG K., GAO R., WANG C., WANG W., YAN W.	69
<i>Spa</i> typing of <i>Staphylococcus aureus</i> isolated from clinical specimens from outpatients in Iraq MOHAMMED K.A.S., ABDULKAREEM Z.H., ALZAALAN A.R., YAQOOB A.K.	79
Diversity of culturable bacteria isolated from highland barley cultivation soil in Qamdo, Tibet Autonomous Region PAN H., ZHOU J., DAWA Z., DAI Y., ZHANG Y., YANG H., WANG C., LIU H., ZHOU H., LU X., TIAN Y.	87
<i>Campylobacter fetus</i> induced proinflammatory response in bovine endometrial epithelial cells CAMPOS-MÚZQUIZ L.G., MÉNDEZ-OLVERA E.T., MARTÍNEZ M.P., MARTÍNEZ-GÓMEZ D.	99
Clonal dissemination of KPC-2, VIM-1, OXA-48-producing <i>Klebsiella pneumoniae</i> ST147 in Katowice, Poland OCHOŃSKA D., KLAMIŃSKA-CEBULA H., DOBRUT A., BULANDA M., BRZYCHCZY-WŁOCH M.	107
A clinical trial to evaluate the efficacy of α -viniferin in <i>Staphylococcus aureus</i> – specific decolonization without depleting the normal microbiota of nares RAHIM M.A., SEO H., KIM S., JEONG Y.K., TAJDOZIAN H., KIM M., LEE S., SONG H.-Y.	117

SHORT COMMUNICATION

Growth inhibition of phytopathogenic fungi and oomycetes by basidiomycete <i>Irpex lacteus</i> and identification of its antimicrobial extracellular metabolites PINEDA-SUAZO D., MONTERO-VARGAS J.M., ORDAZ-ORTIZ J.J., VÁZQUEZ-MARRUFO G.	131
---	-----

INSTRUCTIONS FOR AUTHORS

Instructions for authors: https://www.exeley.com/journal/polish_journal_of_microbiology

The Pathogenesis of *Aspergillus fumigatus*, Host Defense Mechanisms, and the Development of AFMP4 Antigen as a Vaccine

XIANG GU^{1,2#}, YAN-HONG HUA^{2#}, YANG-DONG ZHANG³, DI BAO³, JIN LV^{3*} and HONG-FANG HU^{3*}

¹ College of Law and Political Science, Nanjing University of Information Science and Technology, Nanjing, China

² The University of Hong Kong Li Ka Shing Faculty of Medicine, Hong Kong, China

³ The PLA Rocket Force Characteristic Medical Center, Beijing, China

Submitted 26 August 2020, revised 10 January 2021, accepted 11 January 2021

Abstract

Aspergillus fumigatus is one of the ubiquitous fungi with airborne conidia, which accounts for most aspergillosis cases. In immunocompetent hosts, the inhaled conidia are rapidly eliminated. However, immunocompromised or immunodeficient hosts are particularly vulnerable to most *Aspergillus* infections and invasive aspergillosis (IA), with mortality from 50% to 95%. Despite the improvement of antifungal drugs over the last few decades, the therapeutic effect for IA patients is still limited and does not provide significant survival benefits. The drawbacks of antifungal drugs such as side effects, antifungal drug resistance, and the high cost of antifungal drugs highlight the importance of finding novel therapeutic and preventive approaches to fight against IA. In this article, we systemically addressed the pathogenic mechanisms, defense mechanisms against *A. fumigatus*, the immune response, molecular aspects of host evasion, and vaccines' current development against aspergillosis, particularly those based on AFMP4 protein, which might be a promising antigen for the development of anti-*A. fumigatus* vaccines.

Key words: *Aspergillus fumigatus*, vaccine, *Aspergillus fumigatus* mannoprotein

Introduction

Aspergillus spp. is a genus of saprophytic fungi, which is widely distributed in nature. This genus plays an important role in environmental nitrogen and carbon recycling and relies on conidia to spread in the air (Krüger et al. 2015; Latgé and Chamilos 2019). Among the approximately 200 *Aspergillus* species, less than 20 are pathogenic for humans (Paulussen et al. 2017; Mead et al. 2019). *Aspergillus fumigatus* exerts a major influence on the number of pathogenic *Aspergillus* strains. Statistical data revealed that among multitudinous *Aspergillus* spp. isolates, *A. fumigatus* accounted for 50–60%, *A. flavus*, *A. terreus*, and *A. niger* each made up 10–15% of the isolates, and other uncommon *Aspergillus* spp. were less than 2% (Paulussen et al. 2017; Hoenigl et al. 2018).

Of all pathogenic *Aspergillus* spp., *A. fumigatus* with airborne conidia is a prevailing agent for human infections. The small sizes of conidia allow them to reach

the lung alveoli from the natural environment effortlessly. It is estimated that humans may inhale as many as hundreds of *A. fumigatus* conidia every day (Alanio et al. 2017; Takazono and Izumikawa 2018). In healthy hosts, the inhaled conidia are rapidly eliminated by a competent immune system composed of innate and adaptive immunity. The innate immunity plays pivotal role in destroying most of the inhaled conidia in the respiratory tract by respiratory ciliary movement and proteins on the surface of epithelial cells, and in recognizing and engulfing the remaining conidia by alveolar phagocytes through surface pattern recognition receptors. Simultaneously, phagocytes also induce inflammatory chemokines and cytokines and recruit other immune cells to destroy surviving *A. fumigatus* spores and hyphae. Among them, neutrophils can prevent the formation of hyphae and kill it; monocytes can phagocytose spores to prevent fungal outbreaks. When dendritic cells phagocytose *A. fumigatus*, antigenic components are presented on the cell membrane surface to activate T

Xiang Gu and Yan-Hong Hua contribute equally to this work and are co-first authors.

* Corresponding authors: J. Lv, The PLA Rocket Force Characteristic Medical Center, Beijing, China; e-mail: lvjin6630@hotmail.com
H.-F. Hu, The PLA Rocket Force Characteristic Medical Center, Beijing, China; e-mail: hhf81@126.com

© 2021 Xiang Gu et al.

This work is licensed under the Creative Commons Attribution-NonCommercial-NoDerivatives 4.0 License (<https://creativecommons.org/licenses/by-nc-nd/4.0/>)

cells and B cells, initiating adaptive immunity of the body. Whereas, if the immune responses are excessively intensive, some immunological diseases such as allergic bronchopulmonary aspergillosis will occur. In immunocompromised or immunodeficient hosts, such as the patients with immunosuppressive treatment for autoimmune disease, HIV suffers, and transplantation recipients, the growth of spores and hyphae of *A. fumigatus* cannot be prevented due to the decrease of neutrophils and phagocytes. Eventually, the hyphae of *A. fumigatus* will invade human blood vessels and spread from blood to the whole body, causing multi-system infection (Filler and Sheppard 2006). *A. fumigatus* is the most lethal invasive pathogenic fungus, with the mortality from invasive aspergillosis (IA) above 50%, even up to 95% (Dos Santos et al. 2020), especially for the patients with acute leukemia and hematopoietic stem cell transplantation (HSCT) (van de Peppel et al. 2018).

Despite the wide applications of antifungal drugs, they failed to provide satisfying treatment for invasive aspergillosis patients. Notably, the clear side effects of antifungal drugs such as amphotericin B's kidney toxicity and the potential hepatotoxicity of itraconazole discouraged their clinical use. Although voriconazole had better penetration than amphotericin B and itraconazole, it might cause temporary hepatotoxicity. In addition to the side effects of antifungal drugs, drug resistance and high cost also greatly hindered the use of antifungal drugs. In response to the quest for more efficacious and safer therapeutic options, various new therapeutic drugs and new dosage forms of various therapeutic drugs are also in progress. The latest drugs, such as rifconazole and abaconazole, are being tested in various *in vitro* and *in vivo* trials (Jović et al. 2019). However, more studies still need to provide useful data on the efficacy and safety of new antifungal drugs. In consequence, the development of antifungal vaccines is highly proposed. Recently, *A. fumigatus* mannoprotein 4 (AFMP4) has been recognized as a virulence factor of *A. fumigatus* and expected to serve as an antigen for the development of anti-*A. fumigatus* vaccines. In this article, we systemically review the biological characters of *Aspergillus* spp. and the pathogenic and defense mechanisms of *A. fumigatus* to provide new strategies for the treatment of *A. fumigatus*.

Pathogenicity

Disease caused by *A. fumigatus*

A. fumigatus can cause a broad spectrum of aspergillosis ranging from mild to severe symptoms for immunodeficient or immunosuppressed patients, including allergic syndromes, noninvasive infections, and IA

(Bonnet et al. 2017; Pagano et al. 2017; Gamaletsou et al. 2018; Xiao et al. 2020). The common diseases caused by *A. fumigatus* infection are as follows: (1) allergic bronchopulmonary aspergillosis (ABPA), (2) allergic sinusitis, (3) aspergilloma, (4) necrotizing pulmonary aspergillus (CNPA), (5) cutaneous aspergillosis, and (6) IA. In ABPA, the inflammation due to *Aspergillus* infection of the lungs primarily affects the patients with asthma, cystic fibrosis, and bronchiectasis, which cause allergy symptoms such as fever, cough, wheeze, and generalized malaise. Allergic sinusitis is a noninvasive and recurrent inflammatory sinusitis with the hypertrophic sinus and nasal polyps as the manifested symptoms in patients. Aspergilloma predominantly exhibits mycelial balls in the damaged lung bronchia, pulmonary cyst, or lung cavities, which causes a typical hemoptysis symptom in severe patients, and even threatens lives. CNPA usually occurs in patients with mild-to-moderate immunosuppression, accompanied with chronic symptoms like fever, cough, sputum, anorexia, and weight loss with a duration of 1–6 months (Barac et al. 2017). Cutaneous aspergillosis is a cutaneous manifestation of disseminated *Aspergillus* infection, including erythematous-to-violaceous plaques or papules, commonly characterized by an ulcer or eschar (Sato and Tamai 2019). IA is a severe infection that significantly affects immunocompromised patients, such as those who have had an organ transplant or a stem cell transplant operation. IA can affect each organ, but sinopulmonary diseases are the most common IA symptoms, including nasal congestion and pain, fever, pleuritic chest pain, and hemoptysis.

Molecular basis of *A. fumigatus* virulence

A. fumigatus is an opportunistic pathogen that causes ~90% of IA with very high mortality (Darling and Milder 2018). Why *A. fumigatus* dominates the human pathogenicity is confusing to clinical medical workers, which motivating scientists to explore its pathogenic mechanisms. The pathogenicity of *A. fumigatus* to the host was mainly manifested by a direct attack with the pathogen's virulent factors, the hypersensitivity response of patients, or the innate and adaptive immunity of host evoked by virulent factors during the process of germinating in the host. In recent decades, especially after *A. fumigatus* AF293 strain genome sequencing in 2005, the virulence of *A. fumigatus* was shown to be multifactorial and was related to thermotolerance, cell wall composition and maintenance, resistance to immune response, toxins, nutrient uptake during invasive growth, signaling regulation, and allergens (Darling and Milder 2018; Latgé and Chamilo 2019). Besides, many molecules or genes related to the pathogenicity of *A. fumigatus* have been found,

including galactomannan glycoprotein encoded by *afmp1*, hydrophobic protein Rod A, fumagillin, gliotoxin, helvolic acid, fumigaclavin C, asp-hemolysin, and so on. The genes and molecules associated with *A. fumigatus* virulence either were helpful for the survival of pathogens in the host, or contributed to the process of evading the immune system, such as masking the important PAMPs, inhibition of phagosome-lysosome fusion, production of antioxidants like catalase, SOD, and mannitol, or exerted multiple immunosuppressive actions on the host immunity by producing specific secondary metabolites such as gliotoxin (GT), fumagillin, actibind, and cytochalasin E.

The genes related to thermotolerance

As a thermophilic fungus, *A. fumigatus* can grow at 55°C and survive at temperatures above 75°C. This ability facilitates to thrive in dead or decayed organic matters and to infect mammalian host cells. Thus, the genes related to thermotolerance contribute to the virulence of *A. fumigatus*. Five genes have been proved to be associated with the thermotolerance of *A. fumigatus* (*thtA*, *cgrA*, *afpmt1*, *kre2/afmnt1*, and *hsp1/asp f 12*). The *thtA* gene is necessary for the growth of *A. fumigatus* at 48°C, but it is not involved in the pathogenicity of *A. fumigatus*. The *afpmt1* gene encodes for one mannosyl transferase, which is essential for the growth of *A. fumigatus* over 37°C. It was found that the Δ *afmnt1* mutant was attenuated in a mouse infection model and more sensitive to azoles (Wagener et al. 2008).

Toxins

A. fumigatus produce toxins for protection against predators and competitors, and they can directly attack the host and contribute to the pathogenesis of the fungus. Many toxins are secondary metabolites of fungi. They can affect the synthesis of DNA, RNA, and proteins, or alter cell membrane and impair cellular functions. Many toxins and relevant genes of *A. fumigatus* have been studied, such as diffusible toxic substances from conidia, gliotoxin (*gliP* and *gliZ*), mitogillin (*res/mitF/aspf1*), hemolysin (*aspHS*), verruculogen, fumagillin, and the transcription factor *laeA*. Gliotoxin is the most potent toxin produced by *A. fumigatus* (Zhang et al. 2019), which can suppress macrophage phagocytosis, T cell proliferation, cytotoxic T cell response, and monocyte apoptosis (Schlam et al. 2016; Schmidt et al. 2017; Fraga-Silva et al. 2019). Gliotoxin can also inhibit the NADPH of neutrophils (Tsunawaki et al. 2004), suppress ROS production, and impair the neutrophil's phagocytic capacity (Orciuolo et al. 2007). In addition, it should be noted that the transcription factor *laeA* is a crucial regulator for secondary metabolite biosynthesis (Pfannenstiel et al. 2017), and it has been proved that *laeA* deletion in *A. fumigatus* inhibited the pro-

duction of almost all secondary metabolites containing gliotoxin (Arias et al. 2018).

Allergens

Moreover, *A. fumigatus* can produce a large number of allergens; among them 23 have their official names ranging from Asp f1 to Asp f34 (available at: <http://www.allergen.org/>, updated on July 11, 2019). Some allergens show toxic or enzymatic activities, which are related to the virulence. Other allergenic molecules have no virulence functions. All *Aspergillus* allergens are likely to trigger a Type I hypersensitivity response in patients and induce a high-affinity IgE antibody production. *Aspergillus* allergens can cause hypersensitivities in immunocompetent patients, such as ABPA, allergic rhinosinusitis, asthma, and aspergilloma. In immunocompromised patients, these allergenic molecules can significantly increase the risk of aspergillosis. Many *Aspergillus* allergens have been explored and developed for diagnostic purposes (Masaki et al. 2017).

Other pathogenic factors

So far, none of the pathogenic factors is unique to *A. fumigatus*, and it is necessary to further investigate why *A. fumigatus* is more pathogenic than other common conditional pathogens. Some scholars believed that, unlike other human pathogenic bacteria such as *Candida* and *Cryptococcus*, the pathogenicity of *A. fumigatus* is not caused by one or several pathogenic factors but caused by the result of its unique biological characteristics such as growth and metabolism and the joint action of multiple pathogenic factors.

Recently, based on the homology between fungal endoether glucokinase and AnmK kinase of bacterial cell wall circulatory metabolism, we proposed the hypothesis that fungal cell wall has a mechanism similar to that of bacterial cell wall circulatory metabolism, which plays a role in the growth and reproduction of fungi. Whether this hypothesis is correct and related to the pathogenicity of *A. fumigatus* needs to be further confirmed by research.

Defense mechanism against *A. Fumigatus*

Host immunity to *A. fumigatus*

Innate defense immunity

Anatomical barriers. At the entry point of airborne conidia, the upper respiratory tract's airway epithelium is the first defensive line of innate host immunity against *A. fumigatus*. As an airway epithelium cell, the mucous secreting cell can secrete mucus to trap inhaled conidia. Another airway epithelium cell, a ciliated cell, can drive the trapped conidia to the oropharyngeal junction

(van de Veerdonk et al. 2017). In this way, a significant number of *A. fumigatus* are expelled from the lung. The respiratory epithelium can also secrete some peptides or enzymes to combat *A. fumigatus*, indicating that chitinase produced by epithelium can damage chitin on the cell wall of *A. fumigatus* (Garth et al. 2018).

Professional phagocytes and classical signaling pathways. The dominant role of phagocytes defense against *A. fumigatus* *in vivo* and *in vitro* has been reported (Liu et al. 2017; Almeida et al. 2019; Mackel and Steele 2019). The primary phagocytes responsible for the phagocytosis of *A. fumigatus* are alveolar macrophages (AM) and neutrophils.

In the lung of the immunocompetent host, certain soluble recognition receptors produced by alveolar macrophages such as Pentraxin 3 (PTX3) and surface protein-D (SP-D) can immediately bind to the inhaled conidia of *A. fumigatus*, and enhance the phagocytosis of alveolar macrophages (Smole et al. 2020). Alveolar macrophages then recognize and swallow the conidia through the TLR2/4 and Dectin-1. Toll-like receptors (TLRs) are type I membrane receptors that function in recognition of PAMPs and an intracellular TLR domain required for downstream signaling. TLRs can recognize pathogens and activate transcription factors such as NF- κ B, which mediate the expression of inflammatory cytokines and chemokines (Anthoney et al. 2018). Some studies implicated the membrane receptors TLR2 and TLR4 were the crucial recognition components for host defense against *A. fumigatus* (Dai et al. 2019). An essential role for TLR2 and TLR4 in cytokine production against *A. fumigatus* has been established in many *in vitro* studies (Briard et al. 2019; Gupta et al. 2019). Dectin-1 is a type II transmembrane protein, which is highly expressed in macrophages, neutrophils, and DCs. Dectin-1 can recognize β -glucan on germinating conidium but cannot identify the resting conidia, allowing macrophages to differentiate the various forms of *A. fumigatus* (Li et al. 2019; Dutta et al. 2020). Alveolar macrophages capture conidia leading to a proinflammatory response accompanied by the secretion of many cytokines and chemokines, including TNF- α and CXCL2 (Chemokine (C-X-C motif) ligand 2), which are essential activators for neutrophil recruitment (Guo et al. 2020). The conidia escaped from the phagocytosis by alveolar macrophages continue to germinate and spread. Proinflammatory factors derived by alveolar macrophages and epithelial cells recruit neutrophils to the infection site. Neutrophils perform an effective elimination of the germinating conidia and hyphae.

In the immunocompetent lung, conidia are immediately trapped by the soluble recognition receptors (PTX3, SP-D), promoting conidial phagocytosis by alveolar macrophage (AM). AM also captures conidia through TLRs and Dectin-1, leading to a proinflam-

matory response. The escaped conidia continue to germinate and penetrate through the alveolar epithelial cells. Neutrophils employ the processes of NET formation, degranulation, and lactoferrin production to inactivate germinating conidia and hyphae. Dendritic cells phagocytose, and process germinated conidia for antigens presentation to T cells, and finally activate an adaptive immune response to *A. fumigatus* (Garth and Steele 2017).

Mechanism of innate immune cells removing A. fumigatus. The mechanism includes phagocytosis, reactive oxygen species (ROS) generations mediated by nicotinamide adenine dinucleotide phosphate-oxidase (NADPH), lactoferrin production, and neutrophil extracellular traps (NETs) formation (Schoen et al. 2019; Souza et al. 2019; Shopova et al. 2020). ROS production responds to swollen conidia, but not resting conidia, through NADPH oxidase activation (Ferling et al. 2020; Khani et al. 2020). It has been demonstrated that the ROS-producing complex plays a crucial fungicidal role during *A. fumigatus* infection (Shen et al. 2016). NETs are networks of extracellular fibers, mainly composed of DNA from neutrophils. The NET formation is induced by a variety of proinflammatory mediators such as IL-8. It is significant for defense against large pathogens, such as hyphae of *A. fumigatus* (Li et al. 2020). It has been demonstrated both *in vitro* and *in vivo*, NET formation is dependent on NADPH oxidase and ROS generation (Khan et al. 2019; Ravindran et al. 2019). In addition, dendritic cells (DCs) play a well-established role in the host defense against *A. fumigatus*. Immature DCs can phagocytose conidia and hyphae through PRRs and present the processed antigens of *A. fumigatus* to host T cells, leading to the activation of adaptive immune responses (Wang et al. 2017).

Adaptive immunity mechanism

The elimination of the daily-inhaled conidia mainly depends on the innate immune response, but the treatment for serious *Aspergillus* infections relies on the cooperation of the adaptive immune system, which responds to the signaling generated by innate immunity. Lymphocytes T and B represent the two main parts of the adaptive defensive system.

Role of T cells in adaptive immunity. The T cell immunity system interacts with the innate immune response in many ways. For instance, DCs recruit at the infection sites can load and migrate the *A. fumigatus* antigen to lymph nodes, leading to T lymphocytes' activation (Wang et al. 2017). CD4+ T cells are the dominating organizer, which play a major role in antifungal immunity. These activated T cells are able to invoke phagocytes or restrict the immune response. The initiating of CD4+ T cell immunity occurred between TCR and its cognate antigens on the DC cells. The excessive

inflammatory response secreted by the activated T cells can induce the naïve T cells to differentiate into CD4 T help (Th) subsets while damaging the incident tissues and contributing to the invasive infections of *A. fumigatus*. Th1 response was the predominant cell type that involved the protective immune response to the host through the production of pro-inflammatory cytokines such as IFN- γ , IL-2, IL-12, and TNF- α . In contrast, Th2 immune response was associated with the germination of fungal and exacerbation of disease as well as induced the alternatively activated macrophages in the defense against *A. fumigatus*. The balance between Th1 and Th2 subset determined the quality and outcome of host immune responses. It was also found that Th17 played multiple roles in clearing infections by participating in the production of proinflammatory genes and antimicrobial peptides, recruitment, and activation of neutrophils (Pathakumari et al. 2020). T cell immunity against fungal infections primes Th1 type response (Shenoy et al. 2017). However, in patients with aspergillosis, the predominance of Th2 T cells' immune response was conducted to exacerbate disease (Dewi et al. 2017). Besides, DCs contribute to a damaging inflammatory response by stimulating the Th17 cells and producing IL-23 (Movahed et al. 2018).

Humoral immunity to *A. fumigatus*. The function of *Aspergillus*-specific antibodies in immunocompromised patients with IA has been investigated (Boniche et al. 2020). Early researches indicated that the antibody responses failed to provide effective protection against IA or played only a minor role in fighting aspergillosis (Cutler et al. 2007). However, recent research reported that β -1,3-glucan specific antibodies could not only inhibit *Aspergillus* hyphae but also protect CD2F1 mice against *Aspergillus* challenge (Matveev et al. 2019). Although it is generally acknowledged that T cells immunity plays a vital role in combating fungal aspergillosis (Diaz-Arevalo and Kalkum 2017), there are a variety of ways, such as opsonization, complement activation, and virulence factors neutralization, in which antibodies affect T cells response and suppress the growth, adherence, and germination of fungi (Liedke et al. 2017; Ulrich and Ebel 2020).

Progress of anti-*A. fumigatus* vaccines development

Despite the wide applications of antifungal drugs, they failed to provide satisfying treatment for IA patients. The therapy with antifungal drugs is often associated with side effects, drug-resistance, and high costs. To overcome these disadvantages, the development of alternative methods, including antifungal vaccines, is highly desirable. Antifungal vaccine studies' primary tool is the employment of fungal particulate forms, homogenates, or recombinant proteins. Some

studies revealed that the immunization with conidia, mycelia extracts, or fungal culture filtrates induced effective protection against *Aspergillus* infections (Muthu et al. 2018; Pérez-Cantero et al. 2019). The heat-killed mutant strain was also reported to be a broad-spectrum fungal vaccine that induced host protection against common invasive fungal infections in both immunocompetent and immunocompromised hosts (Wang et al. 2019). However, the crude extracts commonly consist of abundant fungal components as various carbohydrates, nucleic acids, or even some toxins (Shishodia et al. 2019). Thus, vaccination using purified recombinant antigenic protein or peptide-based vaccine (Da Silva et al. 2020) is a more popular method in antifungal vaccine studies, whereas the possibility of potential severe anaphylaxis remains.

Obstacles in vaccine development

Although recently there is some progress published on the study of vaccines against *A. fumigatus* (Chauvin et al. 2019; Khani et al. 2020), several significant obstacles remain to be overcome for producing effective vaccine (Levitz 2017). First of all, since *A. fumigatus* is an opportunistic pathogen and most invasive infections appear in the immunocompromised population, the induction of an effective adaptive immunity in such individuals is a real challenge. One of the feasible measures is the prophylactic vaccination, especially in target population, such as the patients waiting for bone marrow transplant and the patients before the treatment with immunosuppressive agents. Another major problem in developing a vaccine against *A. fumigatus* is related to the fungus' molecular complexity. The extract of *A. fumigatus* is a mixture containing up to 200 different proteins, glycoproteins, and compounds of low molecular weights. In addition, safety issues should also be well addressed because a wide range of allergic diseases correlates with *Aspergillus* allergens. The potential of activating an adverse immunoreaction is also an intractable problem (Dewi et al. 2017).

Adaptive immunity induced by anti-*A. fumigatus* vaccines

Currently, some *A. fumigatus* allergens were identified based on their reactivity to patients' antibodies. Some of these allergens are not effective antigens for vaccine development because they primarily induce Th2 cell response but cannot provide adequate protection against *Aspergillus* infection. Nevertheless, a recombinant allergen of *A. fumigatus* – Asp f3 was confirmed to induce protective response when presented mixed with TM adjuvant in a murine inhalation model (Namvar et al. 2015). It was also reported that various yeast genera could activate innate CD8⁺ T lymphocyte response and generate broad antifungal protection (Bazan et al.

2018). It suggested yeasts as a potential antifungal vaccine candidate to activate antigen-specific CD8+ T cell responses effectively.

For a long time, most antifungal vaccine research intended to activate memory T lymphocytes and raise a Th1 type immune response that would produce some favorable cytokines to enhance phagocytosis or T cell killing (Upadhyaya et al. 2016). Most studies suggested that the protective antifungal reactions induced by vaccines are cell-mediated immune responses. However, some recent investigations focused on protective antibodies. One β -glucan conjugate vaccine was shown to provide good protection against *Candida albicans* and *A. fumigatus* (Catellani et al. 2020). The serum of vaccinated mice significantly inhibited the growth of fungus hyphae. The mechanism of the β -glucan conjugate vaccine might involve specific anti- β -glucan antibody (Matveev et al. 2019).

Optimizing vaccination schedules with *A. fumigatus* mannoprotein (AFMP)

The cell wall of fungi is primarily defensive to a hostile environment (Ruiz-Herrera and Ortiz-Castellanos 2019). Except for physical protection, one central role of the fungus cell wall is the interaction with the hosts. Therefore, the cell wall components are usually the targets to be attacked by the immune cells in hosts. The cell wall of *A. fumigatus* is mainly composed of polysaccharides and proteins. The polysaccharides consist of glucan, mannose, and chitin, which constitute a three-dimensional network. β -(1,3)-glucan branched with β -(1,6)-glucan forms the wall's skeleton. Chitin, a polymer of N-acetylglucosamine is covalently linked to β -glucan. Several proteins of the cell wall are mannosylated. The role of some mannoprotein has been investigated and suggested as antigenic determinants for serodiagnosis.

Mannoproteins (MPs) are natural glycoconjugates expressed mainly on the fungal surface and released into the culture medium during fungal growth. MPs have been implicated as important antigens involved in the induction of T cell-mediated immunity (Schülke 2018; Paulovičová et al. 2019). Therefore, MP may have potential use as an immunomodulator in patients at high risk of IA.

The *afmp* genes were reported to encode some cell wall MPs of *A. fumigatus*. Among them, *afmp1* encodes a protein-AFMP1 with 284 amino acids, which contains some similar sequences present in MP of *Penicillium marneffeii* (Muszewska et al. 2017). AFMP2 also includes a few domains of MP1 (Woo et al. 2018). Remarkably, specific AFMP1 and AFMP2 antibodies were found in the aspergillosis or aspergilloma patients during *A. fumigatus* infections (Woo et al. 2018). More-

over, recombinant AFMP1 protein was also applied in the ELISA assay to detect specific AFMP1 antibodies in hosts, which greatly contributes to the rapid diagnosis of *A. fumigatus*-related aspergillosis (Woo et al. 2018). Based on this research, another two *A. fumigatus* MPs, AFMP3, and AFMP4 proteins were discovered during BLASTP searching conserved sequence domains of AFMP2 (Woo et al. 2018). Furthermore, it was demonstrated that AFMP1 and AFMP4 monoclonal antibodies had been generated and used to develop two ELISA methods to detect AFMP1 and AFMP4. These antigen-capture ELISA methods can rapidly and specifically detect AFMP1 or AFMP4 in the cultures of *A. fumigatus* without the cross-reactivity with other pathogenic *Aspergillus* species (Woo et al. 2018).

In MP1 and AFMP1~AFMP4 proteins, there is a putative signal peptide at the N-terminal site, which instructs secretory proteins to the endoplasmic reticulum route (Woo et al. 2018), as well as several homologous conserved domains detected through phylogenetic analysis. Considering that the virulence role of *Penicillium marneffeii* mannoprotein 1 (MP1) has been confirmed (Woo et al. 2018), AFMPs may contribute to the virulence of *A. fumigatus* likewise. Our collaborators compared the difference in virulence between wild *A. fumigatus* and various *afmp* mutants (Woo et al. 2018). The results showed that among the four *afmp1-afmp4* single knockdown mutants, the virulence of *A. fumigatus* distinctly decreased only in the *afmp4* mutant. The mice infected by the conidia of *afmp1-afmp3* single knockdown strains did not distinguish the survival rates in the mice challenged with conidia of wild type *A. fumigatus*. It implied that *afmp1*, *afmp2*, *afmp3* might not be the crucial toxic factors, whereas *afmp4* is very likely to be a decisive virulence factor for *A. fumigatus* and may be used as a promising antigen for the development of vaccines against *A. fumigatus*.

Conclusions

The multifactorial virulence factors and complex pathogenic mechanism of *A. fumigatus* put forward higher requirements for the prevention and control of fungal. Advances in the understanding of pathogenicity and host immune response to *A. fumigatus* would be conducive to propose new strategies for antifungal vaccines. The AFMP4 protein of *A. fumigatus*, which has been identified at the molecular levels, might serve as a promising candidate antigen for developing vaccines against invasive aspergillosis. Alternatively, a pan-fungal vaccine with a broader antifungal spectrum derived from the conserved fungal cell surface epitopes might be the most promising antifungal vaccine in the future. Also, several studies of animal models, adjuvants, and

immunomodulators would provide novel strategies for the design of antifungal vaccines. Nevertheless, with antifungal vaccines' progress, these vaccines' efficacy and efficiency need to be improved.

ORCID

Jin Lv <https://orcid.org/0000-0002-8429-0687>

Acknowledgments

This work was supported by the National Natural Science Foundation of China (No. 71704082), the Ministry of Education Humanities and Social Sciences Research Program of China (No. 17YJCZH052), and Jiangsu Overseas Visiting Scholar Program for University Prominent Young & Middle-aged Teachers and Presidents.

Conflict of interest

The authors do not report any financial or personal connections with other persons or organizations, which might negatively affect the contents of this publication and/or claim authorship rights to this publication.

Literature

- Alanio A, Desnos-Ollivier M, Garcia-Hermoso D, Bretagne S.** Investigating clinical issues by genotyping of medically important fungi: why and how? *Clin Microbiol Rev.* 2017 Jul;30(3):671–707. <https://doi.org/10.1128/CMR.00043-16>
- Almeida MC, Antunes D, Silva BMA, Rodrigues L, Mota M, Borges O, Fernandes C, Gonçalves T.** Early interaction of *Aspergillus fumigatus* with macrophages. *Mycopathologia.* 2019 Jun;184(3):383–392. <https://doi.org/10.1007/s11046-019-00339-6>
- Anthony N, Foldi I, Hidalgo A.** Toll and Toll-like receptor signaling in development. *Development.* 2018 May 01;145(9):dev156018. <https://doi.org/10.1242/dev.156018>
- Arias M, Santiago L, Vidal-García M, Redrado S, Lanuza P, Comas L, Domingo MP, Rezusta A, Gálvez EM.** Preparations for invasion: modulation of host lung immunity during pulmonary aspergillosis by gliotoxin and other fungal secondary metabolites. *Front Immunol.* 2018 Nov 6;9:2549. <https://doi.org/10.3389/fimmu.2018.02549>
- Barac A, Vukicevic TA, Ilic AD, Rubino S, Zucig V, Stevanovic G.** Complications of chronic necrotizing pulmonary aspergillosis: review of published case reports. *Rev Inst Med Trop São Paulo.* 2017; 59(0):e19. <https://doi.org/10.1590/s1678-9946201759019>
- Bazan SB, Walch-Rückheim B, Schmitt MJ, Breinig F.** Maturation and cytokine pattern of human dendritic cells in response to different yeasts. *Med Microbiol Immunol (Berl).* 2018 Feb;207(1):75–81. <https://doi.org/10.1007/s00430-017-0528-8>
- Boniche C, Rossi SA, Kischkel B, Barbalho FV, Moura ÁND, Nosanchuk JD, Travassos LR, Taborda CP.** Immunotherapy against systemic fungal infections based on monoclonal antibodies. *J Fungi (Basel).* 2020 Feb 29;6(1):31. <https://doi.org/10.3390/jof6010031>
- Bonnet S, Duléry R, Regany K, Bouketouche M, Magro L, Coiteux V, Alfandari S, Berthon C, Quesnel B, Yakoub-Agha I.** Long-term follow up of invasive aspergillosis in allogeneic stem cell transplantation recipients and leukemia patients: differences in risk factors and outcomes. *Curr Res Transl Med.* 2017 Apr-Jun;65(2):77–81. <https://doi.org/10.1016/j.retram.2017.05.003>
- Briard B, Karki R, Malireddi RKS, Bhattacharya A, Place DE, Mavuluri J, Peters JL, Vogel P, Yamamoto M, Kanneganti TD.** Fungal ligands released by innate immune effectors promote inflammatory activation during *Aspergillus fumigatus* infection. *Nat Microbiol.* 2019 Feb;4(2):316–327. <https://doi.org/10.1038/s41564-018-0298-0>
- Catellani M, Lico C, Cerasi M, Massa S, Bromuro C, Torosantucci A, Benvenuto E, Capodicasa C.** Optimised production of an anti-fungal antibody in Solanaceae hairy roots to develop new formulations against *Candida albicans*. *BMC Biotechnol.* 2020 Dec;20(1):15. <https://doi.org/10.1186/s12896-020-00607-0>
- Chauvin D, Hust M, Schütte M, Chesnay A, Parent C, Moreira GMSG, Arroyo J, Sanz AB, Pugnière M, Martineau P, et al.** Targeting *Aspergillus fumigatus* Crf transglycosylases with neutralizing antibody is relevant but not sufficient to erase fungal burden in a neutropenic rat model. *Front Microbiol.* 2019 Mar 26;10:600. <https://doi.org/10.3389/fmicb.2019.00600>
- Cutler JE, Deepe GS Jr, Klein BS.** Advances in combating fungal diseases: vaccines on the threshold. *Nat Rev Microbiol.* 2007 Jan;5(1):13–28. <https://doi.org/10.1038/nrmicro1537>
- Da Silva LBR, Taborda CP, Nosanchuk JD.** Advances in fungal peptide vaccines. *J Fungi (Basel).* 2020 Jul 25;6(3):119. <https://doi.org/10.3390/jof6030119>
- Dai C, Wu J, Chen C, Wu X.** Interactions of thymic stromal lymphopoietin with TLR2 and TLR4 regulate anti-fungal innate immunity in *Aspergillus fumigatus*-induced corneal infection. *Exp Eye Res.* 2019 May;182:19–29. <https://doi.org/10.1016/j.exer.2019.02.020>
- Darling BA, Milder EA.** Invasive aspergillosis. *Pediatr Rev.* 2018 Sep;39(9):476–478. <https://doi.org/10.1542/pir.2017-0129>
- Dewi I, van de Veerdonk F, Gresnigt M.** The multifaceted role of T-helper responses in host defense against *Aspergillus fumigatus*. *J Fungi (Basel).* 2017 Oct 04;3(4):55. <https://doi.org/10.3390/jof3040055>
- Diaz-Arevalo D, Kalkum M.** CD4⁺ T cells mediate aspergillosis vaccine protection. *Methods Mol Biol.* 2017;1625:281–293. https://doi.org/10.1007/978-1-4939-7104-6_19
- Dos Santos RAC, Steenwyk JL, Rivero-Mendez O, Mead ME, Silva LP, Bastos RW, Alastruey-Izquierdo A, Goldman GH, Rokas A.** Genomic and phenotypic heterogeneity of clinical isolates of the human pathogens *Aspergillus fumigatus*, *Aspergillus lentulus*, and *Aspergillus fumigatus affinis*. *Front Genet.* 2020 May 12;11:459. <https://doi.org/10.3389/fgene.2020.00459>
- Dutta O, Espinosa V, Wang K, Avina S, Rivera A.** Dectin-1 promotes type I and III interferon expression to support optimal anti-fungal immunity in the lung. *Front Cell Infect Microbiol.* 2020 Jul 8;10:321. <https://doi.org/10.3389/fcimb.2020.00321>
- Ferling I, Dunn JD, Ferling A, Soldati T, Hillmann F.** Conidial melanin of the human-pathogenic fungus *Aspergillus fumigatus* disrupts cell autonomous defenses in amoebae. *MBio.* 2020 May 26; 11(3):e00862–20. <https://doi.org/10.1128/mBio.00862-20>
- Filler SG, Sheppard DC.** Fungal invasion of normally non-phagocytic host cells. *PLoS Pathog.* 2006;2(12):e129. <https://doi.org/10.1371/journal.ppat.0020129>
- Fraga-Silva TFC, Mimura LAN, Leite LCT, Borim PA, Ishikawa LLW, Venturini J, Arruda MSP, Sartori A.** Gliotoxin aggravates experimental autoimmune encephalomyelitis by triggering neuroinflammation. *Toxins (Basel).* 2019 Jul 26;11(8):443. <https://doi.org/10.3390/toxins11080443>
- Gamaletsou MN, Walsh TJ, Sipsas NV.** Invasive fungal infections in patients with hematological malignancies: emergence of resistant pathogens and new antifungal therapies. *Turk J Haematol.* 2018 Feb 26;35(1):1–11. <https://doi.org/10.4274/tjh.2018.0007>
- Garth JM, Mackel JJ, Reeder KM, Blackburn JP, Dunaway CW, Yu Z, Matalon S, Fitz L, Steele C.** Acidic mammalian chitinase negatively affects immune responses during acute and chronic *Aspergillus fumigatus* exposure. *Infect Immun.* 2018 Apr 30;86(7):e00944–17. <https://doi.org/10.1128/IAI.00944-17>

- Garth JM, Steele C. Innate lung defense during invasive aspergillosis: new mechanisms. *J Innate Immun.* 2017;9(3):271–280. <https://doi.org/10.1159/000455125>
- Guo Y, Kasahara S, Jhingran A, Tosini NL, Zhai B, Aufiero MA, Mills KAM, Gjonbalaj M, Espinosa V, Rivera A, et al. During *Aspergillus* infection, monocyte-derived DCs, neutrophils, and plasmacytoid DCs enhance innate immune defense through CXCR3-dependent crosstalk. *Cell Host Microbe.* 2020 Jul 8;28(1):104–116.e4. <https://doi.org/10.1016/j.chom.2020.05.002>
- Gupta N, Singh PK, Revankar SG, Chandrasekar PH, Kumar A. Pathobiology of *Aspergillus fumigatus* endophthalmitis in immunocompetent and immunocompromised mice. *Microorganisms.* 2019 Aug 28;7(9):297. <https://doi.org/10.3390/microorganisms7090297>
- Hoeningl M, Prattes J, Neumeister P, Wölfler A, Krause R. Real-world challenges and unmet needs in the diagnosis and treatment of suspected invasive pulmonary aspergillosis in patients with haematological diseases: An illustrative case study. *Mycoses.* 2018 Mar; 61(3):201–205. <https://doi.org/10.1111/myc.12727>
- Jović Z, Janković SM, Ružić Zečević D, Milovanović D, Stefanović S, Folić M, Milovanović J, Kostić M. Clinical pharmacokinetics of second-generation triazoles for the treatment of invasive aspergillosis and candidiasis. *Eur J Drug Metab Pharmacokinet.* 2019 Apr; 44(2):139–157. <https://doi.org/10.1007/s13318-018-0513-7>
- Khan MA, Ali ZS, Swezey N, Grasemann H, Palaniyar N. Progression of cystic fibrosis lung disease from childhood to adulthood: neutrophils, neutrophil extracellular trap (NET) formation, and NET degradation. *Genes (Basel).* 2019 Feb 26;10(3):183. <https://doi.org/10.3390/genes10030183>
- Khani S, Seyedjavadi SS, Hosseini HM, Goudarzi M, Valadbeigi S, Khatami S, Ajdary S, Eslamifard A, Amani J, Imani Fooladi AA, et al. Effects of the antifungal peptide Skh-AMP1 derived from *Satureja khuzistanica* on cell membrane permeability, ROS production, and cell morphology of conidia and hyphae of *Aspergillus fumigatus*. *Peptides.* 2020 Jan;123:170195. <https://doi.org/10.1016/j.peptides.2019.170195>
- Krüger T, Luo T, Schmidt H, Shopova I, Kniemeyer O. Challenges and strategies for proteome analysis of the interaction of human pathogenic fungi with host immune cells. *Proteomes.* 2015 Dec 14;3(4):467–495. <https://doi.org/10.3390/proteomes3040467>
- Latgé JP, Chamilos G. *Aspergillus fumigatus* and aspergillosis in 2019. *Clin Microbiol Rev.* 2019 Nov 13;33(1):e00140–18. <https://doi.org/10.1128/CMR.00140-18>
- Levitz SM. *Aspergillus* vaccines: hardly worth studying or worthy of hard study? *Med Mycol.* 2017 Jan 01;55(1):103–108. <https://doi.org/10.1093/mmy/myw081>
- Li T, Zhang Z, Li X, Dong G, Zhang M, Xu Z, Yang J. Neutrophil extracellular traps: signaling properties and disease relevance. *Mediators Inflamm.* 2020 Jul 28;2020:1–14. <https://doi.org/10.1155/2020/9254087>
- Li W, Yan J, Yu Y. Geometrical reorganization of Dectin-1 and TLR2 on single phagosomes alters their synergistic immune signaling. *Proc Natl Acad Sci USA.* 2019 Dec 10;116(50):25106–25114. <https://doi.org/10.1073/pnas.1909870116>
- Liedke SC, Miranda DZ, Gomes KX, Gonçalves JLS, Frases S, Nosanchuk JD, Rodrigues ML, Nimrichter L, Peralta JM, Guimarães AJ. Characterization of the antifungal functions of a WGA-Fc (IgG2a) fusion protein binding to cell wall chitin oligomers. *Sci Rep.* 2017 Dec;7(1):12187. <https://doi.org/10.1038/s41598-017-12540-y>
- Liu C, Wang M, Sun W, Cai F, Geng S, Su X, Shi Y. PU.1 serves a critical role in the innate defense against *Aspergillus fumigatus* via dendritic cell-associated C-type lectin receptor-1 and Toll-like receptors-2 and 4 in THP-1-derived macrophages. *Mol Med Rep.* 2017 Jun;15(6):4084–4092. <https://doi.org/10.3892/mmr.2017.6504>
- Mackel JJ, Steele C. Host defense mechanisms against *Aspergillus fumigatus* lung colonization and invasion. *Curr Opin Microbiol.* 2019 Dec;52:14–19. <https://doi.org/10.1016/j.mib.2019.04.003>
- Masaki K, Fukunaga K, Matsusaka M, Kabata H, Tanosaki T, Mochimaru T, Kamatani T, Ohtsuka K, Baba R, Ueda S, et al. Characteristics of severe asthma with fungal sensitization. *Ann Allergy Asthma Immunol.* 2017 Sep;119(3):253–257. <https://doi.org/10.1016/j.anai.2017.07.008>
- Matveev AL, Krylov VB, Khlusevich YA, Baykov IK, Yashunsky DV, Emelyanova LA, Tsvetkov YE, Karelin AA, Bardashova AV, Wong SSW, et al. Novel mouse monoclonal antibodies specifically recognizing β -(1 \rightarrow 3)-D-glucan antigen. *PLoS One.* 2019 Apr 25;14(4):e0215535. <https://doi.org/10.1371/journal.pone.0215535>
- Mead ME, Knowles SL, Raja HA, Beattie SR, Kowalski CH, Steenwyk JL, Silva LP, Chiaratto J, Ries LNA, Goldman GH, et al. Characterizing the pathogenic, genomic, and chemical traits of *Aspergillus fisheri*, a close relative of the major human fungal pathogen *Aspergillus fumigatus*. *MSphere.* 2019 Feb 20;4(1):e00018–19. <https://doi.org/10.1128/mSphere.00018-19>
- Movahed E, Cheok YY, Tan GMY, Lee CYQ, Cheong HC, Velayuthan RD, Tay ST, Chong PP, Wong WF, Looi CY. Lung-infiltrating T helper 17 cells as the major source of interleukin-17A production during pulmonary *Cryptococcus neoformans* infection. *BMC Immunol.* 2018 Dec;19(1):32. <https://doi.org/10.1186/s12865-018-0269-5>
- Muszewska A, Piłsyk S, Perlińska-Lenart U, Kruszewska JS. Diversity of cell wall related proteins in human pathogenic fungi. *J Fungi (Basel).* 2017 Dec 29;4(1):6. <https://doi.org/10.3390/jof4010006>
- Muthu V, Sehgal IS, Dhooria S, Aggarwal AN, Agarwal R. Utility of recombinant *Aspergillus fumigatus* antigens in the diagnosis of allergic bronchopulmonary aspergillosis: A systematic review and diagnostic test accuracy meta-analysis. *Clin Exp Allergy.* 2018 Sep; 48(9):1107–1136. <https://doi.org/10.1111/cea.13216>
- Namvar S, Warn P, Farnell E, Bromley M, Fraczek M, Bowyer P, Herrick S. *Aspergillus fumigatus* proteases, Asp f 5 and Asp f 13, are essential for airway inflammation and remodelling in a murine inhalation model. *Clin Exp Allergy.* 2015 May;45(5):982–993. <https://doi.org/10.1111/cea.12426>
- Orciuolo E, Stanzani M, Canestraro M, Galimberti S, Carulli G, Lewis R, Petrini M, Komanduri KV. Effects of *Aspergillus fumigatus* gliotoxin and methylprednisolone on human neutrophils: implications for the pathogenesis of invasive aspergillosis. *J Leukoc Biol.* 2007 Oct;82(4):839–848. <https://doi.org/10.1189/jlb.0207090>
- Pagano L, Busca A, Candoni A, Cattaneo C, Cesaro S, Fanci R, Nadali G, Potenza L, Russo D, Tumbarello M, et al.; SEIFEM (Sorveglianza Epidemiologica Infezioni Fungine nelle Emopatie Maligne) Group. Risk stratification for invasive fungal infections in patients with hematological malignancies: SEIFEM recommendations. *Blood Rev.* 2017 Mar;31(2):17–29. <https://doi.org/10.1016/j.blre.2016.09.002>
- Pathakumari B, Liang G, Liu W. Immune defence to invasive fungal infections: A comprehensive review. *Biomed Pharmacother.* 2020 Oct;130:110550. <https://doi.org/10.1016/j.biopha.2020.110550>
- Paulovičová L, Paulovičová E, Farkaš P, Čížová A, Bystrický P, Jančinová V, Turánek J, Pericolini E, Gabrielli E, Vecchiarelli A, et al. Bioimmunological activities of *Candida glabrata* cellular mannan. *FEMS Yeast Res.* 2019 Mar 01;19(2):19. <https://doi.org/10.1093/femsyr/foz009>
- Paulussen C, Hallsworth JE, Álvarez-Pérez S, Nierman WC, Hamill PG, Blain D, Rediers H, Lievens B. Ecology of aspergillosis: insights into the pathogenic potency of *Aspergillus fumigatus* and some other *Aspergillus* species. *Microb Biotechnol.* 2017 Mar; 10(2):296–322. <https://doi.org/10.1111/1751-7915.12367>
- Pérez-Cantero A, Serrano DR, Navarro-Rodríguez P, Schätzlein AG, Uchegbu IF, Torrado JJ, Capilla J. Increased efficacy of oral fixed-dose combination of amphotericin B and AHCC®

- natural adjuvant against aspergillosis. *Pharmaceutics*. 2019 Sep 03; 11(9):456. <https://doi.org/10.3390/pharmaceutics11090456>
- Pfannenstiel BT, Zhao X, Wortman J, Wiemann P, Throckmorton K, Spraker JE, Soukup AA, Luo X, Lindner DL, Lim FY, et al.** Revitalization of a forward genetic screen identifies three new regulators of fungal secondary metabolism in the genus *Aspergillus*. *MBio*. 2017 Nov 08;8(5):e01246–17. <https://doi.org/10.1128/mBio.01246-17>
- Ravindran M, Khan MA, Palaniyar N.** Neutrophil extracellular trap formation: physiology, pathology, and pharmacology. *Biomolecules*. 2019 Aug 14;9(8):365. <https://doi.org/10.3390/biom9080365>
- Ruiz-Herrera J, Ortiz-Castellanos L.** Cell wall glucans of fungi. A review. *The Cell Surface*. 2019 Dec;5:100022. <https://doi.org/10.1016/j.tcs.2019.100022>
- Sato S, Tamai Y.** Cutaneous aspergillosis disseminated from invasive pulmonary aspergillosis. *Int J Infect Dis*. 2019 Oct;87:13–14. <https://doi.org/10.1016/j.ijid.2019.08.005>
- Schlam D, Canton J, Carreño M, Kopinski H, Freeman SA, Grinstein S, Fairn GD.** Gliotoxin suppresses macrophage immune function by subverting phosphatidylinositol 3,4,5-trisphosphate homeostasis. *MBio*. 2016 May 04;7(2):e02242–15. <https://doi.org/10.1128/mBio.02242-15>
- Schmidt S, Tramsen L, Lehrnbecher T.** Natural killer cells in anti-fungal immunity. *Front Immunol*. 2017 Nov 22;8:1623. <https://doi.org/10.3389/fimmu.2017.01623>
- Schoen TJ, Rosowski EE, Knox BP, Bennin D, Keller NP, Huttenlocher A.** Neutrophil phagocyte oxidase activity controls invasive fungal growth and inflammation in zebrafish. *J Cell Sci*. 2019 Dec 20;133(5):133. <https://doi.org/10.1242/jcs.236539>
- Schülke S.** Induction of interleukin-10 producing dendritic cells as a tool to suppress allergen-specific T helper 2 responses. *Front Immunol*. 2018 Mar 19;9:455. <https://doi.org/10.3389/fimmu.2018.00455>
- Shen Q, Zhou W, Li H, Hu L, Mo H.** ROS involves the fungicidal actions of thymol against spores of *Aspergillus flavus* via the induction of nitric oxide. *PLoS One*. 2016 May 19;11(5):e0155647. <https://doi.org/10.1371/journal.pone.0155647>
- Shenoy MK, Iwai S, Lin DL, Worodria W, Ayakaka I, Byanyima P, Kaswabuli S, Fong S, Stone S, Chang E, et al.** Immune response and mortality risk relate to distinct lung microbiomes in patients with HIV and pneumonia. *Am J Respir Crit Care Med*. 2017 Jan; 195(1):104–114. <https://doi.org/10.1164/rccm.201603-0523OC>
- Shishodia SK, Tiwari S, Shankar J.** Resistance mechanism and proteins in *Aspergillus* species against antifungal agents. *Mycology*. 2019 Jul 03;10(3):151–165. <https://doi.org/10.1080/21501203.2019.1574927>
- Shopova IA, Belyaev I, Dasari P, Jahreis S, Stroe MC, Cseresnyés Z, Zimmermann AK, Medyukhina A, Svensson CM, Krüger T, et al.** Human neutrophils produce antifungal extracellular vesicles against *Aspergillus fumigatus*. *MBio*. 2020 Apr 14;11(2):e00596–20. <https://doi.org/10.1128/mBio.00596-20>
- Smole U, Kratzer B, Pickl WF.** Soluble pattern recognition molecules: guardians and regulators of homeostasis at airway mucosal surfaces. *Eur J Immunol*. 2020 May;50(5):624–642. <https://doi.org/10.1002/eji.201847811>
- Souza JAM, Baltazar LM, Carregal VM, Gouveia-Eufrasio L, de Oliveira AG, Dias WG, Campos Rocha M, Rocha de Miranda K, Malavazi I, Santos DA, et al.** Characterization of *Aspergillus fumigatus* extracellular vesicles and their effects on macrophages and neutrophils functions. *Front Microbiol*. 2019 Sep 4;10:2008. <https://doi.org/10.3389/fmicb.2019.02008>
- Takazono T, Izumikawa K.** Recent advances in diagnosing chronic pulmonary aspergillosis. *Front Microbiol*. 2018 Aug 17;9:1810. <https://doi.org/10.3389/fmicb.2018.01810>
- Tsunawaki S, Yoshida LS, Nishida S, Kobayashi T, Shimoyama T.** Fungal metabolite gliotoxin inhibits assembly of the human respiratory burst NADPH oxidase. *Infect Immun*. 2004 Jun;72(6):3373–3382. <https://doi.org/10.1128/IAI.72.6.3373-3382.2004>
- Ulrich S, Ebel F.** Monoclonal antibodies as tools to combat fungal infections. *J Fungi (Basel)*. 2020 Feb 04;6(1):22. <https://doi.org/10.3390/jof6010022>
- Upadhy R, Lam WC, Maybruck B, Specht CA, Levitz SM, Lodge JK.** Induction of protective immunity to cryptococcal infection in mice by a heat-killed, chitosan-deficient strain of *Cryptococcus neoformans*. *MBio*. 2016 Jul 06;7(3):e00547–16. <https://doi.org/10.1128/mBio.00547-16>
- van de Peppel RJ, Visser LG, Dekkers OM, de Boer MGJ.** The burden of invasive aspergillosis in patients with haematological malignancy: A meta-analysis and systematic review. *J Infect*. 2018 Jun;76(6):550–562. <https://doi.org/10.1016/j.jinf.2018.02.012>
- van de Veerdonk FL, Gresnigt MS, Romani L, Netea MG, Latgé JP.** *Aspergillus fumigatus* morphology and dynamic host interactions. *Nat Rev Microbiol*. 2017 Nov;15(11):661–674. <https://doi.org/10.1038/nrmicro.2017.90>
- Wagener J, Echtenacher B, Rohde M, Kotz A, Krappmann S, Heesemann J, Ebel F.** The putative alpha-1,2-mannosyltransferase AfMnt1 of the opportunistic fungal pathogen *Aspergillus fumigatus* is required for cell wall stability and full virulence. *Eukaryot Cell*. 2008 Oct;7(10):1661–1673. <https://doi.org/10.1128/EC.00221-08>
- Wang F, Zhang C, Jiang Y, Kou C, Kong Q, Long N, Lu L, Sang H.** Innate and adaptive immune response to chronic pulmonary infection of hyphae of *Aspergillus fumigatus* in a new murine model. *J Med Microbiol*. 2017 Oct 01;66(10):1400–1408. <https://doi.org/10.1099/jmm.0.000590>
- Wang Y, Wang K, Masso-Silva JA, Rivera A, Xue C.** A Heat-Killed *Cryptococcus* mutant strain induces host protection against multiple invasive mycoses in a murine vaccine model. *MBio*. 2019 Nov 26;10(6):e02145–19. <https://doi.org/10.1128/mBio.02145-19>
- Woo PCY, Lau SKP, Lau CCY, Tung ETK, Au-Yeung RKH, Cai JP, Chong KTK, Sze KH, Kao RY, Hao Q, et al.** Mp1p homologues as virulence factors in *Aspergillus fumigatus*. *Med Mycol*. 2018 Apr 01;56(3):350–360. <https://doi.org/10.1093/mmy/myx052>
- Xiao H, Tang Y, Cheng Q, Liu J, Li X.** Risk prediction and prognosis of invasive fungal disease in hematological malignancies patients complicated with bloodstream infections. *Cancer Manag Res*. 2020 Mar;12:2167–2175. <https://doi.org/10.2147/CMAR.S238166>
- Zhang C, Chen F, Liu X, Han X, Hu Y, Su X, Chen Y, Sun Y, Han L.** Gliotoxin induces cofilin phosphorylation to promote actin cytoskeleton dynamics and internalization of *Aspergillus fumigatus* into type II human pneumocyte cells. *Front Microbiol*. 2019 Jun 18;10:1345. <https://doi.org/10.3389/fmicb.2019.01345>

Epidemiology and Pathogenesis of *Staphylococcus* Bloodstream Infections in Humans: a Review

KLAUDIA LISOWSKA-ŁYSIAK¹ , RYSZARD LAUTERBACH² , JACEK MIĘDZOBRODZKI¹ 
and MAJA KOSECKA-STROJEK^{1*} 

¹Department of Microbiology, Faculty of Biochemistry, Biophysics and Biotechnology,
Jagiellonian University, Kraków, Poland

²Department of Neonatology, Collegium Medicum, Jagiellonian University, Kraków, Poland

Submitted 22 October 2020, revised 18 December 2021, accepted 12 January 2021

Abstract

Staphylococci are among the most frequent human microbiota components associated with the high level of bloodstream infection (BSI) episodes. In predisposed patients, there is a high risk of transformation of BSI episodes to sepsis. Both bacterial and host factors are crucial for the outcomes of BSI and sepsis. The highest rates of BSI episodes were reported in Africa, where these infections were up to twice as high as the European rates. However, there remains a great need to analyze African data for comprehensive quantification of staphylococcal BSI prevalence. The lowest rates of BSI exist in Australia. Asian, European, and North American data showed similar frequency values. World-wide analysis indicated that both *Staphylococcus aureus* and coagulase-negative staphylococci (CoNS) are the most frequent BSI agents. In the second group, the most prevalent species was *Staphylococcus epidermidis*, although CoNS were not identified at the species level in many studies. The lack of a significant worldwide decrease in BSI episodes indicates a great need to implement standardized diagnostic methods and research etiological factors using advanced genetic methods.

Key words: bacteremia, carriage, infection, sepsis, *Staphylococcus*

Introduction

Staphylococcus aureus is one of the most frequently isolated pathogens from the hospital or community-acquired infections. Staphylococci are a large group of bacteria in every environment; however, these bacteria can proliferate only in humans or animals. Many staphylococcal species colonize the skin and mucosal membranes, especially the perineum and pharynx. The other sites that harbor these bacteria are the gastrointestinal tract, vagina, and axilla, but carriage in those areas is less frequent (Kosecka-Strojek et al. 2018). Traditionally, staphylococci have been divided into two groups based on the production of extracellular enzyme coagulase: coagulase-positive staphylococci (CoPS) and coagulase-negative staphylococci (CoNS). The first group is represented by well-known opportunistic pathogens such as *Staphylococcus aureus*, *Staphylococcus schleiferi*, *Staphylococcus intermedius*, and *Staphylococcus pseud-intermedius*, and the second group traditionally includes

nonpathogenic or opportunistic pathogens; however, recently, several clinical reports have presented CoNS as dangerous pathogens, particularly for newborns or immunocompromised patients (Heilmann et al. 2019). A few species, namely *Staphylococcus hyicus*, *Staphylococcus agnetis*, and *Staphylococcus felis*, belong to the third group – coagulase-variable staphylococci. These species are usually grouped with CoPS but cannot produce clumping factors, and coagulase production tests give variable results (Becker et al. 2014). As opportunistic pathogens, staphylococci exhibit saprophytic characteristics under physiological conditions, but the bacteria become severe pathogens under additional infection-facilitating conditions.

Staphylococci are etiological agents of diseases with various localizations, manifestations and/or courses of infection. The most frequent infections are local infections, and the bacteria can cause lesions in various anatomical tissues. Overall, the infections are grouped into skin and soft tissue infections (SSTIs) with

* Corresponding author: M. Kosecka-Strojek, Department of Microbiology, Faculty of Biochemistry, Biophysics and Biotechnology, Jagiellonian University, Kraków, Poland, e-mail: maja.kosecka-strojek@uj.edu.pl

© 2021 Klaudia Lisowska-Łysiak et al.

This work is licensed under the Creative Commons Attribution-NonCommercial-NoDerivatives 4.0 License (<https://creativecommons.org/licenses/by-nc-nd/4.0/>).

manifestations such as dermatitis, abscesses, furunculosis, boils, folliculitis, impetigo, or mastitis, and also includes other severe diseases such as staphylococcal foodborne disease, toxic shock syndrome, and staphylococcal scalded skin syndrome (SSSS) (Foster 2012; Tong et al. 2015). Staphylococci are also common pathogens of deep tissue infections, including foreign bodies infection. Most studies focused on *S. aureus* infections, but there is strong evidence of the CoNS involvement in severe diseases. Osteomyelitis, otitis, wound infection, endophthalmitis, urinary tract infection, meningitis, or even pneumonia may be caused by *S. epidermidis*, *Staphylococcus saprophyticus*, *Staphylococcus lugdunensis*, and *S. schleiferi* (von Eiff et al. 2002; Becker et al. 2014; Argemi et al. 2019). When staphylococci gain entry into the bloodstream, colonization becomes systemic as bacteremia and then advances to infection.

The literature was screened based on a PubMed search using the terms „staphylococci”, „*Staphylococcus*” and „bloodstream infections” and/or „sepsis”. The publications were then evaluated based on a citation index. Specific criteria were used to describe the worldwide occurrence of *S. aureus*, and CoNS bloodstream infections and/or sepsis, such as: only original articles were included; the data from different geographical regions/countries were analyzed; the articles with the highest number of participants and bacterial strains isolated, and those containing long-term studies or the recent data, were selected to the analysis.

Bacteremia, bloodstream infection, and sepsis

Bacteremia. Bacteremia is characterized by the presence of pathogens in the blood (Pai et al. 2015). Transient bacteremia is limited to one or two days, without any manifestations, and may be caused by some staphylococcal species. Furthermore, the phenomenon does not indicate any further manifestation in healthy hosts (Samet et al. 2006). The presence of bacteria in the blood is eliminated by immunological defense systems and is known in the literature as „natural bacteremia” or „physiological bacteremia”.

Bloodstream infection. However, in predisposed hosts, bacteremia advances to bloodstream infection (BSI), manifesting as an inflammatory response against microorganisms or/and against their metabolites present in the body (Dayan et al. 2016). The BSI can be successfully treated or advances to sepsis (Thomer et al. 2016; Michalik et al. 2020). Sepsis is related to organ dysfunction, perfusion disturbances, or hypotension with accompanying lacticaemia, oliguria, and/or psychological disorders (Samet et al. 2006; Hotchkiss et al. 2016).

Therefore, some *S. aureus* bacteremia complications, such as endocarditis, attributable mortality, embolic

stroke, or recurrent infection during the 12-week follow-up period, are circumstances associated with the increased sepsis frequency from 11% to 43%. When the inflammatory response is triggered by the massive release of pro-inflammatory Th1 cytokines, such as TNF- α , IL-1 β , IL-6, and IFN- γ , a septic shock may occur (Dayan et al. 2016).

Sepsis. Sepsis is the incorrect, inflammatory response of the host organism to infection, and often, it is a result of systemic bloodstream infections. Recently, sepsis is defined as life-threatening organ dysfunction caused by a dysregulated host response to infection (Singer et al. 2016). Untreated sepsis can lead to severe sepsis or septic shock and, consequently, multiple organ failure (Sequential Organ Failure Assessment, SOFA) and death (Stevenson et al. 2016). Sepsis is a critical clinical stage of general toxemia and organ dysfunction, and a patient’s inflammatory response interferes with the functioning of vital organs, such as the heart, kidneys, lungs, or liver. Sepsis-3 recommends a new sepsis scoring system, rapid sequential assessment of organ failure (qSOFA), consisting of 3 elements: an altered mental state, respiratory rate, and systolic blood pressure (Minejima et al. 2019). Patients with suspected infection expected to have a prolonged ICU stay can be identified at the bedside with quick SOFA, i.e., alteration in mental status, systolic blood pressure ≤ 100 mmHg, or respiratory rate ≥ 22 /min. Moreover, patients with septic shock can be identified with a clinical construct of sepsis with persisting hypotension requiring vasopressors to maintain MAP ≥ 65 mmHg and having a serum lactate level > 2 mmol/l (18 mg/dl) despite adequate volume resuscitation (Singer et al. 2016).

Pathogenicity of staphylococcal bloodstream infections

Antibiotic resistance. Staphylococci exhibit a wide resistance to antibiotics. One of the most dangerous features of staphylococci is their multi-resistance. Research indicates that both the CoPS and CoNS species have staphylococcal chromosome cassettes *mec* (*SCCmec*) that determine resistance to methicillin in both groups. Furthermore, the *SCCmec* elements of CoNS present extreme diversity, which causes many diagnostic problems (Hosseinkhani et al. 2018). The increase of methicillin-resistant *S. aureus* (MRSA) isolates in hospital and the community due to horizontal gene transfer across bacterial species occurred. The environmental and animal-associated CoNS may be underestimated factor for the spread of the resistance genes into more pathogenic species like *S. aureus* (Kosecka-Strojek et al. 2016; Lisowska-Łysiak et al. 2019). Methicillin and

vancomycin resistance remain the major antimicrobial resistance phenotype of concern. Although still relatively infrequent, multi-resistant CoNS with reduced susceptibility to glycopeptides are emerging pathogens of clinical concern and should be kept in mind in empirical and rational therapy of BSI (Veach et al. 1990; Natoli et al. 2009). In recent years an emerging spread of linezolid-resistant *Staphylococcus capitis* and *S. epidermidis* strains in Europe was shown (Tevell et al. 2017; Kosecka-Strojek et al. 2020). An increased resistance is the result of antibiotic pressure, which could select resistant clones among staphylococci.

Virulence determinants and other invasion/evasion determinants. Staphylococci exhibit a strong capacity to infect human hosts by using specific strategies to enable the adherence, invasion, persistence, and evasion of the host's immunity mechanisms. However, the infection ability is not similar for all species within the *Staphylococcus* genus. In general, CoNS isolates present lower levels of virulence determinants than CoPS, but the factors involved in colonization support invasion in the host (Becker et al. 2014). It is especially true in extremely immature infants, in whom more than 80% of late-onset sepsis (diagnosed after 72 hours of life) is caused by CoNS (Lauterbach et al. 2016; Wójkowska-Mach et al. 2019). However, despite the relatively low level of virulence, immature infants with sepsis caused by these pathogens present a wide range of clinical symptoms (Lauterbach et al. 2016). It was shown that *S. lugdunensis* was responsible for sepsis and endocarditis on the 1st day of life in a term newborn, which underwent lotus birth (Ittleman and Szabo 2018). In contrast, *S. aureus* strains often exhibit a vast arsenal of toxins and enzymes involved in staphylococcal pathogenesis. Toxins can lead to a weak response of the human organism because they can degrade certain host cells, manipulate the innate and adaptive immune response, and degrade intercellular junctions, contributing to the *S. aureus* proliferation (Oliveira et al. 2018).

Toxins. One of *S. aureus* toxicity mechanisms is damage to host cell membranes caused by hemolysins, bicomponent leukocidins, or phenol-soluble modulins (Herrera et al. 2016). However, it has been proven that CoNS also secrete toxins and enzymes. Based on CoNS strains whole-genome sequencing (WGS) performed by Argemi et al. (2019), the presence of proteases, lipases, and hemolysins genes in *S. epidermidis*, *S. capitis*, and *Staphylococcus caprae* was shown. Moreover, enterotoxin genes in *S. epidermidis* and *Staphylococcus haemolyticus* genomes were shown (Nanoukon et al. 2018; Argemi et al. 2019). Other toxins produced by *S. aureus* are usually infection-specific, such as enterotoxins or toxic shock syndrome toxin. Furthermore, bacteria-host interactions depend on extracellular

enzymes, and the largest group of enzymes includes proteases. This category consists of serine proteases, the metalloprotease aureolysin, and staphopains that are engaged in the evasion of complement-mediated killing, host tissue destruction, immunoglobulin degradation, and deregulation of fibrinolysis (Miedzobrodzki et al. 2002; Sabat et al. 2008; Kalińska et al. 2012; Martínez-García et al. 2018).

Biofilm formation. Biofilm formation is an additional factor associated with CoPS and CoNS infections (Grzebyk et al. 2013; Argemi et al. 2019). Biofilm formation is one of the staphylococcal survival strategies within host organisms. The presence of staphylococcal biofilms is a key factor involved in bacterial resistance to various groups of antibiotics. Bacterial biofilms are defined as communities of bacterial colonies attached to the host surface and surrounded by exopolymeric matrix substances strictly regulated by numerous proteins engaged in the biofilm life cycle. It was shown that biofilms could evade the host immune response, which leads to the persistence of staphylococci. Bhattacharya et al. (2018) proved that *S. aureus* biofilms could release leukocidins, which affect extracellular trap formation and allow evasion of neutrophil-mediated killing. Biofilm production has also been proven for CoNS species, including *S. lugdunensis* that produces adhesins and other biofilm promoters (Argemi et al. 2017). Staphylococcal pathogenesis is a process that involves an array of extracellular proteins, biofilm, and cell wall components that are coordinately expressed in different phases of infection. The expression or suppression of two divergent loci, accessory gene regulator (*agr*) and staphylococcal accessory regulator (*sar*) are recognized as critical regulators of virulence in staphylococci (Arya and Princy 2013).

Risk factors present in humans: predisposed patients. Several studies have shown that host risk factors may significantly enhance the effects of BSIs, including mortality. The high-risk group of staphylococcal infections contains mostly patients with indwelling medical devices. The highly predisposed groups also contain premature newborns or elderly patients or multimorbid, chronically ill, or immunosuppressed patients. A large group of the patients infected is also those with inserted foreign plastic bodies, such as implants and venflons.

The essential patients' factors that determine bloodstream infections and complications are age, presence of comorbidities, and appropriate initial antibiotic treatment (Ayau et al. 2017). Bloodstream infections occur in elderly patients over 75 years old, resulting in increased mortality (Gasch et al. 2013). A 9-year study performed by Ayau et al. (2017) underlined risk factors that increased the probability of mortality, such as age, cancer, heart disease, neurological disease, nursing

home residence, and Charlson score greater than 3. In fact, cancer itself increases the 30-day mortality, but Bello-Chavolla et al. (2018) reported additional risk factors, including hematologic malignancy, hyperglycemia, abdominal source of infection, and endocarditis, based on studies conducted on patients with cancer. Malignancy was also confirmed to be a key factor associated with poor outcomes of infection in other studies (Papadimitriou-Olivgeris et al. 2019).

Epidemiology: Worldwide distribution of staphylococcal bloodstream infections

Staphylococcal bloodstream infections are currently a challenging issue for clinicians, diagnosticians, and microbiologists, primarily due to their high frequency worldwide. Studies on bloodstream infection episodes differ slightly from each other because of the high number of patients and the number of institutions involved in providing the data. Interestingly, all of these studies confirmed a high number of staphylococci isolated from blood samples, ranging from 23.9 to 79.2% (Table I). In many cases, *S. aureus*, usually MRSA isolates, and CoNS were the predominant species involved in BSI episodes. However, most importantly, staphylococcal bloodstream infections affect the whole world, not only developing countries. It is imperative to analyze the data to implement standard diagnostic methods, to compare the results among various countries, to evaluate existing preventive measures, and to plan effective infection prevention and control programs or establish new programs, including the use of advanced genetic methods (Dik et al. 2016; Sabat et al. 2017; Kosecka-Strojek et al. 2019). This study compares staphylococcal bloodstream infections in the world. The evaluation of *S. aureus* and CoNS as etiological agents of BSI of the cited publications was made under the following criteria: the studies included patients with symptoms of BSI/sepsis; pathogens grew on at least one percutaneous blood culture and a culture of the catheter tip; bacteria have been identified as *S. aureus* or CoNS species using commercial/automated identification tests; susceptibility testing was performed, and CoNS species from positive blood samples were included in comprehensive data for analysis except where specified in the laboratory records as contaminants.

Europe. The epidemiology of BSI episodes in Europe was analyzed in detail. The European Centre for Disease Prevention and Control (ECDC 2008; 2018) presented that CoNS were the most numerous bloodstream infections pathogens isolated in Europe. Moreover, the biggest groups of infected patients consisted of neonates and children, and the probability of serious complications such as long-term adverse neurological outcomes

or mortality remained high for these infections (Zingg et al. 2017). Deptuła et al. (2018) reported that catheter-related BSI episodes in Poland occurred in 48.9% of the patients analyzed, and the predominant pathogens were CoNS. These results suggest a strong need for the construction of functional incidence-based surveillance programs in Poland to reduce BSI episodes. The Neonatology Surveillance Network (PNSN) prepared one of these programs and focused on late-onset BSI (LO-BSI) in very-low-birth-weight infants. The study showed that CoNS were the most common cause of LO-BSI (Wójkowska-Mach et al. 2014). Both studies confirmed that it is necessary to implement a national program for infectious disease monitoring and prevention.

Another study in Germany focused on pediatric BSI was based on 20 years of sample collection at a tertiary care hospital. This study conducted a complex observation of a large group of BSI episodes. The results showed an increasing number of CoNS to be responsible for these infections (Hufnagel et al. 2008). Similar results were published by Buetti et al. (2017), which were based on a 7-year surveillance study in Switzerland, although the major pathogen isolated was *Escherichia coli*. These findings were confirmed by other studies performed in Switzerland when staphylococci caused a big group of BSI episodes, but the major isolated pathogens were Gram-negative rods (Papadimitriou-Olivgeris et al. 2019).

On the other hand, an increase in the presence of CoNS was observed, but a minority of studies identified bacteria to the species level. One of these studies was performed in Sweden and showed the CoNS were related to newborns' sepsis from 1987 to 2014. The authors presented that *S. epidermidis* (67.4%) was the most frequent pathogen, followed by *S. haemolyticus* (10.5%), and *S. capitis* (9.6%) (Ehlersson et al. 2017). The epidemiological study in France was partially consistent with previously mentioned research and showed that *E. coli* was the primary pathogen in 36% of BSI episodes, followed by *S. aureus* (16%), and CoNS (8%). The other investigation from France showed the median rate of CoNS in sepsis (12.2%), and all of these strains belonged to *S. capitis* species (Butin et al. 2017). However, studies in the United Kingdom, Greece, Netherlands, and Romania confirmed that CoNS were predominant pathogens in BSI episodes and sepsis (Cailes et al. 2018; Zlatian et al. 2018; Gkentzi et al. 2019; Zonnenberg et al. 2019).

Asia. A study designed in Japan by Takeshita et al. (2017) showed that the major pathogens isolated from BSIs were CoNS (736 cases, 23%), but *S. aureus* isolates were also among the most commonly isolated strains. These results were comparable to those observed in Europe (Takeshita et al. 2017). The authors also focused on 30-day mortality associated with the species and the

Table I
Worldwide distribution of staphylococcal bloodstream infections. The gray areas consist of the primary pathogen isolated in studies provided according to adequate reference.

No.	Continent	Country	No. of institutions	Years of isolation	Total number of BSI episodes	Staphylococcus	Staphylococcus (%)	S. aureus	S. aureus (%)	CoNS	CoNS (%)	Reference
1	Africa	Ghana	1	2010–2013	1,763	507	28.8	76	4.3	431	24.4	Labi et al. 2016
2	Africa	Egypt	1	2013–2015	65	26	40.1	6	9.3	20	30.8	Seliem and Sultan 2018
3	Africa	Ethiopia	1	2016–2017	88	38	43.0	16	18.0	22	25.0	Sorsa et al. 2019
4	Africa	Zambia	1	2013–2014	103	13	12.0	6	6.0	7	6.0	Kabwe et al. 2016
5	Asia	Japan	5	2012–2013	3,284	1,030	32.2	294	9.2	736	23.0	Takeshita et al. 2017
6	Asia	South Korea	55	2013–2014	717	349	48.7	81	11.3	268	37.4	Lee et al. 2015
7	Asia	Arab States	4	2013–2015	785	289	36.85	17	2.2	272	34.65	Hammond et al. 2017
8	Asia	China	1	2015–2016	133	64	60.3	8	7.5	56	52.8	Jiang et al. 2016
9	Asia	Nepal	1	2017	56	50	89.2	11	19.6	39	69.6	Thapa et al. 2019
10	Asia	India	1	2012–2014	183	87	47.4	42	22.9	45	24.5	Bandyopadhyay et al. 2018
11	Asia	Taiwan	1	2008–2013	2,090	485	23.2	57	2.7	428	20.5	Chen et al. 2016
12	Australia	Australia	23	2008–2012	9,418	3,160	36.4	1,429	18.0	1,731	18.4	Si et al. 2016
13	Australia	Australia	1	2005–2016	203	115	40.3	46	16.1	69	24.2	Worth et al. 2018
14	Australia	Australia	1	2005–2016	146	79	54.1	26	17.8	53	36.3	Gowda et al. 2017
15	Europe	Turkey	1	2003–2009; 2010–2016	925	542	58.6	46	5.0	496	53.6	Mutlu et al. 2019
16	Europe	Switzerland	20	2008–2014	1,823	535	30.0	300	17.0	235	13.0	Buetti et al. 2017
17	Europe	Switzerland	1	2014–2017	404	78	19.3	68	16.8	10	2.5	Papadimitriou-Olivgeris et al. 2019
18	Europe	Poland	nd	2012–2015	329	150	45.6	53	16.1	97	29.5	Deptula et al. 2018
19	Europe	Germany	1	1985–1995; 1997–2006	1,646	650	79.2	241	28.1	409	51.1	Hufnagel et al. 2008
20	Europe	Romania	1	2016–2017	170	81	47.65	63	37.06	18	10.59	Zlatian et al. 2018
21	Europe	Holland	1	2008–2014	93	84	90.4	70	75.3	14	15.1	Zonnenberg et al. 2019
22	Europe	France	1	2011–2012	201	28	12.2	0	0.0	28	12.2	Butin et al. 2017
23	Europe	United Kingdom	30	2005–2014	3,903	2,466	65.0	233	8.0	2,233	57.0	Cailles et al. 2017
24	Europe	Greece	16	2012–2015	459	140	30.4	2	0.4	138	30.0	Gkentzi et al. 2019
25	North America	USA	1	2002–2012	8,196	4,254	51.9	721	8.8	3,533	43.1	Larru et al. 2016
26	North America	USA	1	2006–2017	92	39	42.4	7	7.6	32	34.8	Wagstaff et al. 2019
27	North America	USA	10	2015–2018	5,066	1,500	29.0	1,115	22.0	355	7.0	Khare et al. 2019
28	North America	USA	1	2013–2017	97	29	29.9	17	17.5	12	12.4	Black et al. 2019
29	South America	Brazil	28	2016	47	17	36.2	6	12.8	11	23.4	Braga et al. 2018
30	South America	Latin America	32	2001–2013	3,066	1,625	53.0	267	8.7	1,358	44.3	Escalante et al. 2018

nd – no data

group of pathogens. They concluded that the highest mortality rates were exhibited by hospital-acquired BSI (HA-BSI) pathogens, followed by community-onset healthcare-associated BSI (CHA-BSI), and the most dangerous species were CoNS and *Klebsiella pneumoniae*. The study from South Korea showed that CoNS were the most frequent pathogens engaged in neonatal sepsis (Lee et al. 2015). Studies in India proved a high staphylococci frequency in BSI episodes, however, gram-negative rods were mostly isolated in majority from blood samples (Bandyopadhyay et al. 2018). On the other hand, CoNS became the major isolated pathogen in neonatal sepsis in China, Nepal, Taiwan, Turkey and the Arab States, which proves widespread staphylococcal-caused sepsis in Asia (Jiang et al. 2016; Chen et al. 2017; Hammoud et al. 2017; Thapa and Sapkota 2019; Mutlu et al. 2020). These findings strongly correlate with European data.

North America and South America. In the USA research performed by Larru et al. (2016) presented similar results as European or Asian studies. The most commonly isolated pathogens were CoNS and *S. aureus*, and these pathogens were associated with healthcare-acquired BSI. Moreover, the authors confirmed that all the CoNS were evidenced as pathogens and not as contaminants. Another study from the USA showed a significant majority of *S. aureus* strains involved in neonate sepsis (Khare et al. 2020). The predisposed patients' characteristics were also comparable to those observed in Europe. These studies showed that the most endangered group consists of children and infants, especially with prolonged hospitalization.

Interestingly, children hospitalized since birth exhibited a significantly low prevalence of hospital-onset *S. aureus* bacteremia (Burke et al. 2009). For comparison with the USA, Latin American countries were also analyzed for staphylococcal bloodstream infections. Arias et al. (2017) presented a paper summarizing the results for nine South American countries, from Mexico to Argentina. This study did not evaluate the number of coagulase-negative staphylococci but showed many MRSA strains found in BSI samples from these countries. Notably, the highest number of participants with MRSA-associated BSI was reported in Brazil. Other studies confirmed that the prevalence of intensive-care unit-acquired infections was higher in Brazilian hospitals than in European countries and in the USA (Braga et al. 2018). On the other hand, the highest rates of CoNS (44.3%) were present in NEOCOSUR studies on five Latin American countries: Argentina, Chile, Paraguay, Peru and Uruguay (Escalante et al. 2018).

Africa. The World Health Organization (WHO) reported that, to date, information regarding bloodstream infections in Africa is scarce due to the lack of

research (Bagheri Nejad et al. 2011). However, it was estimated that the incidence of bloodstream infections (up to 14.8%) in developing countries in Africa was up to twice as high as the average European prevalence (7.1%) (ECDC 2008). The studies cited were not correlated with each other with respect to the microbiological data; the major BSI-associated pathogens presented, such as *Pseudomonas aeruginosa*, *E. coli*, *K. pneumoniae*, *Enterobacter* spp., and *S. aureus*, varied among papers (Bagheri Nejad et al. 2011). Besides, the most recent investigations showed a significant increase in CoNS prevalence in BSI episodes in Africa. Labi et al. (2016) showed a high number of positive blood culture samples (21.9%) among neonates, and the significant pathogens were CoNS. Nanoukon et al. (2017) obtained similar results in Benin, where *S. haemolyticus* and *S. epidermidis* were identified as the most frequently isolated pathogens. Similar results were also obtained in Egypt and Malawi (Mashaly and El-Mahdy 2017; Musicha et al. 2017). CoNS were confirmed as a major pathogen isolated in further investigations on smaller groups of patients, mostly neonates in Egypt and Ethiopia (Seliem and Sultan 2018; Sorsa et al. 2019). In contrast, a study from Zambia reports that the most frequent pathogen isolated from neonates with sepsis was *Klebsiella* sp. (Kabwe et al. 2016).

Australia. The rate of healthcare-associated BSIs in Australia is lower than reported elsewhere in the world, which was confirmed by a study in Queensland on 23 public hospitals and by research conducted by the Victorian Healthcare Associated Infection Surveillance System (VICNISS) Coordinating Centre in Victoria (Si et al. 2016; Gowda et al. 2017; Worth et al. 2018). Papers showed that the most frequently reported pathogens responsible for BSI episodes were CoNS, from 18.4 to 24.2%, and *S. aureus*, from 15.2 to 16.1%.

The distribution of all of the aforementioned staphylococcal bloodstream infections is presented in Table I.

***S. aureus* is one of the most frequent bloodstream infection agents**

According to the ECDC report, *S. aureus* is one of the major agents causing bloodstream infections in Europe. Based on the studies conducted in 25 European countries, the ECDC estimated the dynamic changes in *S. aureus* clones associated with BSI episodes. The report states that the *S. aureus* BSI infection mortality rate was 19.4% of the episodes' total number. Moreover, as expected, the MRSA all-cause mortality (24.4%) was higher than that of MSSA infections (17.1%).

***Spa* types related to *S. aureus* from BSI in Europe.** ECDC also estimated 20 of the most frequent MRSA and MSSA *spa* types. The first group included the

5 most frequent *spa* types, namely, t032 (ST22, 17.9%), t003 (ST225, 8.8%), t008 (ST8, 8.4%), t002 (ST5, 7.7%), and t067 (ST125, 4.4%). Interestingly, the significant increase in incidence was related to the multilocus variable number of tandem repeats analysis type (MLVA type) ST22, and this lineage constituted 36% of the top-ranking isolates in 2011. This MRSA clone was first identified in England and was further detected in Ireland, Germany, Hungary, Portugal, and Northern Italy. The fifth most abundant *spa* type t067 was firstly described in Spain (Grundmann et al. 2014). In comparison, the rates of MSSA *spa*-type frequency were lower than those of MRSA isolates, and the 7 most popular types were t091 (ST7, 5.3%), t084 (ST15, 4.7%), t002 (ST5, 4.6%), t015 (ST45, 3.7%), t008 (ST8, 3.7%), t012 (ST30, 3.4%), and t0127 (ST1, 3.2%) (Grundmann et al. 2014). Two *spa* types (t008 and t002) were present in both MRSA and MSSA infections, which was probably a result of the high overall global frequency of these types, according to Ridom SpaServer (www.spaserver.ridom.de).

***Spa* types related to *S. aureus* from BSI in Poland.**

S. aureus, a key pathogen in BSI episodes, was also identified in a study conducted by our group (Ilczyszyn et al. 2016). This study, performed on neonates and children in Poland, showed the most frequent MRSA genotype to be *spa* type t003-CC5, which is consistent with the data presented by ECDC. Among MSSA strains, the most frequent genotypes belonged to the following *spa* types: t091-CC7, t037-CC30, t008-CC8, and t240-CC10. Additionally, some of the observed genotypes exhibited age-related patterns, and the *spa* type t003, *spa*-CC 002, and CC5 were strongly associated with invasive infections in infants and young children (Ilczyszyn et al. 2016).

***Spa* types related to *S. aureus* from BSI outside Europe.** A study in China, performed for five years, examined *S. aureus* BSI samples and identified the most frequent *S. aureus spa* types and virulence factors. According to these data, the most frequent MRSA *spa* type in China was t030/t037, belonging to MLVA type ST239. These isolates also harbored SCC*mec* III cassette, which represents the hospital-acquired strains, and an *agr* system I. In comparison, the most frequent Chinese MSSA isolates presented the t318 type ST188 and also harbored *agr* I (Liu et al. 2018).

Latin American research divided the most numerous MRSA strains into three clades (A, B, and C) based on phylogenetic reconstruction. Strains in clade A belonged to ST5, ST105, and ST1011, and a majority of these strains harbored the gene cassette SCC*mec* I or II (HA-MRSA). Clade B consisted of the MLS types ST8, ST88, ST97, and ST72, accompanied by SCC*mec* IV variants. The last clade included Argentinian strains belonging to ST30 (Arias et al. 2017).

Non-*S. aureus* staphylococci as bloodstream infection agents

Human skin is colonized by various staphylococcal species, although the most invasive is *S. aureus*, followed by *Staphylococcus auricularis*, *S. capitis*, *S. epidermidis*, *S. haemolyticus*, *Staphylococcus hominis*, *S. saprophyticus*, *Staphylococcus simulans* and *Staphylococcus warneri* (Yu et al. 2017). The CoNS are among the most commonly isolated microorganisms from blood samples. Compared to *S. aureus* strains, which are classified as invasive pathogens, the clinical significance of CoNS needs to be proven. It is essential to estimate whether the presence of CoNS represents true bacteremia or sample contamination. Many of the studies conducted have not estimated the real impact of CoNS associated with blood infections, mainly because these species are less frequent overall; have not identified these bacteria at the species level; or have not distinguished the species' differences. However, several studies have shown that CoNS can cause serious bloodstream infections (Grzebyk et al. 2013; Li et al. 2016; Szczuka et al. 2016). Therefore, host-specific capabilities and strain-specific features need to be reconsidered for an improved understanding of the course of every particular infection, as under favorable conditions, CoNS species may become highly pathogenic (Becker et al. 2014).

CoNS as BSI agents in Europe. A study performed in Belgium showed that most isolated bloodstream infection-associated CoNS strains belonged to *S. epidermidis*, and 77% of these strains were identified as methicillin-resistant *S. epidermidis* (MRSE). All of these strains presented resistance to a wide range of antibiotics, especially erythromycin (*ermA*, *ermC*, and *msrA*), aminoglycosides (*aacA-aphD* and *aadC*), tetracycline (*tetK*), and mupirocin (*mupA*). Molecular typing of these strains assigned 85% of the MRSE strains to clonal complex (CC) 2, consisting of the ST2, ST5, ST59, and ST88 MLVA types (Deplano et al. 2016). Another study on *S. warneri* strains from Poland showed their wide range of pathogenicity factors. These strains were able to adhere to host cells, produce biofilms, invade and destroy epithelial cells, which strongly facilitated bacterial persistence (Szczuka et al. 2016). This finding warrants reconsideration of the role of CoNS in bloodstream infections.

CoNS as BSI agents in the USA. In studies conducted in the USA, many CoNS isolates (n = 602) were found in blood samples from years 2013–2014. The most frequently isolated strains belonged to *S. epidermidis*, *S. lugdunensis*, *S. hominis*, and *S. capitis* (Sader et al. 2016). A high number of blood samples was also analyzed in Japan by Yamada et al. (2017), and 314 methicillin-resistant CoNS (MRCoNS) strains were found. Among the Japanese strains, the predominant strains

belonged to *S. epidermidis* (78.6%), *S. haemolyticus* (14.3%), and *S. capitis* subsp. *ureolyticus*. A high number of CoNS-associated BSI episodes and increasing resistance rate should also be confirmation of the danger based on the presence and spread of these bacteria.

Conclusions

Staphylococci are among the most frequent pathogens causing bloodstream infections, which can advance to sepsis and are often observed in patients with indwelling medical devices or neonates. A high number of *S. aureus* and CoNS-related BSI episodes in high-risk patients had evidenced a significant challenge for clinicians. Many institutions widely document BSI episodes, and there has not been a worldwide decrease in these episodes. It is vital to improve existing prevention and control programs based on analysis of the data to implement standard diagnostic methods and conduct research on etiological factors, including via the usage of advanced genetic methods.

ORCID

Klaudia Lisowska-Łysiak <https://orcid.org/0000-0001-8659-9947>

Ryszard Lauterbach <https://orcid.org/0000-0003-1431-6252>

Jacek Międzobrodzki <https://orcid.org/0000-0003-4252-880X>

Maja Kosecka-Strojek <https://orcid.org/0000-0001-8337-6975>

Authors' contributions

JM and MKS brought the idea of the project. KL-Ł and MKS performed the literature research and data analysis. KL-Ł, JM and MKS drafted the work. RL provided clinical consultation of the data. All authors critically revised the work.

Acknowledgments

This project was financed by funds No N19/MNS/000016 (to MKS) of the Faculty of Biochemistry, Biophysics and Biotechnology, Jagiellonian University.

Conflict of interest

The authors do not report any financial or personal connections with other persons or organizations, which might negatively affect the contents of this publication and/or claim authorship rights to this publication.

Literature

Argemi X, Hansmann Y, Prola K, Prévost G. Coagulase-negative staphylococci pathogenomics. *Int J Mol Sci*. 2019 Mar 11;20(5):1215. <https://doi.org/10.3390/ijms20051215>

Argemi X, Hansmann Y, Riegel P, Prévost G. Is *Staphylococcus lugdunensis* significant in clinical samples? *J Clin Microbiol*. 2017 Nov;55(11):3167–3174. <https://doi.org/10.1128/JCM.00846-17>

Arias CA, Reyes J, Carvajal LP, Rincon S, Diaz L, Panesso D, Ibarra G, Rios R, Munita JM, Salles MJ, et al. A prospective cohort multicenter study of molecular epidemiology and phylogenomics of *Staphylococcus aureus* bacteremia in nine Latin American countries. *Antimicrob Agents Chemother*. 2017 Oct;61(10):e00816–17. <https://doi.org/10.1128/AAC.00816-17>

Arya R, Princy SA. An insight into pleiotropic regulators Agr and Sar: molecular probes paving the new way for antivirulent therapy. *Future Microbiol*. 2013 Oct;8(10):1339–1353. <https://doi.org/10.2217/fmb.13.92>

Ayau P, Bardossy AC, Sanchez G, Ortiz R, Moreno D, Hartman P, Rizvi K, Prentiss TC, Perri MB, Mahan M, et al. Risk Factors for 30-day mortality in patients with methicillin-resistant *Staphylococcus aureus* bloodstream infections. *Int J Infect Dis*. 2017 Aug;61:3–6. <https://doi.org/10.1016/j.ijid.2017.05.010>

Bandyopadhyay T, Kumar A, Saili A, Randhawa VS. Distribution, antimicrobial resistance and predictors of mortality in neonatal sepsis. *J Neonatal Perinatal Med*. 2018 Jul 05;11(2):145–153. <https://doi.org/10.3233/NPM-1765>

Becker K, Heilmann C, Peters G. Coagulase-negative staphylococci. *Clin Microbiol Rev*. 2014 Oct;27(4):870–926. <https://doi.org/10.1128/CMR.00109-13>

Bello-Chavolla OY, Bahena-Lopez JP, Garciadiego-Fosass P, Volkow P, Garcia-Horton A, Velazquez-Acosta C, Vilar-Compte D. Bloodstream infection caused by *S. aureus* in patients with cancer: a 10-year longitudinal single-center study. *Support Care Cancer*. 2018 Dec;26(12):4057–4065. <https://doi.org/10.1007/s00520-018-4275-1>

Bhattacharya M, Berends ETM, Chan R, Schwab E, Roy S, Sen CK, Torres VJ, Wozniak DJ. *Staphylococcus aureus* biofilms release leukocidins to elicit extracellular trap formation and evade neutrophil-mediated killing. *Proc Natl Acad Sci USA*. 2018 Jul 10;115(28):7416–7421. <https://doi.org/10.1073/pnas.1721949115>

Black CG, Tavares L, Stachel A, Ratner AJ, Randis TM. Distribution of late-onset neonatal sepsis pathogens differs in inpatient and outpatient settings. *Am J Perinatol*. 2019 Sep;36(11):1136–1141. <https://doi.org/10.1055/s-0038-1675643>

Braga IA, Campos PA, Gontijo-Filho PP, Ribas RM. Multi-hospital point prevalence study of healthcare-associated infections in 28 adult intensive care units in Brazil. *J Hosp Infect*. 2018 Jul;99(3):318–324. <https://doi.org/10.1016/j.jhin.2018.03.003>

Buetti N, Atkinson A, Kottanattu L, Bielicki J, Marschall J, Kronenberg A; Swiss Centre for Antibiotic resistance (ANRESIS). Patterns and trends of pediatric bloodstream infections: a 7-year surveillance study. *Eur J Clin Microbiol Infect Dis*. 2017 Mar;36(3):537–544. <https://doi.org/10.1007/s10096-016-2830-6>

Burke RE, Halpern MS, Baron EJ, Gutierrez K. Pediatric and neonatal *Staphylococcus aureus* bacteremia: epidemiology, risk factors, and outcome. *Infect Control Hosp Epidemiol*. 2009 Jul;30(7):636–644. <https://doi.org/10.1086/597521>

Butin M, Rasigade JP, Subtil F, Martins-Simões P, Pralong C, Freydière AM, Vandenesch F, Tigaud S, Picaud JC, Laurent F. Vancomycin treatment is a risk factor for vancomycin-nonsusceptible *Staphylococcus capitis* sepsis in preterm neonates. *Clin Microbiol Infect*. 2017 Nov;23(11):839–844. <https://doi.org/10.1016/j.cmi.2017.03.022>

Cailles B, Kortsalioudaki C, Buttery J, Pattanayak S, Greenough A, Matthes J, Bedford Russell A, Kennea N, Heath PT; neonIN network. Epidemiology of UK neonatal infections: the neonIN infection surveillance network. *Arch Dis Child Fetal Neonatal Ed*. 2018 Nov;103(6):F547–F553. <https://doi.org/10.1136/archdischild-2017-313203>

Chen CY, Tien FM, Sheng WH, Huang SY, Yao M, Tang JL, Tsay W, Tien HF, Hsueh PR. Clinical and microbiological characteristics of bloodstream infections among patients with hematological malignancies with and without neutropenia at a medical centre in northern Taiwan, 2008–2013. *Int J Antimicrob Agents*. 2017 Mar;49(3):272–281. <https://doi.org/10.1016/j.ijantimicag.2016.11.009>

Dayan GH, Mohamed N, Scully IL, Cooper D, Begier E, Eiden J, Jansen KU, Gurtman A, Anderson AS. *Staphylococcus aureus*: the

- current state of disease, pathophysiology and strategies for prevention. *Expert Rev Vaccines*. 2016 Nov;15(11):1373–1392. <https://doi.org/10.1080/14760584.2016.1179583>
- Deplano A, Vandendriessche S, Nonhoff C, Dodémont M, Roisinienis O. National surveillance of *Staphylococcus epidermidis* recovered from bloodstream infections in Belgian hospitals. *J Antimicrob Chemother*. 2016 Jul;71(7):1815–1819. <https://doi.org/10.1093/jac/dkw086>
- Deptuła A, Trejnowska E, Dubiel G, Wanke-Rytt M, Deptuła M, Hryniewicz W. Healthcare associated bloodstream infections in Polish hospitals: prevalence, epidemiology and microbiology – summary data from the ECDC Point Prevalence Survey of Healthcare Associated Infections 2012–2015. *Eur J Clin Microbiol Infect Dis*. 2018 Mar;37(3):565–570. <https://doi.org/10.1007/s10096-017-3150-1>
- Dik JWH, Poelman R, Friedrich AW, Panday PN, Lo-Ten-Foe JR, Assen S, van Gemert-Pijnen JEWC, Niesters HGM, Hendrix R, Sinha B. An integrated stewardship model: antimicrobial, infection prevention and diagnostic (AID). *Future Microbiol*. 2016 Jan;11(1):93–102. <https://doi.org/10.2217/fmb.15.99>
- ECDC. Annual epidemiological report on communicable diseases in Europe 2008. Stockholm (Sweden): European Centre for Disease Prevention and Control; 2008.
- ECDC. Healthcare-associated infections acquired in intensive care units. In: ECDC. Annual epidemiological report for 2016. Stockholm (Sweden): European Centre for Disease Prevention and Control; 2018.
- Ehlersson G, Hellmark B, Svartström O, Stenmark B, Söderquist B. Phenotypic characterisation of coagulase-negative staphylococci isolated from blood cultures in newborn infants, with a special focus on *Staphylococcus capitis*. *Acta Paediatr*. 2017 Oct;106(10):1576–1582. <https://doi.org/10.1111/apa.13950>
- Escalante MJ, Ceriani-Cernadas JM, D'Apremont I, Bancalari A, Webb V, Genes L, Villarreal L, Munoz E, Tapia JL; NEOCOSUR Neonatal Network. Late onset sepsis in very low birth weight infants in the South American NEOCOSUR Network. *Pediatr Infect Dis J*. 2018 Oct;37(10):1022–1027. <https://doi.org/10.1097/INF.0000000000001958>
- Foster AP. Staphylococcal skin disease in livestock. *Vet Dermatol*. 2012 Aug;23(4):e342–e343, e344. <https://doi.org/10.1111/j.1365-3164.2012.01093.x>
- Gasch O, Camoez M, Dominguez MA, Padilla B, Pintado V, Almirante B, Molina J, Lopez-Medrano F, Ruiz E, Martinez JA, et al.; REIPI/GEIH Study Groups. Predictive factors for mortality in patients with methicillin-resistant *Staphylococcus aureus* bloodstream infection: impact on outcome of host, microorganism and therapy. *Clin Microbiol Infect*. 2013 Nov;19(11):1049–1057. <https://doi.org/10.1111/1469-0691.12108>
- Gkentzi D, Kortsalioudaki C, Cailles BC, Zaoutis T, Kopsidas J, Tsolia M, Spyridis N, Siahaniidou S, Sarafidis K, Heath PT, et al.; Neonatal Infection Surveillance Network in Greece. Epidemiology of infections and antimicrobial use in Greek Neonatal Units. *Arch Dis Child Fetal Neonatal Ed*. 2019 May;104(3):F293–F297. <https://doi.org/10.1136/archdischild-2018-315024>
- Gowda H, Norton R, White A, Kandasamy Y. Late-onset neonatal sepsis – A 10-year review from North Queensland, Australia. *Pediatr Infect Dis J*. 2017 Sep;36(9):883–888. <https://doi.org/10.1097/INF.0000000000001568>
- Grundmann H, Schouls LM, Aanensen DM, Pluister GN, Tami A, Chlebowicz M, Glasner C, Sabat AJ, Weist K, Heuer O, et al.; ESCMID Study Group on Molecular Epidemiological Markers; European Staphylococcal Reference Laboratory Working Group. The dynamic changes of dominant clones of *Staphylococcus aureus* causing bloodstream infections in the European region: results of a second structured survey. *Euro Surveill*. 2014 Dec 11;19(49):20987. <https://doi.org/10.2807/1560-7917.ES2014.19.49.20987>
- Grzebyk M, Brzychczy-Włoch M, Piotrowska A, Krzyściak P, Heczko PB, Bulanda M. [Phenotypic evaluation of hydrophobicity and the ability to produce biofilm in coagulase-negative staphylococci isolated from infected very-low-birthweight newborns] (in Polish). *Med Dosw Mikrobiol*. 2013;65(3):149–159.
- Hammoud MS, Al-Taiar A, Al-Abdi SY, Bozaid H, Khan A, AlMuhairi LM, Rehman MU. Late-onset neonatal sepsis in Arab states in the Gulf region: two-year prospective study. *Int J Infect Dis*. 2017 Feb;55:125–130. <https://doi.org/10.1016/j.ijid.2017.01.006>
- Heilmann C, Ziebuhr W, Becker K. Are coagulase-negative staphylococci virulent? *Clin Microbiol Infect*. 2019 Sep;25(9):1071–1080. <https://doi.org/10.1016/j.cmi.2018.11.012>
- Herrera A, Vu BG, Stach CS, Merriman JA, Horswill AR, Salgado-Pabón W, Schlievert PM. *Staphylococcus aureus* β -toxin mutants are defective in biofilm ligase and sphingomyelinase activity, and causation of infective endocarditis and sepsis. *Biochemistry*. 2016 May 03;55(17):2510–2517. <https://doi.org/10.1021/acs.biochem.6b00083>
- Hosseinkhani F, Tammes Buirs M, Jabalameli F, Emaneini M, van Leeuwen WB. High diversity in SCCmec elements among multidrug-resistant *Staphylococcus haemolyticus* strains originating from paediatric patients; characterization of a new composite island. *J Med Microbiol*. 2018 Jul 01;67(7):915–921. <https://doi.org/10.1099/jmm.0.000776>
- Hotchkiss RS, Moldawer LL, Opal SM, Reinhart K, Turnbull IR, Vincent JL. Sepsis and septic shock. *Nat Rev Dis Primers*. 2016 Dec 22;2(1):16045. <https://doi.org/10.1038/nrdp.2016.45>
- Hufnagel M, Burger A, Bartelt S, Henneke P, Berner R. Secular trends in pediatric bloodstream infections over a 20-year period at a tertiary care hospital in Germany. *Eur J Pediatr*. 2008 Oct;167(10):1149–1159. <https://doi.org/10.1007/s00431-007-0651-4>
- Ilczyszyn WM, Sabat AJ, Akkerboom V, Szkarlat A, Klepacka J, Sowa-Sierant I, Wasik B, Kosecka-Strojek M, Buda A, Miedzobrodzki J, et al. Clonal structure and characterization of *Staphylococcus aureus* strains from invasive infections in paediatric patients from South Poland: association between age, spa types, clonal complexes, and genetic markers. *PLoS One*. 2016 Mar 18;11(3):e0151937. <https://doi.org/10.1371/journal.pone.0151937>
- Ittleman BR, Szabo JS. *Staphylococcus lugdunensis* sepsis and endocarditis in a newborn following lotus birth. *Cardiol Young*. 2018 Nov; 28(11):1367–1369. <https://doi.org/10.1017/S1047951118001300>
- Jiang Y, Kuang L, Wang H, Li L, Zhou W, Li M. The clinical characteristics of neonatal sepsis infection in Southwest China. *Intern Med*. 2016;55(6):597–603. <https://doi.org/10.2169/internalmedicine.55.3930>
- Kabwe M, Tembo J, Chilukutu L, Chilufya M, Ngulube F, Lukwesa C, Kapasa M, Enne V, Wexner H, Mwananyanda L, et al. Etiology, antibiotic resistance and risk factors for neonatal sepsis in a large referral center in Zambia. *Pediatr Infect Dis J*. 2016 Jul; 35(7):e191–e198. <https://doi.org/10.1097/INF.0000000000001154>
- Kalińska M, Kantyka T, Greenbaum DC, Larsen KS, Władyska B, Jabaiah A, Bogyo M, Daugherty PS, Wysocka M, Jaros M, et al. Substrate specificity of *Staphylococcus aureus* cysteine proteases – Staphopains A, B and C. *Biochimie*. 2012 Feb;94(2):318–327. <https://doi.org/10.1016/j.biochi.2011.07.020>
- Khare R, Kothari T, Castagnaro J, Hemmings B, Tso M, Juretschko S. Active monitoring and feedback to improve blood culture fill volumes and positivity across a large integrated health system. *Clin Infect Dis*. 2020 Jan 2;70(2):262–268. <https://doi.org/10.1093/cid/ciz198>
- Kosecka-Strojek M, Buda A, Miedzobrodzki J. Staphylococcal ecology and epidemiology. In: Savini V, editor. Pet-to-man travelling staphylococci. A world in progress. Cambridge (USA): Academic Press; 2018. p. 11–24. <https://doi.org/10.1016/B978-0-12-813547-1.00002-9>

- Kosecka-Strojek M, Ilczyszyn WM, Buda A, Polakowska K, Murzyn K, Panz T, Bialecka A, Kasprowicz A, Jakubczak A, Krol J, et al. Multiple-locus variable-number tandem repeat fingerprinting as a method for rapid and cost-effective typing of animal-associated *Staphylococcus aureus* strains from lineages other than sequence type 398. *J Med Microbiol*. 2016 Dec 16;65(12):1494–1504. <https://doi.org/10.1099/jmm.0.000378>
- Kosecka-Strojek M, Sabat AJ, Akkerboom V, Becker K, van Zanten E, Wisselink G, Miedzobrodzki J, Kooistra-Smid AMDM, Friedrich AW. Development and validation of a reference data set for assigning *Staphylococcus* species based on next-generation sequencing of the 16S-23S rRNA region. *Front Cell Infect Microbiol*. 2019 Aug 7;9:278. <https://doi.org/10.3389/fcimb.2019.00278>
- Kosecka-Strojek M, Sadowy E, Gawryszewska I, Klepacka J, Tomasik T, Michalik M, Hryniewicz W, Miedzobrodzki J. Emergence of linezolid-resistant *Staphylococcus epidermidis* in the tertiary children's hospital in Cracow, Poland. *Eur J Clin Microbiol Infect Dis*. 2020 Sep;39(9):1717–1725. <https://doi.org/10.1007/s10096-020-03893-w>
- Labi AK, Obeng-Nkrumah N, Bjerrum S, Enweronu-Laryea C, Newman MJ. Neonatal bloodstream infections in a Ghanaian Tertiary Hospital: are the current antibiotic recommendations adequate? *BMC Infect Dis*. 2016 Dec;16(1):598. <https://doi.org/10.1186/s12879-016-1913-4>
- Larru B, Gong W, Vendetti N, Sullivan KV, Localio R, Zaoutis TE, Gerber JS. Bloodstream infections in hospitalized children: epidemiology and antimicrobial susceptibilities. *Pediatr Infect Dis J*. 2016 May;35(5):507–510. <https://doi.org/10.1097/INF.0000000000001057>
- Lauterbach R, Wilk B, Bocheńska A, Hurkała J, Radziszewska R. Nonactivated protein c in the treatment of neonatal sepsis: a retrospective analysis of outcome. *Pediatr Infect Dis J*. 2016 Sep;35(9):967–971. <https://doi.org/10.1097/INF.0000000000001247>
- Lee SM, Chang M, Kim KS. Blood culture proven early onset sepsis and late onset sepsis in very-low-birth-weight infants in Korea. *J Korean Med Sci*. 2015 Oct;30(Suppl 1):S67–74. <https://doi.org/10.3346/jkms.2015.30.S1.S67>
- Li S, Guo Y, Zhao C, Chen H, Hu B, Chu Y, Zhang Z, Hu Y, Liu Z, Du Y, et al. *In vitro* activities of tedizolid compared with other antibiotics against Gram-positive pathogens associated with hospital-acquired pneumonia, skin and soft tissue infection and bloodstream infection collected from 26 hospitals in China. *J Med Microbiol*. 2016 Oct 18;65(10):1215–1224. <https://doi.org/10.1099/jmm.0.000347>
- Lisowska-Łysiak K, Kosecka-Strojek M, Bialecka J, Kasprowicz A, Garbacz K, Piechowicz L, Kmet V, Savini V, Miedzobrodzki J. New insight into genotypic and phenotypic relatedness of *Staphylococcus aureus* strains from human infections or animal reservoirs. *Pol J Microbiol*. 2019;68(1):93–104. <https://doi.org/10.21307/pjm-2019-011>
- Liu Y, Du F, Liu P, Mei Y, Wan L, Wei D, Xu H, Zhang W. Molecular epidemiology and virulence features of *Staphylococcus aureus* bloodstream isolates in a regional burn center in China, 2012–2016. *Microb Drug Resist*. 2018 Nov;24(9):1354–1360. <https://doi.org/10.1089/mdr.2017.0209>
- Martínez-García S, Rodríguez-Martínez S, Cancino-Díaz ME, Cancino-Díaz JC. Extracellular proteases of *Staphylococcus epidermidis*: roles as virulence factors and their participation in biofilm. *APMIS*. 2018 Mar;126(3):177–185. <https://doi.org/10.1111/apm.12805>
- Mashaly GES, El-Mahdy RH. Vancomycin heteroresistance in coagulase negative *Staphylococcus* blood stream infections from patients of intensive care units in Mansoura University Hospitals, Egypt. *Ann Clin Microbiol Antimicrob*. 2017 Dec;16(1):63. <https://doi.org/10.1186/s12941-017-0238-5>
- Michalik S, Sundaramoorthy N, Murr A, Depke M, Völker U, Bröker BM, Aamot HV, Schmidt F. Early-stage *Staphylococcus aureus* bloodstream infection causes changes in the concentrations of lipoproteins and acute-phase proteins and is associated with low antibody titers against bacterial virulence factors. *mSystems*. 2020 Jan 21;5(1):e00632–19. <https://doi.org/10.1128/mSystems.00632-19>
- Miedzobrodzki J, Kaszycki P, Bialecka A, Kasprowicz A. Proteolytic activity of *Staphylococcus aureus* strains isolated from the colonized skin of patients with acute-phase atopic dermatitis. *Eur J Clin Microbiol Infect Dis*. 2002 Apr;21(4):269–276. <https://doi.org/10.1007/s10096-002-0706-4>
- Minejima E, Delayo V, Lou M, Ny P, Nieberg P, She RC, Wong-Beringer A. Utility of qSOFA score in identifying patients at risk for poor outcome in *Staphylococcus aureus* bacteremia. *BMC Infect Dis*. 2019 Dec;19(1):149. <https://doi.org/10.1186/s12879-019-3770-4>
- Musicha P, Cornick JE, Bar-Zeev N, French N, Masesa C, Denis B, Kennedy N, Mallewa J, Gordon MA, Msefula CL, et al. Trends in antimicrobial resistance in bloodstream infection isolates at a large urban hospital in Malawi (1998–2016): a surveillance study. *Lancet Infect Dis*. 2017 Oct;17(10):1042–1052. [https://doi.org/10.1016/S1473-3099\(17\)30394-8](https://doi.org/10.1016/S1473-3099(17)30394-8)
- Mutlu M, Aslan Y, Aktürk Acar F, Kader Ş, Bayramoğlu G, Yılmaz G. Changing trend of microbiologic profile and antibiotic susceptibility of the microorganisms isolated in the neonatal nosocomial sepsis: a 14 years analysis. *J Matern Fetal Neonatal Med*. 2020 Nov; 33(21):3658–3665. <https://doi.org/10.1080/14767058.2019.1582633>
- Nanoukon C, Affolabi D, Keller D, Tollo R, Riegel P, Baba-Moussa L, Prévost G. Characterization of human type C enterotoxin produced by clinical *S. epidermidis* isolates. *Toxins (Basel)*. 2018 Mar 27;10(4):139. <https://doi.org/10.3390/toxins10040139>
- Nanoukon C, Argemi X, Sogbo F, Orekan J, Keller D, Affolabi D, Schramm F, Riegel P, Baba-Moussa L, Prévost G. Pathogenic features of clinically significant coagulase-negative staphylococci in hospital and community infections in Benin. *Int J Med Microbiol*. 2017 Jan;307(1):75–82. <https://doi.org/10.1016/j.ijmm.2016.11.001>
- Natoli S, Fontana C, Favaro M, Bergamini A, Testore GP, Minelli S, Bossa MC, Casapulla M, Broglio G, Beltrame A, et al. Characterization of coagulase-negative staphylococcal isolates from blood with reduced susceptibility to glycopeptides and therapeutic options. *BMC Infect Dis*. 2009 Dec;9(1):83. <https://doi.org/10.1186/1471-2334-9-83>
- Nejad SB, Allegranzi B, Syed S, Ellis B, Pittet D. Health-care-associated infection in Africa: a systematic review. *Bull World Health Organ*. 2011 Oct 1;89(10):757–765. <https://doi.org/10.2471/BLT.11.088179>
- Oliveira D, Borges A, Simões M. *Staphylococcus aureus* toxins and their molecular activity in infectious diseases. *Toxins (Basel)*. 2018 Jun 19;10(6):252. <https://doi.org/10.3390/toxins10060252>
- Pai S, Enoch DA, Aliyu SH. Bacteremia in children: epidemiology, clinical diagnosis and antibiotic treatment. *Expert Rev Anti Infect Ther*. 2015 Sep 02;13(9):1073–1088. <https://doi.org/10.1586/14787210.2015.1063418>
- Papadimitriou-Olivgeris M, Psychogiou R, Garessus J, Camaret AD, Fourre N, Kanagaratnam S, Jecker V, Nusbaumer C, Monnerat LB, Kocher A, et al. Predictors of mortality of bloodstream infections among internal medicine patients in a Swiss hospital: role of quick Sequential Organ Failure Assessment. *Eur J Intern Med*. 2019 Jul;65:86–92. <https://doi.org/10.1016/j.ejim.2019.05.003>
- Sabat AJ, van Zanten E, Akkerboom V, Wisselink G, van Slochteren K, de Boer RF, Hendrix R, Friedrich AW, Rossen JWA, Kooistra-Smid AMD. Targeted next-generation sequencing of the 16S–23S rRNA region for culture-independent bacterial identification – increased discrimination of closely related species. *Sci Rep*. 2017 Dec;7(1):3434. <https://doi.org/10.1038/s41598-017-03458-6>

- Sabat AJ, Wladyka B, Kosowska-Shick K, Grundmann H, van Dijk J, Kowal J, Appelbaum PC, Dubin A, Hryniewicz W. Polymorphism, genetic exchange and intragenic recombination of the aureolysin gene among *Staphylococcus aureus* strains. *BMC Microbiol.* 2008;8(1):129. <https://doi.org/10.1186/1471-2180-8-129>
- Sader HS, Farrell DJ, Flamm RK, Streit JM, Mendes RE, Jones RN. Antimicrobial activity of ceftaroline and comparator agents when tested against numerous species of coagulase-negative *Staphylococcus* causing infection in US hospitals. *Diagn Microbiol Infect Dis.* 2016 May;85(1):80–84. <https://doi.org/10.1016/j.diagmicrobio.2016.01.010>
- Samet A, Bronk M, Sledzińska A, Labon M, Rybak B. [Nosocomial bacteremia] (in Polish). *Przegl Epidemiol.* 2006;60(1):35–41.
- Seliem WA, Sultan AM. Etiology of early onset neonatal sepsis in neonatal intensive care unit – Mansoura, Egypt. *J Neonatal Perinatal Med.* 2018 Sep 28;11(3):323–330. <https://doi.org/10.3233/NPM-17128>
- Si D, Runnegar N, Marquess J, Rajmohan M, Playford EG. Characterising health care-associated bloodstream infections in public hospitals in Queensland, 2008–2012. *Med J Aust.* 2016 Apr; 204(7):276. <https://doi.org/10.5694/mja15.00957>
- Singer M, Deutschman CS, Seymour CW, Shankar-Hari M, Annane D, Bauer M, Bellomo R, Bernard GR, Chiche JD, Coopersmith CM, et al. The third international consensus definitions for sepsis and septic shock (Sepsis-3). *JAMA.* 2016 Feb 23; 315(8):801–810. <https://doi.org/10.1001/jama.2016.0287>
- Sorsa A, Früh J, Stötter L, Abdissa S. Blood culture result profile and antimicrobial resistance pattern: a report from neonatal intensive care unit (NICU), Asella teaching and referral hospital, Asella, south East Ethiopia. *Antimicrob Resist Infect Control.* 2019 Dec;8(1):42. <https://doi.org/10.1186/s13756-019-0486-6>
- Stevenson M, Pandor A, Martyn-St James M, Rafia R, Uttley L, Stevens J, Sanderson J, Wong R, Perkins GD, McMullan R, et al. Sepsis: the LightCycler SeptiFast Test MGRADE®, SepsiT[™] and IRIDICA BAC BSI assay for rapidly identifying bloodstream bacteria and fungi – a systematic review and economic evaluation. *Health Technol Assess.* 2016 Jun;20(46):1–246. <https://doi.org/10.3310/hta20460>
- Szczuka E, Krzysińska S, Kaznowski A. Clonality, virulence and the occurrence of genes encoding antibiotic resistance among *Staphylococcus warneri* isolates from bloodstream infections. *J Med Microbiol.* 2016 Aug 01;65(8):828–836. <https://doi.org/10.1099/jmm.0.000287>
- Takehita N, Kawamura I, Kurai H, Araoka H, Yoneyama A, Fujita T, Ainoda Y, Hase R, Hosokawa N, Shimanuki H, et al. Unique characteristics of community-onset healthcare-associated bloodstream infections: a multi-centre prospective surveillance study of bloodstream infections in Japan. *J Hosp Infect.* 2017 May; 96(1):29–34. <https://doi.org/10.1016/j.jhin.2017.02.022>
- Tevell S, Hellmark B, Nilsson-Augustinsson Å, Söderquist B. *Staphylococcus capitis* isolated from prosthetic joint infections. *Eur J Clin Microbiol Infect Dis.* 2017 Jan;36(1):115–122. <https://doi.org/10.1007/s10096-016-2777-7>
- Thapa S, Sapkota LB. Changing trend of neonatal septicemia and antibiotic susceptibility pattern of isolates in Nepal. *Int J Pediatr.* 2019 Feb 06;2019:1–7. <https://doi.org/10.1155/2019/3784529>
- Thomer L, Schneewind O, Missiakas D. Pathogenesis of *Staphylococcus aureus* bloodstream infections. *Annual Review of Pathology: Mechanisms of Disease.* 2016 May 23;11(1):343–364. <https://doi.org/10.1146/annurev-pathol-012615-044351>
- Tong SYC, Davis JS, Eichenberger E, Holland TL, Fowler VG Jr. *Staphylococcus aureus* infections: epidemiology, pathophysiology, clinical manifestations, and management. *Clin Microbiol Rev.* 2015 Jul;28(3):603–661. <https://doi.org/10.1128/CMR.00134-14>
- Veach LA, Pfaller MA, Barrett M, Koontz FP, Wenzel RP. Vancomycin resistance in *Staphylococcus haemolyticus* causing colonization and bloodstream infection. *J Clin Microbiol.* 1990;28(9):2064–2068. <https://doi.org/10.1128/JCM.28.9.2064-2068.1990>
- von Eiff C, Peters G, Heilmann C. Pathogenesis of infections due to coagulase-negative staphylococci. *Lancet Infect Dis.* 2002 Nov;2(11): 677–685. [https://doi.org/10.1016/S1473-3099\(02\)00438-3](https://doi.org/10.1016/S1473-3099(02)00438-3)
- Wagstaff JS, Durrant RJ, Newman MG, Eason R, Ward RM, Sherwin CMT, Enioutina EY. Antibiotic treatment of suspected and confirmed neonatal sepsis within 28 days of birth: A retrospective analysis. *Front Pharmacol.* 2019 Oct 15;10:1191. <https://doi.org/10.3389/fphar.2019.01191>
- Wójkowska-Mach J, Chmielarczyk A, Strus M, Lauterbach R, Heczko P. Neonate bloodstream infections in organization for economic cooperation and development countries: an update on epidemiology and prevention. *J Clin Med.* 2019 Oct 21;8(10):1750. <https://doi.org/10.3390/jcm8101750>
- Wójkowska-Mach J, Gulczyńska E, Nowiczewski M, Borszewska-Kornacka M, Domańska J, Merritt TA, Helwich E, Kordek A, Pawlik D, Gadzinowski J, et al. Late-onset bloodstream infections of very-low-birth-weight infants: data from the Polish Neonatology Surveillance Network in 2009–2011. *BMC Infect Dis.* 2014 Dec; 14(1):339. <https://doi.org/10.1186/1471-2334-14-339>
- Worth LJ, Daley AJ, Spelman T, Bull AL, Brett JA, Richards MJ. Central and peripheral line-associated bloodstream infections in Australian neonatal and paediatric intensive care units: findings from a comprehensive Victorian surveillance network, 2008–2016. *J Hosp Infect.* 2018 May;99(1):55–61. <https://doi.org/10.1016/j.jhin.2017.11.021>
- Yamada K, Namikawa H, Fujimoto H, Nakaie K, Takizawa E, Okada Y, Fujita A, Kawaguchi H, Nakamura Y, Abe J, et al. Clinical characteristics of methicillin-resistant coagulase-negative staphylococcal bacteremia in a tertiary hospital. *Intern Med.* 2017;56(7):781–785. <https://doi.org/10.2169/internalmedicine.56.7715>
- Yu W, Kim HK, Rauch S, Schneewind O, Missiakas D. Pathogenic conversion of coagulase-negative staphylococci. *Microbes Infect.* 2017 Feb;19(2):101–109. <https://doi.org/10.1016/j.micinf.2016.12.002>
- Zingg W, Hopkins S, Gayet-Ageron A, Holmes A, Sharland M, Suetens C, Almeida M, Asembergiene J, Borg MA, Budimir A, et al.; ECDC PPS study group. Health-care-associated infections in neonates, children, and adolescents: an analysis of paediatric data from the European Centre for Disease Prevention and Control point-prevalence survey. *Lancet Infect Dis.* 2017 Apr;17(4):381–389. [https://doi.org/10.1016/S1473-3099\(16\)30517-5](https://doi.org/10.1016/S1473-3099(16)30517-5)
- Zlatian O, Balasoiu A, Balasoiu M, Cristea O, Docea A, Mitrut R, Spandidos D, Tsatsakis A, Bancescu G, Calina D. Antimicrobial resistance in bacterial pathogens among hospitalised patients with severe invasive infections. *Exp Ther Med.* 2018 Sep 14;16(6):4499–4510. <https://doi.org/10.3892/etm.2018.6737>
- Zonnenberg IA, van Dijk-Lokkert EM, van den Dungen FAM, Vermeulen RJ, van Weissenbruch MM. Neurodevelopmental outcome at 2 years of age in preterm infants with late-onset sepsis. *Eur J Pediatr.* 2019 May;178(5):673–680. <https://doi.org/10.1007/s00431-019-03339-2>

Microbiota: A Missing Link in The Pathogenesis of Chronic Lung Inflammatory Diseases

AGNIESZKA MAGRYŚ*

Chair and Department of Medical Microbiology, Medical University of Lublin, Lublin, Poland

Submitted 7 December 2020, revised 8 February 2021, accepted 18 February 2021

Abstract

Chronic respiratory diseases account for high morbidity and mortality, with asthma, chronic obstructive pulmonary disease (COPD), and cystic fibrosis (CF) being the most prevalent globally. Even though the diseases increase in prevalence, the exact underlying mechanisms have still not been fully understood. Despite their differences in nature, pathophysiologies, and clinical phenotypes, a growing body of evidence indicates that the presence of lung microbiota can shape the pathogenic processes underlying chronic inflammation, typically observed in the course of the diseases. Therefore, the characterization of the lung microbiota may shed new light on the pathogenesis of these diseases. Specifically, in chronic respiratory tract diseases, the human microbiota may contribute to the disease's development and severity. The present review explores the role of the microbiota in the area of chronic pulmonary diseases, especially COPD, asthma, and CF.

Key words: microbiota, asthma, COPD, cystic fibrosis, lungs

Introduction

The Human Microbiome Project launched in 2007 approximated the human microbiome's complexity and led to significant growth in understanding its role in health and disease (Moffatt and Cookson 2017). In 2020, an international panel of experts proposed an updated definition of the microbiota, describing it as the assemblage of living microorganisms belonging to different kingdoms (Prokaryotes [Bacteria, or Archea], Eucaryotes [e.g., Protozoa, Fungi, and Algae]) (Berg et al. 2020). The human microbiome represents not only the entire community of commensal, symbiotic, and pathogenic microorganisms but also their “theatre of activity”, involving the whole spectrum of molecules produced by the microorganisms (their structural elements and metabolites), and molecules produced by coexisting hosts embedded in the environmental habitat (Berg et al. 2020). This complex ecosystem plays a fundamental role in controlling most aspects of physiology. Inhabiting various anatomical body sites, such as skin, mucosa, the gastrointestinal tract, and the respiratory tract, the microbiota is crucial in regulating the homeostasis and metabolism of hematopoiesis, inflamma-

tion, and immunity of its host (Moffatt and Cookson 2017). The microbiome's size and composition evolve in response to environmental and host factors, and in any imbalance, a negative impact can be seen upon human health (Ogunrinola et al. 2020). Shifts in the microbiota composition may lead to dysbiosis by decreasing the number of symbionts and increasing potential dangerous pathogens. Microbial dysbiosis has been found to be involved in a growing list of human diseases, including chronic respiratory diseases (Paudel et al. 2020).

Chronic respiratory diseases account for high morbidity and mortality, with asthma, chronic obstructive pulmonary disease (COPD), and cystic fibrosis (CF) being the most prevalent globally (Paudel et al. 2020). Even though the diseases increase in prevalence, the exact underlying mechanisms have still not been fully understood. Despite their differences in nature, pathophysiologies, and clinical phenotypes, a growing body of evidence indicate that the presence of lung microbiota has the potential to shape the pathogenic processes underlying chronic inflammation typically observed in the course of the diseases (Dima et al. 2019; Loverdos et al. 2019). The characterization of the lung microbiota may therefore shed new light on the pathogenesis

* Corresponding author: A. Magryś, Chair and Department of Medical Microbiology, Medical University of Lublin, Lublin, Poland;
e-mail: agnieszka.magrys@umlub.pl

© 2021 Agnieszka Magryś

This work is licensed under the Creative Commons Attribution-NonCommercial-NoDerivatives 4.0 License (<https://creativecommons.org/licenses/by-nc-nd/4.0/>).

of these diseases. Specifically, in chronic respiratory tract diseases, the human microbiota may contribute to the disease's development and severity. The present review aims at exploring the role of the microbiota in chronic pulmonary diseases, especially COPD, asthma, and CF, and, in particular, the possible mechanisms of airway microbiome contributing to the pathogenesis of these diseases. The main hypothesis is that interactions between the bacterial microbiome and host inflammation are related to chronic lung diseases and their exacerbations. For this purpose, a comprehensive literature search was conducted using PubMed to collect current studies concerning lung microbiome in COPD, asthma, and CF. The following keywords were used 1. microbiome and chronic pulmonary disease; 2. asthma; 3. COPD; 4. CF; 5. microbiota and immunity; 6. airway microbiome; 7. airway microbiota and combinations thereof.

Healthy lung microbiota

A microbiome analysis based on 16S rRNA sequencing has identified unique microbiota in organs previously considered sterile, such as the lower respiratory tract. Currently, there is no doubt that the mucous membrane of the lungs has its own resident microbiome (Huffnagle et al. 2017). Moreover, increasing evidence indicates that pulmonary microbiota, acting on resident immune cells, plays a key role in maintaining homeostasis in the organs (Dickson et al. 2013).

Lungs, being constantly in contact with environmental air, full of microorganisms and inhaled particles, are at the frontline of immunity (Wang et al. 2017; Sommariva et al. 2020). The lower respiratory tract is a rather hostile environment for microbes. Ciliary epithelium and numerous mucin-releasing secretory cells of bacteriostatic properties mainly line it, creating an immune barrier. Moreover, the immunity of healthy lungs is conditioned by the presence of lung-resident lymphocytes and alveolar macrophages, which additionally protects them against external threats (Malinowska et al. 2017; Wang et al. 2017). In addition to its essential role in immunity against pathogens, perhaps the pulmonary immune system's most important function is to maintain a state of immunotolerance to non-dangerous environmental particles and self-antigens (Ramírez-Labrada et al. 2020; Sommariva et al. 2020). Cross-talk between alveolar macrophages, dendritic cells, and regulatory T cells (Treg) is the most critical to maintaining an immunological tone of the airways (Lloyd and Marsland 2017; Ramírez-Labrada et al. 2020; Sommariva et al. 2020). Of note, depletion of naturally occurring regulatory cells is characteristic of many chronic inflammatory diseases, including allergies, CF,

and COPD, and their downregulation are strongly connected with disease progression (Ramírez-Labrada et al. 2020; Sommariva et al. 2020). Accumulating evidence shows that resident pulmonary Treg cells' functionality can be significantly shaped by local lung microbiota (Ramírez-Labrada et al. 2020; Sommariva et al. 2020).

Lung microbiota is a relatively small bacterial community containing 10^3 – 10^5 cells/g of bronchial tissue. Comparatively, colon microbiota, which represents the most abundant ecosystem, comprises 10^{11} – 10^{12} cells/g of luminal content (Loverdos et al. 2019). Similar to other body sites, lungs present a complex bacterial community (Sommariva et al. 2020). According to numerous studies, the most common bacterial phyla that constitute the lung microbial ecosystem belong to *Bacteroides* and *Firmicutes* genera. It was also found that oral commensals, such as *Prevotella*, *Veilonella*, and *Streptococcus*, are the most prominent in healthy individuals' lungs (Ramírez-Labrada et al. 2020; Sommariva et al. 2020; Xu et al. 2020). This neutral community is acquired mostly during microaspiration of pharyngeal particles or direct migration along airway mucosa, and all their members equally participate in creating the regional growth conditions, i.e., the lung microenvironment (Ramírez-Labrada et al. 2020). Thus, it appears that the microbes' composition in the lungs is dynamic, mainly determined by the balance between microbial migration from the upper respiratory tract during microaspiration, elimination by coughing, mucociliary clearance, and immune system activity (Ramírez-Labrada et al. 2020; Sommariva et al. 2020; Xu et al. 2020). Different external and internal factors can influence the composition of the lung microbiome. Age, nutrition, lifestyle, pollution or tobacco smoke, inherited genes, and underlying diseases all can shape the type and number of lung microbiota, eventually leading to dysbiosis (Ogunrinola et al. 2019).

The respiratory microbiota both impacts and is impacted by immunity and disease. To avoid chronic inflammation under healthy condition, the lung microbiota has a fundamental role in shaping pulmonary immune tolerance. Microbes boost and calibrate innate and adaptive immunity, contribute to metabolic activities, and provide resistance to invasion by respiratory pathogens. Commensals can promote the establishment of a hostile environment and protect its host from pathogenic colonization (Ramírez-Labrada et al. 2020). This growth restriction may be caused by several mechanisms, such as altering of nutrient availability and production of antimicrobial metabolites (Ramírez-Labrada et al. 2020). Aside from the fact that microbiota can act on invasive microbes preventing their growth and spread, it plays a pivotal role in regulating immune tolerance in the lung environment. For homeostasis to be effectively managed, a balance must be maintained

between several factors, including Th cell activation and suppression by regulatory Treg cells (Belkaid and Hand 2014; Belkaid and Harrison 2017). As mentioned before, a local lung commensal can significantly modulate the activity of resident pulmonary immune cells. Indeed, microbiota participates in shaping an immune tolerant environment influencing the recruitment and activation of Treg cells as well as macrophages and tolerogenic dendritic cells (Ramírez-Labrada et al. 2020; Sommariva et al. 2020).

An optimal microbiota-host interaction impacts the formation of a symbiotic relationship between commensal bacteria and their host. Beneficial as microbiota may be in maintaining health, its perturbation disrupts homeostatic processes promoting dysfunction and disease (Sommariva et al. 2020).

Lung microbiota in chronic pulmonary diseases

Inflammation represents a host response to many harmful stimuli, including pro-inflammatory mediators, environmental toxins, and chronic infection (Huffnagle et al. 2017). In contrast to acute inflammatory response, chronic inflammation represents a long-term reaction, characteristic of predominant recruitment of mononuclear leucocytes. A growing body of evidence suggests that the dysregulation of the human lung microbiota is involved in shaping the pathogenetic processes underlying nearly all kinds of chronic inflammatory respiratory diseases (Wang et al. 2017; Loverdos et al. 2019). This has been achieved by culture-independent sequencing techniques that in patients with chronic pulmonary diseases microbiota can be found that profoundly differs from that of healthy lungs, which indeed, determines a chronic inflammatory status. The reason for the problem – inflammation – suggests that microbiota can modulate the environment, in which it lives. Admittedly, disturbances in the microbial community can drastically change the local growth conditions by changing the resident immune cells' activation state. During chronic inflammation, the lung habitat becomes unstable, and its species composition changes from “healthy” to a “pathogenic” state (Kovaleva et al. 2019).

Although the role of specific bacteria in the development of specific lung pathologies is still being established, a shift often occurs towards *Proteobacteria* the bacterial class of common lung-associated Gram-negative pathogens (mostly *Neisseria*, *Moraxella*, and *Haemophilus*) (Huffnagle et al. 2017; Sommariva et al. 2020). Particular metabolites and toxins with immunoregulatory properties are released, and other permissive niches for other species to reside there are created (O'Dwyer et al. 2016; Toraldo and Conte 2019). There is growing evidence that their metabolites, toxins, and cell

lysis products by enriching the local microenvironment activate the host's inflammatory cells and, therefore, contribute to lung diseases' pathogenesis (Huffnagle et al. 2017; Sommariva et al. 2020).

Key environmental factors that influence commensal bacteria growth and survival, such as temperature, pH, oxygen tension, and host immune cells, change dramatically. Nutrients, limited during the steady-state, are made available in abundance with the introduction of mucus and vascular permeability (Huang et al. 2017; Sommariva et al. 2020). These profound changes in the community composition of the respiratory microbiota, directly influencing the immune system regulation, are now believed to be involved in a rapid increase of chronic inflammatory diseases (Belkaid and Hand 2014; O'Dwyer et al. 2016). It must also be considered that numerous byproducts of inflammation: catecholamines, and inflammatory cytokines, positively influence the growth and survival of some potentially pathogenic groups of bacteria, especially members of *Proteobacteria*. During chronic inflammation, bacteria that can benefit from inflammation outcompete bacteria that cannot thrive in such an unfavorable environment, resulting in a reduction in microbiome diversity (Huffnagle et al. 2017; Loverdos et al. 2019).

The basis of chronic lung diseases is a variety of biological and genetic mechanisms and dysbiosis, which significantly contributes to injury to the host. The microbiota's metabolites and toxins are responsible for the changes in maintaining the steady-state of the lung microenvironment. However, it is not a single species or bacterial product responsible for this imbalance, but the entire cascade of events is an underlying cause of lung diseases. Thus, pathological changes in the composition and abundance of the lung microbiota might contribute to and result from chronic inflammation (Huang et al. 2017; Huffnagle et al. 2017; Sommariva et al. 2020) (Fig. 1).

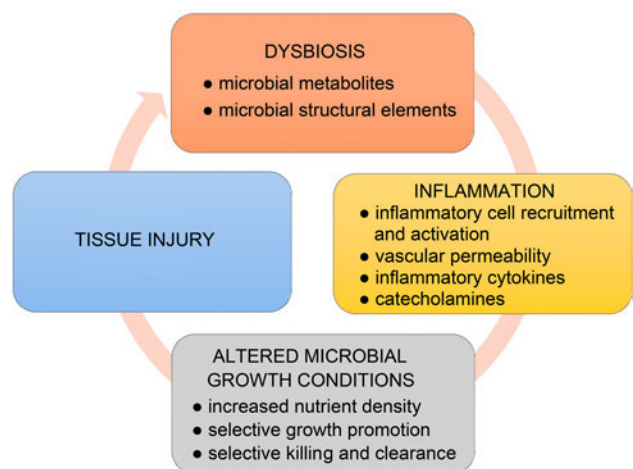


Fig. 1. A circle of dysbiosis and inflammation in chronic pulmonary diseases.

Airway microbiome in asthma

Asthma is a complex disease of the respiratory airways characteristic of chronic inflammation in the lungs, reversible airflow obstruction, mucus overproduction, and tissue neutrophilia or eosinophilia (Paudel et al. 2020). There is not a single cause of asthma (Kozik and Huang 2019). Existing data point to genetic and exogenous risks, including cigarette smoke, viral and bacterial infections, and obesity, associated with severe asthma and exacerbations of the disease (Kozik and Huang 2019; Paudel et al. 2020).

The role of the lung microbiome in the pathogenesis of asthma has not yet been fully elucidated. However, the most constant finding among lung microbiome studies is an observed increase in bacterial load and dominance of *Proteobacteria*, particularly *Haemophilus* spp. and *Moraxella catarrhalis* (Castro-Nallar et al. 2015; Noval Rivas et al. 2016; Loverdos et al. 2019). Dysbiotic communities may substantially contribute to the course or severity of the disease. On the other hand, a reduction in bacterial diversity could influence the inflammatory asthma phenotypes (Chung 2017; Sverrild et al. 2017). Different studies have shown that in patients with neutrophilic asthma, the microbiota composition is altered, and organisms, such as *M. catarrhalis*, *Haemophilus* spp. and *Streptococcus* spp. predominate. Their presence is associated with severe airflow obstruction, longer asthma duration, and neutrophilic infiltration, possibly via Th-17 – driven mechanism (Chung et al. 2017; Sverrild et al. 2017; Kozik and Huang 2019; Goto 2020; Paudel et al. 2020). In patients with worse asthma symptoms, airway enrichment with potentially pathogenic *Proteobacteria* members correlates with the level of IL-8, the neutrophilic pro-inflammatory marker. Interestingly, neutrophilic asthma is also associated with inadequate response to the first-line corticosteroid treatment. In corticosteroid-resistant patients, an overgrowth of *Haemophilus parainfluenzae* has been noted. Moreover, *Haemophilus influenzae* and *Tropheryma* have been reported in sputum samples of patients with poorly controlled severe cases (Simpson et al. 2016; Chung 2017). As inhaled steroids are a mainstay of the therapy, the involvement of particular bacterial genera in resistance mechanisms may explain the cause of steroidunresponsive asthma.

Eosinophilic asthma results from the activation of Th2 response that leads to airway infiltration by eosinophils. Here, in contrast to neutrophilic phenotype, microbiota's role is less clear and more heterogeneous (Taylor et al. 2018; Barcik et al. 2020). As observed, eosinophil infiltration of bronchial tissue is associated with low bacterial burden and diversity (Denner et al. 2016; Cait et al. 2018). The same studies found a nega-

tive correlation between *Proteobacteria* and *Firmicutes* and lung eosinophilia (Huang et al. 2015; Denner et al. 2016; Cait et al. 2018). It is now suggested that fungi, such as *Aspergillus* spp. rather than bacteria play a more significant role in eosinophilic asthma. This finding is supported by the fact that fungi, being significant allergens, can induce a strong eosinophilic allergic reaction in asthmatic patients. Nevertheless, the role of fungal microbiota in asthma remains poorly understood (Durack et al. 2017; Kozik and Huang 2019; Loverdos et al. 2019).

Respiratory viruses, mainly rhinoviruses, are detected in more than 75% of patients with acute exacerbation of asthma. For a long time, the bacterial role in asthma exacerbations has not been considered, since traditionally, no microbes were grown from patients' clinical specimens. Also, no clinical benefits of early antibiotic therapy were noticed in patients with acute exacerbation of the disease. However, culture-independent approaches, surprisingly, demonstrated the presence of atypical bacteria, such as *Mycoplasma pneumoniae* and *Chlamydia pneumoniae* (Dickson et al. 2014). However, their role in exacerbations of asthma is less clear than that of viral infections. It is believed that these bacterial pathogens may be somewhat involved in asthma persistence than exacerbations (Papadopoulos et al. 2011).

Airway microbiome in cystic fibrosis

Although cystic fibrosis (CF) is a multisystem disease, the disease's most tremendous burden falls upon the respiratory tract, characteristic of chronic airway infection and inflammation (Cribbs and Beck 2016). Recent studies have demonstrated that the lung microbiome is associated with the pathogenesis of this disease.

Cystic fibrosis arises from mutations in the cystic fibrosis transmembrane conductance regulator (CFTR) gene that is required for the homeostatic control of chloride ions in the lung. The CFTR gene's role is crucial, and its mutations lead to mucin overproduction along airways and disruption of the regular mucociliary activity and transport (Cribbs and Beck 2016; Françoise and Héry-Arnaud 2020). This defect also promotes polymicrobial proliferation and microbial imbalance along the respiratory tract, as mucin is a rich nutritional resource, which can support bacterial growth (Françoise and Héry-Arnaud 2020). In CF, the subsequent activation of neutrophilic inflammatory response leads to uncontrolled inflammation and progressive lung disease that severely limits pulmonary function (LiPuma 2010; Belkaid and Hand 2014). Polymicrobial chronic airway infections, which are characteristic of

CF, lead to persistent inflammation and periodic episodes of acute pulmonary exacerbation.

Traditionally, only a few bacteria have been associated with CF. *Pseudomonas aeruginosa*, *Staphylococcus aureus*, *H. influenzae*, and *Burkholderia cepacia* are the most often CF airway constituents (Belkaid and Hand 2014; Surette 2014; Cuthbertson et al. 2020). However, next-generation sequencing significantly advanced our knowledge about bacterial communities within a CF lung. Lines of evidence now show that CF lung microbiome is more complex, polymicrobial, highly diverse with overexpression of *Actinobacteria* and *Proteobacteria*, and potentially pathogenic anaerobes (Gillanders et al. 2011; Cuthbertson et al. 2020; Françoise and Héry-Arnaud 2020). The changes in the bacterial community might play an essential role in CF airway microenvironment condition. Bacteria within the CF lung contribute to horizontal gene transfer, especially in the presence of biofilm. They may affect the host by shedding different bioactive molecules that interact with host cells in shaping immune response and triggering inflammatory cytokines and growth factors (Cribbs and Beck 2017).

Microbial diversity is a marker of lung function (Françoise and Héry-Arnaud 2020). In CF, bacterial diversity correlates with the patient's age, the disease stage, and recurrent antibiotic therapies. A frequent broad-spectrum antibiotic therapy to treat pulmonary infections together with airway inflammation appears to be a significant driver of a fall in bacterial diversity that increases with age. This reduction is additionally associated with the establishment of species that are regarded as pathogens, usually, *H. influenzae*, *S. aureus*, and *P. aeruginosa* (Cox et al. 2010; Rogers et al. 2017; Françoise and Héry-Arnaud 2020). Consequently, the collapse in community diversity is associated with reduced lung function and disease progression (Cox et al. 2010). Data on strain changes in patients with pulmonary exacerbations remain unclear and contradictory (Carmody et al. 2013; Surette et al. 2014; Acosta et al. 2017). Many authors indicate that a total load of bacteria does not generally change at exacerbation onset. They also noticed that exacerbations are not related to significant in microbial diversity changes, but the microbiota composition that was more diverse at baseline tended to change over time (Hoffman and Surette 2013). Some studies report that *P. aeruginosa* and anaerobes are the critical components of pulmonary exacerbations. According to the observations of Carmody et al. (2013) facultatively anaerobic bacteria of the genus *Gemella* increased by 83% during exacerbation. Although the pathogenic potential of *Gemella* is not known, its abundance in patients during exacerbation makes it a potential biomarker candidate of the acute stage of the disease (Hoffman and Surette 2013).

Airway microbiome in chronic obstructive pulmonary disease (COPD)

Chronic obstructive pulmonary disease (COPD), one of the most prevalent respiratory diseases, is characteristic of persistent symptoms and airway obstruction due to inflammation. Traditionally, culture-based methods of analysis of COPD samples frequently revealed *H. influenzae*, *S. pneumoniae*, *M. catarrhalis* and *P. aeruginosa* as the most prominent pathogenic bacteria involved in the pathogenesis of the disease. Recent use of high throughput 16S rRNA gene-based sequencing has provided additional evidence of the presence of dysbiosis in COPD. Culture-independent methods confirmed that in COPD, aerobic and anaerobic bacteria colonize the airways, with *Proteobacteria* (*Haemophilus* spp.) being more common than *Bacteroides* (*Prevotella* spp.) being significantly reduced (Einarsson et al. 2016; Haldar et al. 2020). In addition, in stable COPD, a higher level of colonization with potentially pathogenic bacteria, such as *H. influenzae*, *S. pneumoniae*, and *M. catarrhalis* is associated with a greater chance of exacerbation and a more severe airflow obstruction (Martinez et al. 2013; Ditz et al. 2020). These bacteria are found in more than 75% of cases and are regarded as a "core" pulmonary microbiome in COPD (Martinez et al. 2013; Einarsson et al. 2016).

The disease is characteristic of a chronic inflammatory state, and bacteria colonizing COPD patients' airways are believed to participate in this dysregulation and provoke the host inflammatory response (Dima 2019; Haldar et al. 2020). Even at the state of bacterial colonization in stable COPD, many authors have reported excessive inflammation. In patients with COPD, persistent neutrophilic inflammation likely represents a local host immune response to chronic microbial colonization (Burgel et al. 2017). In addition, it has been confirmed that the profile of colonization-induced inflammation is similar to that observed during exacerbation. Therefore, it is likely that chronic microbial infection with potential bacterial pathogens serves as an activator of an immune response (Martinez et al. 2013; Wang et al. 2016; Burgel et al. 2017).

In patients with acute exacerbation, augmenting neutrophilic or eosinophilic inflammation is typically observed. As expected, bacteria-associated COPD exacerbations are associated with airway neutrophilia, accompanied by elevated levels of the primary mediators of inflammation, including IL-1 β , IL-8, and TNF. Subsequently, an increased number of neutrophils and inflammatory markers in the airways can cause significant damage to the respiratory tissue (Burgel et al. 2017; Ditz et al. 2020).

Conclusions and perspectives

While the study of the exact influence of the microbiome on lung health is still a relatively new field, it is clear that respiratory microbiome changes accompany chronic lung diseases of a non-infectious etiology, as previously believed. The composition of the lung microbiome is increasingly well characterized, and a specific spectrum of pathogenic microorganisms observed in association with several chronic respiratory diseases such as asthma, cystic fibrosis, and chronic obstructive pulmonary disease is already described. Indeed, the lung microbiome in chronic pulmonary diseases has a dynamic nature and is influenced by many factors, such as age, environmental exposure, treatment, etc.

It is also now becoming clear that chronic respiratory diseases' pathogenesis is a cascade of events in a self-amplifying cycle of altered microbial growth conditions, respiratory dysbiosis, and airway inflammation. In this cycle of events, changes in lung microbial community composition and abundance provoke airway inflammation, injuring the delicate lung tissue. And then, inflammation of the airways alters microbial environmental growth conditions promoting dysbiosis.

Lung microbiota does not seem to be the only microbial factor contributing to chronic pulmonary diseases. The gut microbiota's influence on lung immunity has been well documented and linked to disease development in the lungs with immune response changes when the gut microbiota community is altered (Pulvirenti et al. 2019). Mounting evidence indicates that the immune cells and cytokines induced by the gut microbiota components or metabolites, especially short-chain fatty acids (SCFAs), can modulate lung immunity and inflammatory responses, with specific taxa able to influence the pathogenesis of chronic pulmonary diseases (Samuelson et al. 2015; Cait et al. 2018). Although there is a growing body of evidence for the role of the gut/lung axis in lung diseases, several unanswered questions still exist for its clinical relevance.

Environmental factors such as pollution, cigarette smoke, antibiotics, and diet can also modulate microbiota composition and affect disease susceptibility. Indeed, it is broadly accepted that cigarette smoking and air pollution are the most substantial risk factors for developing COPD (Allais et al. 2016). At the same time, an increased risk of asthma has been associated with microbial dysbiosis in the gut in early life. Simultaneously, the use of antibiotics in children has also been implicated in the development of asthma (Yang et al. 2019).

Although many of the underlying mechanisms are likely disease-specific, the microbiome's exploration is promising and provides a solid background for developing innovative strategies for diagnostic, preventative, and therapeutic approaches.

Conflict of interest

The authors do not report any financial or personal connections with other persons or organizations, which might negatively affect the contents of this publication and/or claim authorship rights to this publication.

Literature

- Acosta N, Whelan FJ, Somayaji R, Poonja A, Surette MG, Rabin HR, Parkins MD. The evolving cystic fibrosis microbiome: a comparative cohort study spanning 16 years. *Ann Am Thorac Soc*. 2017 Aug;14(8):1288–1297. <https://doi.org/10.1513/AnnalsATS.201609-668OC>
- Allais L, Kerckhof FM, Verschuere S, Bracke KR, De Smet R, Laukens D, Van den Abbeele P, De Vos M, Boon N, Brusselle GG, et al. Chronic cigarette smoke exposure induces microbial and inflammatory shifts and mucin changes in the murine gut. *Environ Microbiol*. 2016 May;18(5):1352–1363. <https://doi.org/10.1111/1462-2920.12934>
- Barcik W, Boutin RCT, Sokolowska M, Finlay BB. The role of lung and gut microbiota in the pathology of asthma. *Immunity*. 2020 Feb 18;52(2):241–255. <https://doi.org/10.1016/j.immuni.2020.01.007>
- Belkaid Y, Hand TW. Role of the microbiota in immunity and inflammation. *Cell*. 2014 Mar;157(1):121–141. <https://doi.org/10.1016/j.cell.2014.03.011>
- Belkaid Y, Harrison OJ. Homeostatic immunity and the microbiota. *Immunity*. 2017 Apr;46(4):562–576. <https://doi.org/10.1016/j.immuni.2017.04.008>
- Berg G, Rybakova D, Fischer D, Cernava T, Vergès MCC, Charles T, Chen X, Cocolin L, Eversole K, Corral GH, et al. Microbiome definition re-visited: old concepts and new challenges. *Microbiome*. 2020 Dec;8(1):103. <https://doi.org/10.1186/s40168-020-00875-0>
- Burgel P-R, Contoli M, López-Campos JL. Acute exacerbations of the pulmonary diseases. Sheffield (UK): European Respiratory Society; 2017. <https://doi.org/10.1183/2312508X.erm7717>
- Cait A, Hughes MR, Antignano F, Cait J, Dimitriu PA, Maas KR, Reynolds LA, Hacker L, Mohr J, Finlay BB, et al. Microbiome-driven allergic lung inflammation is ameliorated by short-chain fatty acids. *Mucosal Immunol*. 2018 May;11(3):785–795. <https://doi.org/10.1038/mi.2017.75>
- Carmody LA, Zhao J, Schloss PD, Petrosino JF, Murray S, Young VB, Li JZ, LiPuma JJ. Changes in cystic fibrosis airway microbiota at pulmonary exacerbation. *Ann Am Thorac Soc*. 2013 Jun; 10(3):179–187. <https://doi.org/10.1513/AnnalsATS.201211-107OC>
- Castro-Nallar E, Shen Y, Freishtat RJ, Pérez-Losada M, Manimaran S, Liu G, Johnson WE, Crandall KA. Integrating microbial and host transcriptomics to characterize asthma-associated microbial communities. *BMC Med Genomics*. 2015 Dec;8(1):50. <https://doi.org/10.1186/s12920-015-0121-1>
- Chung KF. Airway microbial dysbiosis in asthmatic patients: A target for prevention and treatment? *J Allergy Clin Immunol*. 2017 Apr; 139(4):1071–1081. <https://doi.org/10.1016/j.jaci.2017.02.004>
- Cox MJ, Allgaier M, Taylor B, Baek MS, Huang YJ, Daly RA, Karaoz U, Andersen GL, Brown R, Fujimura KE, et al. Airway microbiota and pathogen abundance in age-stratified cystic fibrosis patients. *PLoS One*. 2010 Jun 23;5(6):e11044. <https://doi.org/10.1371/journal.pone.0011044>
- Cribbs SK, Beck JM. Microbiome in the pathogenesis of cystic fibrosis and lung transplant-related disease. *Transl Res*. 2017 Jan; 179:84–96. <https://doi.org/10.1016/j.trsl.2016.07.022>
- Cuthbertson L, Walker AW, Oliver AE, Rogers GB, Rivett DW, Hampton TH, Ashare A, Elborn JS, De Soyza A, Carroll MP, et al.

- Lung function and microbiota diversity in cystic fibrosis. *Microbiome*. 2020 Dec;8(1):45.
<https://doi.org/10.1186/s40168-020-00810-3>
- Denner DR, Sangwan N, Becker JB, Hogarth DK, Oldham J, Castillo J, Sperling AI, Solway J, Naureckas ET, Gilbert JA, et al.** Corticosteroid therapy and airflow obstruction influence the bronchial microbiome, which is distinct from that of bronchoalveolar lavage in asthmatic airways. *J Allergy Clin Immunol*. 2016 May; 137(5):1398–1405.e3. <https://doi.org/10.1016/j.jaci.2015.10.017>
- Dickson RP, Erb-Downward JR, Huffnagle GB.** The role of the bacterial microbiome in lung disease. *Expert Rev Respir Med*. 2013 Jun;7(3):245–257. <https://doi.org/10.1586/ers.13.24>
- Dickson RP, Martinez FJ, Huffnagle GB.** The role of the microbiome in exacerbations of chronic lung diseases. *Lancet*. 2014 Aug; 384(9944): 691–702.
[https://doi.org/10.1016/S0140-6736\(14\)61136-3](https://doi.org/10.1016/S0140-6736(14)61136-3)
- Dima E, Kyriakoudi A, Kaponi M, Vasileiadis I, Stamou P, Koutsoukou A, Koulouris NG, Rovina N.** The lung microbiome dynamics between stability and exacerbation in chronic obstructive pulmonary disease (COPD): Current perspectives. *Respir Med*. 2019 Oct;157:1–6. <https://doi.org/10.1016/j.rmed.2019.08.012>
- Ditz B, Christenson S, Rossen J, Brightling C, Kerstjens HAM, van den Berge M, Faiz A.** Sputum microbiome profiling in COPD: beyond singular pathogen detection. *Thorax*. 2020 Apr;75(4):338–344.
<https://doi.org/10.1136/thoraxjnl-2019-214168>
- Durack J, Lynch SV, Nariya S, Bhakta NR, Beigelman A, Castro M, Dyer AM, Israel E, Kraft M, Martin RJ, et al.; National Heart, Lung and Blood Institute’s “AsthmaNet”.** Features of the bronchial bacterial microbiome associated with atopy, asthma, and responsiveness to inhaled corticosteroid treatment. *J Allergy Clin Immunol*. 2017 Jul;140(1):63–75. <https://doi.org/10.1016/j.jaci.2016.08.055>
- Einarsson GG, Comer DM, McIlreavey L, Parkhill J, Ennis M, Tunney MM, Elborn JS.** Community dynamics and the lower airway microbiota in stable chronic obstructive pulmonary disease, smokers and healthy non-smokers. *Thorax*. 2016 Sep;71(9):795–803.
<https://doi.org/10.1136/thoraxjnl-2015-207235>
- Françoise A, Héry-Arnaud G.** The microbiome in cystic fibrosis pulmonary disease. *Genes (Basel)*. 2020 May 11;11(5):536.
<https://doi.org/10.3390/genes11050536>
- Gillanders LJ, Elborn JS, Gilpin DE, Schneiders T, Tunney MM.** The airway microbiome in cystic fibrosis: challenges for therapy. *Therapy*. 2011 Nov;8(6):645–660.
<https://doi.org/10.2217/thy.11.81>
- Goto T.** Airway microbiota as a modulator of lung cancer. *Int J Mol Sci*. 2020 Apr 26;21(9):3044.
<https://doi.org/10.3390/ijms21093044>
- Haldar K, George L, Wang Z, Mistry V, Ramsheh MY, Free RC, John C, Reeve NF, Miller BE, Tal-Singer R, et al.** The sputum microbiome is distinct between COPD and health, independent of smoking history. *Respir Res*. 2020 Dec;21(1):183.
<https://doi.org/10.1186/s12931-020-01448-3>
- Hoffman L, Surette M.** What to expect when you’re expectorating: cystic fibrosis exacerbations and microbiota. *Ann Am Thorac Soc*. 2013 Jun;10(3):249–250.
<https://doi.org/10.1513/AnnalsATS.201304-086ED>
- Huang YJ, Erb-Downward JR, Dickson RP, Curtis JL, Huffnagle GB, Han MK.** Understanding the role of the microbiome in chronic obstructive pulmonary disease: principles, challenges, and future directions. *Transl Res*. 2017 Jan;179:71–83.
<https://doi.org/10.1016/j.trsl.2016.06.007>
- Huang YJ, Nariya S, Harris JM, Lynch SV, Choy DE, Arron JR, Boushey H.** The airway microbiome in patients with severe asthma: associations with disease features and severity. *J Allergy Clin Immunol*. 2015 Oct;136(4):874–884.
<https://doi.org/10.1016/j.jaci.2015.05.044>
- Huffnagle GB, Dickson RP, Lukacs NW.** The respiratory tract microbiome and lung inflammation: a two-way street. *Mucosal Immunol*. 2017 Mar;10(2):299–306.
<https://doi.org/10.1038/mi.2016.108>
- Kovaleva OV, Romashin D, Zborovskaya IB, Davydov MM, Shogenov MS, Gratchev A.** Human lung microbiome on the way to cancer. *J Immunol Res*. 2019 Jul 29;2019:1394191.
<https://doi.org/10.1155/2019/1394191>
- Kozik AJ, Huang YJ.** The microbiome in asthma: Role in pathogenesis, phenotype, and response to treatment. *Ann Allergy Asthma Immunol*. 2019 Mar;122(3):270–275.
<https://doi.org/10.1016/j.anai.2018.12.005>
- LiPuma JJ.** The changing microbial epidemiology in cystic fibrosis. *Clin Microbiol Rev*. 2010 Apr;23(2):299–323.
<https://doi.org/10.1128/CMR.00068-09>
- Lloyd CM, Marsland BJ.** Lung homeostasis: influence of age, microbes and the immune system. *Immunity*. 2017 Apr;46(4):549–561.
<https://doi.org/10.1016/j.immuni.2017.04.005>
- Loverdos K, Bellos G, Kokolatou L, Vasileiadis I, Giamarellos E, Pecchiari M, Koulouris N, Koutsoukou A, Rovina N.** Lung microbiome in asthma: Current perspective. *J Clin Med*. 2019 Nov 14; 8(11):1967. <https://doi.org/10.3390/jcm8111967>
- Malinowska M, Tokarz-Deptuła B, Deptuła W.** [Mikrobiom człowieka] (in Polish). *Postepy Mikrobiol*. 2017;56(1):33–42.
- Martinez FJ, Erb-Downward JR, Huffnagle GB.** Significance of the microbiome in chronic obstructive pulmonary disease. *Ann Am Thorac Soc*. 2013 Dec;10 Supplement:S170–S179.
<https://doi.org/10.1513/AnnalsATS.201306-204AW>
- Moffatt ME, Cookson WO.** The lung microbiome in health and disease. *Clin Med (Lond)*. 2017 Dec;17(6):525–529.
<https://doi.org/10.7861/clinmedicine.17-6-525>
- Noval Rivas M, Crother TR, Arditi M.** The microbiome in asthma. *Curr Opin Pediatr*. 2016 Dec;28(6):764–771.
<https://doi.org/10.1097/MOP.0000000000000419>
- O’Dwyer DN, Dickson RP, Moore BB.** The lung microbiome, immunity and the pathogenesis of chronic lung disease. *J Immunol*. 2016 Jun 15;196(12):4839–4847.
<https://doi.org/10.4049/jimmunol.1600279>
- Ogunrinola GA, Oyewale JO, Oshamika OO, Olasehinde GI.** The human microbiome and its impacts on health. *Int J Microbiol*. 2020 Jun 12;2020:1–7.
<https://doi.org/10.1155/2020/8045646>
- Papadopoulos NG, Christodoulou I, Rohde G, Agache I, Almqvist C, Bruno A, Bonini S, Bont L, Bossios A, Bousquet J, et al.** Viruses and bacteria in acute asthma exacerbations – A GA²LEN-DARE* systematic review. *Allergy*. 2011 Apr;66(4): 458–468.
<https://doi.org/10.1111/j.1398-9995.2010.02505.x>
- Paudel KR, Dharwal V, Patel VK, Galvao I, Wadhwa R, Malyla V, Shen SS, Budden KE, Hansbro NG, Vaughan A, et al.** Role of lung microbiome in innate immune response associated with chronic lung diseases. *Frontiers in Medicine*. 2020 Sep 18;7:554.
<https://doi.org/10.3389/fmed.2020.00554>
- Pulvirenti G, Parisi GF, Giallongo A, Papale M, Manti S, Savasta S, Licari A, Marseglia GL, Leonardi S.** Lower airway microbiota. *Front Pediatr*. 2019 Sep 27;7:393.
<https://doi.org/10.3389/fped.2019.00393>
- Ramírez-Labrada AG, Isla D, Artal A, Arias M, Rezusta A, Pardo J, Gálvez EM.** The influence of lung microbiota on lung carcinogenesis, immunity and immunotherapy. *Trends Cancer*. 2020 Feb;6(2):86–97.
<https://doi.org/10.1016/j.trecan.2019.12.007>
- Rogers GB, Bruce KD, Hoffman LR.** How can the cystic fibrosis respiratory microbiome influence our clinical decision-making? *Curr Opin Pulm Med*. 2017 Nov;23(6):536–543.
<https://doi.org/10.1097/MCP.0000000000000419>

- Samuelson DR, Welsh DA, Shellito JE.** Regulation of lung immunity and host defense by the intestinal microbiota. *Front Microbiol.* 2015 Oct 7;6:1085. <https://doi.org/10.3389/fmicb.2015.01085>
- Simpson JL, Daly J, Baines KJ, Yang IA, Upham JW, Reynolds PN, Hodge S, James AL, Hugenholtz P, Willner D, et al.** Airway dysbiosis: *Haemophilus influenzae* and *Tropheryma* in poorly controlled asthma. *Eur Respir J.* 2016 Mar;47(3):792–800. <https://doi.org/10.1183/13993003.00405-2015>
- Sommariva M, Le Noci V, Bianchi F, Camelliti S, Balsari A, Tagliabue E, Sfondrini L.** The lung microbiota: role in maintaining pulmonary immune homeostasis and its implications in cancer development and therapy. *Cell Mol Life Sci.* 2020 Jul;77(14):2739–2749. <https://doi.org/10.1007/s00018-020-03452-8>
- Surette MG.** The cystic fibrosis lung microbiome. *Ann Am Thorac Soc.* 2014 Jan;11 Suppl 1:S61–S65. <https://doi.org/10.1513/AnnalsATS.201306-159MG>
- Sverrild A, Kiilerich P, Brejnrod A, Pedersen R, Porsbjerg C, Bergqvist A, Erjefält JS, Kristiansen K, Backer V.** Eosinophilic airway inflammation in asthmatic patients is associated with an altered airway microbiome. *J Allergy Clin Immunol.* 2017 Aug;140(2):407–417.e11. <https://doi.org/10.1016/j.jaci.2016.10.046>
- Taylor SL, Leong LEX, Choo JM, Wesselingh S, Yang IA, Upham JW, Reynolds PN, Hodge S, James AL, Jenkins C, et al.** Inflammatory phenotypes in patients with severe asthma are associated with distinct airway microbiology. *J Allergy Clin Immunol.* 2018 Jan;141(1):94–103.e15. <https://doi.org/10.1016/j.jaci.2017.03.044>
- Toraldo DM, Conte L.** Influence of the lung microbiota dysbiosis in chronic obstructive pulmonary disease exacerbations: the controversial use of corticosteroid and antibiotic treatments and the role of eosinophils as a disease marker. *J Clin Med Res.* 2019;11(10):667–675. <https://doi.org/10.14740/jocmr3875>
- Wang J, Li F, Tian Z.** Role of microbiota on lung homeostasis and diseases. *Sci China Life Sci.* 2017 Dec;60(12):1407–1415. <https://doi.org/10.1007/s11427-017-9151-1>
- Wang Z, Bafadhel M, Haldar K, Spivak A, Mayhew D, Miller BE, Tal-Singer R, Johnston SL, Ramsheh MY, Barer MR, et al.** Lung microbiome dynamics in COPD exacerbations. *Eur Respir J.* 2016 Apr;47(4):1082–1092. <https://doi.org/10.1183/13993003.01406-2015>
- Xu N, Wang L, Li C, Ding C, Li C, Fan W, Cheng C, Gu B.** Microbiota dysbiosis in lung cancer: evidence of association and potential mechanisms. *Transl Lung Cancer Res.* 2020 Aug;9(4):1554–1568. <https://doi.org/10.21037/tlcr-20-156>
- Yang X, Feng H, Zhan X, Zhang C, Cui R, Zhong L, Ying S, Chen Z.** Early-life vancomycin treatment promotes airway inflammation and impairs microbiome homeostasis. *Aging (Albany NY).* 2019 Apr 13; 11(7):2071–2081. <https://doi.org/10.18632/aging.101901>

Effects of Different Ambient Temperatures on Caecal Microbial Composition in Broilers

YUTING YANG^{1#}, XING LI^{1#}, ZHENHUI CAO¹, YINGING QIAO¹, QIUYE LIN², JIANPING LIU³, ZHIYONG ZHAO⁴,
QINGCONG AN¹, CHUNYONG ZHANG¹, HONGFU ZHANG⁵ and HONGBIN PAN^{1*} 

¹ Yunnan Provincial Key Laboratory of Animal Nutrition and Feed Science, Faculty of Animal Science and Technology, Yunnan Agricultural University, Kunming, The People's Republic of China

² College of Food Science and Technology, Yunnan Agricultural University, Kunming, The People's Republic of China

³ Jiangsu Key Laboratory for Molecular and Medical Biotechnology, College of Life Sciences, Nanjing Normal University, Nanjing, The People's Republic of China

⁴ Yunnan Animal Science and Veterinary Institute, Kunming, The People's Republic of China

⁵ Institute of Animal Science Chinese Academy of Agricultural Sciences, Beijing, The People's Republic of China

Submitted 26 September 2020, revised 24 December 2020, accepted 27 December 2020

Abstract

Short-term or acute temperature stress affect the immune responses and alters the gut microbiota of broilers, but the influences of long-term temperature stress on stress biomarkers and the intestinal microbiota remains largely unknown. Therefore, we examined the effect of three long-term ambient temperatures (high (HC), medium (MC), and low (LC) temperature groups) on the gene expression of broilers' heat shock proteins (Hsps) and inflammation – related genes, as well as the caecal microbial composition. The results revealed that Hsp70 and Hsp90 levels in HC group significantly increased, and levels of Hsp70, Hsp90, IL-6, TNF- α , and NFKB1 in LC group were significantly higher than in MC group ($p < 0.05$). In comparison with the MC group, the proportion of Firmicutes increased in HC and LC groups, while that of Bacteroidetes decreased in LC group at phylum level ($p < 0.05$). At genus level, the proportion of *Escherichia/Shigella*, *Phascolarctobacterium*, *Parabacteroides*, and *Enterococcus* increased in HC group; the fraction of *Faecalibacterium* was higher in LC group; and the percentage of *Barnesiella* and *Alistipes* decreased in both HC and LC groups ($p < 0.05$). Functional analysis based on communities' phylogenetic investigation revealed that the pathways involved in environmental information processing and metabolism were enriched in the HC group. Those involved in cellular processes and signaling, metabolism, and gene regulation were enriched in LC group. Hence, we conclude that the long-term temperature stress can greatly alter the intestinal microbial communities in broilers and may further affect the host's immunity and health.

Key words: broiler, temperature, 16S rRNA sequencing, caecal microbial composition, KEGG pathway

Introduction

Poultry provides an crucial protein source in the human diet and thus has enormous economic value. The broiler breeds were produced by selecting a high growth rate and feed conversion in intensive poultry farming, but they display a low tolerance to ambient temperature change (Lara and Rostagno 2013). Temperature stress may adversely affect poultry immunity, growth performance, physiology, and intestinal morphology and may further cause several health problems such as immunosuppression, microbial infection, and

other diseases (Song et al. 2018; Rioja-Lang et al. 2019). Heat shock proteins (Hsps) and inflammatory proteins (such as NF- κ B and TNF- α) were reported to be associated with the function of immune systems (Tsan and Gao 2009). Hsps have been identified as important modulators of adaptive immunity and can be induced during multiple types of cellular stresses (Santoro 2000). Besides, extracellular Hsps can interact with dendritic cells (DCs) and macrophages, subsequently activating NF- κ B signaling pathway and enhancing the expression of the inflammatory cytokines IL-1, IL-6, and TNF- α (Appenheimer and Evans 2018).

Yuting Yang and Xing Li contribute equally to this work and are co-first authors.

* Corresponding author: H. Pan, Yunnan Provincial Key Laboratory of Animal Nutrition and Feed Science, Faculty of Animal Science and Technology, Yunnan Agricultural University, Kunming, The People's Republic of China; e-mail: ynsdyz@163.com

© 2021 Yuting Yang et al.

This work is licensed under the Creative Commons Attribution-NonCommercial-NoDerivatives 4.0 License (<https://creativecommons.org/licenses/by-nc-nd/4.0/>).

The gastrointestinal compartments of chickens are densely populated with diverse and complex microbial communities, with the most densely populated microbiota found in the caecum (Mohd Shaufi et al. 2015; Shang et al. 2018). The close symbiosis between the host and its intestinal microbes is critical for maintaining the host's health (Chow et al. 2010). Gut microbes produce various essential metabolites that play vital roles in nutrient digestion, metabolism, and immunity modulation (Hou et al. 2016). Furthermore, caecal microbiota and its modulation are closely associated with poultry health, productivity, and disease control (Montoro-Dasi et al. 2020). The environmental temperature could affect the composition of intestinal microbiota (Wang et al. 2018). For example, the composition of broilers' gut microbiome varies seasonally (Oakley et al. 2018). The microbial community structure in the ileum and caecum altered with short-term heat stress (Burkholder et al. 2008), and exposure to low temperature led to remarkable changes in the gut microbiota composition (Chevalier et al. 2015).

Although much is known about the effect of acute or continuous heat and cold stresses on the host immune responses and gut microbiota of broilers, little evidence is available regarding how temperature stress that span the entire cycle of broilers (e.g. lasting over 40 days) impact the Hsps, the expression of inflammatory genes and caecal microbiota. Therefore, in this study, we investigated the effects of 42-day temperature stress on the expression of heat shock proteins and inflammation-related genes in the liver, and the composition and function of caecal microbiota in broilers. Our results may provide experimental evidence for designing optimal breeding temperature and developing useful probiotics.

Experimental

Materials and Methods

Ethics statement. All experiments performed in this study were approved by the International Animal Care and Use Committee of the Yunnan Agricultural University (permission code: YNAU20160016). The study complied with the guidelines of the Institutional Administrative Committee and Ethics Committee of Laboratory Animals.

Animal and management. A total of 36 one-day-old Avian chickens (Hunan Shuncheng Industrial Co. Ltd., Hunan, China) were randomly split into three open-circuit calorimetry chambers (Sun et al. 2017) in a commercial chicken farm. One chamber was for the high-temperature treatment (HC), the second one for the medium temperature treatment (MC), and the third one for the low temperature treatment (LC). The temperature of the MC group originated from the

Avian 500 broiler feeding standard of Beijing Poultry Breeding Co., Ltd., while the temperatures for HC and LC groups were increased or decreased by 3°C, respectively. The temperature schedule was started at 36.5°C (HC), 33.5°C (MC), and 30.5°C (LC), and respectively reduced to 22°C, 19°C, and 16°C on day 42 as shown in Table SI. Chickens in each chamber were further subdivided into three replicates (four chickens for each) and provided with a bedding of rice husks, feed, and water ad libitum. Aside from the different temperatures, the chickens in all three groups received the same treatments, including the National Research Council (NRC) diet and environment (Table SII).

Samples collection. On day 42, four chickens from each replicate were euthanized by cervical dislocation. The caecal contents and liver samples from all 36 broilers were obtained and immediately stored in liquid nitrogen for further 16S rRNA amplicon sequencing and quantitative real-time polymerase chain reaction (qPCR).

Quantitative real-time PCR. qPCR analysis was performed to compare the relative expression level of Hsp70, Hsp90, tumor necrosis factor alpha (TNF- α), and NF- κ B signaling pathway-related genes (NFKB1, NFKB2) in the three temperature groups. Total RNA from the 36 liver samples was extracted using RNA simple total RNA kit (Tiangen Co. Ltd., Cat. #DP419) according to the manufacturer's recommendations. Primers were designed with Primer Premier 5.0 and shown in Table I. The cDNA was synthesized using FastKing RT kit with gDNAase (Tiangen Co. Ltd., Cat. #KR116). The SYBR Green SuperReal PreMix Plus kit (Tiangen Co. Ltd., Cat. #FP205) was used in the qPCR analysis (CFX96 Real-time system, Bio-Rad) to assess the mRNA expression levels. The data were analyzed by the $2^{-\Delta\Delta C_t}$ method with normalization by the Ct of the housekeeping gene ACTB (β -Actin) (Livak and Schmittgen 2001).

Microbial DNA extraction and 16S rRNA sequencing. Genomic DNA of caecal contents samples was extracted with QIAamp® Fast DNA Stool Mini Kit (Qiagen, Cat No.19593, Dusseldorf, Germany) following the manufacturer's recommendations. The amplification of the hypervariable V3-V4 region of the 16S rRNA gene was performed following the recommendations of the 16S Metagenomic Sequencing Library Preparation guide (Illumina, San Diego, CA, USA) using the primer pair 341 F 5'-CCTACGGGGRSGCAGCAG-3' and 806 R 5'-GGACTACVVGGGTATCTAATC-3'. Amplicons were electrophoresed in 2% agarose gels before they were extracted from the gel and purified using the AxyPrep DNA Gel Extraction Kit (Axygen Biosciences, Union City, CA, U.S.) according to the manufacturer's instructions and quantified using Qubit®2.0 (Invitrogen, CA, U.S.). The prepared library

Table I
List of primer sequences for qPCR.

Gene	Forward primer (5'→3')	Reverse primer (5'→3')	Gene accession number
ACTB	CTCGGCTGTGGTGGTGAA	CCATCTATGAAGGCTACGC	AB495648
Hsp70	TGGTGGGAATGGTGGTGTAC	ATCTGCTCCTGTTGGATGTCA	MH422508.1
Hsp90	CAGCAGCAGTATCATCTTCATC	CCTGTCCTCTGGCTTTAGTTT	NM001109785.1
NF-κB1	AGTTCAGGATGCACCAAGAGT	AGTCAACGCAGGACCTAAAGA	GGAF000241
NF-κB2	TGACGGTGGGATAGGTCTTGT	CTGCCTGGATGGGATTGACTA	U00111
IL-6	CCTAGAAGGAAATGAGAATGCCTAT	CGTTTATGGAGAAGACCGTGAG	AJ309540
TNF-α	GCTTACTTCCCTTCTTCTCC	TCTACATCTGACCCATCCC	XM015284187

Table II
Library diversity of the 16S rRNA genes from the chicken cecum¹.

Group ID	HC	MC	LC
OTUs	292 ± 22.70	297 ± 42.57	271 ± 52.59
Chao1	334.06 ± 22.72 ^{ab}	351.67 ± 44.98 ^a	316.75 ± 45.95 ^b
Observed species	289.16 ± 22.77	294.25 ± 42.11	267.66 ± 53.71
Shannon	4.93 ± 0.43	4.62 ± 0.64	4.83 ± 1.01
Simpson	0.91 ± 0.03	0.86 ± 0.05	0.89 ± 0.11
PD whole tree	17.32 ± 1.18	17.83 ± 2.11	16.64 ± 2.88
Good's Coverage	0.9983 ± 0.0001	0.9981 ± 0.0002	0.9983 ± 0.0002

^{a,b} – Different superscripts in the same row indicate significant difference ($p < 0.05$)

¹ – $n = 12$ per treatment group (Mean ± SD)

was sequenced in the HiSeq 2500 platform (Illumina, San Diego, CA, USA) for paired-end reads of 250 bp. The reads were deposited in the NCBI sequence archive (SRA) under accession no. PRJNA573420.

Bioinformatics analyses. Bioinformatics analyses were performed as previously described (Li et al. 2019). In brief, paired-end reads in the fastq files were assembled through PANDAsq software (<https://github.com/neufeld/pandaseq/releases/tag/v2.8.1>). The quality control and the filtering process were made pursuant as suggested (Caporaso et al., 2010). The clean reads were clustered and classified into the same operational taxonomic units (OTUs) with a similarity of 97% using UPARSE (<http://drive5.com/uparse/>), while the chimeric sequences were identified and removed using Userach (version 7.0). Each representative read was assigned to a taxon by RDP Classifier against the Ribosomal Database Project (RDP) database (<http://rdp.cme.msu.edu/>) with a threshold value of 0.8–1. According to the bacterial annotation, taxonomic information, and each sample's community composition at various classification levels (Kingdom, Phylum, Class, Order, Family, Genus) were assessed. Alpha diversity of Chao1 values, Good's Coverage values, Shannon indices, observed species indices, PD whole tree indices, Simpson indices, and beta diversity of principal component analysis (PCA) were calculated using QIIME (version 1.9.1) (Caporaso et al. 2010). The linear discriminant analysis (LDA) effect size (LEfSe) method was used

to identify the different taxa between the three groups (Segata et al. 2011). Phylogenetic Investigation of Communities by Reconstruction of Unobserved States (PICRUSt) based on closed-reference OTUs was used to predict the abundance of functional categories in the Kyoto Encyclopedia of Genes and Genomes (KEGG) ortholog (KO) (Langille et al. 2013).

Statistical analysis. The SPSS 22.0 software (IBM SPSS Statistics for Windows, NY) was used to analyze the experimental data. The general linear model analysis with Duncan's multiple comparison test was used to analyze the gene expression data. Microbial data were analyzed using the Kruskal-Wallis rank test by the SPSS software.

Results

Expression of the genes encoding for heat shock proteins and inflammation-related genes in the liver. Compared to the MC group, the Hsp70 and Hsp90 mRNA expression increased in HC and LC groups ($p < 0.05$). The NF-κB1 mRNA expression in LC group was upregulated when compared to MC and HC groups ($p < 0.05$), while higher mRNA expression of IL-6 and TNF-α was observed in the LC group than in the MC group (Fig. 1).

High-throughput 16S rDNA sequencing. HiSeq sequencing of the 16S rRNA gene amplicons generated

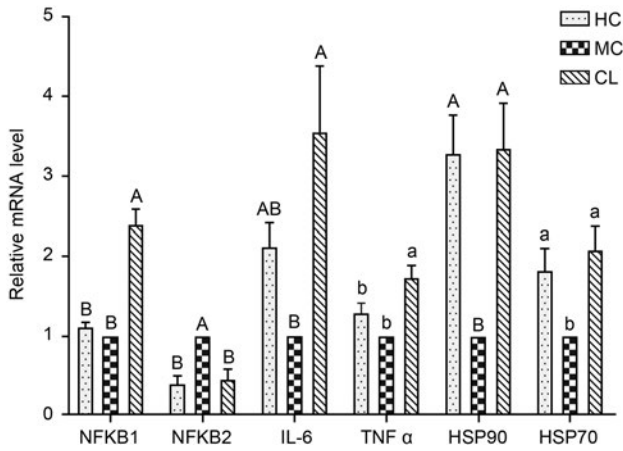


Fig. 1. The relative mRNA expression level of heat shock proteins and inflammation-related genes in the liver of chickens. Different uppercase and lowercase letters indicate the significance of difference at $p < 0.01$ and $p < 0.05$, respectively. The same letters indicate no significant difference.

2,100,180 clean reads (mean length of 414 bp), yielding an average of 58,338 clean reads (52,667–64,809) per sample. Then we rarefied the library size to 32,296 tags per sample using the rarefy function to minimize the impact of the sequencing depth on microbial composition (Table SIII). With a 97% sequence similarity as a cutoff, we obtained 460, 537, and 547 OTUs from the HC, MC, and LC groups, in which the proportion of the core microbiome was 79%, 68%, and 67%, respectively (Fig. S1). Alpha diversity demonstrated different temperature treatments changes in terms of richness and evenness, as summarized in Table II. The Chao1 index in the MC group was significantly higher than that in the LC group ($p < 0.05$).

Effects of temperature stress on taxonomic composition. Out of the classifiable sequences, 10 phyla

were identified (Fig. S2). Out of the classifiable sequences, ten phyla were identified (Fig. S2). The significant changes of dominant microbiota at the phylum level were determined between the HC, MC, and LC groups (Fig. 2). In the MC group, Bacteroidetes (60.70%) and Firmicutes (36.22%) were the dominant phyla, followed by Actinobacteria (1.00%), Proteobacteria (0.93%), and Tenericutes (0.23%). In comparison, the HC group displayed a 9.02% decrease in the relative abundance of Bacteroidetes ($p > 0.05$), an 8.67% increase of Firmicutes ($p < 0.05$). The LC group also exhibited considerable phylum-level changes: 17.43% reduction in the relative abundance of Bacteroidetes ($p < 0.01$), 14.56% increase of Firmicutes ($p < 0.01$), and 1.65% increase of Proteobacteria ($p > 0.05$). Meanwhile, the ratio of Firmicutes/Bacteroidetes in LC group increased by 23.31% and 43.98% compared to the HC and MC ($p < 0.05$) groups, respectively.

At the genus level, the most abundant phylotypes were *Barnesiella*, *Bacteroides*, *Alistipes*, *Faecalibacterium*, and *Clostridium* XIVa, which accounted for 29.48%, 24.19%, 4.59%, 2.33%, and 1.92% of the cecal microbiota of the MC group, respectively (Fig. S3). The remarkable alteration of dominant microbiota at the genus level was noticed between the the HC, MC, and LC groups (Fig. 3). In comparison to MC group, HC group manifested the decrease of 11.12% in the relative abundance of *Barnesiella* ($p < 0.01$), and *Alistipes* (1.34%, $p < 0.01$), as well as increase of *Escherichia/Shigella* by 1.28% ($p < 0.05$), *Phascolarctobacterium* (1.21%, $p < 0.05$), *Parabacteroides* (1.58%, $p < 0.001$), and *Enterococcus* (0.67%, $p < 0.01$). The LC group also exhibited considerable changes, including a 15.11% decrease in the relative abundance of *Barnesiella* ($p < 0.001$), a 2.38% increase in that of *Faecalibacte-*

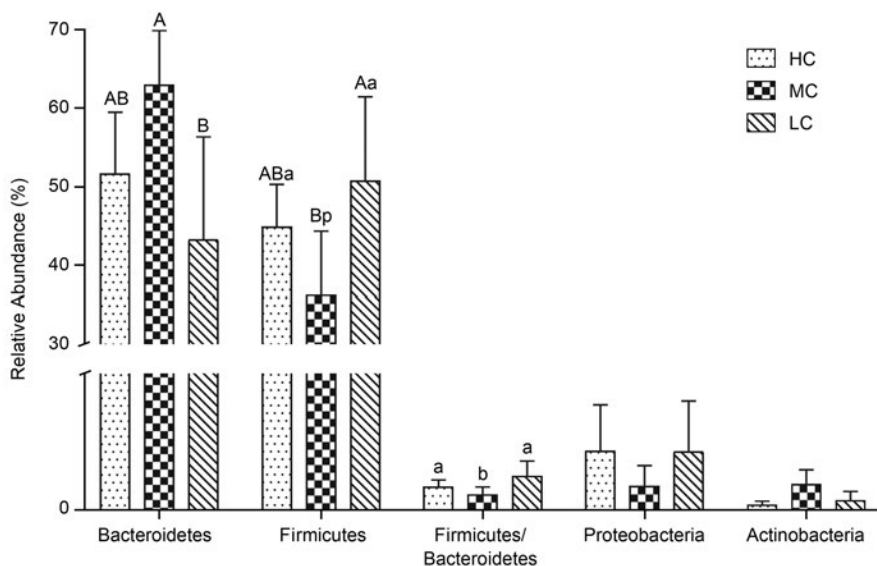


Fig. 2. Composition of the dominant microbiome at the phylum level. Different uppercase and lowercase letters indicate significant differences at $p < 0.01$ and $p < 0.05$, respectively. The same letters indicate no significant difference.

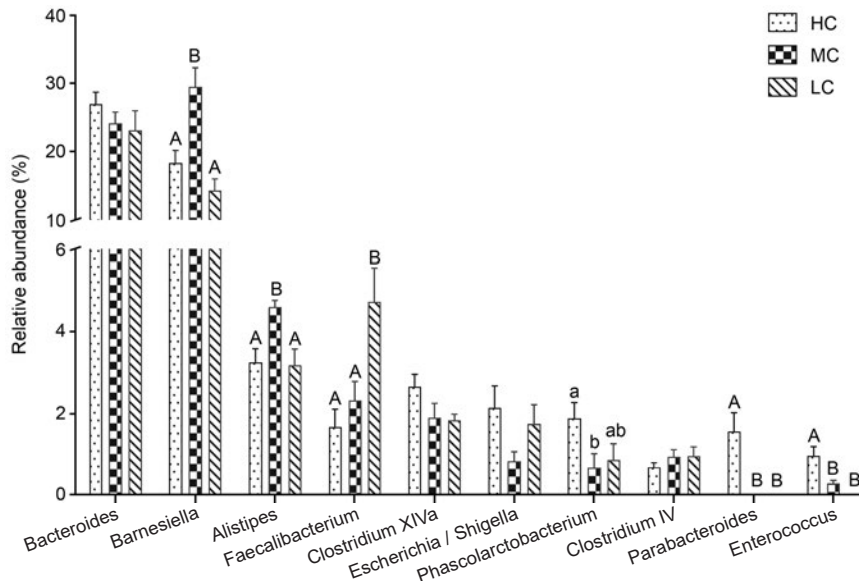


Fig. 3. Composition of the dominant microbiome at the genus level. Different uppercase and lowercase letters indicate significant differences at $p < 0.01$ and $p < 0.05$, respectively. The same letters indicate no significant difference.

rium ($p < 0.01$), and a 1.39% decrease in that of *Alistipes* ($p < 0.01$), respectively.

The effects of temperature stress on the caecal microbial communities. PCA analysis revealed a clear separation of the community structure of caecal microbiota in the three groups (Fig. 4), indicating that the high- and low-temperature treatments principally affected the microbial composition.

LefSe revealed that the three phyla (Bacteroidetes, Actinobacteria, and Proteobacteria) enriched in the MC group included three classes (Bacteroidia, Actinobacteria, and Deltaproteobacteria), four orders (Bacteroidales, Coriobacteriales, Bifidobacteriales, and Actinomycetales), five families (Porphyromonadaceae, Rikenellaceae, Coriobacteriaceae, Bifidobacteriaceae, and Oxalobacteraceae) and three genera (*Barnesiella*, *Alistipes*, and *Bifidobacterium*). Then, three major phyla (Bacteroidetes, Firmicutes, and Proteobacteria) from the LC group consisted of two classes (Clostridia and Betaproteobacteria), two orders (Clostridiales and Burkholderiales), three families (Burkholderiaceae, Brucellaceae, and Prevotellaceae), nine genera (*Faecalibacterium*, *Veillonella*, *Pandora*, *Lactococcus*, *Pseudochrobacterium*, *Oscillibacter*, *Prevotella*, *Anaerostipes*, and *Subdoligranulum*). Lastly, two dominant phyla (Bacteroidetes and Firmicutes) were found in the HC group, which were comprised of two classes (Bacilli and Erysipelotrichia), two orders (Lactobacillales and Erysipelotrichales), two families (Enterococcaceae and Erysipelotrichaceae), and five genera (*Parabacteroides*, *Enterococcus*, *Erysipelotrichaceae incertae sedis*, *Butyrivococcus*, and *Turicibacter*) (Fig. 5). We suggested that the temperature stress greatly influences the composition of the broilers' caecal microbiota.

The effects of temperature stress on the microbial functions of caecal microbiota. We observed a striking difference in the KEGG Orthologs (KO) composition of the caecal microbiota.

There were 328 differentially enriched KEGG pathways at the L3 hierarchy between the three groups, among which 41 pathways had $LDA > 2$ (Fig. 6). The pathways enriched in the LC group were related to cellular processes and signaling (e.g. sporulation, signal transduction mechanisms), metabolism (e.g., porphyrin and chlorophyll metabolism, propanoate metabolism, valine, leucine, and isoleucine biosynthesis, fatty acid biosynthesis, and lipid biosynthesis), and gene regulation (e.g., sulfur relay system, transcription factors). The pathways enriched in the HC group were related to environmental information processing (e.g., ABC transporters, G protein-coupled receptors, phosphotransferase system, and transporters) and metabolism (e.g. methane metabolism, and pyruvate metabolism). The pathways enriched in the MC group were related to metabolism (e.g. other glycan degradation, alanine, aspartate, and glutamate metabolism, purine metabolism, sphingolipid metabolism, lipopolysaccharide biosynthesis, ubiquinone and other terpenoid-quinone biosynthesis, pyrimidine metabolism, streptomycin biosynthesis, citrate acid cycle, cyanoamino acid metabolism, carbon fixation in photosynthetic organisms, phenylpropanoid biosynthesis, polyketide sugar unit biosynthesis, carbon fixation pathways in prokaryotes, prenyltransferases, one carbon pool by folate, and amino acid related enzymes), cellular processes (e.g. lysosome, peroxisome), and gene regulation (e.g. chaperones and folding catalysts, RNA degradation, and protein processing in the endoplasmic reticulum).

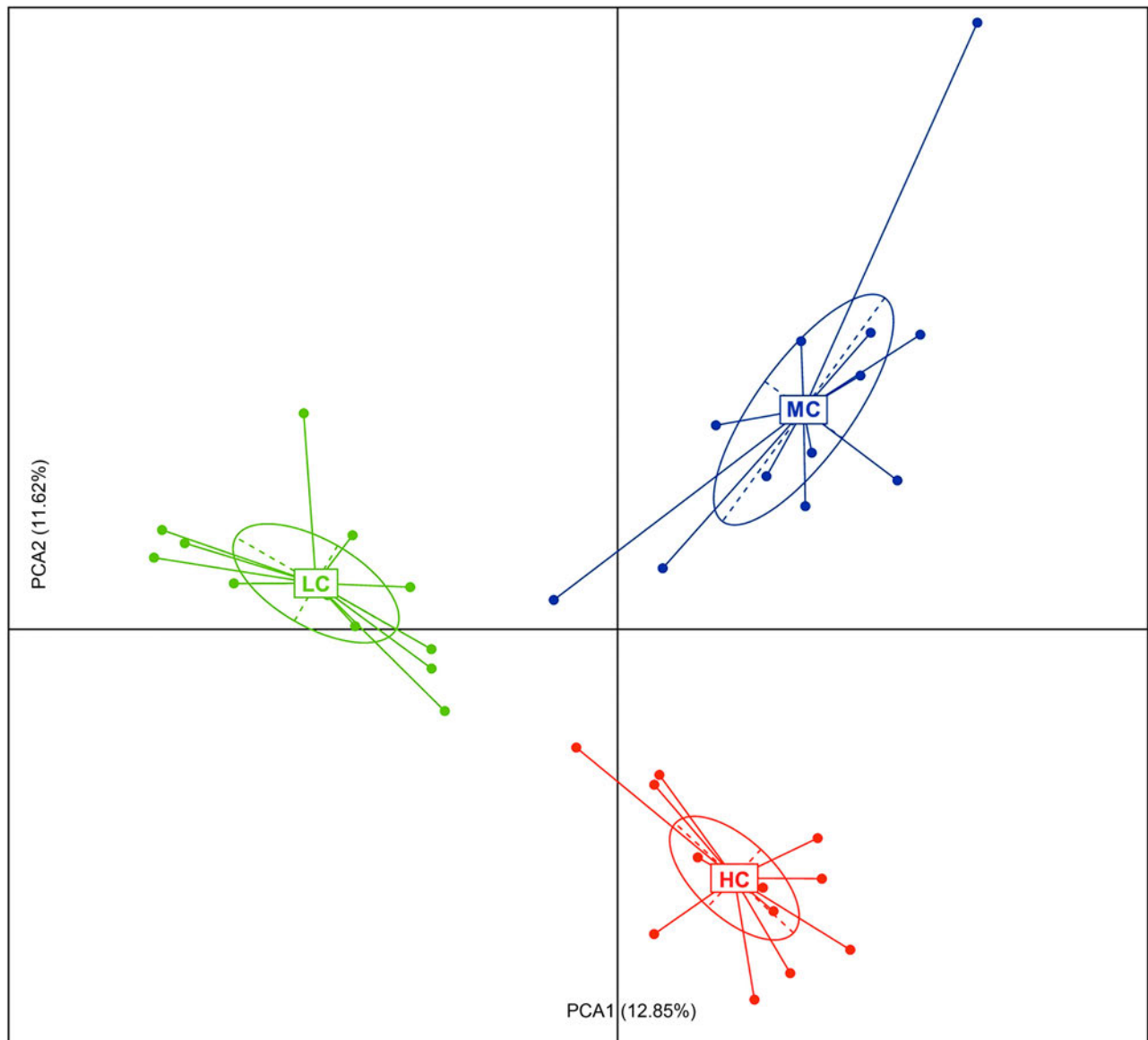


Fig. 4. The effects of ambient temperatures on the caecal microbial communities. Principal component analysis (PCA) of the abundance profiling of microbes based on OTUs.

Discussion

Temperature stress causes huge losses to poultry producers (Attia et al. 2011), as stresses from low or high temperatures exerted wide-ranging effects on host physiochemical and immune responses (Thaxton 1978). On the one hand, long-term exposure of poultry to high and low environmental temperatures had markedly increased feed consumption and the ratio of feed gain, while low temperature decreased chickens' final body weight (Yang et al. 2020). On the other hand, both heat and cold stresses could influence the immune responses, such as depression of immune and endocrine functions, elevated expression of heat shock proteins (Hsps), and upregulation of inflammatory genes (such as NF- κ B and TNF- α) (Hangalapura et al. 2004; Zhao et al. 2014). Also, increased gene expression of Hsps and NF- κ B was

reported to be associated with inflammation activation (Vidal Martins et al. 2016; Chebotareva et al. 2020). It was previously reported that cold stress could enhance the cytokine expression levels of IL-6 and TNF- α in humans (Rhind et al. 2001). The Hsp70 mRNA level in the pigs' muscle increased after exposure to continuous high environmental temperature ($35^{\circ}\text{C} \pm 1^{\circ}\text{C}$) (Abdelnour et al. 2019). In the present study, the Hsp70 and Hsp90 mRNA expression increased in HC and LC groups, while higher NF- κ B 1, IL-6, and TNF- α mRNA expression in the LC group was observed in the MC group. Consequently, our results were consistent with previous findings that both long-term heat and cold stress increased liver inflammation of broilers.

Firmicutes, Bacteroidetes, and Proteobacteria are the most dominant phyla in chickens' caecal microbiota (Luo et al. 2013; Oakley et al. 2018), which was

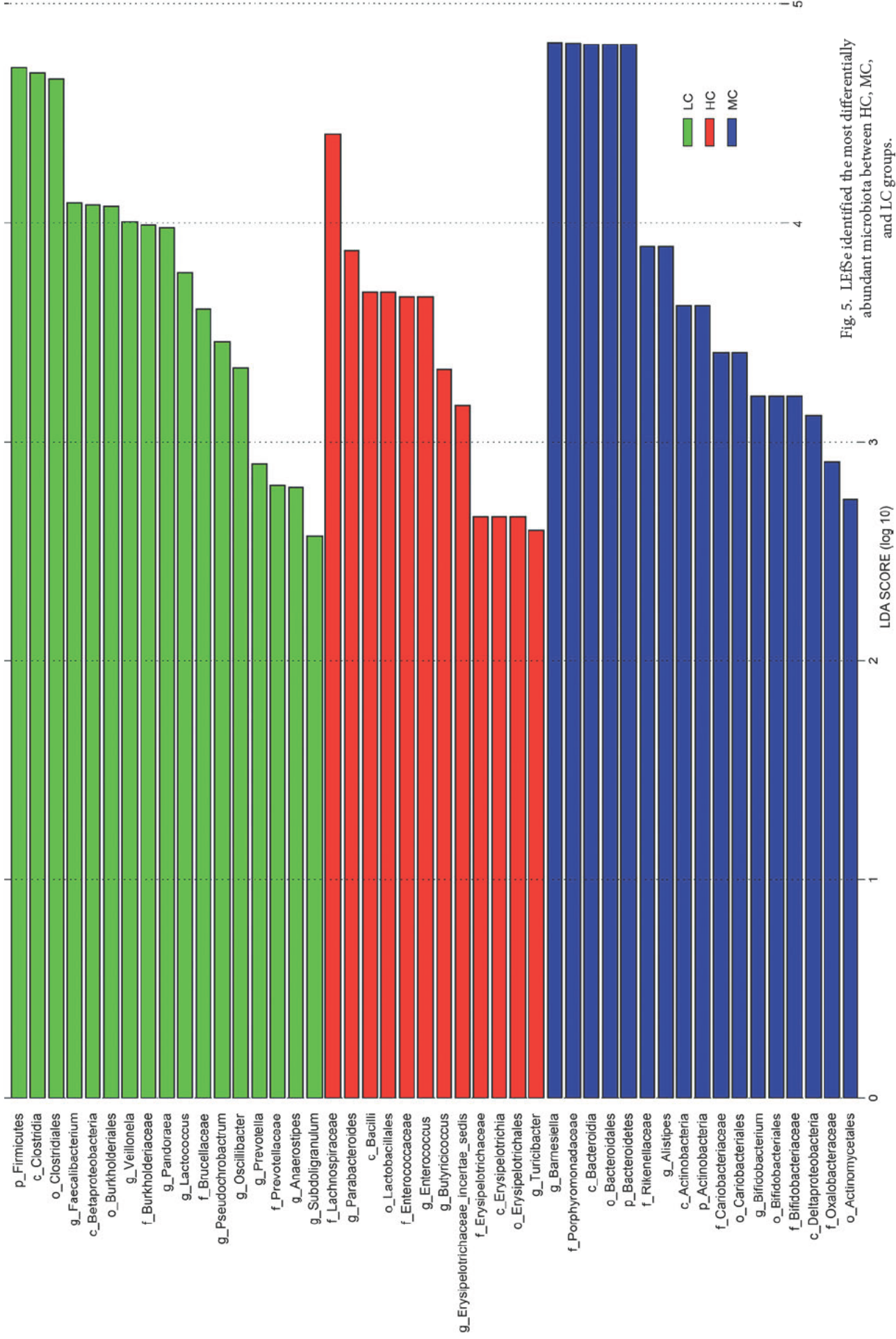


Fig. 5. LEfSe identified the most differentially abundant microbiota between HC, MC, and LC groups.

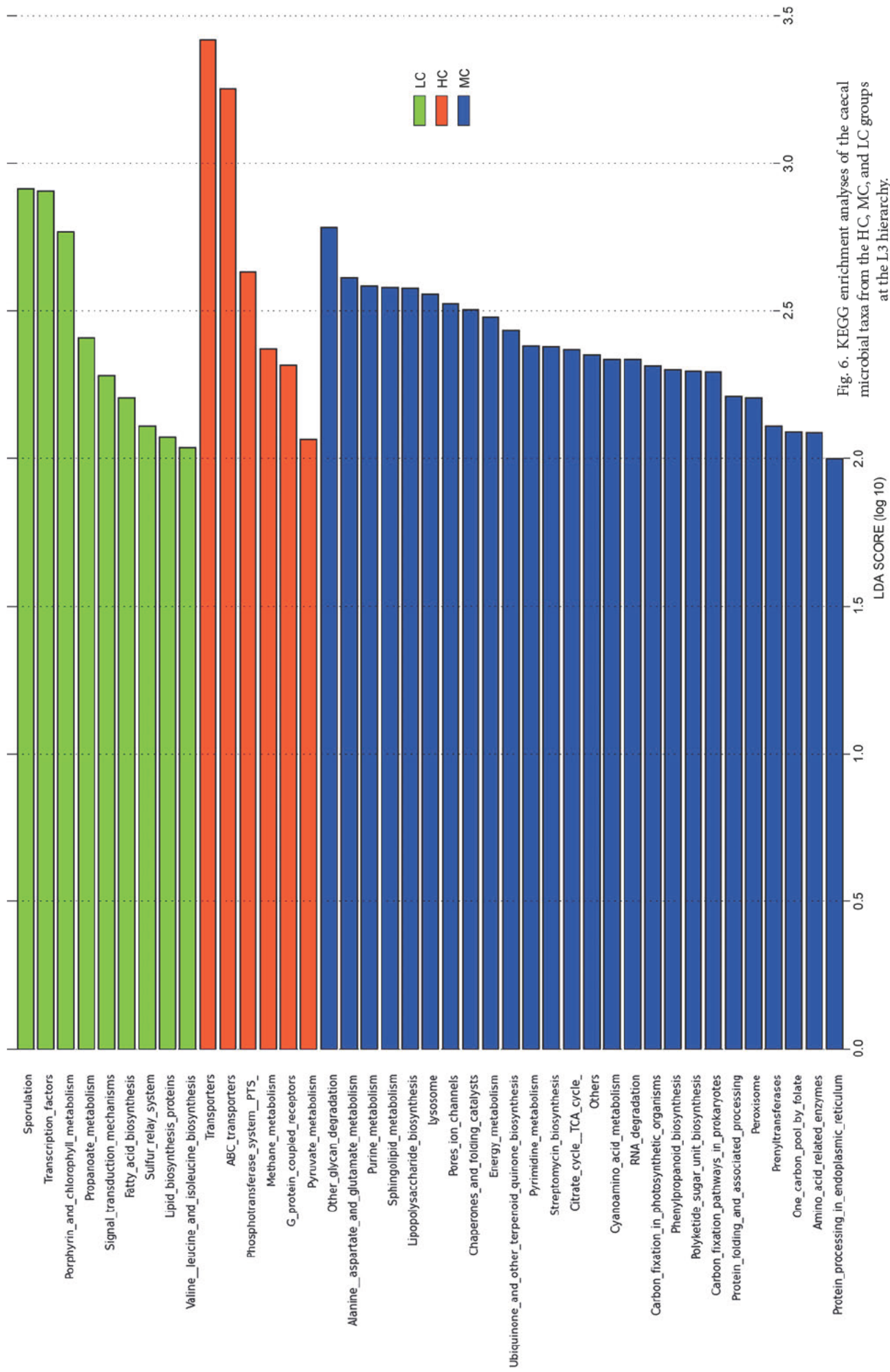


Fig. 6. KEGG enrichment analyses of the caecal microbial taxa from the HC, MC, and LC groups at the L3 hierarchy.

corroborated by our data from the MC group. Firmicutes is one of the most abundant phyla of the broilers' gut microbiome (Corrigan et al. 2011; Hume et al. 2011). Many Firmicutes species are involved in nutrient absorption (Komaroff 2017), and some microbes can survive under extreme conditions (Filippidou et al. 2016). A mouse study revealed that fecal microbial composition changed when the animals were exposed to a cold environment (6°C), during which the relative abundance of Firmicutes increased from 19% to 61%, whereas that of Bacteroidetes decreased from 73% to 35% (Chevalier et al. 2015). In this study, Firmicutes was significantly increased by 9% and 15% in the HC and LC groups, respectively, in comparison with the MC group. These findings suggest that the increase in the proportion of Firmicutes is probably a consequence of the chickens' physiological adaptations to the temperature stress.

Bacteroides, which belong to Bacteroidetes are generally associated with the degradation of polysaccharides, especially starch and glucans, and the production of short-chain fatty acids (Beckmann et al. 2006). It has been shown that *Bacteroides* was the most abundant genus in the caecum (Saxena et al. 2016), in line with the findings from our present study. *Faecalibacterium prausnitzii* in the genus *Faecalibacterium* is one of the most abundant and important symbiotic bacteria of the human intestinal microflora producing butyrate and other short-chain fatty acids through the fermentation of dietary fiber, and thus improve the intestinal tract immune function (Ferreira-Halder et al. 2017). The abundances of *Faecalibacterium* in the LC group increased compared with that in the MC group. Therefore, changes in the relative abundances *Faecalibacterium* may help utilize intestinal nutrients, maintain immune function, and further alleviate the adverse effects of long-term low environmental temperature on broilers.

Barnesiella is a genus in the family of Porphyromonadaceae, and is associated with hyperglycemia, insulin resistance, hepatic steatosis, and inflammation in rodents (Le Roy et al. 2013). *Barnesiella* is also one of the most abundant genera in human feces and can be used to treat vancomycin-resistant *Streptococcus faecalis* colonization (Wylie et al. 2012). In addition, it has been reported that *Barnesiella intestinihominis* from *Barnesiella* is an intestinal symbiotic bacteria, which can change the tumor microenvironment, reduce regulatory T cells, stimulate the anti-cancer immunomodulator cyclophosphamide (CTL) reaction, and further promote the antitumor efficacy of cyclophosphamide (CTX) (Daillère et al. 2016). In the present study, the relative abundances of *Barnesiella* in HC and LC groups were significantly lower than in the MC group, indicating *Barnesiella* as one of the

most abundant genera in broilers, with its abundance influenced by both heat and cold stresses.

In the present study, the proportion of *Escherichia/Shigella* and *Enterococcus* increased in HC group compared to that in the MC group. Both *Enterococcus* and *Escherichia/Shigella* are potentially harmful bacteria from Enterobacteriaceae family (Kong et al. 2019). *Enterococcus faecalis* is a common commensal organism in humans' intestines, which can damage eukaryotic cellular DNA in colonic epithelial cells by producing extracellular superoxides and hydroperoxides (Jones et al. 2008). Also, the percentage of *Salmonella* in Enterobacteriaceae was reported higher in heat-stressed birds than that in the control group (Alhenaky et al. 2017), and the increases of Enterobacteriaceae may be related to mice diarrhea (Yuan et al. 2018). Therefore, *Escherichia/Shigella* and *Enterococcus* may trigger inflammation through elevated Hsps and inflammatory genes.

PICRUSt analysis revealed that 41 pathways were differentially enriched between the three groups. Many of the enriched pathways in the HC group were potentially related to environmental information processing and metabolism, such as ABC transporters (LDA = 3.26), G protein-coupled receptors (GPCRs, LDA = 2.32), the phosphotransferase system (PTS, LDA = 2.64) and transporters (LDA = 3.42). ABC transporters were involved in transferring a variety of substrates, including sugars, amino acids, glycans, cholesterol, phospholipids, peptides, proteins, toxins, antibiotics, and xenobiotics (Gottesman and Ambudkar 2001). GPCRs were the receptors for hormones, neurotransmitters, ions, photons, and other stimuli, comprising the essential components of communications between the intracellular and extracellular environments (Rosenbaum et al. 2009). The phosphotransferase system (PTS) catalyzed the uptake of carbohydrates and subsequent their conversion into phosphodiester (Deutscher et al. 2006). Therefore, the enhancement of environmental information processing related signal pathways in the HC group may help regulate the intestinal mucosal function and further meet broilers' metabolic needs.

Many KEGG pathways enriched in the LC group were potentially related to cellular processes and signaling, metabolism, and gene regulation. The enriched metabolism pathways in the LC group included fatty acid biosynthesis (LDA = 2.21), lipid biosynthesis proteins (LDA = 2.07), porphyrin and chlorophyll metabolism (LDA = 2.78), propanoate metabolism (LDA = 2.41), and valine, leucine, and isoleucine biosynthesis (LDA = 2.04). Previous studies suggested that cells prefer glycolysis as a rapid compensatory mechanism to meet energy requirements for adaptive thermogenic responses under cold stress (Sajjanar et al. 2019), and that maintenance of body temperature in cold-exposed animals require increased energy

intake and expenditure (Iossa et al. 2001). Our previous study demonstrated that long-term low temperature increased feed consumption but reduced body weight gain (Yang et al. 2020). Altogether, these results indicated that the microbiota in long-term cold stress might maintain the normal body temperature by elevating broilers' energy and lipid metabolism with a tradeoff of decreased growth performance.

In conclusion, our data revealed that long-term high and low temperatures elevated immune-inflammatory responses in the liver. Stresses from high temperature led to increased potentially harmful bacteria proportion (such as *Escherichia/Shigella* and *Enterococcus*) in the caecum. Also, long-term cold stress may upregulate energy and lipid metabolism to maintain broilers' normal body temperature. Therefore, avoiding unfavorable temperature is a critical factor in the maintenance of broiler birds' production, welfare, and immune status.

ORCID

Hongbin Pan <https://orcid.org/0000-0002-9289-2434>

Acknowledgments

This study was supported by the National Key R&D Program of China (2016YFD0500501).

Conflict of interest

The authors do not report any financial or personal connections with other persons or organizations, which might negatively affect the contents of this publication and/or claim authorship rights to this publication.

Literature

- Abdelnour SA, Abd El-Hack ME, Khafaga AF, Arif M, Taha AE, Noreldin AE. Stress biomarkers and proteomics alteration to thermal stress in ruminants: A review. *J Therm Biol.* 2019;79:120–134. <https://doi.org/10.1016/j.jtherbio.2018.12.013>
- Alhenaky A, Abdelqader A, Abuajamieh M, Al-Fataftah AR. The effect of heat stress on intestinal integrity and *Salmonella* invasion in broiler birds. *J Therm Biol.* 2017;70(Pt B):9–14. <https://doi.org/10.1016/j.jtherbio.2017.10.015>
- Appenheimer MM, Evans SS. Temperature and adaptive immunity. *Handb Clin Neurol.* 2018;156:397–415. <https://doi.org/10.1016/B978-0-444-63912-7.00024-2>
- Attia YA, Hassan RA, Tag El-Din AE, Abou-Shehema BM. Effect of ascorbic acid or increasing metabolizable energy level with or without supplementation of some essential amino acids on productive and physiological traits of slow-growing chicks exposed to chronic heat stress. *J Anim Physiol Anim Nutr (Berl).* 2011;95(6):744–755. <https://doi.org/10.1111/j.1439-0396.2010.01104.x>
- Beckmann L, Simon O, Vahjen W. Isolation and identification of mixed linked beta-glucan degrading bacteria in the intestine of broiler chickens and partial characterization of respective 1,3-1,4-beta-glucanase activities. *J Basic Microbiol.* 2006;46(3):175–185. <https://doi.org/10.1002/jobm.200510107>
- Burkholder KM, Thompson KL, Einstein ME, Applegate TJ, Patterson JA. Influence of stressors on normal intestinal microbiota, intestinal morphology, and susceptibility to *Salmonella* enteritidis colonization in broilers. *Poult Sci.* 2008;87(9):1734–1741. <https://doi.org/10.3382/ps.2008-00107>

- Caporaso JG, Kuczynski J, Stombaugh J, Bittinger K, Bushman FD, Costello EK, Fierer N, Peña AG, Goodrich JK, Gordon JI, et al. QIIME allows analysis of high-throughput community sequencing data. *Nat Methods.* 2010;7(5):335–336. <https://doi.org/10.1038/nmeth.f.303>
- Chebotareva N, Vinogradov A, Gindis A, Tao E, Moiseev S. Heat shock protein 90 and NFκB levels in serum and urine in patients with chronic glomerulonephritis. *Cell Stress Chaperones.* 2020;25(3):495–501. <https://doi.org/10.1007/s12192-020-01089-x>
- Chevalier C, Stojanović O, Colin DJ, Suarez-Zamorano N, Tarallo V, Veyrat-Durebex C, Rigo D, Fabbiano S, Stevanović A, Hagemann S, et al. Gut microbiota orchestrates energy homeostasis during cold. *Cell.* 2015;163(6):1360–1374. <https://doi.org/10.1016/j.cell.2015.11.004>
- Chow J, Lee SM, Shen Y, Khosravi A, Mazmanian SK. Host-bacterial symbiosis in health and disease. *Adv Immunol.* 2010;107:243–274. <https://doi.org/10.1016/B978-0-12-381300-8.00008-3>
- Corrigan A, Horgan K, Clipson N, Murphy RA. Effect of dietary supplementation with a *Saccharomyces cerevisiae* mannan oligosaccharide on the bacterial community structure of broiler cecal contents. *Appl Environ Microbiol.* 2011;77(18):6653–6662. <https://doi.org/10.1128/AEM.05028-11>
- Daillère R, Vétizou M, Waldschmitt N, Yamazaki T, Isnard C, Poirier-Colame V, Duong CPM, Flament C, Lepage P, Roberti MP, et al. *Enterococcus hirae* and *Barnesiella intestinihominis* facilitate cyclophosphamide-induced therapeutic immunomodulatory effects. *Immunity.* 2016;45(4):931–943. <https://doi.org/10.1016/j.immuni.2016.09.009>
- Deutscher J, Francke C, Postma PW. How phosphotransferase system-related protein phosphorylation regulates carbohydrate metabolism in bacteria. *Microbiol Mol Biol Rev.* 2006;70(4):939–1031. <https://doi.org/10.1128/MMBR.00024-06>
- Ferreira-Halder CV, Faria AVS, Andrade SS. Action and function of *Faecalibacterium prausnitzii* in health and disease. *Best Pract Res Clin Gastroenterol.* 2017;31(6):643–648. <https://doi.org/10.1016/j.bpg.2017.09.011>
- Filippidou S, Wunderlin T, Junier T, Jeanneret N, Dorador C, Molina V, Johnson DR, Junier P. A combination of extreme environmental conditions favor the prevalence of endospore-forming Firmicutes. *Front Microbiol.* 2016;7:1707. <https://doi.org/10.3389/fmicb.2016.01707>
- Gottesman MM, Ambudkar SV. Overview: ABC transporters and human disease. *J Bioenerg Biomembr.* 2001;33(6):453–458. <https://doi.org/10.1023/a:1012866803188>
- Hangalapura BN, Nieuwland MG, Buysse J, Kemp B, Parmentier HK. Effect of duration of cold stress on plasma adrenal and thyroid hormone levels and immune responses in chicken lines divergently selected for antibody responses. *Poult Sci.* 2004;83(10):1644–1649. <https://doi.org/10.1093/ps/83.10.1644>
- Hou Q, Kwok LY, Zheng Y, Wang L, Guo Z, Zhang J, Huang W, Wang Y, Leng L, Li H, et al. Differential fecal microbiota are retained in broiler chicken lines divergently selected for fatness traits. *Sci Rep.* 2016;6:37376. <https://doi.org/10.1038/srep37376>
- Hume ME, Barbosa NA, Dowd SE, Sakomura NK, Nalian AG, Martynova-Van Kley A, Oviedo-Rondón EO. Use of pyrosequencing and denaturing gradient gel electrophoresis to examine the effects of probiotics and essential oil blends on digestive microflora in broilers under mixed *Eimeria* infection. *Foodborne Pathog Dis.* 2011;8(11):1159–1167. <https://doi.org/10.1089/fpd.2011.0863>
- Iossa S, Lionetti L, Mollica MP, Crescenzo R, Barletta A, Liverini G. Effect of cold exposure on energy balance and liver respiratory capacity in post-weaning rats fed a high-fat diet. *Br J Nutr.* 2001;85(1):89–96. <https://doi.org/10.1079/bjn2000219>
- Jones BV, Begley M, Hill C, Gahan CG, Marchesi JR. Functional and comparative metagenomic analysis of bile salt hydrolase activ-

- ity in the human gut microbiome. *Proc Natl Acad Sci USA*. 2008; 105(36):13580–13585. <https://doi.org/10.1073/pnas.0804437105>
- Komaroff AL**. The microbiome and risk for obesity and diabetes. *JAMA*. 2017;317(4):355–356. <https://doi.org/10.1001/jama.2016.20099>
- Kong C, Gao R, Yan X, Huang L, Qin H**. Probiotics improve gut microbiota dysbiosis in obese mice fed a high-fat or high-sucrose diet. *Nutrition*. 2019;60:175–184. <https://doi.org/10.1016/j.nut.2018.10.002>
- Langille MG, Zaneveld J, Caporaso JG, McDonald D, Knights D, Reyes JA, Clemente JC, Burkpile DE, Vega Thurber RL, Knight R, et al.** Predictive functional profiling of microbial communities using 16S rRNA marker gene sequences. *Nat Biotechnol*. 2013;31(9):814–821. <https://doi.org/10.1038/nbt.2676>
- Lara LJ, Rostagno MH**. Impact of heat stress on poultry production. *Animals (Basel)*. 2013;3(2):356–369. <https://doi.org/10.3390/ani3020356>
- Le Roy T, Llopis M, Lepage P, Bruneau A, Rabot S, Bevilacqua C, Martin P, Philippe C, Walker F, Bado A, et al.** Intestinal microbiota determines development of non-alcoholic fatty liver disease in mice. *Gut*. 2013;62(12):1787–1794. <https://doi.org/10.1136/gutjnl-2012-303816>
- Li X, Cao Z, Yang Y, Chen L, Liu J, Lin Q, Qiao Y, Zhao Z, An Q, Zhang C, et al.** Correlation between jejunal microbial diversity and muscle fatty acids deposition in broilers reared at different ambient temperatures. *Sci Rep*. 2019;9(1):11022. <https://doi.org/10.1038/s41598-019-47323-0>
- Livak KJ, Schmittgen TD**. Analysis of relative gene expression data using real-time quantitative PCR and the 2^{(-Delta Delta C(T))} method. *Methods*. 2001;25(4):402–408. <https://doi.org/10.1006/meth.2001.1262>
- Luo YH, Peng HW, Wright AD, Bai SB, Ding XM, Zeng QF, Li H, Zheng P, Su ZW, Cui R, et al.** Broilers fed dietary vitamins harbor higher diversity of cecal bacteria and higher ratio of *Clostridium*, *Faecalibacterium*, and *Lactobacillus* than broilers with no dietary vitamins revealed by 16S rRNA gene clone libraries. *Poult Sci*. 2013;92(9):2358–2366. <https://doi.org/10.3382/ps.2012-02935>
- Mohd Shaufi MA, Siew CC, Chong CW, Gan HM, Ho YW**. Deciphering chicken gut microbial dynamics based on high-throughput 16S rRNA metagenomics analyses. *Gut Pathog*. 2015;7:4. <https://doi.org/10.1186/s13099-015-0051-7>
- Montoro-Dasi L, Villagra A, de Toro M, Pérez-Gracia MT, Vega S, Marin C**. Fast and slow-growing management systems: characterisation of broiler caecal microbiota development throughout the growing period. *Animals*. 2020;10(8):1401. <https://doi.org/10.3390/ani10081401>
- Oakley BB, Vasconcelos EJR, Diniz PPVP, Calloway KN, Richardson E, Meinersmann RJ, Cox NA, Berrang ME**. The cecal microbiome of commercial broiler chickens varies significantly by season. *Poult Sci*. 2018;97(10):3635–3644. <https://doi.org/10.3382/ps/pey214>
- Rhind SG, Castellani JW, Brenner IK, Shephard RJ, Zamecnik J, Montain SJ, Young AJ, Shek PN**. Intracellular monocyte and serum cytokine expression is modulated by exhausting exercise and cold exposure. *Am J Physiol Regul Integr Comp Physiol*. 2001; 281(1):R66–R75. <https://doi.org/10.1152/ajpregu.2001.281.1.R66>
- Rioja-Lang FC, Brown JA, Brockhoff EJ, Faucitano L**. A review of swine transportation research on priority welfare issues: A Canadian perspective. *Front Vet Sci*. 2019;6:36. <https://doi.org/10.3389/fvets.2019.00036>
- Rosenbaum DM, Rasmussen SG, Kobilka BK**. The structure and function of G-protein-coupled receptors. *Nature*. 2009;459(7245):356–363. <https://doi.org/10.1038/nature08144>
- Sajjanar B, Siengdee P, Trakooljul N, Liu X, Kalbe C, Wimmers K, Ponsuksili S**. Cross-talk between energy metabolism and epigenetics during temperature stress response in C2C12 myoblasts. *Int J Hyperthermia*. 2019;36(1):776–784. <https://doi.org/10.1080/02656736.2019.1639834>
- Santoro MG**. Heat shock factors and the control of the stress response. *Biochem Pharmacol*. 2000;59(1):55–63. [https://doi.org/10.1016/s0006-2952\(99\)00299-3](https://doi.org/10.1016/s0006-2952(99)00299-3)
- Saxena S, Saxena VK, Tomar S, Sapkota D, Gonmei G**. Characterisation of caecum and crop microbiota of Indian indigenous chicken targeting multiple hypervariable regions within 16S rRNA gene. *Br Poult Sci*. 2016;57(3):381–389. <https://doi.org/10.1080/00071668.2016.1161728>
- Segata N, Izard J, Waldron L, Gevers D, Miropolsky L, Garrett WS, Huttenhower C**. Metagenomic biomarker discovery and explanation. *Genome Biol*. 2011;12(6):R60. <https://doi.org/10.1186/gb-2011-12-6-r60>
- Shang Y, Kumar S, Oakley B, Kim WK**. Chicken gut microbiota: importance and detection technology. *Front Vet Sci*. 2018;5:254. <https://doi.org/10.3389/fvets.2018.00254>
- Song ZH, Cheng K, Zheng XC, Ahmad H, Zhang LL, Wang T**. Effects of dietary supplementation with enzymatically treated *Artemisia annua* on growth performance, intestinal morphology, digestive enzyme activities, immunity, and antioxidant capacity of heat-stressed broilers. *Poult Sci*. 2018;97(2):430–437. <https://doi.org/10.3382/ps/pex312>
- Sun YK, Yan XG, Ban ZB, Yang HM, Hegarty RS, Zhao YM**. The effect of cysteamine hydrochloride and nitrate supplementation on *in-vitro* and *in-vivo* methane production and productivity of cattle. *Anim Feed Sci Tech*. 2017;232:49–56. <https://doi.org/10.1016/j.anifeeds.2017.03.016>
- Thaxton P**. Influence of temperature on the immune response of birds. *Poult Sci*. 1978;57(5):1430–1440. <https://doi.org/10.3382/ps.0571430>
- Tsan MF, Gao B**. Heat shock proteins and immune system. *J Leukoc Biol*. 2009;85(6):905–910. <https://doi.org/10.1189/jlb.0109005>
- Vidal Martins M, Montezano de Carvalho IM, Magalhães Caetano MM, Lopes Toledo RC, Avelar Xavier A, De Queiroz JH**. Neuroprotective effect of *Sapucaia* nuts (*Lecythis pisonis*) on rats fed with high-fat diet. *Nutr Hosp*. 2016;33(6):1424–1429. <https://doi.org/10.20960/nh.805>
- Wang XJ, Feng JH, Zhang MH, Li XM, Ma DD, Chang SS**. Effects of high ambient temperature on the community structure and composition of ileal microbiome of broilers. *Poult Sci*. 2018;97(6):2153–2158. <https://doi.org/10.3382/ps/pey032>
- Wylie KM, Truty RM, Sharpton TJ, Mihindukulasuriya KA, Zhou Y, Gao H, Sodergren E, Weinstock GM, Pollard KS**. Novel bacterial taxa in the human microbiome. *Plos One* 2012;7(6):e35294. <https://doi.org/10.1371/journal.pone.0035294>
- Yang Y, Gao H, Li X, Cao Z, Li M, Liu J, Qiao Y, Ma L, Zhao Z, Pan H**. Correlation analysis of muscle amino acid deposition and gut microbiota profile of broilers reared at different ambient temperatures. *Anim Biosci*. 2021 Jan;34(1):93–101. <https://doi.org/10.5713/ajas.20.0314>
- Yuan L, Zhang S, Li H, Yang F, Mushtaq N, Ullah S, Shi Y, An C, Xu J**. The influence of gut microbiota dysbiosis to the efficacy of 5-fluorouracil treatment on colorectal cancer. *Biomed Pharmacother*. 2018;108:184–193. <https://doi.org/10.1016/j.biopha.2018.08.165>
- Zhao FQ, Zhang ZW, Qu JP, Yao HD, Li M, Li S, Xu SW**. Cold stress induces antioxidants and Hsps in chicken immune organs. *Cell Stress Chaperones*. 2014;19(5):635–648. <https://doi.org/10.1007/s12192-013-0489-9>

The Effects of Different Modes of Delivery on the Structure and Predicted Function of Intestinal Microbiota in Neonates and Early Infants

KAIYU PAN^{1#*}, CHENGYUE ZHANG^{2*} and JUN TIAN¹

¹ Department of Paediatrics, The First People's Hospital of Xiaoshan District, Hangzhou, China

² Xiangya School of Medicine, Central South University, Changsha, China

Submitted 14 October 2020, revised 27 December 2020, accepted 7 January 2021

Abstract

Several studies have shown that an increased risk of metabolic and immune disorders associated with cesarean section mode of delivery may exist. However, such studies have not been conducted in the Chinese population. Stool sample sequencing of the gene encoding the 16S rRNA of 82 prospectively enrolled 3- and 30–42-day-old vaginal and cesarean section delivered newborns was performed to study the composition and predicted function of the intestinal microbiota. In the samples from the 3-day-old neonates, the levels of *Escherichia-Shigella* in the two groups were similar. The genera *Bifidobacterium*, *Lactobacillus*, and *Bacteroides* were more prominent in the vaginal delivery than in the cesarean section group, which showed a predominance of *Staphylococcus*, *Streptococcus*, and *Corynebacterium*. The differences between the two groups were statistically significant ($p < 0.05$). In the samples from 30- to 42-day-old infants, *Bifidobacterium*, *Lactobacillus*, *Escherichia-Shigella*, and *Bacteroides* were the main genera present in the vaginal delivery group, while in the cesarean section delivery group; the predominant genera were *Escherichia-Shigella*, *Bifidobacterium*, *Bacteroides*, and *Staphylococcus*. Predicted functions of the vaginal delivery group revealed higher metabolic and biodegradation rates of carbohydrates, vitamins, and xenobiotics than those in the cesarean section group, which contributed to the stability of the microbiota in the former. The abundance of probiotic bacteria such as *Bifidobacterium* and *Lactobacillus*, and the negative correlation between obesity and *Bacteroides* presence were higher in vaginally delivered infants than in cesarean-delivered infants at both studied time points.

Key words: vaginal delivery, cesarean section delivery, early infants, intestinal microbiota, predicted function

Introduction

Previous studies have found that the intestinal microbiota composed of colonizing bacteria plays an important regulatory role in human metabolism, cell differentiation, and immune function (Blaser and Falkow 2009). The interaction between the intestinal microbiota and their host is mechanistically involved in health and disease pathogenesis (Hegazy et al. 2017; Smith and Ravel 2017; Meisel et al. 2018). The colonization and maturity of the intestinal microbiota are affected by various factors, such as the modes of delivery, gestational age, feeding methods, and the use of antibiotics, especially in infants and young children (Madan et al. 2016; Chu et al. 2017; Uberos 2020).

In recent years, owing to an increase in cesarean deliveries worldwide, several studies on the effects of delivery modes on the structure and predicted function of the intestinal microbiota in infants had been conducted. These studies have shown that an increased risk of metabolic disorders, such as respiratory illness, and immune disorders, such as allergies and autoimmune diseases, may be associated with the cesarean section mode of delivery (Baumfeld et al. 2018; Reyman et al. 2019). However, to the best of our knowledge, such studies have not been conducted in the Chinese population.

We sought to determine the effects of the delivery modes and their potential confounders or modifiers on the structure and predicted function of intestinal microbiota in early infants in China.

Kaiyu Pan and Chengyue Zhang contribute equally to this work and are co-first authors.

* Corresponding author: K. Pan, Department of Paediatrics, The First People's Hospital of Xiaoshan District, Hangzhou, China; **e-mail:** 804489145@qq.com

© 2021 Kaiyu Pan et al.

This work is licensed under the Creative Commons Attribution-NonCommercial-NoDerivatives 4.0 License (<https://creativecommons.org/licenses/by-nc-nd/4.0/>).

Experimental

Materials and Methods

Volunteers and samples. We enrolled 82 healthy newborns (39 boys and 43 girls), of which 51 were delivered vaginally and 31 by cesarean section. The 82 recruited infants were born between the 15th of January and the 30th of November of 2019. All infants belonged to the Han Chinese ethnicity, were born between the gestational ages of 37 and 42 weeks, presented a weight at birth of 2.5–4 kg, and did not receive perinatal antibiotics. In all cases, the time between premature rupture of membranes and delivery was less than 18 hours. There were no significant differences between the two groups in gender, gestational age, birth weight, time of premature rupture of membranes, and Hb. Cesarean section was indicated according to the expert consensus on the procedure by the National Health Commission. The detailed information is presented in Table I.

Sequencing analysis of the gene encoding the 16S rRNA was performed in stool samples on days 3 and 30–42 after delivery. The structure and predicted functions of the stool microbiota were analyzed. The rate of cesarean delivery was similar to the Chinese incidence (38.1% versus 36.7%, respectively). The Ethics Board of The First People's Hospital of Xiaoshan (2019-XS-04) approved this project, and written informed consents were obtained from all participants.

Sequencing experiment flow. Herein, 200 mg of fresh fecal samples collected by the parents were trans-

ferred to 2 ml centrifuge tubes. Next, 1 ml RNA was added to each centrifuge tube, and the samples were mixed thoroughly and incubated at 4°C for 8–12 hours before freezing at –80°C. The samples were then transported over dry ice to Bio-science (Hangzhou, Zhejiang) for 16S rRNA sequencing. The DNA extracted from the stool samples was pooled and sequenced using 1% agarose gel electrophoresis, PCR amplification, fluorescence quantification, construction, and MiSeq library sequencing.

Biological information analysis process. We sequenced the hypervariable regions of the 16S ribosomal gene from the extracted DNA. Then, an interactive cloud analysis of the diversity in the microbial community was conducted. The diversity within samples (α -diversity) and between samples (β -diversity) was evaluated using the operational taxonomic unit (OTU) table. For α -diversity measurements, the indices were calculated using the sobs index, and the significance was determined using Student's *t*-test. Phylogenetic (UniFrac) distance matrices were determined for β -diversity measurements. Community heatmaps were generated using the R package *vegan*. Cumulative distribution plots of β -diversity distances were generated using Qiime 1.9.1. Heatmap-based KEGG pathways were generated using PICRUSt 1.0.0 for the predicted function.

Statistical analysis. SPSS 22.0 software was used for statistical analysis. The Student's *t*-test was used for normal distribution data, and the Wilcoxon signed-rank test was used for non-normal distribution data

Table I
Description of 82 participants of this study.

Group	Vaginal delivery (n = 51)	Cesarean delivery (n = 31)	<i>p</i> -value
Sex (%)			0.907
Boys	24 (47.1%)	15 (48.4%)	
Girls	27 (52.9%)	16 (51.6%)	
Gestational age (w)	39.0 ± 0.9	39.2 ± 1.0	0.532
Birth weight (g)	3,091.0 ± 299.7	3,117.4 ± 260.4	0.685
Hb (g/l)	163.9 ± 12.0	161.2 ± 10.2	0.296
Premature rupture of membranes (h)	3.2 ± 2.1	3.3 ± 2.5	0.836
Feeding (%) 3-day-old			0.687
Breast-fed	24 (47.1%)	12 (38.7%)	
Mixed-fed	16 (31.4%)	10 (32.3%)	
Fomula-fed	11 (21.6%)	9 (29.0%)	
Feeding (%) 30–42-day-old			0.853
Breast-fed	21 (41.2%)	11 (35.5%)	
Mixed-fed	16 (31.3%)	10 (32.3%)	
Fomula-fed	14 (27.5%)	10 (32.3%)	

Mean ± SD for continuous variables: *p*-value was calculated by linear regression model.
% for categorical variables: *p*-value was calculated by *chi*-square test.

to compare the two groups. P -values < 0.05 were considered statistically significant.

Results

Effects of the delivery mode on the structure of intestinal microbiota. The intestinal microbiota structure of the two groups (vaginal delivery and cesarean

section) in 3-day-old neonates and 30–42-day-old infants is shown in Fig. 1 and 2, respectively. As shown in Fig. 1, in the 3-day-old neonates, there were no significant differences in the levels of *Escherichia-Shigella* in the two groups ($p > 0.05$). The genera *Bifidobacterium*, *Lactobacillus*, and *Bacteroides* were more prominent in the vaginal delivery group than the cesarean section group, which had higher levels of *Staphylococcus*, *Streptococcus*, and *Corynebacterium*. The difference

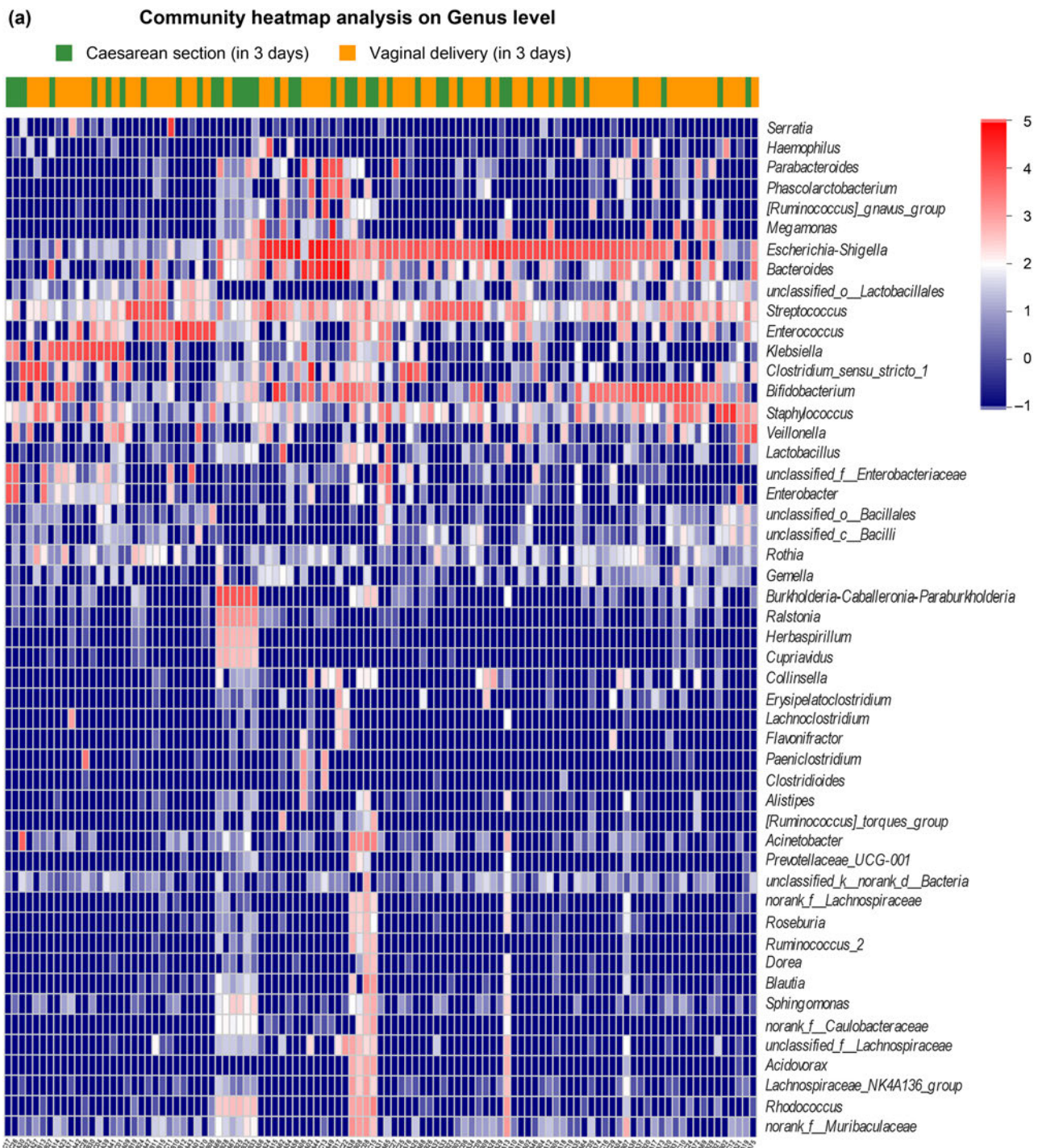


Fig. 1. Intestinal microbiota community structure of 2 groups (vaginal delivery and cesarean section) in 3 days neonates.

(A) Intestinal microbiota community heatmap analysis on the genus level of the two groups.

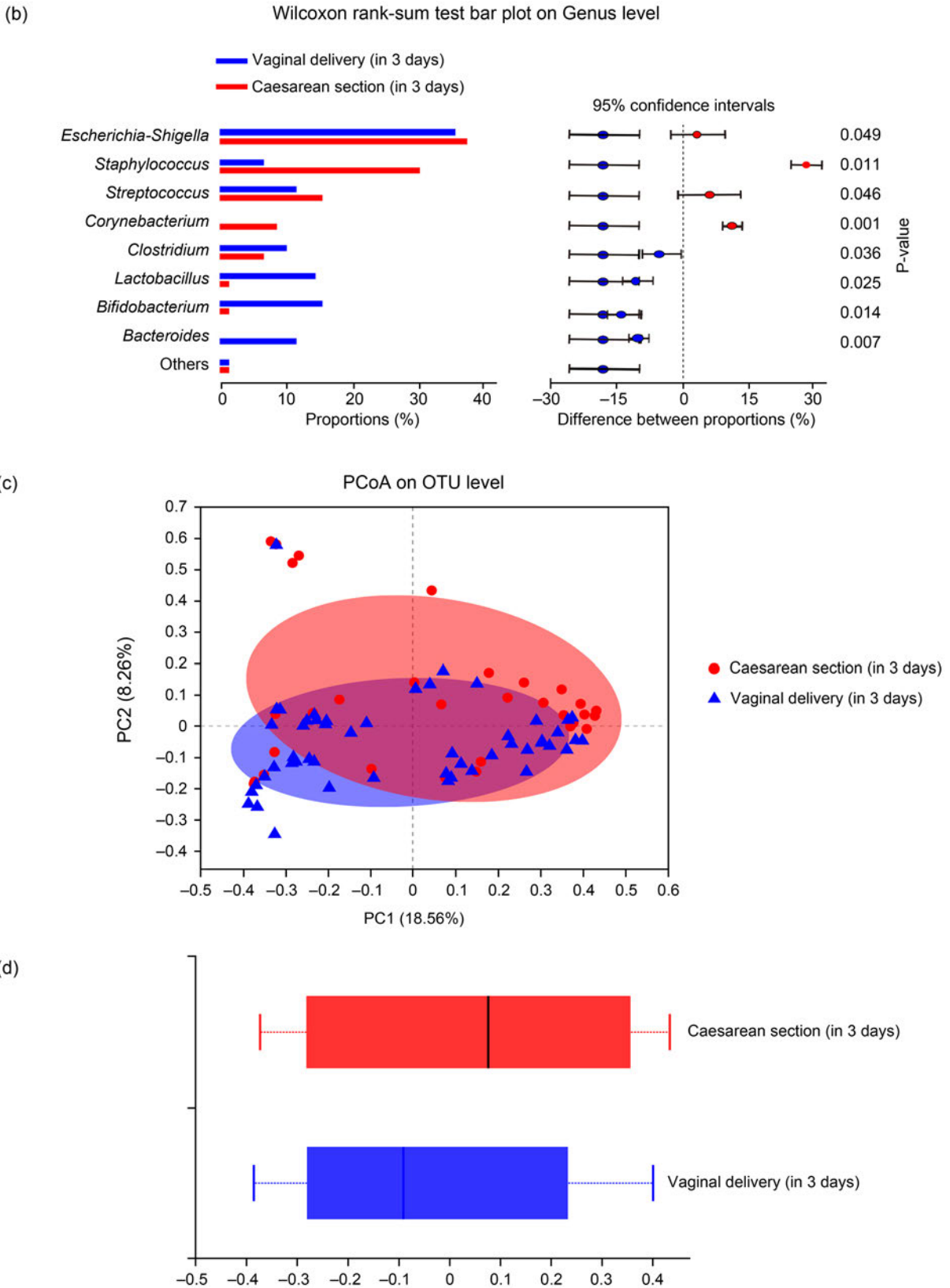


Fig. 1. Intestinal microbiota community structure of 2 groups (vaginal delivery and cesarean section) in 3 days neonates.

(B) Wilcoxon rank-sum test bar plot on the genus level between the two groups.

(C) Principal coordinate analysis (PCoA) on unweighted UniFrac distances between the neonatal microbiota is shown along the first two principal coordinates (PC) axes. Each point represents a single sample and is colored by a delivery mode: vaginal delivery, blue; cesarean section, red. The closer the two sample points are, the more similar the species composition is.

(D) PCoA box diagram. Represents the discrete distribution of different groups of samples on the PC1 axis: vaginal delivery, blue; cesarean section, red.

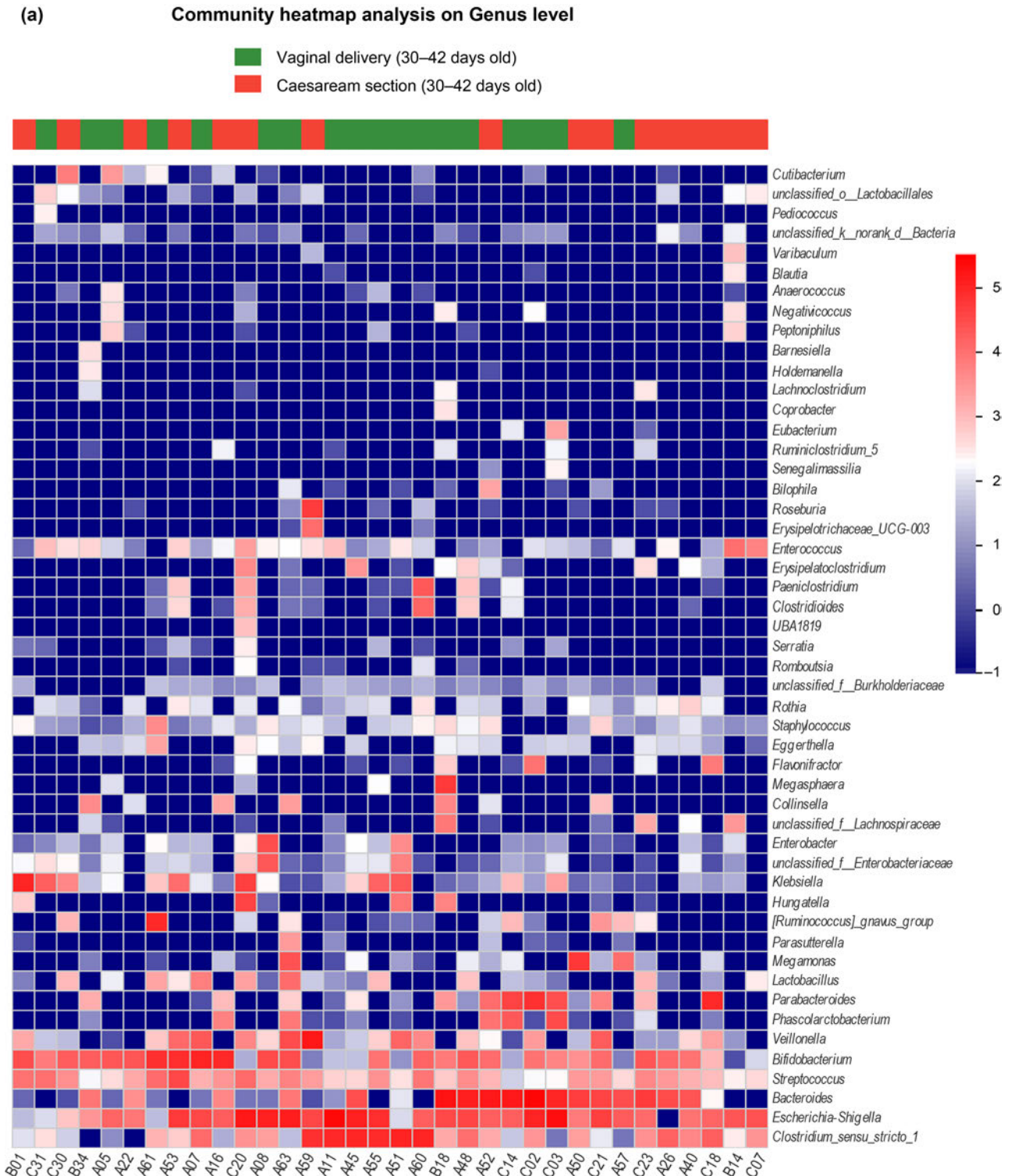


Fig. 2. Intestinal microbiota community structures of two groups (vaginal delivery and cesarean section) in 30–42 days infants.

(A) Intestinal microbiota community heatmap analysis on the genus level of the two groups.

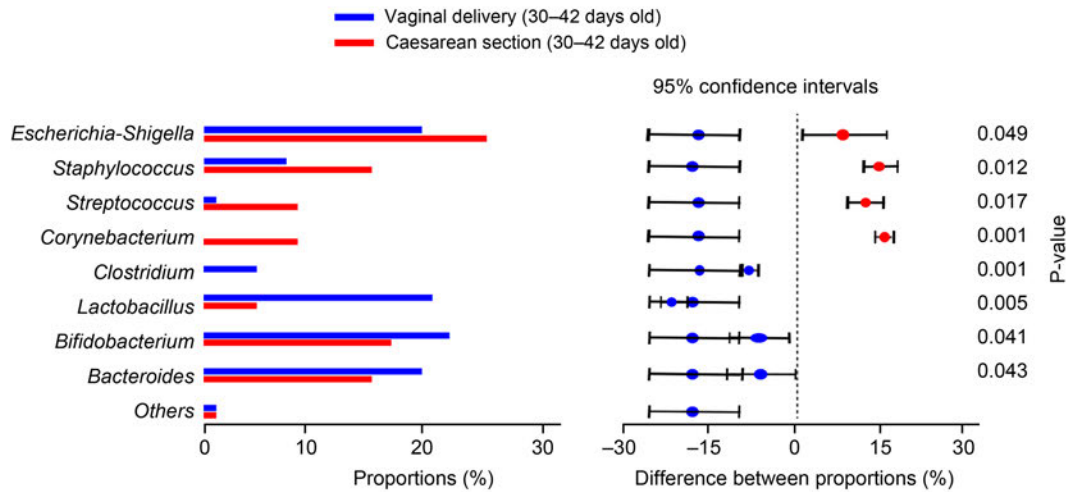
between the two groups was statistically significant ($p < 0.05$). Furthermore, as shown in Fig. 2, in the 30–42-day-old early infants, *Bifidobacterium*, *Lactobacillus*, *Escherichia-Shigella*, and *Bacteroides* were the prominent genera in the vaginal delivery group, whereas *Escherichia-Shigella*, *Bifidobacterium*, *Bacteroides*, and *Staphylococcus* were the main observed genera in the

cesarean section group. The difference between the two groups was statistically significant ($p < 0.05$).

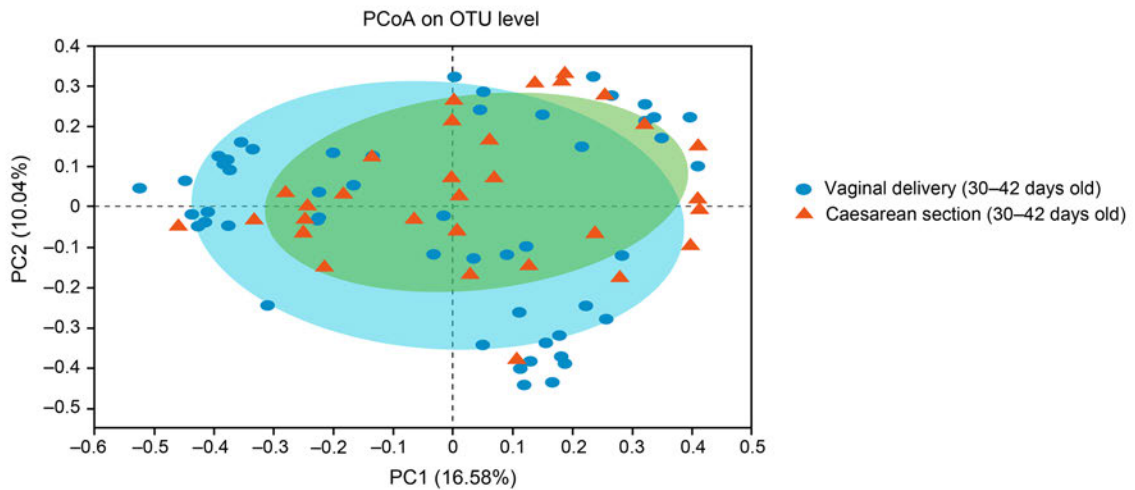
Sobs index analysis for α -diversity measurement.

The Student's *t*-test was used to calculate the significance of the intestinal microbiota's sobs index in the vaginal delivery and cesarean section groups in 3- and 30–42-day-old infants shown in Fig. 3. The microbiota

(b)

Wilcoxon rank-sum test bar plot on Genus level

(c)



(d)

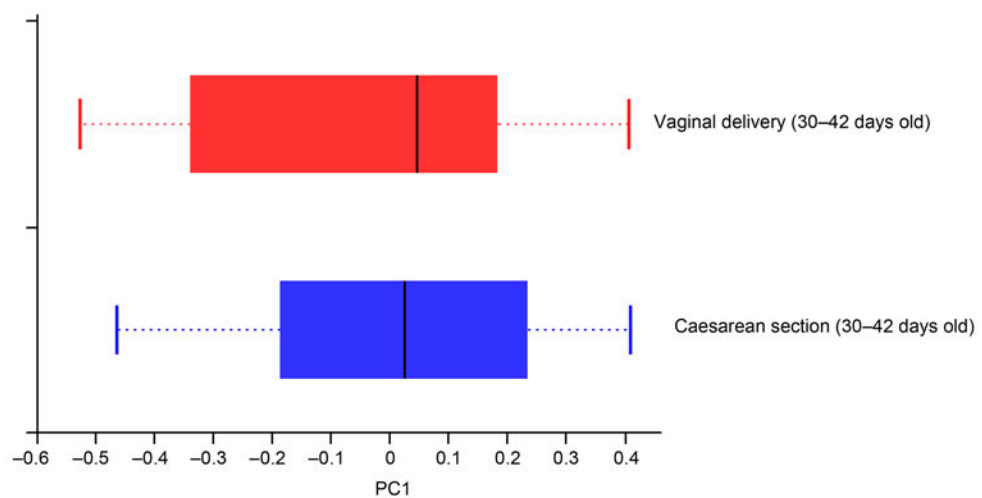


Fig. 2. Intestinal microbiota community structures of two groups (vaginal delivery and cesarean section) in 30–42 days infants.

(B) Wilcoxon rank-sum test bar plot on the genus level between the two groups.

(C) Principal coordinate analysis (PCoA) on unweighted UniFrac distances between the infants' intestinal microbiota is shown along the first two principal coordinates (PC) axes. Each point represents a single sample and is colored by delivery mode: vaginal delivery, blue; cesarean section, red. The closer the two sample points are, the more similar the species composition is.

(D) PCoA box diagram. Represents the discrete distribution of different groups of samples on the PC1 axis: vaginal delivery, red; cesarean section, blue.

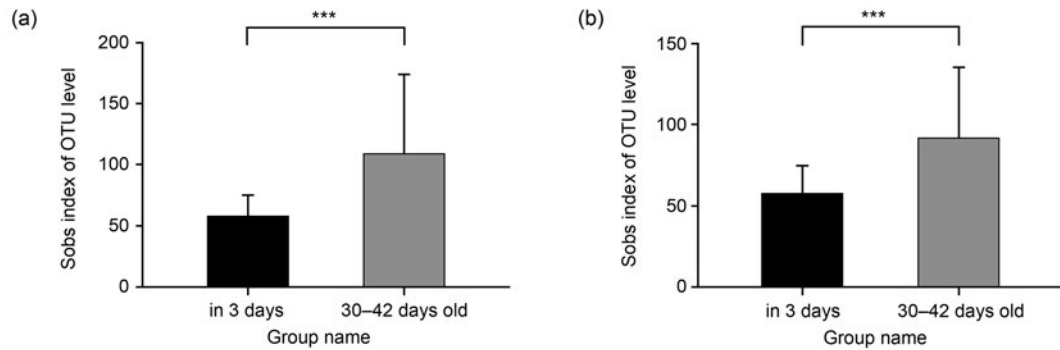


Fig. 3. Student's *t*-test for sobs index of vaginal delivery and cesarean section groups' intestinal microbiota at two points (in 3 days and 30-42 days old).

(A) Sobs index at the two points of vaginal delivery infants. (B) Sobs index at the two points of cesarean section infants.

was detected in all the stool samples from the 3-day-old neonates, but their sobs index (α -diversity) was at significantly lower levels than that of the 30-42-day-old group, irrespective of vaginal or cesarean section modes of delivery ($p < 0.001$).

Predicted function of the intestinal microbiota.

The predicted function of the intestinal microbiota of the vaginal delivery and cesarean section groups of both 3- and 30-42-day-old infants is shown in Fig. 4. Heatmap of the Kyoto Encyclopedia of Genes and Genomes (KEGG) pathway level 2 at the two points belonged to the categories that showed statistical differences between vaginal delivery and cesarean section groups. Compared to the cesarean delivery group, the vaginal delivery group presented a higher carbohydrate and vitamin metabolism level. A higher rate of biodegradation and metabolism of xenobiotics in both neonates and infants favors their microbiota community's stability.

Discussion

In this study, we found that *Escherichia-Shigella* levels were significantly high in all stool samples of the 3-day-old infants. These data confirmed previous observations on the typical microbial constituents of early infant stools at this age (Backhed et al. 2015; Nagpal et al. 2017). Previously reported OTUs were considered to be derived from the maternal stool (Chu et al. 2017). Additionally, the levels of *Escherichia-Shigella* did not vary significantly between the modes of delivery. Furthermore, we found that the delivery mode has a much more significant influence on the presence and abundance of several other notable taxa in early infants' intestinal microbiota. Accordingly, the vaginally delivered infants' intestinal microbiota has high levels of *Bifidobacterium*, *Lactobacillus*, and *Bacteroides*, whereas the cesarean section-delivered infants harbor *Staphylococcus*, *Streptococcus*, and *Corynebacterium*. In infants delivered by cesarean section, the amniotic membrane

does not rupture at birth; this prevents the mother's birth-tract flora from entering the baby. Thus, vaginally delivered infants are enriched in bacterial communities resembling those found in the maternal vagina, whereas the cesarean-section delivered infants harbor skin microbiota. In the stool samples of the vaginally delivered 30-42-day-old early infants, *Bifidobacterium*, *Lactobacillus*, *Escherichia-Shigella*, and *Bacteroides* were the prominent genera, whereas those in the cesarean section group showed a predominance of *Escherichia-Shigella*, *Bifidobacterium*, *Bacteroides*, and *Staphylococcus*. The differences in each genus's levels between the two groups were statistically significant ($p < 0.05$). Although microbiota was detected in all the first-pass stool samples, their α -diversity was relatively lower in the 3-day-old neonates than in the 30-42-day-old early infants, irrespective of the mode of delivery ($p < 0.001$). It has been previously shown that the abundance and growth of the intestinal microbiota progress with age (Chu et al. 2017). An endpoint of approximately 30-42 days postpartum was chosen because the infants at this age have limited person-to-person contact and are not yet exposed to the wide variety of environmental microbes. At 30-42 days of age, significant levels of *Bifidobacterium* and *Lactobacillus* continued to be present in the vaginally delivered infants. However, the infants delivered by cesarean section showed delayed colonization of bifidobacteria and a gradual rise in lactobacilli levels compared to those delivered vaginally (Wampach et al. 2017; Reyman et al. 2019). *Bifidobacterium* is a probiotic bacterium that promotes gut health and provides defense against pathogens (Tamburini et al. 2016). Acetate and lactate are the primary end products of bifidobacterial fermentation and important energy sources for colonocytes (Fukuda et al. 2011). Moreover, intestinal bifidobacteria produce essential nutrients, including riboflavin and folate (Sugahara et al. 2015). *Lactobacillus* is also a probiotic bacterium that regulates the gastrointestinal tract's normal microbiota and maintains the micro-ecological balance to reduce



Fig. 4. Predicted function: Heatmap of KEGG pathway level 2.

(A) Heatmap showing distinct microbial gene (KEGG pathway level 2) profiles of the two groups' stool in 3 days after delivery: vaginal delivery, red; cesarean section, green.

serum cholesterol, improve gastrointestinal function, inhibit the growth of intestinal putrefactive bacteria, and increase immune functions. The abundance of lactobacilli was lower than that of bifidobacteria in the gut of infants delivered vaginally at both time points studied; our findings are similar to those reported previ-

ously (Yang et al. 2019). Furthermore, there is evidence that *Bifidobacterium* and *Lactobacillus* supplementation has positive effects in protecting the human gut from different intestinal infections (Tamburini et al. 2016) and has also been associated with the production of beneficial metabolites (Arboleya et al. 2015).

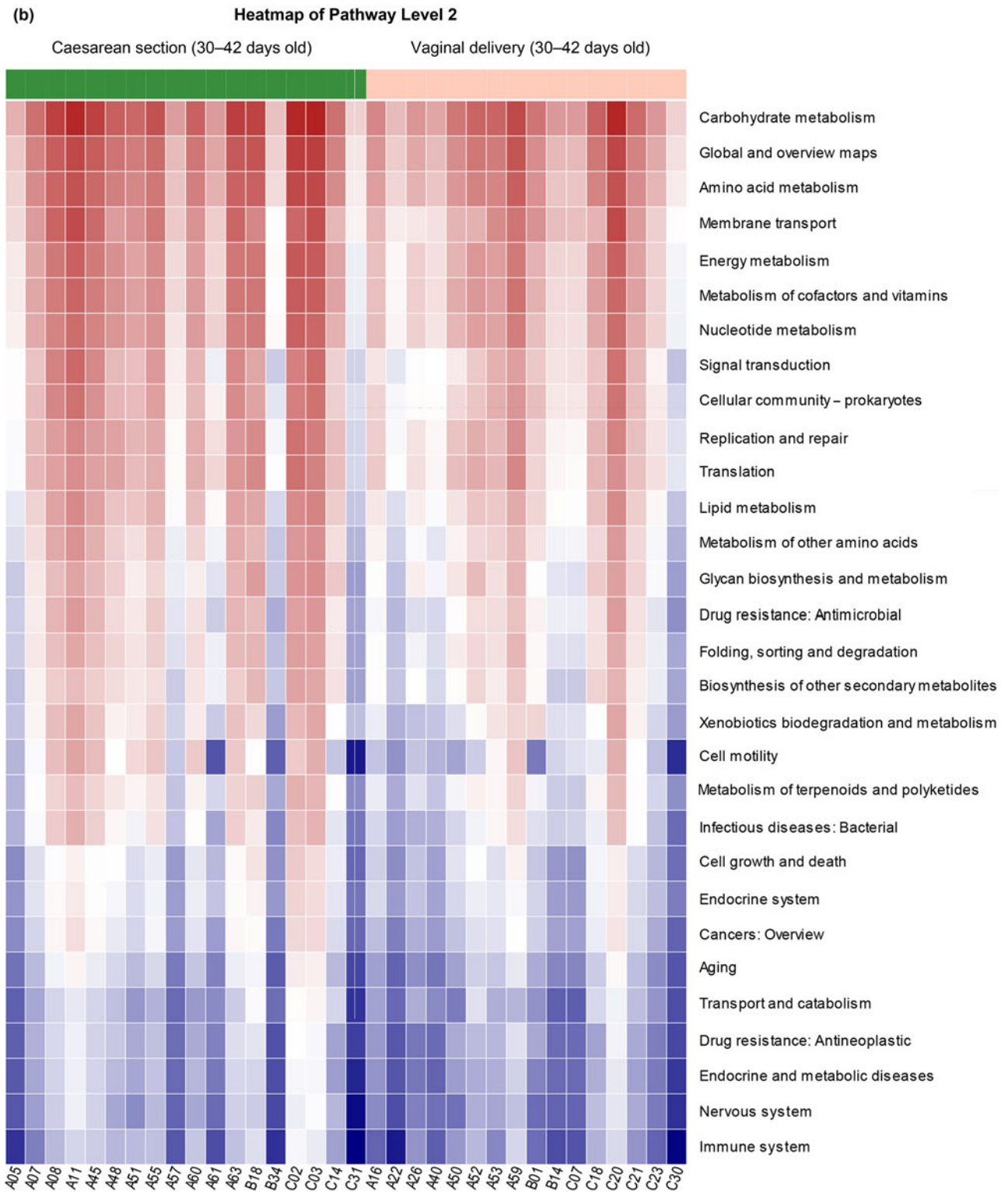


Fig. 4. Predicted function: Heatmap of KEGG pathway level 2.

(B) Heatmap showing distinct microbial gene (KEGG pathway level 2) profiles of 2 groups in 30–42 days old: vaginal delivery, green; cesarean section, red.

Bacteroides counts were low in both groups of 3-day-old neonates. This early reduction in diversity could be due to a decrease in the *Bacteroides* genus's diversity within the *Bacteroidetes* phylum (Fallani et al. 2010). As opposed to a previous study by Wopereis et al. (2014),

the stool samples of 30- to 42-day-old early infants showed significantly greater clustering of *Bacteroides* in the vaginally delivered infants than in the cesarean-delivered infants, irrespective of their ethnic factors. *Bacteroides* are efficient fermenters of human milk

oligosaccharides, which may have been underestimated in early life due to a molecular bias. Furthermore, they may protect against the development of milk allergy (Hoyles and McCartney 2009). Previous studies have also shown that *Bacteroides* in the gut are negatively correlated to obesity. Here, we showed that the *Bacteroides* levels were significantly higher in the vaginally-delivered group than in the cesarean-delivered group in the 30–42-day-old infants. These data are consistent with previous findings on the correlation with obesity (Mueller et al. 2019). The abundances of *Staphylococcus*, *Streptococcus*, and *Corynebacterium* were higher in cesarean section delivered infants than in those delivered the vaginally, and these differences between the two groups are consistent with the data on human skin microbiota (Akagawa et al. 2019). Furthermore, these genera are neutral in the intestines of infants in their early life as human symbiotic bacteria or conditional pathogens. Thus, they were not analyzed in this study.

Predicted function revealed that the vaginal delivery group presented higher levels of carbohydrate and vitamin metabolism, biodegradation and metabolism of xenobiotics, and a more stable microbiota when compared to the cesarean delivery group.

In this study, we explored the effects of different delivery modes on the structure and predicted function of intestinal microbiota in neonates and early infants in the Chinese population. Furthermore, we provided scientific data for the construction of an early infant intestinal microbiota bank in China. However, there are certainly worth noting limitations. First, the feeding habits of the infants were variable at the end of the study. The potential impact of feeding habits cannot be overruled as a factor explaining the differences observed between vaginal delivery and cesarean section groups. Second, a study by Savage et al. (2018) reported that maternal diets with a high intake of vegetables and a low intake of processed meats and deep-fried foods present a positive correlation with the *Lactobacillus* abundance in the intestinal microbiota of infants. Thus, the lack of a food frequency questionnaire about maternal diet constitutes a limitation of our study.

16S rRNA sequencing technology was chosen to study the stool samples. 16S rRNA gene is located on the small subunit of prokaryotic ribosomes, including nine hypervariable regions and ten conserved regions. The conserved regions have few differences among bacteria, and the hypervariable regions have a specificity that varies with the kinship of genus or species. Therefore, 16S rRNA can be used as a characteristic nucleic acid sequence suggesting biological species and is considered to be the most suitable indicator for bacterial phylogeny and taxonomic identification (Caporaso et al. 2011). 16S rRNA amplicon sequencing usually selects one or several mutated regions and uni-

versal primers for amplification to obtain PCR products and then performs sequencing, analysis, and strain identification. It is an important means for studying environmental samples for microbial composition and structure (Youssef et al. 2009). At present, 16S rRNA sequencing technology is widely used worldwide and is also being gradually developed in China.

Overall, we have found that the abundance of probiotic bacteria, such as *Bifidobacterium* and *Lactobacillus* in vaginally delivered infants was higher than in the infants delivered by cesarean section at both studied time points. The level of *Bacteroides* in the cesarean section group was lower than that in the vaginal delivery group; hence, the former is associated with the risk of obesity. Further follow-up is needed to monitor the growth of *Bacteroides* with age dynamically. Screening of infants, especially those delivered by cesarean section, for excess weight gain, may help guide the primordial prevention of obesity. It is suggested that long-term follow-up of growth and development should be undertaken for children delivered by cesarean section to protect against the risk of obesity. Furthermore, this study also concludes that 16S rRNA sequencing technology is effective and reliable in detecting intestinal microbiota in early infants.

ORCID

Kaiyu Pan <https://orcid.org/0000-0002-3177-6624>

Author contributions

KYP, CYZ and JT contributed to the data collection, analysis, and writing of the manuscript. KYP contributed to the study design and editing of the manuscript.

Ethical statement

The Institutional Review Board of The First People's Hospital of Xiaoshan District approved this study (Protocol Number: 2019-XS-04).

Funding

This research is supported by major scientific and technological plan projects for social development in Xiaoshan District (No. 2018201). Also is supported by Hangzhou Science and Technology Plan Guidance Project in Hangzhou city (No. 20181228Y81).

Conflict of interest

The authors do not report any financial or personal connections with other persons or organizations, which might negatively affect the contents of this publication and/or claim authorship rights to this publication.

Literature

Akagawa S, Tsuji S, Onuma C, Akagawa Y, Yamaguchi T, Yamagishi M, Yamanouchi S, Kimata T, Sekiya S, Ohashi A, et al. Effect of delivery mode and nutrition on gut microbiota in neonates. *Ann Nutr Metab.* 2019;74(2):132–139. <https://doi.org/10.1159/000496427>

- Arbolea S, Sánchez B, Milani C, Duranti S, Solís G, Fernández N, de los Reyes-Gavilán CG, Ventura M, Margolles A, Gueimonde M. Intestinal microbiota development in preterm neonates and effect of perinatal antibiotics. *J Pediatr*. 2015 Mar;166(3):538–544. <https://doi.org/10.1016/j.jpeds.2014.09.041>
- Bäckhed F, Roswall J, Peng Y, Feng Q, Jia H, Kovatcheva-Datchary P, Li Y, Xia Y, Xie H, Zhong H, et al. Dynamics and stabilization of the human gut microbiome during the first year of life. *Cell Host Microbe*. 2015 Jun;17(6):852. <https://doi.org/10.1016/j.chom.2015.05.012>
- Baumfeld Y, Walfisch A, Wainstock T, Segal I, Sergienko R, Landau D, Sheiner E. Elective cesarean delivery at term and the long-term risk for respiratory morbidity of the offspring. *Eur J Pediatr*. 2018 Nov;177(11):1653–1659. <https://doi.org/10.1007/s00431-018-3225-8>
- Blaser MJ, Falkow S. What are the consequences of the disappearing human microbiota? *Nat Rev Microbiol*. 2009 Dec;7(12):887–894. <https://doi.org/10.1038/nrmicro2245>
- Caporaso JG, Lauber CL, Walters WA, Berg-Lyons D, Lozupone CA, Turnbaugh PJ, Fierer N, Knight R. Global patterns of 16S rRNA diversity at a depth of millions of sequences per sample. *Proc Natl Acad Sci USA*. 2011 Mar 15;108 Supplement_1:4516–4522. <https://doi.org/10.1073/pnas.1000080107>
- Chu DM, Ma J, Prince AL, Antony KM, Seferovic MD, Aagaard KM. Maturation of the infant microbiome community structure and function across multiple body sites and in relation to mode of delivery. *Nat Med*. 2017 Mar;23(3):314–326. <https://doi.org/10.1038/nm.4272>
- Fallani M, Young D, Scott J, Norin E, Amarri S, Adam R, Aguilera M, Khanna S, Gil A, Edwards CA, et al. Other Members of the INFABIO Team. Intestinal microbiota of 6-week-old infants across Europe: geographic influence beyond delivery mode, breast-feeding, and antibiotics. *J Pediatr Gastroenterol Nutr*. 2010 Jul;51(1):77–84. <https://doi.org/10.1097/MPG.0b013e3181d1b11e>
- Fukuda S, Toh H, Hase K, Oshima K, Nakanishi Y, Yoshimura K, Tobe T, Clarke JM, Topping DL, Suzuki T, et al. Bifidobacteria can protect from enteropathogenic infection through production of acetate. *Nature*. 2011 Jan;469(7331):543–547. <https://doi.org/10.1038/nature09646>
- Hegazy AN, West NR, Stubbington MJT, Wendt E, Suijker KIM, Datsi A, This S, Danne C, Campion S, Duncan SH, et al. Circulating and tissue-resident CD4+ T cells with reactivity to intestinal microbiota are abundant in healthy individuals and function is altered during inflammation. *Gastroenterology*. 2017 Nov;153(5):1320–1337.e16. <https://doi.org/10.1053/j.gastro.2017.07.047>
- Hoyle L, McCartney AL. What do we mean when we refer to *Bacteroidetes* populations in the human gastrointestinal microbiota? *FEMS Microbiol Lett*. 2009 Oct;299(2):175–183. <https://doi.org/10.1111/j.1574-6968.2009.01741.x>
- Madan JC, Hoen AG, Lundgren SN, Farzan SF, Cottingham KL, Morrison HG, Sogin ML, Li H, Moore JH, Karagas MR. Association of cesarean delivery and formula supplementation with the intestinal microbiome of 6-week-old infants. *JAMA Pediatr*. 2016 Mar 01;170(3):212–219. <https://doi.org/10.1001/jamapediatrics.2015.3732>
- Meisel JS, Sfyroera G, Bartow-McKenney C, Gimblet C, Bugayev J, Horwinski J, Kim B, Brestoff JR, Tyldsley AS, Zheng Q, et al. Commensal microbiota modulate gene expression in the skin. *Microbiome*. 2018 Dec;6(1):20. <https://doi.org/10.1186/s40168-018-0404-9>
- Mueller NT, Zhang M, Hoyo C, Østbye T, Benjamin-Neelon SE. Does cesarean delivery impact infant weight gain and adiposity over the first year of life? *Int J Obes*. 2019 Aug;43(8):1549–1555. <https://doi.org/10.1038/s41366-018-0239-2>
- Nagpal R, Tsuji H, Takahashi T, Nomoto K, Kawashima K, Nagata S, Yamashiro Y. Ontogenesis of the gut microbiota composition in healthy, full-term, vaginally born and breast-fed infants over the first 3 years of life: a quantitative bird's-eye view. *Front Microbiol*. 2017 Jul 21;8:1388. <https://doi.org/10.3389/fmicb.2017.01388>
- Reyman M, van Houten MA, van Baarle D, Bosch AATM, Man WH, Chu MLJN, Arp K, Watson RL, Sanders EAM, Fuentes S, et al. Impact of delivery mode-associated gut microbiota dynamics on health in the first year of life. *Nat Commun*. 2019 Dec;10(1):4997. <https://doi.org/10.1038/s41467-019-13014-7>
- Savage JH, Lee-Sarwar KA, Sordillo JE, Lange NE, Zhou Y, O'Connor GT, Sandel M, Bacharier LB, Zeiger R, Sodergren E, et al. Diet during pregnancy and infancy and the infant intestinal microbiome. *J Pediatr*. 2018 Dec;203:47–54.e4. <https://doi.org/10.1016/j.jpeds.2018.07.066>
- Smith SB, Ravel J. The vaginal microbiota, host defence and reproductive physiology. *J Physiol*. 2017 Jan 15;595(2):451–463. <https://doi.org/10.1113/JP271694>
- Sugahara H, Odamaki T, Hashikura N, Abe F, Xiao J. Differences in folate production by bifidobacteria of different origins. *Biosci Microbiota Food Health*. 2015;34(4):87–93. <https://doi.org/10.12938/bmfh.2015-003>
- Tamburini S, Shen N, Wu HC, Clemente JC. The microbiome in early life: implications for health outcomes. *Nat Med*. 2016 Jul;22(7):713–722. <https://doi.org/10.1038/nm.4142>
- Uberos J. Perinatal microbiota: review of its importance in newborn health. *Arch Argent Pediatr*. 2020 Jun;118(3):e265–e270. <https://doi.org/10.5546/aap.2020.eng.e265>
- Wampach L, Heintz-Buschart A, Hogan A, Muller EEL, Narayanasamy S, Laczny CC, Hugerth LW, Bindl L, Bottu J, Andersson AF, et al. Colonization and succession within the human gut microbiome by archaea, bacteria, and microeukaryotes during the first year of life. *Front Microbiol*. 2017 May 02;8:738. <https://doi.org/10.3389/fmicb.2017.00738>
- Wopereis H, Oozeer R, Knipping K, Belzer C, Knol J. The first thousand days – intestinal microbiology of early life: establishing a symbiosis. *Pediatr Allergy Immunol*. 2014 Aug;25(5):428–438. <https://doi.org/10.1111/pai.12232>
- Yang B, Chen Y, Stanton C, Ross RP, Lee YK, Zhao J, Zhang H, Chen W. *Bifidobacterium* and *Lactobacillus* composition at species level and gut microbiota diversity in infants before 6 weeks. *Int J Mol Sci*. 2019 Jul 05;20(13):3306. <https://doi.org/10.3390/ijms20133306>
- Youssef N, Sheik CS, Krumholz LR, Najjar FZ, Roe BA, Elshahed MS. Comparison of species richness estimates obtained using nearly complete fragments and simulated pyrosequencing-generated fragments in 16S rRNA gene-based environmental surveys. *Appl Environ Microbiol*. 2009 Aug 15;75(16):5227–5236. <https://doi.org/10.1128/AEM.00592-09>

Antibiotic and Disinfectant Resistance in Tap Water Strains – Insight into the Resistance of Environmental Bacteria

AGATA SIEDLECKA*^{ORCID}, MIRELA J. WOLF-BACA^{ORCID} and KATARZYNA PIEKARSKA^{ORCID}

Department of Environmental Protection Engineering, Faculty of Environmental Engineering,
Wrocław University of Science and Technology, Wrocław, Poland

Submitted 24 October 2020, revised 30 December 2020, accepted 11 January 2021

Abstract

Although antibiotic-resistant bacteria (ARB) have been isolated from tap water worldwide, the knowledge of their resistance patterns is still scarce. Both horizontal and vertical gene transfer has been suggested to contribute to the resistance spread among tap water bacteria. In this study, ARB were isolated from finished water collected at two independent water treatment plants (WTPs) and tap water collected at several point-of-use taps during summer and winter sampling campaigns. A total of 24 strains were identified to genus or species level and subjected to antibiotic and disinfectant susceptibility testing. The investigated tap water ARB belonged to phyla *Proteobacteria*, *Bacteroidetes*, *Actinobacteria*, and *Firmicutes*. The majority of the isolates proved multidrug resistant and resistant to chemical disinfectant. Neither seasonal nor WTP-dependent variabilities in antibiotic or disinfectant resistance were found. Antibiotics most effective against the investigated isolates included imipenem, tetracyclines, erythromycin, and least effective – aztreonam, cefotaxime, amoxicillin, and ceftazidime. The most resistant strains originate from *Afipia* sp. and *Methylobacterium* sp. Comparing resistance patterns of isolated tap water ARB with literature reports concerning the same genera or species confirms intra-genus or even intra-specific variabilities of environmental bacteria. Neither species-specific nor acquired resistance can be excluded.

Key words: susceptibility testing, antibiograms, MIC testing, drinking water bacteria, environmental strains

Introduction

Antibiotic resistance of environmental bacteria, including bacteria dwelling in aquatic ecosystems, is a thoroughly investigated phenomenon (Baquero et al. 2008; Martinez 2009). Due to increased antibiotic consumption (ESAC-Net 2020; Roberts and Zembower 2020), antibiotic resistance is considered emerging environmental contamination (Pruden et al. 2006). Natural waters can be reservoirs of autochthonous antibiotic-resistant bacteria (ARB) and could be additionally contaminated by antibiotics, ARB and antibiotic resistance genes (ARGs) due to human activities such as wastewater effluents discharge, aquaculture, or agriculture (Berglund 2015). Antibiotic resistance determinants may not be removed entirely in water treatment plants (WTPs) and can enter distribution systems. Although tap water is commonly considered drinking water in many countries, knowledge regarding

ARB biodiversity in drinking water distribution systems (DWDSs) is still scarce.

Bai et al. (2015) found antibiotic-resistant *Bacillus* sp., *Sinorhizobium* sp., *Bradyrhizobiaceae* sp., *Comamonadaceae* sp., *Enterobacter hormaechei*, *Sphingomonas* sp., *Enterobacter* sp., and *Ensifer* sp. in finished water at WTP in Shanghai, China. Antibiotic-resistant *Proteobacteria* were frequently isolated from tap water in Porto, Portugal (Vaz-Moreira et al. 2011; 2012; 2017; Figueira et al. 2012; Narciso-da-Rocha et al. 2013; 2014). Furthermore, antibiotic-resistant *Pseudomonas* spp. were found in tap water produced from a karstic springs system during turbid events in Le Havre, France (Flores-Ribeiro et al. 2014). Khan et al. (2016a; 2016b) isolated antibiotic and disinfectant resistant *Paenibacillus*, *Burkholderia*, *Escherichia*, *Sphingomonas*, and *Dermacoccus* representatives and other bacteria possessing ARGs from tap water in Glasgow, Scotland. Antibiotic-resistant *Methylobacterium* spp. were found

* Corresponding author: A. Siedlecka, Department of Environmental Protection Engineering, Faculty of Environmental Engineering, Wrocław University of Science and Technology, Wrocław, Poland: e-mail: agata.siedlecka@pwr.edu.pl

© 2021 Agata Siedlecka et al.

This work is licensed under the Creative Commons Attribution-NonCommercial-NoDerivatives 4.0 License (<https://creativecommons.org/licenses/by-nc-nd/4.0/>).

in a nation-wide study of hospital tap water in Japan (Furuhata et al. 2006). Various ARB were identified in tap water in Wrocław, Poland, in the previous study (Leginowicz et al. 2018). Moreover, Shi et al. (2013) found intestinal ARB in finished water and tap water in Nanjing, China. According to these reports, tap water bacteria's antibiotic resistance can be regarded as a global problem that requires further research. Even if most tap water bacteria remain unculturable, culture-dependent methods should not be neglected because they could broaden the current state of knowledge regarding environmental ARB.

Resistance dissemination could be facilitated by horizontal gene transfer (HGT) within water supply networks (Shi et al. 2013; Ma et al. 2017). Moreover, subinhibitory concentrations of disinfectants were revealed to enhance the intra-genus conjugation transfer of genes (Zhang et al. 2017), suggesting the potential spread of antibiotic resistance in suboptimally chlorinated drinking water. Other findings indicated the critical role of vertical gene transfer (VGT) in this phenomenon because some ARB's resistance patterns were revealed to be species-specific (Vaz-Moreira et al. 2011; 2012; Narciso-da-Rocha et al. 2013; 2014).

The influence of ARB from drinking water on consumer health is still unclear and requires further investigation (Vaz-Moreira et al. 2014; Sanganyado and Gwenzi 2019). Swallowed bacteria have been determined to exchange genes with human intestinal microflora (Salyers et al. 2004). Moreover, Khan et al. (2020) have recently confirmed the possibility of disseminating the *mcr-1* gene, known as the last resort ARGs, from drinking water to the healthy mouse gut.

Next to being resistant to antibiotics, bacteria dwelling in drinking water have been reported to be chlorine or monochloramine tolerant (Shrivastava et al. 2004; Furuhata et al. 2007; Chiao et al. 2014; Khan et al. 2016a). Like antibiotic resistance, resistance to disinfectants could be facilitated by HGT (Stokes and Gillings 2011). A risk of co-selection of ARB associated with drinking water chlorination has been suggested (Shi et al. 2013; Pruden 2014; Proctor and Hammes 2015), although this hypothesis requires verification (Lin et al. 2016). Antibiotic and disinfectant susceptibility testing of tap water bacteria could contribute to elucidating this issue.

This study's objective was to investigate ARB dwelling in bulk tap water supplied by two independent WTPs within one DWDS during the summer and winter seasons. Next to antibiotic resistance, the resistance to disinfectants was tested. The resistance patterns of isolated strains were also compared with literature reports to gain a preliminary insight into resistance prevalence in tap water bacteria and expand knowledge in this issue.

Experimental

Materials and Methods

DWDS, sample collection, and ARB cultivation.

The DWDS in Wrocław, Poland, is primarily supplied by two independent WTPs: Na Grobli (NG) and Mokry Dwór (MD). Both WTPs (NG and MD) draw source water from the Oława and Nysa Kłodzka Rivers. In WTP NG, however, groundwater recharge is implemented as the first step of treatment, resulting in water adopting groundwater properties. WTP NG consists of the following treatment processes: groundwater recharge, aeration, filtration, ozonation, adsorption on activated carbon, pH correction, and disinfection. WTP MD consists of the following treatment processes: coagulation, filtration, ozonation, adsorption on activated carbon, pH correction, and disinfection. In both WTPs, chlorine and chlorine dioxide are used for disinfection purposes; residual chlorine is also provided in the distribution system (Siedlecka et al. 2020b).

Finished water samples from both WTPs (NG1 and MD1) and tap water samples from point-of-use taps, three in each WTP supply area (NG2, NG3, NG4 and MD2, MD3, MD4), were collected twice a season (in July and August 2018 for summer and in January and February 2019 for winter), as described previously (Siedlecka et al. 2020b). The Municipal Water and Sewerage Company kindly provided free and total residual chlorine concentrations of each water sample.

Before sample collection, each tap was disinfected and flushed until the water temperature stabilized to avoid plumbing influence. Samples were collected in sterile, plastic containers, supplemented with 0.1 g/l sodium thiosulfate (Chempur) to neutralize the disinfectants (Vaz-Moreira et al. 2017), and immediately transported to the laboratory. Then, 1 l of each sample was divided into four, and each of 250 ml aliquots was concentrated by filtration through a mixed cellulose membrane of 0.2 µm pore diameter (Whatman) with the application of a sterile filtration set (Nalgene). Next, each membrane was placed on a plate of R2A (BTL) supplemented with an antibiotic (Sigma-Aldrich), prepared following guidelines (EUCAST 2020) as presented in Table I.

These antibiotics represent the groups of high consumption rates in Poland (ESAC-Net 2020). Plates with membranes were incubated at 22°C for seven days. For quality control, *Escherichia coli* ATCC 25922 and *Pseudomonas aeruginosa* ATCC 27853 (BioMaxima) were inoculated on each prepared batch plates. Next, ARB representatives of different colony morphology (size, shape, color, opacity, surface, and texture) from various antibiotic supplemented plates, both WTPs and each sampling campaign, were selected.

Table I
R2A media supplementation for the cultivation of antibiotic-resistant bacteria (ARB) (Siedlecka et al. 2020a; 2020b).

Antibiotic (abbreviation, final concentration)	ARB
Amoxicillin (AML, 8 mg/l)	Bacteria resistant to β -lactams
Ciprofloxacin (CIP, 2 mg/l)	Bacteria resistant to fluoroquinolones
Ceftazidime (CAZ, 8 mg/l)	Bacteria resistant to 3 rd generation cephalosporins
Tetracycline (TE, 16 mg/l)	Bacteria resistant to tetracyclines

Molecular identification of strains. Each selected colony of ARB was subject to the streak-plate inoculation technique to isolate the pure strain. The bacteria were streaked on an R2A medium supplemented with the same antibiotic as previously incubated. The strains were Gram stained and observed under an optical microscope to confirm their purity, and apply the appropriate DNA extraction procedure. Next, genomic DNA was extracted with a Genomic Mini kit (A&A Biotechnology) under the manufacturer's instructions, depending on Gram-staining results. DNA concentration and purity were measured on NanoPhotometer N60 (Implen).

Nearly full 16S rRNA gene was amplified with a primer set 27F (AGAGTTTGATCMTGGCTCAG) and 1492R (TACGGYTACCTTGTACGACTT) (Siedlecka et al. 2020b). The PCR mixture consisted of: 4 μ l of 5 \times Silver Hot Start PCR Mix (Synegn), 0.4 μ l of each 10 μ M primer, 2 μ l of DNA, and 13.2 μ l of water (A&A Biotechnology). Touchdown PCR protocol was as follows: initial denaturation at 95°C for 15 min, followed by 25 cycles of denaturation at 95°C for 15 s, annealing at 55–50°C for 30 s, elongation at 72°C for 60 s, and final elongation at 72°C for 7 min. Negative control was applied to confirm the lack of contamination in the reaction. After PCR amplification, 5 μ l of each sample was mixed with 1 μ l of 6x loading buffer (A&A Biotechnology) and separated by electrophoresis in 1% agarose gel (Sigma-Aldrich) stained with Green DNA Gel Stain (Synegen). The products were electrophoresed at 120 V for 15 min, and at 80 V for 60 min in 1 \times TBE buffer and visualized by UV (UVITEC). The amplicon size was compared with DNA Marker 3 (A&A Biotechnology). The remaining products were purified with Clean-up Concentrator (A&A Biotechnology) following the manufacturer's instructions. The DNA concentration of the purified PCR products was determined using NanoPhotometer N60 (Implen) and subjected to Sanger sequencing (Genomed).

Sequences 27F and 1492R were subject to quality control and aligned with MEGA-X. The consensus of each aligned pair of strands was created with BioEdit. The obtained consensus sequences were identified with BLAST (<https://blast.ncbi.nlm.nih.gov/Blast.cgi>).

Antibiotic and disinfectant susceptibility testing.

Before susceptibility testing, each strain was transferred to Mueller-Hinton (BioMaxima) agar plate to ensure adaptation to the richer medium. Eighteen antibiotics and two disinfectants were tested through the Kirby-Bauer disk diffusion method (antibiogram). The antibiograms were prepared in accordance with guidelines (EUCAST 2020). Briefly, fresh bacterial culture was suspended in sterile saline (0.89% NaCl, Chempur) to achieve turbidity of 0.5 McFarland standard (BioMerieux). Then, the suspension was inoculated on Mueller-Hinton by swabbing three times, every time turning the plate by 60 degrees. Next, the disks containing the antibiotics (BioMaxima) were placed on plates with inoculated bacteria utilizing a dispenser (BioMaxima). The antibiotics selected for testing included (abbreviation, disk content in μ g): ampicillin (AM, 10), aztreonam (ATM, 30), ertapenem (ETP, 10), imipenem (IMP, 10) meropenem (MEM, 10), ofloxacin (OFX, 5), cefotaxime (CTX, 5), cefepime (FEP, 30), doxycycline (DO, 30), oxytetracycline (T, 30), vancomycin (VA, 30), gentamycin (CN, 30), streptomycin (S, 300), sulphamethoxazole/trimethoprim (SXT, 23.75/1.25), erythromycin (E, 15), rifampicin (RA, 5), chloramphenicol (C, 30), and polymyxin B (PB, 300). Sterile disks were simultaneously soaked in 14.5% sodium hypochlorite (Chempur), commercial disinfectant Melsept (Braun) at the working solution, and sterile water as a control and placed on plates with inoculated bacteria. All disks were placed within 15 min after inoculation of the strains on the plates. The plates were incubated at 22°C for 7 d due to the psychrophilic properties and prolonged growth of environmental bacteria. For quality control, *E. coli* ATCC 25922 and *P. aeruginosa* ATCC 27853 (BioMaxima) were subject to antibiotic susceptibility testing in the same manner. Then, the diameter of the zone of inhibition was measured for each disk. Because the guidelines for inhibition zone data interpretation are provided only for clinically relevant species, the epidemiological cut-off values (ECOFFs) taken from the EUCAST database (<https://mic.eucast.org/Eucast2/SearchController/>) were adopted for the purpose of differentiation on susceptible (criteria as for wild type) and resistant (criteria

as for non-wild type) phenotypes. EUCAST provides different ECOFFs for various species. In this study, the lowest ECOFF among those proposed by EUCAST was adopted for each antibiotic to avoid resistant phenotypes' overestimation. If no ECOFFs was provided in the EUCAST database, bacteria presenting inhibition zone diameter ≥ 10 mm were considered susceptible. In the case of disinfectant susceptibility testing, the inhibition zone diameter ≤ 20 mm was adopted to consider bacteria to be resistant, as proposed by Khan et al. (2016a).

Minimal inhibitory concentration (MIC) testing.

MIC testing was performed for four antibiotics representative of the most commonly consumed groups of antibiotics in Poland (ESAC-Net 2020), namely AML, CIP, CAZ, and TE, and two of such antibiotics with additives, i.e., AML with clavulanic acid and CAZ with avibactam. For antibiotic resistance screening, each strain was inoculated on four R2A plates supplemented with antibiotics: AML, CIP, CAZ, and TE, as described in section 2.1. Only strains able to grow on R2A in the presence of a given antibiotic were subject to further MIC testing. The strains that did not grow on R2A plates supplemented with a given antibiotic (prepared as presented in Table I) were considered sensitive, and they were not subject to MIC testing.

Each antibiotic-resistant strain was inoculated on a Mueller-Hinton plate, as described in section 2.3. Within 15 min, MIC strips (BioMaxima) were placed on the plates. The MIC strips included (abbreviation, concentration range in $\mu\text{g/ml}$): amoxicillin (AML, 0.016–256), amoxicillin with clavulanic acid (AMC, 0.016–256), ciprofloxacin (CIP, 0.002–32), ceftazidime (CAZ, 0.016–256), ceftazidime with avibactam (CZA, 0.016–256), and tetracycline (TE, 0.016–256). The plates were incubated at 22°C for 7 d due to the psychrophilic properties and prolonged growth of environmental bacteria. For quality control, *E. coli* ATCC 25922 and *P. aeruginosa* ATCC 27853 (BioMaxima) were subject to MIC testing in the same manner.

Statistical analysis. The normality of data was verified using a Shapiro-Wilk test. A Mann-Whitney *U*-test was conducted to evaluate the effect of the season (summer and winter) or WTP (NG and MD) on the total number of antibiotics to which each strain was resistant, as well as on inhibition zones of chlorine and commercial disinfectant disk diffusion testing.

Correlations between the total number of antibiotics to which each strain was resistant, and MICs results, as well as inhibition zones of chlorine and commercial disinfectant disk diffusion testing, were assessed using Spearman analysis. The significance level was set at $p < 0.05$ throughout the study. All statistical analyses were done in Microsoft Excel software (Microsoft Office 365 ProPlus).

Results and Discussion

Antibiotic and disinfectant susceptibility testing. As a result, 24 strains were isolated. The molecular identification of the strains, antibiotic and disinfectant susceptibility testing, and MIC testing are presented in Tables II, III, and IV, respectively. Free and total residual chlorine concentrations in collected tap water were in a range of 0.00 to 0.31 and 0.10 to 0.49 mg/l across the study, respectively. The data on the percentage of ARB in total bacteria, and other microbiological and physical-chemical analyses of the collected tap water samples, have been previously published (Siedlecka et al. 2020b).

The majority of bacteria belonged to the phylum *Proteobacteria* (15/24), including classes *Alphaproteobacteria* (13/24) and *Betaproteobacteria* (2/24). Representatives of *Bacteroidetes* (4/24), *Actinobacteria* (4/24), and *Firmicutes* (1/24) were also found. Unfortunately, *Caulobacter* sp. was excluded from further analyses because the strain did not grow evenly on Mueller-Hinton medium. A similar problem with tap water bacteria cultivation was reported by Khan et al. (2016a).

Some strains were identified to the same genera or species. These isolates generally presented similar resistance patterns despite their origin from different sampling points (*Achromobacter* sp., *Mycobacterium frederiksbergense*) or sampling campaigns (*Bosea massiliensis*). However, both *Sphingomonas* sp. isolates were obtained from the same sample, suggesting their affinity (the strains were primarily isolated on R2A medium supplemented with AML and CIP, respectively). Interestingly, all *Brevundimonas* isolates were isolated from WTP NG finished water. Two of them, identified as *Brevundimonas mediterranea*, from the same sample, also suggested their affinity (the strains were primarily isolated on R2A medium supplemented with AML and CAZ antibiotics, respectively).

The results of statistical analyses revealed that neither seasonal nor WTP dependent variabilities were found in the total number of antibiotics to which each strain was resistant, and inhibition zones of chlorine and commercial disinfectant disk diffusion testing. Weak but statistically significant correlations were found between the total number of ineffective drugs and AML ($\rho = 0.45$) and AMC ($\rho = 0.50$) MIC results for strains subject to MIC testing.

Among the antibiotics tested by the disk diffusion method, ATM and CTX, belonging to monobactams and 3rd generation cephalosporins groups, respectively (WHO ATC Index (https://www.whocc.no/atc_ddd_index/)), proved the least effective against the investigated bacteria, whereas all strains were susceptible to IMP. Apart from IMP, other carbapenems were not as effective against investigated strains. Tetracyclines and E also proved to be highly effective against tap water

Table II
Results of molecular identification of strains, % identity of sequence with the reference sequence in the BLAST database, accession No. of the reference sequence.

Strain No.	Origin*	Identification	% Identity	Accession
1	MD4VII(AML)	<i>Chryseobacterium</i> sp.	91.28%	MK095762.1
2	MD4VII(CIP)	<i>Bosea massiliensis</i>	100.00%	KM114964.1
3	NG1VIII(CAZ)	<i>Mycobacterium frederiksbergense</i>	99.55%	LN613126.1
4	NG1VIII(AML)	<i>Brevundimonas mediterranea</i>	99.84%	CP048751.1
5	NG2VIII(CIP)	<i>Sphingomonas sanxanigenens</i>	99.23%	KY078833.1
6	NG4VIII(CIP)	<i>Sphingomonas</i> sp.	99.69%	HM191725.1
7	NG4VIII(AML)	<i>Sphingomonas</i> sp.	99.77%	HM191725.1
8	MD2VIII(CIP)	<i>Dyadobacter</i> sp.	98.78%	MK271730.1
9	MD4VIII(CIP)	<i>Microbacterium</i> sp.	99.70%	MT542332.1
10	MD4VIII(TE)	<i>Afiptia</i> sp.	99.54%	MK402948.2
11	MD4VIII(CIP)	<i>Bosea massiliensis</i>	99.69%	MF101018.1
12	NG1I(AML)	<i>Brevundimonas mediterranea</i>	99.69%	CP048751.1
13	NG1I(CAZ)	<i>Brevundimonas mediterranea</i>	99.84%	CP048751.1
14	NG2I(CAZ)	<i>Nocardia asteroides</i>	99.85%	MT355847.1
15	NG2I(CAZ)	<i>Sphingobium abikonense</i>	98.92%	MK696981.3
16	NG3I(AML)	<i>Achromobacter</i> sp.	99.39%	KT826375.1
17	NG4I(AML)	<i>Pedobacter</i> sp.	100%	EF660750.1
18	NG4I(CAZ)	<i>Flavobacterium</i> sp.	99.32%	JQ977667.1
19	MD1I(CAZ)	<i>Bacillus zhangzhouensis</i>	95.24%	MG651160.1
20	MD3I(AML)	<i>Achromobacter</i> sp.	94.86%	KT826375.1
21	MD4I(CIP)	<i>Caulobacter</i> sp.	97.92%	KM252977.1
22	NG1II(CIP)	<i>Brevundimonas</i> sp.	99.92%	CP045456.1
23	NG3II(CAZ)	<i>Mycobacterium frederiksbergense</i>	100%	LN613126.1
24	MD3II(CAZ)	<i>Methylobacterium</i> sp.	91.84%	HM327817.1

* – sample collection site and month, where: NG refers to WTP Na Grobli, MD refers to WTP Mokry Dwór, Arabic numerals refer to consecutive sampling points (1 – finished water at each WTP, 2, 3, 4 – consecutive sampling points in the distribution system within each WTP supply area), Roman numerals refer to the month of sample collection, abbreviations in brackets refer to R2A media supplementation – the plate from which the strain was initially isolated. Strains are ordered by the month of collection.

bacteria in this study. Among the antibiotics tested by means of MIC, the least effective was CAZ, followed by AML, both belonging to β -lactam antibiotics (WHO ATC Index (https://www.whocc.no/atc_ddd_index/)). Interestingly, AML and CAZ MICs exceeded 256 mg/l for 7 and 15 strains, respectively, suggesting strong resistance of tap water bacteria to these antibiotics. Moreover, the results of MIC testing suggest that all but one (strain No. 14) strains tested for AML exhibit β -lactamase activity. The addition of clavulanic acid, known as a competitive inhibitor of β -lactamases (Kim et al. 2009), decreased effective drug concentration. Among strains tested for CAZ, 8 (i.e., strains No. 1, 5, 6, 11, 12, 15, 16, and 20) proved to be sensitive to the avibactam additive, also suggesting β -lactamase activity (Wang et al. 2016). Nevertheless, the presence and activity of β -lactamases in the strains need to be confirmed by further studies. The majority of strains

subject to AML or CAZ MIC testing (except for strains No. 15, 18, and 23) were resistant to at least one other antibiotic belonging to the β -lactam antibiotic class. All strains subject to CIP MIC testing were resistant to OFX, another representative of fluoroquinolones. Two strains resistant to TE (9 and 10) were also resistant to T and both tetracyclines used in the disk diffusion method, respectively. Contrary to the presented results, aminopenicillins and aminoglycoside resistance were reported to be common in tap water bacteria in Porto, Portugal (Vaz-Moreira et al. 2011; 2012; 2017; Narciso-da-Rocha et al. 2013). The differences in resistance of tap water bacteria in Wrocław and Porto could be region-dependent or taxon-dependent, because the other genera were investigated in these two DWDSs.

The majority of strains were resistant to 14.5% standard sodium hypochlorite, suggesting strong disinfectant resistance of tap water bacteria. However, no

Table III
Results of antibiotic and disinfectant susceptibility testing.

Strain No.	Aminopenicillins		Carbapenems			Fluoroquinolones	Cephalosporins		Tetracyclines		Glyco-peptides	Aminoglycosides		Sulfonamides	Macrolides	Others			Total	Disinfectants	
	AM	ATM	ETP	IMP	MEM	OFX	CTX	FEP	DO	T	VA	CN	S	SXT	E	RA	C	PB		Cl ₂	D
1	•	•	•		•													•	5	•	•
2		•									•								2	•	•
3		•																	1	•	•
4	•	•	•			•	•	•						•					7	•	•
5		•	•			•	•	•					•			•	•		8	•	•
6	•	•	•			•	•					•	•	•		•			9	•	•
7	•	•	•			•	•						•	•		•			8	•	•
8		•				•	•	•			•	•							6	•	•
9		•				•	•	•		•				•		•	•	•	9	•	•
10	•	•			•		•		•	•	•	•		•		•	•	•	12	•	•
11		•																	1	•	
12	•	•				•	•	•											5	•	•
13	•	•				•	•	•						•					6	•	•
14							•	•								•	•		4	•	•
15																•		•	2		
16	•						•					•				•			4	•	•
17	•	•				•	•				•	•						•	7	•	•
18																			0		
19							•												1	•	
20	•						•					•				•			4	•	•
21	-	-	-	-	-	-	-	-	-	-	-	-	-	-	-	-	-	-	-	-	-
22		•				•	•							•					4	•	•
23																			0	•	
24	•	•	•		•	•	•				•	•		•	•		•	•	12	•	•
Total	11	16	6	0	3	11	16	7	1	2	5	7	3	8	1	9	5	6			

• - resistant; - - not included in the testing

Cl₂ - 14.5% sodium hypochlorite; D - commercial disinfectant

The abbreviations of antibiotics are explained in the Materials and Methods section.

Antibiotic groups are in accordance with ATC Classification System (WHO ATC Index).

correlations were found between inhibition zones against each disinfectant and the total number of ineffective antibiotics, nor antibiotic MICs, contrary to the results of Khan et al. (2016a), who found weak (but significant) correlations between chlorine-tolerance and MIC against TE, sulphamethoxazole, and AML. Four strains (11, 19, 23, 24) resistant to 14.5% standard sodium hypochlorite were revealed to be susceptible to working solution of Melspet, suggesting that other antimicrobial agents present in commercial composition disinfectant were more effective against tap water bacteria than chlorine. The disinfectant susceptibility testing of the investigated strains suggests that resistance to strong chemical disinfectants is frequent among tap

water ARB. An approach alternative to tap water chlorination should be considered in the future. For example, in some European WTPs, treatment is based on biofiltration without final disinfection or residual disinfectant use (Proctor and Hammes 2015). It remains unknown, however, whether this approach is successful in limiting ARB prevalence in tap water.

Methylobacterium sp. and *Afipia* sp. proved resistant to the highest total number of antibiotics tested in this study using the disk diffusion method. The MIC testing results confirm the strong resistance of these two strains. On the other hand, *M. frederiksbergense* (strain No.23) and *Flavobacterium* sp. were susceptible to all antibiotics tested with the disk diffusion method

Table IV
Results of MIC testing ($\mu\text{g/ml}$).

Strain No.	AML	AMC	CIP	CAZ	CZA	TE
1	>256	0.75	–	32	0.75	–
2	10	<0.016	–	32	32	–
3	10	0.25	–	>256	>256	–
4	>256	2	4	>256	>256	–
5	16	0.5	>32	>256	<0.016	–
6	96	1.5	12	10	<0.016	–
7	24	8	4	–	–	–
8	10	0.047	>32	>256	>256	–
9	–	–	6	>256	>256	24
10	64	4	–	>256	>256	>256
11	–	–	–	10	0.38	–
12	>256	2	–	96	64	–
13	>256	1.5	–	>256	>256	–
14	10	24	–	>256	>256	–
15	10	0.5	–	>256	64	–
16	>256	1.5	–	10	4	–
17	32	24	>32	>256	>256	–
18	10	0.5	–	>256	>256	–
19	–	–	–	>256	>256	–
20	>256	0.5	–	10	1	–
21	–	–	–	–	–	–
22	10	0.125	4	>256	>256	–
23	12	1	–	>256	>256	–
24	>256	24	>32	>256	>256	–

– – not included in the testing (strain susceptible to the antibiotic)
The abbreviations of antibiotics are explained in the Materials and Methods section.

and resistant only to AML and CAZ. The majority of strains proved multi-drug resistant (MDR), i.e., they were resistant to three or more antibiotic groups (Falagas and Karageorgopoulos 2008). The present study's results seem to confirm MDR among bacteria dwelling in tap water, reported previously (Vaz-Moreira et al. 2011; 2012; Narciso-da-Rocha et al. 2014; Leginowicz et al. 2018). Among genera identified in this study, MDR isolates of *Brevundimonas*, *Microbacterium*, *Pedobacter*, *Bosea*, and *Afipia* were also found in bottled mineral water (Falcone-Dias et al. 2012). Interestingly, the resistance of bacteria belonging to these genera might have been acquired because taxonomically related strains isolated from various mineral water brands presented different resistance profiles (Falcone-Dias et al. 2012).

Intra-genus and intra-specific variability in antibiotic resistance of environmental bacteria – comparison of the obtained results with literature reports. Lack of guidelines for antibiotic susceptibility testing for environmental species makes the comparison of scientific reports complicated (Leginowicz et al. 2018).

Nevertheless, the comparison of data presented in this paper with resistance patterns of bacteria belonging to the same genera or species reported previously in literature could shed new light on antibiotic resistance spread in environmental bacteria. Unless stated otherwise, this review concerns only drugs tested in this study.

Some data regarding the antibiotic resistance of representatives of genera *Achromobacter*, *Chryseobacterium*, *Pedobacter*, and *Microbacterium* are available. Carbapenems and SXT have been claimed to be the most effective antibiotics against *Achromobacter* spp., opportunistic human pathogens (Almuzara et al. 2010). It is in accordance with the results presented in this paper. On the other hand, a literature review concerning genera *Chryseobacterium*, *Pedobacter*, and *Microbacterium* reveals some discrepancies. *Chryseobacterium* spp. were reported to be inherently resistant to E, C, linezolid, polymyxins, aminoglycosides, tetracyclines, and many β -lactams, and intermediately sensitive to VA and clindamycin (Kirby et al. 2004; Loch and Faisal 2015), but susceptible to RA, CIP and SXT (Kirby et al. 2004; Chen et al. 2013b). Another study revealed that out of

Chryseobacterium spp. isolates obtained from aquatic habitats, 97% were resistant to AM, 89% to PB, 62% to E, 54% to T, 21.5% to florfenicol, and 69% were sensitive to SXT (Michel et al. 2005; Loch and Faisal 2015). *Pedobacter* spp. were considered environmental superbugs, probably intrinsically resistant to many antibiotics and having β -lactamases. They have been reported to be resistant to AMC, AM, ATM, FEP, CAZ, C, CIP, CN, S, TE, and VA, but susceptible to IMP and SXT (Viana et al. 2018). *Microbacterium* spp. isolates have been reported to be resistant to CTX, CIP, DO, E, CN, RA, and VA (Gneiding et al. 2008). Findings regarding *Chryseobacterium* sp., *Pedobacter* sp., and *Microbacterium* sp. presented in this study are, therefore, partially in contradiction with literature reports.

Some discrepancies are also found in resistance patterns of representatives of genera *Dyadobacter* and *Flavobacterium*. For example, *Dyadobacter alkalitolerans* first isolated from desert sand in China was susceptible to TE and RA, but resistant to AM, E, VA, and AML (Tang et al. 2009), and *Dyadobacter arcticus* first isolated from Arctic soil in Svalbard was susceptible to PB, TE, VA, CIP, OFX, S, and SXT, but resistant to AM, CN, and CAZ (Chen et al. 2013a). *Flavobacterium psychrophilum* isolates obtained from trout in Turkey demonstrated reduced susceptibility to T, but susceptibility to AML (Saticioglu et al. 2019). In contrast, *Flavobacterium columnare* isolates obtained from pound cultures in Nigeria proved resistant to S, T, C, OFX, CN, and AML, but susceptible to CIP and SXT (Ogbonne et al. 2019). Moreover, clinical isolates of *Flavobacterium* spp. were resistant to E (Aber et al. 1978). The resistance patterns of *Dyadobacter* sp. and *Flavobacterium* sp. isolates investigated in this study differ from those mentioned above.

Afipia sp. and *Methylobacterium* sp. were resistant to most of the antibiotics tested in this study. *Afipia* spp. has been formerly isolated from tap water samples (Zhang et al. 2009). Within this genus, *Afipia felis*, a putative cat-scratch disease agent, has been suggested to be resistant to most antibiotics, remaining susceptible to aminoglycosides, IMP, RA, amikacin, and tobramycin (Maurin et al. 1993). *Methylobacterium* spp. isolates formerly proved resistant to AML, E, and C, but the majority of them were susceptible to TE and CN (Hiraishi et al. 1995). On the other hand, *Methylobacterium* spp. isolates obtained from hospital tap water in Japan were resistant to AM, CN, E, VA, C, and OFX but susceptible to IMP and TE (Furuhata et al. 2006). Therefore, resistance patterns of *Afipia* sp. and *Methylobacterium* sp. investigated in this study, and those reported previously in the literature show certain differences.

Sphingomonadaceae are common inhabitants of tap water. This family has been suggested to be intrinsically resistant to colistin. Resistance to fluoroquinolones, cephalosporins, and sulphonamides is possibly acquired

in these bacteria (Vaz-Moreira et al. 2011; Narciso-da-Rocha et al. 2014). The most antibiotic-resistant genera of the family *Sphingomonadaceae* proved to be *Sphingomonas* and *Sphingobium* (Vaz-Moreira et al. 2011), both investigated in the present paper. *Sphingomonas* representatives have been reported to be resistant to IMP, MEM, FEP, CAZ, CIP, CN, and SXT, and *Sphingobium* representatives to MEM, FEP, CAZ, CIP, CN, and SXT, respectively (moreover, resistance to β -lactams has been suggested to be intrinsic in genus *Sphingobium*) (Vaz-Moreira et al. 2011; Narciso-da-Rocha et al. 2014). The comparison of these resistance patterns with results presented in this paper, therefore, reveals some intra-genus differences.

Some intra-specific variability in antibiotic resistance was also observed based on the examples of the *Sphingobium abikonense*, *Nocardia asteroides*, and *B. massiliensis*. *S. abikonense* was first isolated in India. Its resistance pattern differed from the results presented in this study in terms of AM, RA, and PB (Kumari et al. 2009). The antibiotic resistance of *Nocardia* spp. has been suggested to be species-specific. Nevertheless, linezolid and SXT appear to be effective against this genus, although emerging resistance to SXT has also been reported (Schlaberg et al. 2014; Hashemi-Shahraki et al. 2015; McTaggart et al. 2015; Zhao et al. 2017). *N. asteroides* isolates have formerly proved susceptible to SXT, MEM, CTX, and CN, but resistant or moderate-resistant to AMC, CIP, FEP, AM, VA, and RA; whereas resistance to IMP differed among the studies (Schlaberg et al. 2014; Hashemi-Shahraki et al. 2015; Zhao et al. 2017). In the present study, the resistance pattern of *N. asteroides* differed in terms of AM, CTX, VA, and CIP, suggesting intra-specific diversity of antibiotic resistance. Moreover, *B. massiliensis* first isolated from hospital tap water in France has been reported to be susceptible only to DO (La Scola et al. 2003) in contrary to results presented in this paper. Both *B. massiliensis* isolates investigated in this study were susceptible to most drugs (including DO), also suggesting intra-specific diversity.

Finally, some data regarding *M. frederiksbergense*, *Brevundimonas*, and *Bacillus zhangzhouensis* are also available. *M. frederiksbergense* was first isolated from soil in Denmark (Willumsen et al. 2001). This species has been confirmed to potentially lead to infection while being sensitive to drugs commonly used to treat non-tuberculous mycobacteria (Senozan et al. 2015). *Brevundimonas* spp. isolates were most frequently resistant to AM, ATM, FEP, AMC, CIP, and CAZ, although other resistance patterns were also reported (Ryan and Pembroke 2018). Results presented in this paper generally appear to be in line with these reports. *B. zhangzhouensis* was first isolated from a shrimp farm in China. Unfortunately, no resistance pattern was described for this strain (Liu et al. 2016). The isolate investigated in

this study was only resistant to CTX and CAZ, both belonging to the 3rd generation cephalosporins group.

To sum up, the comparison of results presented in this paper with previous literature reports points to intra-genus differences in resistance patterns of tap water strains identified to the genus level in this study (*Chryseobacterium* sp., *Pedobacter* sp., *Microbacterium* sp., *Dyadobacter* sp., *Flavobacterium* sp., *Afipia* sp., *Methylobacterium* sp., and *Sphingomonas* sp.). This observation, however, does not exclude species-specific resistance. Nevertheless, some strains identified to the species level in this study (*S. abikonense*, *N. asteroides*, and *B. massiliensis*) also presented resistance patterns different from those reported in the literature, suggesting intra-specific diversity and acquired resistance. Similarly, according to Narciso-da-Rocha et al. (2013), *Acinetobacter* spp. isolates (obtained from WTP and tap water) of the same sequence types presented wild type or non-wild type against some antibiotics. On the other hand, some strains identified in this study as belonging to the same genus or species presented very similar (*M. frederiksbergense*, *B. massiliensis*, *B. mediterranea*) or identical (*Achromobacter* sp.) resistance patterns among each other, despite being isolated from different sampling points or campaigns, which reduces the likelihood of their affinity. Therefore, both HGT and VGT appear to play a role in the resistance spread among tap water ARB.

Conclusions

Tap water bacteria could be MDR and disinfectant-resistant. Neither seasonal nor WTP-dependent variabilities were found in terms of bacterial resistance to antibiotics and disinfectants. IMP proved the most effective, and CAZ the least effective drug against tap water isolates. The comparison of resistance patterns of the strains investigated in this study with previous literature reports indicated the existence of intra-genus and intra-specific variabilities, suggesting acquired resistance of tap water bacteria. Nevertheless, some isolates' species-specific resistance could not be excluded because most strains were only identified to the genus level. Moreover, some strains identified in this study as belonging to the same genus or species presented very similar (*M. frederiksbergense*, *B. massiliensis*, *B. mediterranea*) or identical (*Achromobacter* sp.) resistance patterns among each other. It appears that both horizontal and vertical gene transfer could shape resistance phenotypes of tap water bacteria.

ORCID

Agata Siedlecka <https://orcid.org/0000-0002-5027-4670>

Mirela Wolf-Baca <https://orcid.org/0000-0003-0348-9385>

Katarzyna Piekarska <https://orcid.org/0000-0002-6975-5298>

Acknowledgments

The authors would like to thank the Municipal Water and Sewerage Company in Wrocław to help sample collection and provide data on tap water supply network and physico-chemical tap water properties.

Funding

The research was financed from the statutory funds of Faculty of Environmental Engineering, Wrocław University of Science and Technology from the project 0402/0138/17.

Conflict of interest

The authors do not report any financial or personal connections with other persons or organizations, which might negatively affect the contents of this publication and/or claim authorship rights to this publication

Literature

- Aber RC, Wennersten C, Moellering RC Jr.** Antimicrobial susceptibility of flavobacteria. *Antimicrob Agents Chemother.* 1978 Sep 01;14(3):483–487. <https://doi.org/10.1128/AAC.14.3.483>
- Almuzara M, Limansky A, Ballerini V, Galanternik L, Familietti A, Vay C.** *In vitro* susceptibility of *Achromobacter* spp. isolates: comparison of disk diffusion, Etest and agar dilution methods. *Int J Antimicrob Agents.* 2010 Jan;35(1):68–71. <https://doi.org/10.1016/j.ijantimicag.2009.08.015>
- Bai X, Ma X, Xu F, Li J, Zhang H, Xiao X.** The drinking water treatment process as a potential source of affecting the bacterial antibiotic resistance. *Sci Total Environ.* 2015 Nov;533:24–31. <https://doi.org/10.1016/j.scitotenv.2015.06.082>
- Baquero F, Martínez JL, Cantón R.** Antibiotics and antibiotic resistance in water environments. *Curr Opin Biotechnol.* 2008 Jun; 19(3):260–265. <https://doi.org/10.1016/j.copbio.2008.05.006>
- Berglund B.** Environmental dissemination of antibiotic resistance genes and correlation to anthropogenic contamination with antibiotics. *Infect Ecol Epidemiol.* 2015 Jan;5(1):28564. <https://doi.org/10.3402/iee.v5.28564>
- Chen FL, Wang GC, Teng SO, Ou TY, Yu FL, Lee WS.** Clinical and epidemiological features of *Chryseobacterium indologenes* infections: analysis of 215 cases. *J Microbiol Immunol Infect.* 2013b Dec;46(6):425–432. <https://doi.org/10.1016/j.jmii.2012.08.007>
- Chen L, Jiang F, Xiao M, Dai J, Kan W, Fang C, Peng F.** *Dyadobacter arcticus* sp. nov., isolated from Arctic soil. *Int J Syst Evol Microbiol.* 2013a May 01;63(Pt_5):1616–1620. <https://doi.org/10.1099/ijs.0.044198-0>
- Chiao TH, Clancy TM, Pinto A, Xi C, Raskin L.** Differential resistance of drinking water bacterial populations to monochloramine disinfection. *Environ Sci Technol.* 2014 Apr;48(7):4038–4047. <https://doi.org/10.1021/es4055725>
- ESAC-Net.** [Internet]. European Surveillance of Antimicrobial Consumption Network; 2020 [cited 2020 Oct 12]. Available from <https://www.ecdc.europa.eu/en/about-us/partnerships-and-networks/disease-and-laboratory-networks/esac-net>
- EUCAST.** Växjö (Sweden): The European Committee on Antimicrobial Susceptibility Testing; 2020 [cited 2020 Oct 12]. Available from <https://www.eucast.org/>
- Falagas ME, Karageorgopoulos DE.** Pandrug resistance (PDR), extensive drug resistance (XDR), and multidrug resistance (MDR) among Gram-negative bacilli: need for international harmonization in terminology. *Clin Infect Dis.* 2008 Apr;46(7):1121–1122.

<https://doi.org/10.1086/528867>

Falcone-Dias MF, Vaz-Moreira I, Manaia CM. Bottled mineral water as a potential source of antibiotic resistant bacteria. *Water Res.* 2012 Jul;46(11):3612–3622.

<https://doi.org/10.1016/j.watres.2012.04.007>

Figueira V, Serra EA, Vaz-Moreira I, Brandão TRS, Manaia CM. Comparison of ubiquitous antibiotic-resistant *Enterobacteriaceae* populations isolated from wastewaters, surface waters and drinking waters. *J Water Health.* 2012 Mar 01;10(1):1–10.

<https://doi.org/10.2166/wh.2011.002>

Flores Ribeiro A, Bodilis J, Alonso L, Buquet S, Feuilleley M, Dupont JP, Pawlak B. Occurrence of multi-antibiotic resistant *Pseudomonas* spp. in drinking water produced from karstic hydro-systems. *Sci Total Environ.* 2014 Aug;490:370–378.

<https://doi.org/10.1016/j.scitotenv.2014.05.012>

Furuhata K, Kato Y, Goto K, Hara M, Yoshida S, Fukuyama M. Isolation and identification of *Methylobacterium* species from the tap water in hospitals in Japan and their antibiotic susceptibility. *Microbiol Immunol.* 2006 Jan;50(1):11–17.

<https://doi.org/10.1111/j.1348-0421.2006.tb03765.x>

Furuhata K, Kato Y, Goto K, Saitou K, Sugiyama JI, Hara M, Fukuyama M. Identification of yellow-pigmented bacteria isolated from hospital tap water in Japan and their chlorine resistance. *Bio-control Sci.* 2007;12(2):39–46. <https://doi.org/10.4265/bio.12.39>

Gneiding K, Frodl R, Funke G; Encountered in Human Clinical Specimens. Identities of *Microbacterium* spp. encountered in human clinical specimens. *J Clin Microbiol.* 2008 Nov 01;46(11):3646–3652. <https://doi.org/10.1128/JCM.01202-08>

Hashemi-Shahraki A, Heidari H, Bostanabad SZ, Hashemzadeh M, Feizabadi MM, Schraufnagel D, Mirsaeidi M. Genetic diversity and antimicrobial susceptibility of *Nocardia* species among patients with nocardiosis. *Sci Rep.* 2015 Dec;5(1):17862.

<https://doi.org/10.1038/srep17862>

Hiraishi A, Furuhashi K, Matsumoto A, Koike KA, Fukuyama M, Tabuchi K. Phenotypic and genetic diversity of chlorine-resistant *Methylobacterium* strains isolated from various environments. *Appl Environ Microbiol.* 1995;61(6):2099–2107.

<https://doi.org/10.1128/AEM.61.6.2099-2107.1995>

Khan H, Miao X, Liu M, Ahmad S, Bai X. Behavior of last resort antibiotic resistance genes (*mcr-1* and *bla_{NDM-1}*) in a drinking water supply system and their possible acquisition by the mouse gut flora. *Environ Pollut.* 2020 Apr;259:113818.

<https://doi.org/10.1016/j.envpol.2019.113818>

Khan S, Beattie TK, Knapp CW. Relationship between antibiotic and disinfectant-resistance profiles in bacteria harvested from tap water. *Chemosphere.* 2016a Jun;152:132–141.

<https://doi.org/10.1016/j.chemosphere.2016.02.086>

Khan S, Knapp CW, Beattie TK. Antibiotic resistant bacteria found in municipal drinking water. *Environ Process.* 2016b Sep;3(3):541–552. <https://doi.org/10.1007/s40710-016-0149-z>

Kim DJ, King JA, Zuccarelli L, Ferris CF, Koppel GA, Snowdon CT, Ahn CH. Clavulanic acid: A competitive inhibitor of beta-lactamases with novel anxiolytic-like activity and minimal side effects. *Pharmacol Biochem Behav.* 2009 Aug;93(2):112–120. <https://doi.org/10.1016/j.pbb.2009.04.013>

Kirby JT, Sader HS, Walsh TR, Jones RN. Antimicrobial susceptibility and epidemiology of a worldwide collection of *Chryseobacterium* spp.: report from the SENTRY Antimicrobial Surveillance Program (1997–2001). *J Clin Microbiol.* 2004 Jan 01;42(1):445–448. <https://doi.org/10.1128/JCM.42.1.445-448.2004>

Kumari H, Gupta SK, Jindal S, Katoch P, Lal R. *Sphingobium lactosutens* sp. nov., isolated from a hexachlorocyclohexane dump site and *Sphingobium abikonense* sp. nov., isolated from oil-contaminated soil. *Int J Syst Evol Microbiol.* 2009 Sep 01;59(9):2291–2296. <https://doi.org/10.1099/ijs.0.004739-0>

La Scola B, Mallet MN, Grimont PAD, Raoult D. *Bosea eneeae* sp. nov., *Bosea massiliensis* sp. nov. and *Bosea vestrii* sp. nov., isolated from hospital water supplies, and emendation of the genus *Bosea* (Das et al. 1996). *Int J Syst Evol Microbiol.* 2003 Jan 01;53(1):15–20. <https://doi.org/10.1099/ijs.0.02127-0>

Leginowicz M, Siedlecka A, Piekarska K. Biodiversity and antibiotic resistance of bacteria isolated from tap water in Wrocław, Poland. *Environ Prot Eng.* 2018;44(4):85–98.

<https://doi.org/10.37190/epe180406>

Lin W, Zhang M, Zhang S, Yu X. Can chlorination co-select antibiotic-resistance genes? *Chemosphere.* 2016 Aug;156:412–419.

<https://doi.org/10.1016/j.chemosphere.2016.04.139>

Liu Y, Lai Q, Du J, Shao Z. *Bacillus zhangzhouensis* sp. nov. and *Bacillus australimaris* sp. nov. *Int J Syst Evol Microbiol.* 2016 Mar 01;66(3):1193–1199. <https://doi.org/10.1099/ijsem.0.000856>

Loch TP, Faisal M. Emerging flavobacterial infections in fish: A review. *J Adv Res.* 2015 May;6(3):283–300.

<https://doi.org/10.1016/j.jare.2014.10.009>

Ma L, Li B, Jiang XT, Wang YL, Xia Y, Li AD, Zhang T. Catalogue of antibiotic resistance and host-tracking in drinking water deciphered by a large scale survey. *Microbiome.* 2017 Dec;5(1):154. <https://doi.org/10.1186/s40168-017-0369-0>

Martinez JL. The role of natural environments in the evolution of resistance traits in pathogenic bacteria. *Proc Biol Sci.* 2009 Jul 22;276(1667):2521–2530. <https://doi.org/10.1098/rspb.2009.0320>

Maurin M, Lepoche H, Mallet D, Raoult D. Antibiotic susceptibilities of *Afpia felis* in axenic medium and in cells. *Antimicrob Agents Chemother.* 1993 Jul 01;37(7):1410–1413.

<https://doi.org/10.1128/AAC.37.7.1410>

McTaggart LR, Doucet J, Witkowska M, Richardson SE. Antimicrobial susceptibility among clinical *Nocardia* species identified by multilocus sequence analysis. *Antimicrob Agents Chemother.* 2015 Jan;59(1):269–275. <https://doi.org/10.1128/AAC.02770-14>

Michel C, Matte-Tailliez O, Kerouault B, Bernardet JF. Resistance pattern and assessment of phenolic agents' minimum inhibitory concentration in multiple drug resistant *Chryseobacterium* isolates from fish and aquatic habitats. *J Appl Microbiol.* 2005 Aug;99(2):323–332. <https://doi.org/10.1111/j.1365-2672.2005.02592.x>

Narciso-da-Rocha C, Vaz-Moreira I, Manaia CM. Genotypic diversity and antibiotic resistance in *Sphingomonadaceae* isolated from hospital tap water. *Sci Total Environ.* 2014 Jan;466-467:127–135. <https://doi.org/10.1016/j.scitotenv.2013.06.109>

Narciso-da-Rocha C, Vaz-Moreira I, Svensson-Stadler L, Moore ERB, Manaia CM. Diversity and antibiotic resistance of *Acinetobacter* spp. in water from the source to the tap. *Appl Microbiol Biotechnol.* 2013 Jan;97(1):329–340.

<https://doi.org/10.1007/s00253-012-4190-1>

Ogbonne FC, Osegbo AN, Nwokwu CP, Ukazu ER, Egbe FC, Akhiromen DI, Aguta OJ. Genotypic characterization and resistance patterns of *Flavobacterium columnare* from pond-cultured *Clarias gariepinus*. *Middle East J Appl Sci Technol.* 2019;2(1):54–61.

Proctor CR, Hammes F. Drinking water microbiology – from measurement to management. *Curr Opin Biotechnol.* 2015 Jun;33:87–94. <https://doi.org/10.1016/j.copbio.2014.12.014>

Pruden A, Pei R, Storteboom H, Carlson KH. Antibiotic resistance genes as emerging contaminants: studies in northern Colorado. *Environ Sci Technol.* 2006 Dec;40(23):7445–7450.

<https://doi.org/10.1021/es060413l>

Pruden A. Balancing water sustainability and public health goals in the face of growing concerns about antibiotic resistance. *Environ Sci Technol.* 2014 Jan 07;48(1):5–14.

<https://doi.org/10.1021/es403883p>

Roberts SC, Zembower TR. Global increases in antibiotic consumption: a concerning trend for WHO targets. *Lancet Infect Dis.* 2021 Jan;21(1):10–11. [https://doi.org/10.1016/S1473-3099\(20\)30456-4](https://doi.org/10.1016/S1473-3099(20)30456-4)

- Ryan MP, Pembroke JT. *Brevundimonas* spp: emerging global opportunistic pathogens. *Virulence*. 2018 Dec 31;9(1):480–493. <https://doi.org/10.1080/21505594.2017.1419116>
- Salyers A, Gupta A, Wang Y. Human intestinal bacteria as reservoirs for antibiotic resistance genes. *Trends Microbiol*. 2004 Sep; 12(9):412–416. <https://doi.org/10.1016/j.tim.2004.07.004>
- Sanganyado E, Gwenzi W. Antibiotic resistance in drinking water systems: Occurrence, removal, and human health risks. *Sci Total Environ*. 2019 Jun;669:785–797. <https://doi.org/10.1016/j.scitotenv.2019.03.162>
- Saticioglu IB, Duman M, Smith P, Wiklund T, Altun S. Antimicrobial resistance and resistance genes in *Flavobacterium psychrophilum* isolates from Turkey. *Aquaculture*. 2019 Oct;512:734293. <https://doi.org/10.1016/j.aquaculture.2019.734293>
- Schlaberg R, Fisher MA, Hanson KE. Susceptibility profiles of *Nocardia* isolates based on current taxonomy. *Antimicrob Agents Chemother*. 2014 Feb;58(2):795–800. <https://doi.org/10.1128/AAC.01531-13>
- Senozan EA, Adams DJ, Giamanco NM, Warwick AB, Eberly MD. A catheter-related bloodstream infection with *Mycobacterium frederiksbergense* in an immunocompromised child. *Pediatr Infect Dis J*. 2015 Apr;34(4):445–447. <https://doi.org/10.1097/INF.0000000000000563>
- Shi P, Jia S, Zhang XX, Zhang T, Cheng S, Li A. Metagenomic insights into chlorination effects on microbial antibiotic resistance in drinking water. *Water Res*. 2013 Jan;47(1):111–120. <https://doi.org/10.1016/j.watres.2012.09.046>
- Shrivastava R, Upreti RK, Jain SR, Prasad KN, Seth PK, Chaturvedi UC. Suboptimal chlorine treatment of drinking water leads to selection of multidrug-resistant *Pseudomonas aeruginosa*. *Ecotoxicol Environ Saf*. 2004 Jun;58(2):277–283. [https://doi.org/10.1016/S0147-6513\(03\)00107-6](https://doi.org/10.1016/S0147-6513(03)00107-6)
- Siedlecka A, Wolf-Baca M, Piekarska K. Spatiotemporal changes of antibiotic resistance and bacterial communities in drinking water distribution system in Wrocław, Poland. *Water*. 2020b Sep 17;12(9):2601. <https://doi.org/10.3390/w12092601>
- Siedlecka A, Wolf-Baca M, Piekarska K. Seasonal variability of antibiotic resistance and biodiversity of tap water bacteria in Wrocław, Poland. *Environ Prot Eng*. 2020a;46(2):93–109. <https://doi.org/10.37190/epe200207>
- Stokes HW, Gillings MR. Gene flow, mobile genetic elements and the recruitment of antibiotic resistance genes into Gram-negative pathogens. *FEMS Microbiol Rev*. 2011 Sep;35(5):790–819. <https://doi.org/10.1111/j.1574-6976.2011.00273.x>
- Tang Y, Dai J, Zhang L, Mo Z, Wang Y, Li Y, Ji S, Fang C, Zheng C. *Dyadobacter alkaliolerans* sp. nov., isolated from desert sand. *Int J Syst Evol Microbiol*. 2009 Jan 01;59(1):60–64. <https://doi.org/10.1099/ijs.0.001404-0>
- Vaz-Moreira I, Nunes OC, Manaia CM. Bacterial diversity and antibiotic resistance in water habitats: searching the links with the human microbiome. *FEMS Microbiol Rev*. 2014 Jul;38(4):761–778. <https://doi.org/10.1111/1574-6976.12062>
- Vaz-Moreira I, Nunes OC, Manaia CM. Diversity and antibiotic resistance patterns of *Sphingomonadaceae* isolates from drinking water. *Appl Environ Microbiol*. 2011 Aug 15;77(16):5697–5706. <https://doi.org/10.1128/AEM.00579-11>
- Vaz-Moreira I, Nunes OC, Manaia CM. Diversity and antibiotic resistance in *Pseudomonas* spp. from drinking water. *Sci Total Environ*. 2012 Jun;426:366–374. <https://doi.org/10.1016/j.scitotenv.2012.03.046>
- Vaz-Moreira I, Nunes OC, Manaia CM. Ubiquitous and persistent *Proteobacteria* and other Gram-negative bacteria in drinking water. *Sci Total Environ*. 2017 May;586:1141–1149. <https://doi.org/10.1016/j.scitotenv.2017.02.104>
- Viana AT, Caetano T, Covas C, Santos T, Mendes S. Environmental superbugs: the case study of *Pedobacter* spp. *Environ Pollut*. 2018 Oct;241:1048–1055. <https://doi.org/10.1016/j.envpol.2018.06.047>
- Wang DY, Abboud MI, Markoulides MS, Brem J, Schofield CJ. The road to avibactam: the first clinically useful non- β -lactam working somewhat like a β -lactam. *Future Med Chem*. 2016 Jun;8(10): 1063–1084. <https://doi.org/10.4155/fmc-2016-0078>
- Willumsen P, Karlson U, Stackebrandt E, Kroppenstedt RM. *Mycobacterium frederiksbergense* sp. nov., a novel polycyclic aromatic hydrocarbon-degrading *Mycobacterium* species. *Int J Syst Evol Microbiol*. 2001 Sep 01;51(5):1715–1722. <https://doi.org/10.1099/00207713-51-5-1715>
- Zhang P, Hozalski RM, Leach LH, Camper AK, Goslan EH, Parsons SA, Xie YE, LaPara TM. Isolation and characterization of haloacetic acid-degrading *Afipia* spp. from drinking water. *FEMS Microbiol Lett*. 2009 Aug;297(2):203–208. <https://doi.org/10.1111/j.1574-6968.2009.01687.x>
- Zhang Y, Gu AZ, He M, Li D, Chen J. Subinhibitory concentrations of disinfectants promote the horizontal transfer of multidrug resistance genes within and across genera. *Environ Sci Technol*. 2017 Jan 03;51(1):570–580. <https://doi.org/10.1021/acs.est.6b03132>
- Zhao P, Zhang X, Du P, Li G, Li L, Li Z. Susceptibility profiles of *Nocardia* spp. to antimicrobial and antituberculous agents detected by a microplate Alamar Blue assay. *Sci Rep*. 2017 May;7(1):43660. <https://doi.org/10.1038/srep43660>

Chemotaxis Toward Crude Oil by an Oil-Degrading *Pseudomonas aeruginosa* 6-1B Strain

KAIQIANG LIANG^{1,2*}, RUIMIN GAO², CHENGJUN WANG³, WEIBO WANG² and WEI YAN¹

¹Department of Environmental Science and Engineering, Xi'an Jiaotong University, Xi'an, China

²Research Institute of Yanchang Petroleum (Group) Co. Ltd., Xi'an, China

³College of Chemistry and Chemical Engineering, Xi'an Shiyou University, Xi'an, China

Submitted 16 October 2020, revised 6 January 2021, accepted 17 January 2021

Abstract

The chemotactic properties of an oil-degrading *Pseudomonas aeruginosa* strain 6-1B, isolated from Daqing Oilfield, China, have been investigated. The strain 6-1B could grow well in crude oil with a specific rhamnolipid biosurfactant production. Furthermore, it exhibits chemotaxis toward various substrates, including glycine, glycerol, glucose, and sucrose. Compared with another oil-degrading strain, T7-2, the strain 6-1B presented a better chemotactic response towards crude oil and its vital component, *n*-alkenes. Based on the observed distribution of the strain 6-1B cells around the oil droplet in the chemotactic assays, the potential chemotaxis process of bacteria toward crude oil could be summarized in the following steps: searching, moving and consuming.

Key words: chemotaxis, crude oil, *Pseudomonas aeruginosa* 6-1B, swarm plate assay, modified agarose plug assay

Introduction

Microbial enhanced oil recovery (MEOR) is an environment-friendly process that may be useful to petroleum recovery. MEOR may be an efficient and inexpensive alternative method to enhance the physicochemical recovery of oil (EOR) (Kryachko 2018). Microorganisms can be used to reduce the paraffin build-up in producing wells, produce solvents or polymers above ground, and for pumping into the oil-bearing formation, as in EOR (Brown 2010). It is widely accepted that microorganisms can enhance oil recovery by their ability to produce some metabolic products, including biosurfactants. Biosurfactants are one of the most important microbial metabolic products that can reduce surface tension in oil and facilitate the emulsification of oil in with water. The latter increases the bioavailability of the residual crude oil and enhances its biodegradability (Batista et al. 2006). Furthermore, the properties of the microbes themselves, such as high cell surface hydrophobicity and motility, help them to attach to the interface and the surface of oil droplets in sandstones and carbonate strata (Rocha et al. 2020). The degradation of crude oil generally occurs at

oil-water points of contact. The oil-water contact provides conditions that are the most conducive to microbial activity. The transport of hydrocarbons from the oil droplets will provide a plentiful supply of electron donors needed for metabolism, whereas inorganic nutrients required for microbial growth can be transported by water flow or diffusion to the biosphere on the oil-water contact (Head et al. 2003).

Flagellum-dependent chemotaxis is an important advantage of motile bacteria. These bacteria move through a fluid medium by rotating one or more flagella (Nakamura and Minamino 2019). Both metabolism-dependent and independent chemotaxis of *Pseudomonas* sp. toward aromatic compounds had been studied (Sampedro et al. 2015). Chemotactic bacteria, such as *Escherichia coli*, *Pseudomonas putida*, *Pseudomonas aeruginosa*, *Rhodococcus erythropolis*, and others can adapt to the chemical environment by detecting changes in concentrations of certain chemicals and by changing their movement patterns essentially based on the chemical gradient present (Waite et al. 2018). The bacterial chemotaxis ability provides more opportunities for bacterial cells to move into an area with high

* Corresponding author: K. Liang, Department of Environmental Science and Engineering, Xi'an Jiaotong University, Xi'an, China; e-mail: lkq886@163.com

© 2021 Kaiqiang Liang et al.

This work is licensed under the Creative Commons Attribution-NonCommercial-NoDerivatives 4.0 License (<https://creativecommons.org/licenses/by-nc-nd/4.0/>).

concentrations of the necessary chemical attractants (Ni et al. 2020; Yang et al. 2020). Some microorganisms have evolved to use chemotaxis to resist degradation and survive conditions that lead them to utilize poisonous carbon sources, such as non-aqueous phase liquids (NAPLs), especially when there are no usable growth substrates available (Parales and Harwood 2002). Bacterial chemotaxis here is an important prelude to metabolism, as it can increase the degradation rate of NAPL-associated hydrophobic compounds (Law and Aitken 2003). Marx and Aitken (2000) have reported that chemotaxis to naphthalene by *Pseudomonas putida* G7 increased the rate of naphthalene degradation in an aqueous system in which a concentration gradient of naphthalene was imposed.

Crude oil contains NAPL-associated compounds, which are mainly composed of hydrocarbons, and aromatic compounds. It has been reported that hydrocarbon-degrading microbes migrate toward pure alkanes by chemotaxis, which may enhance the alkanes' biodegradation rate by facilitating microbial contact with the substrate (Lanfrancioni et al. 2003). Favorable chemotactic properties may allow oil-degrading bacteria to efficiently detect and migrate towards oil droplets, which could be utilized as a carbon source (Meng et al. 2019). However, experimental demonstrations on chemotaxis of oil-degrading microbes towards crude oil are still limited. The potential role of chemotaxis of oil-degrading microbes in EOR has not yet received much attention. Therefore, this study investigated the chemotactic characteristics of a *Pseudomonas aeruginosa* oil-degrading strain, 6-1B, elicited by various substrates, and the chemotactic response towards crude oil via the swarm plate assay and the modified agarose plug assay. A potential chemotaxis mechanism of the 6-1B strain toward crude oil has been proposed based on the experimental results.

Experimental

Materials and Methods

Materials and media. The crude oil used in this study was light oil obtained from the Daqing Oilfield (China). It has been sterilized using high-pressure steam before use (Table S1). Tridecane and liquid paraffin were obtained from Sinopharm Chemical Reagent Co., Ltd.

Rhodococcus erythropolis T7-2 strain was cultivated in the lab (Huang et al. 2007). The bacteria were incubated in two different kinds of mineral salt media, namely medium M1 (in g/l: KH_2PO_4 0.2, Na_2HPO_4 0.6, NaNO_3 2.0, CaCl_2 0.01, FeSO_4 0.01, $\text{MgSO}_4 \cdot 7\text{H}_2\text{O}$ 0.615, and yeast extract 0.5), and medium M2 (in g/l: Na_2HPO_4 1.5, KH_2PO_4 3.48, $(\text{NH}_4)_2\text{SO}_4$ 4.0, MgSO_4 0.7, and yeast extract 0.01), respectively. The pH values of both media

were adjusted to 7.2. The media were then autoclaved at 121°C for 30 min.

Screening of oil-degrading bacterial strains. The strain 6-1B, used in this study, was isolated from the oil-water of Daqing Oilfield. The strain can degrade crude oil efficiently with the production of biosurfactants. The isolation method was as follows: 10% of oil-water (w/v) was added into the mineral medium M1 supplemented with 0.2% sucrose (w/v) and 2.0% liquid paraffin (w/v) as the carbon sources and was shaken with 150 rpm at 42°C for seven days. After subculturing twice in this medium, 5% seed culture (v/v) was transferred into medium M2 supplemented with 2% liquid paraffin (w/v) as the sole carbon source. The bacteria were incubated for five days at 42°C and were subcultured for more than five times to ensure the selected strains' activity. After enriching the bacteria in the M2 medium, aliquots were diluted and smeared on Luria-Bertani (LB) agar plates to screen for single colonies. The selected colonies on the LB plate were then respectively cultured in the M2 medium at 42°C, supplemented with 2% crude oil (w/v) as the sole carbon source, and these enriched cultures were collected for subsequent testing. The degradation rate of crude oil was analyzed by a standard test method for oil and grease and petroleum hydrocarbons in water (ASTM D3921-85.1990), commonly known as the IR method. Absorbance readings were then taken by following the manufacturer's instructions, using a fixed wavelength model DM600 IR analyzer (AilunGroup, CHN). The measurement range of the IR is 0.1–10,000 ppm.

Bacterial characteristics. The biosurfactant formed by the strain 6-1B from liquid paraffin, which was the sole carbon source needed for production, was analyzed as previously reported (Patowary et al. 2017). The fermentation products of strains 6-1B and T7-2, which could emulsify diesel oil with an Emulsification Index (EI24) value of 100%, were also characterized according to respective methods well-described previously (Gandhimathi et al. 2009). In order to assess cell surface hydrophobicity (CSH), the bacterial adherence to hydrocarbon (BATH) assay was performed as described previously (Gomes et al. 2013). The taxonomy of the isolated strain 6-1B was identified according to the BLAST result of the 16S rDNA sequence with the GenBank database. The 16s rDNA was extracted from isolated colonies of the strain 6-1B and amplified using universal primers 27F (5'-AGAGTTTGTACCTG-GCTCAG-3') and 1492R (5'-GGTTACCTTGTTAC-GACTT-3'). The 16S rDNA sequence was then deposited in NCBI with an accession number of JQ012217.

Chemotaxis assays. Swarm plate assay. To characterize the chemotactic behavior of the strain 6-1B toward crude oil, the swarm plate assay was performed as previously described (Ha et al. 2014). Briefly,

cells grown on oil were collected by centrifugation at $8,000 \times g$ for 5 min and washed twice with a chemotaxis buffer, which contained 25 mM Na_2HPO_4 , 25 mM KH_2PO_4 , and 0.01% yeast extract. Cells were then resuspended in the chemotaxis buffer at a final concentration of 1×10^9 CFU/ml. 0.01 ml of suspension of the strain 6-1B in the chemotaxis buffer was gently poured on the centre of the swarm medium agar plate, which contained (g/l): Na_2HPO_4 1.5, KH_2PO_4 3.48, $(\text{NH}_4)_2\text{SO}_4$ 4.0, MgSO_4 0.7, 0.01% of Triton X-100, 0.01% yeast extract (v/v), and 0.01% of attractants (crude oil, liquid paraffin, and tridecane, v/v). The 0.01% of Triton X-100 (v/v) and the yeast extract were added to the swarm agar plate to improve the oil solubility and keep the mobility of cells, respectively. Overnight cultures of *P. aeruginosa* PAO-1 and *R. erythropolis* T7-2 in LB broth were used as controls. The plates were incubated at 42°C, 30°C, and 37°C, respectively, and were observed every six hours.

Modified agarose plug assay. The agarose plug assay was performed as described previously (Roggo et al. 2018), with a slight modification, by adding a coverslip on top of a concave slide to form a chamber. The cells used in these assays were harvested in the mid-logarithmic phase, washed, and resuspended with the chemotaxis buffer (with a density of about 1×10^7 CFU/ml). Plugs with crude oil sample, or melted agarose in the chemotaxis buffer (negative control), were dropped in the chamber's center. Then, 50 μl of the freshly harvested bacterial culture was then infused around the crude oil droplets. A glass coverslip was placed on top of the chamber, which was then sealed with petroleum jelly (Vaseline) to ensure that there were no air bubbles in the chamber. The movement of cells of the strain 6-1B towards the oil droplets was analyzed under the phase-contrast microscope (Olympus BH2 microscope, Japan) using the Scion Image 3b Software (Scion, Frederick, MD). The chemotaxis of the strain 6-1B was determined based on a relative velocity. A chosen $50 \mu\text{m} \times 50 \mu\text{m}$ area was magnified 500 times to determine the relative velocity of the strain 6-1B.

The chemotaxis videos were divided into frames, and an average relative velocity (derived from the average of $n = 5$ independent experiments) was determined from observed cell movements that had relatively straight trajectories. The area magnified and visualized was the interface between the oil and water; the number of cells in the field of view was counted. The changes in the pixel intensity (ranging from 0–255 PPI) reflected the bacterial density in the oil droplet's vicinity.

Morphology and image analysis. The morphology of the bacteria used in this study was observed through transmission electron microscopy (TEM, Philips EM400-ST, Japan). Chemotactic responses were observed at respective magnifications of 100 \times , 125 \times , 400 \times , and 500 \times , using a phase-contrast microscope (Olympus BH2 microscope, Japan) equipped with a CCD camera (Hitachi KP-D50 Colour Digital, Tokyo, Japan), and Axio-Vision software. The sizes of the chemotactic rings were determined using Axio-Vision software. Videos were analyzed by the method previously described (Boudko et al. 2003). The Scion Image 3b software was used to make line scan image plots.

Results and Discussion

The isolation of the strain chemotactic towards crude oil. The strain 6-1B was isolated from an oil/water sample collected in the Daqing Oilfield and can degrade crude oil upon producing a rhamnolipid biosurfactant. A 16S rRNA sequence-based phylogenetic analysis revealed that the strain 6-1B represented *Pseudomonas aeruginosa* species and was named *P. aeruginosa* 6-1B. The biosurfactant produced by the strain 6-1B was detected in the mineral salts medium M1 culture, which was supplemented with 2.0% (w/v) liquid paraffin as a carbon source. Strain 6-1B can also grow with *n*-alkanes (C_8 to C_{20}) as its sole carbon and energy source. The oil degradation rate of strain 6-1B was up to 60% (Table I).

Table I
The characteristics of the strains used in this study.

Strain characteristics	<i>Pseudomonas aeruginosa</i> 6-1B	<i>Rhodococcus erythropolis</i> T7-2	<i>Pseudomonas aeruginosa</i> PAO1
Optimum temperature (°C)	42	30	37
Fermentation product ²	Rhamnolipid	Saccharides, protein, lipid	ND
Emulsification index (EI_{24})	100%	100%	ND
Cell surface hydrophobicity (CSH%) ¹	38%	85%	16%
Degradation range of <i>n</i> -alkenes	C_8 - C_{20}	C_{12} - C_{36}	ND
Degradation rate of crude oil ³	60.09%	75.43%	ND

¹ – bacteria were cultivated until the exponential period in LB broth

² – mineral salt medium M1 with 2.0% (w/v) liquid paraffin as the carbon source was used for biosurfactant fermentation

³ – crude oil was obtained from the Daqing Oilfield, China

ND – not detected

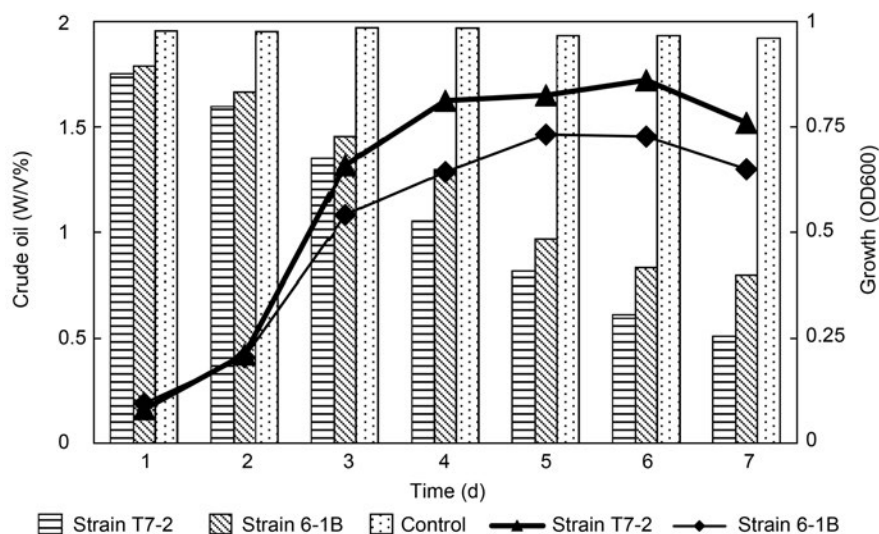


Fig. 1. Growth and degradation of crude oil by *P. aeruginosa* 6-1B and *R. erythropolis* T7-2 strains.

R. erythropolis T7-2, a non-motile strain isolated from the Daqing Oilfield, did not exhibit chemotaxis towards crude oil (Dan 2008). However, the strains T7-2 can also grow with both pure hydrocarbons as its sole carbon source (Table I). Both strains 6-1B and T7-2 were oil-degrading strains; they exhibited insignificant differences in their cell surface structures according to the results of TEM (Fig. S1), and in the cell surface hydrophobicity values (CSH%) (Table I). The TEM image showed that the strain 6-1B has a polar flagellum, while T7-2 does not. The CSH value of the strain T7-2 was 85%, which was much higher than that of the strain 6-1B (38%). Furthermore, when cultured with crude oil, the strain 6-1B showed a maximum growth at day fifth. It exhibited approximately a 15% decrease in the specific growth rate, as compared with strain T7-2.

Chemotaxis of *P. aeruginosa* 6-1B to crude oil in both the swarm plate and the modified agarose plug assays. To investigate the chemotaxis of the isolated strain towards crude oil and its components, both the swarm plate assay and modified agarose plug assay have been carried out. The results have provided several interesting insights on the chemotaxis of this oil-degrading strain towards crude oil.

First, the strain 6-1B showed chemotaxis to crude oil and its partial components, including *n*-alkanes. In the swarm plate assay, the enriched culture of the strain 6-1B was gently poured on the centre of swarm plates containing attractants, which were also the carbon source. In these plates, actively metabolizing the strain 6-1B generated a gradient of the carbon sources present. Chemotactic bacteria and their growth correspondingly following such a gradient resulted in the so-called swarm rings' formation. Therefore, the swarm rings' presence indicated the strain 6-1B's chemotactic behavior towards all the three attractants, includ-

ing crude oil, liquid paraffin, and tridecane (Fig. 2). Bacterial growth, typical of a chemotactic response to a self-generated gradient, was observed in tridecane-

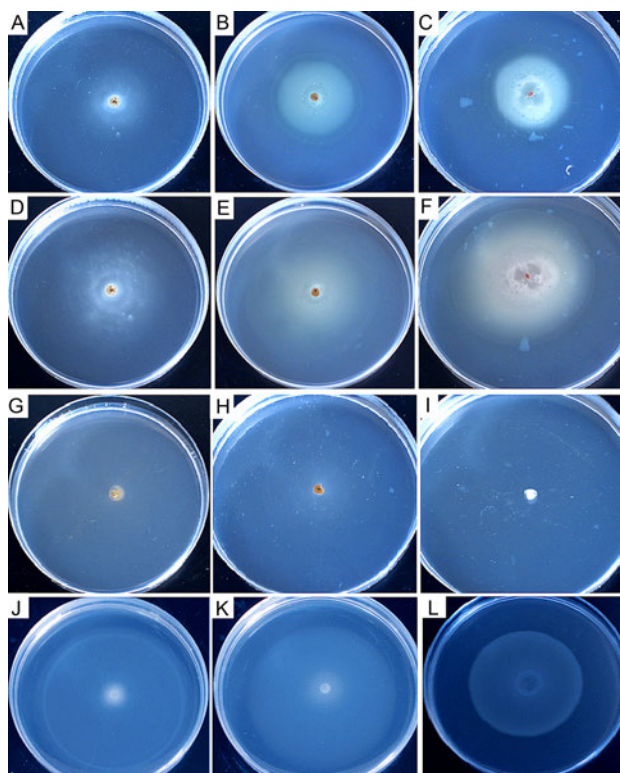


Fig. 2. Chemotaxis of the strain 6-1B towards tridecane, liquid paraffin, and crude oil in the swarm plate assay.

The chemotaxis of the strain 6-1B towards 0.01% of tridecane (A) and (D), liquid paraffin (B) and (E), crude oil (C) and (F), and the chemotaxis buffer without attractant (G) were determined, respectively. The chemotactic responses of the control strain *R. erythropolis* T7-2, and *P. aeruginosa* PAO-1 to crude oil are shown in (H) and (I). Among them, Fig. 2A, 2B, and 2C were photographed after 24 hours of cultivation; Fig. 2D, 2E, 2F, 2G, 2H, and 2I were taken after 48 hours of incubation. The chemotactic responses of the strain 6-1B towards sucrose, glycine, glycerol after 24 hours of cultivation are also shown in Fig. 2J, 2K, and 2L separately.

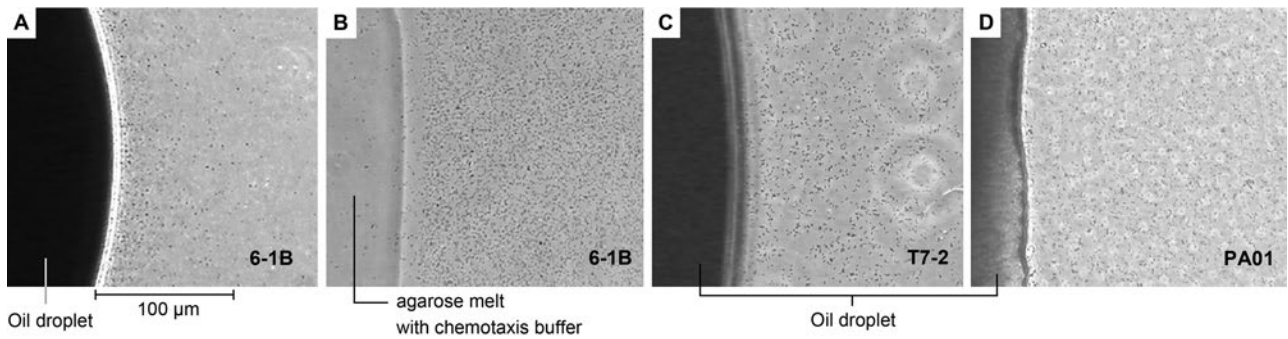


Fig. 3. The chemotactic responses of the strain 6-1B (A), T7-2 (C), and PAO1 (D) towards crude oil via modified agarose plug assay. The chemotaxis of the strain 6-1B towards the chemotaxis buffer served as the negative control (B).

(Fig. 2A and 2D), liquid paraffin- (Fig. 2B and 2E), and crude oil- (Fig. 2C and 2F) containing plates after 24 or 48 hours of incubation.

Similarly, the results of the modified agarose plug assay demonstrated that the strain 6-1B, which was in the exponential phase of growth, retained a strong ability to move and adapt its chemotactic ability towards crude oil, as shown by the chemotactic ring formed around the oil attractant (Fig. 3A). Several studies have examined the chemotactic responses of bacteria toward their carbon source and demonstrated that chemotaxis enables bacteria to position themselves in environments favorable for survival (Pandey and Jain 2002; Pedit et al. 2002; Zheng et al. 2020). Zheng et al. (2020) determined that chemotactic motility plays a crucial role in microbial oil degradation. Microbes' chemotactic motility could cause a continuous bump onto the oil drop, resulting in mechanical disruption of the oil-

water interface and dispersion of the oil components into the surrounding motility buffer. This phenomenon likely created a concentration gradient, which chemotactically attracted more bacteria toward their carbon source. Furthermore, chemotactic responses to the Daqing Crude oil components indicated that the strain 6-1B is chemotactic to *n*-alkenes, such as dodecane, tridecane, tetradecane, pentadecane, hexadecane. Simultaneously, no chemotactic response towards aromatic hydrocarbons naphthalene, diphenyl, and sulfur was observed (Table II). However, the chemotaxis ring formed around some *n*-alkanes, such as tridecane, was not as apparent as those formed around the liquid paraffin and crude oil (Fig. 2). This difference may be due to many hydrocarbons in the liquid paraffin and crude oil plates. Another potential explanation could be related to the relatively low extent of tridecane's degradability (56%). The chemotaxis ring observed around the liquid

Table II

Chemotaxis responses of the different strains to various components of the Daqing crude oil and their respective relative degradation rates.

Attractants ¹	<i>Pseudomonas aeruginosa</i> 6-1B		<i>Rhodococcus erythropolis</i> T7-2		<i>Pseudomonas aeruginosa</i> PAO-1	
	Chemotaxis response ²	Oil degrading rate (%) ³	Chemotaxis response ²	Oil degrading rate (%) ³	Chemotaxis response ²	Oil degrading rate (%) ³
Dodecane	+	63.22	-	78.17	-	ND
Tridecane	+	56.18	-	75.62	-	ND
Tetradecane	+	54.28	-	67.57	-	ND
Pentadecane	+	57.97	-	62.84	-	ND
Hexadecane	+	55.54	-	59.73	-	ND
Liquid paraffin	+	58.13	-	65.11	-	ND
Crude oil	+	60.09	-	75.43	-	ND
Naphthalene	-	ND	-	ND	-	ND
Diphenyl	-	ND	-	ND	-	ND
Sulfur	-	ND	-	ND	-	ND

¹ - all the attractants was tested at a concentration of 0.01% (w/v)

² - chemotactic response was tested by the swarm plate assay

³ - the degradation rate of crude oil was tested by an IR analyzer

+

- - there is no chemotactic response

ND - not detected

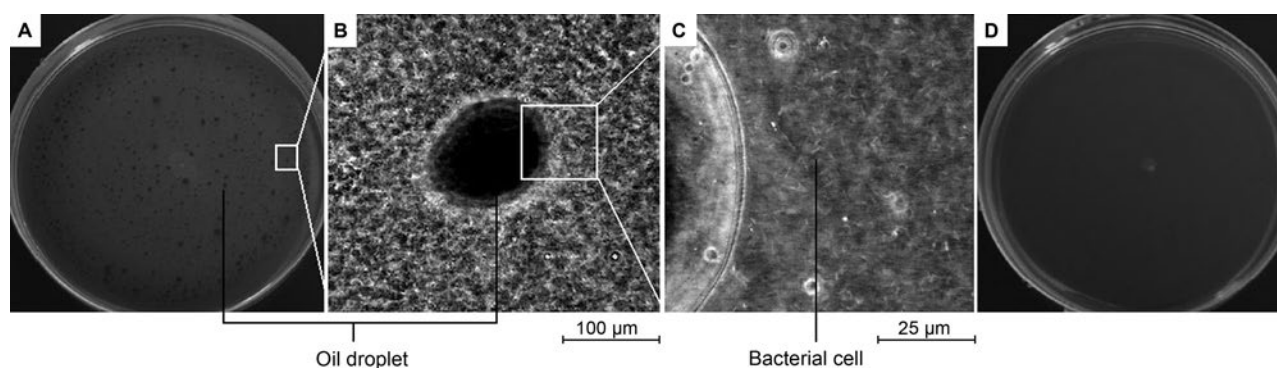


Fig. 4. The visualization of chemotaxis rings in the swarm plate using microscopy.

The chemotaxis of the strain 6-1B toward crude oil (0.1%) visualized using a phase-contrast microscope (Olympus BH2 microscope, Japan) with magnifications of 0× (A), 125× (B) and 500× (C), respectively; the control swarm plate which contained the same composition except for crude oil, visualized at a magnification of 0× (D).

paraffin was evident and similar to that of the crude oil, probably because liquid paraffin is mainly composed of linear *n*-alkanes ranging from C_{12} to C_{18} . The strain 6-1B did not migrate toward other Daqing Crude oil compositions, such as aromatic hydrocarbons, naphthalene, diphenyl, and sulfur within the same timeframe. We proposed that this oil-degrading strain showed chemotaxis to crude oil mainly because it has chemotactic responses to linear hydrocarbons, which bacteria can use as growth substrates. We, therefore, hypothesize that oil-degrading strains show chemotaxis towards *n*-alkanes, which is a component of the crude oil, and that the phenomenon of chemotaxis towards crude oil is, in fact, the chemotactic response towards the hydrocarbons present in the crude oil.

Another notable insight into the degrading strain's displayed chemotaxis is that not all oil-degrading strains exhibit the chemotactic response towards crude oil. Our study also evaluated the chemotactic process of another oil-degrading strain *R. erythropolis* T7-2 and found that T7-2 showed chemotaxis towards crude oil is neither the swarm plate assay (Fig. 2H) nor the modified agarose plug assay (Fig. 3C). A standard laboratory strain *P. aeruginosa* PAO-1, which could neither degrade nor chemotaxis toward crude oil, was used as a control (Fig. 2I and 3D). These results suggest that not all oil-degrading bacterial strains are chemotactic towards the crude oil. Some strains were not even mobile and failed to form chemotactic rings, although they could efficiently degrade crude oil. These microorganisms usually have unique properties, such as a high cell surface hydrophobicity observed for Gram-positive bacteria and unique cell surface structures in other bacteria (Zita and Hermansson 1997; Liu et al. 2004). As previously reported, bacterial adhesion is also a strategy for oil-degrading bacteria to attach to the surface of crude oil, which mainly depends on the bacterial hydrophobic property (Bruinsma et al. 2001). The *R. erythropolis* T7-2 strain, for example, known for

its high cell surface hydrophobicity, displays mycolic acids with carbon chain lengths ranging from 27 to 54 on its cell surface. These observations provide a foundation for biological applications in demulsifying crude oil emulsions in water obtained from oil fields. The T7-2 strain cells' surface is strongly hydrophobic (Table I), which allowed this strain to come into contact with organic compounds, such as crude oil, more efficiently. The T7-2 strain was shown to be able to use *n*-alkanes from C_{12} to C_{36} , with about a 60% extent of hexadecane degradation (Huang et al. 2007). Shaking facilitated fermentation of the oil degradation medium of T7-2 improved the adherence of bacterial cells to the crude oil, as well as the rate of degradation. This type of microorganism, which is used in EOR might depend mainly on their biosurfactant productivity and hydrophobic properties *in situ*.

Furthermore, our results support the existence of chemotactic migration of the strain 6-1B towards crude oil. To analyze the chemotactic process of *P. aeruginosa* 6-1B further, we modified the swarm plate to an oil plate by maintaining the same composition while increasing the concentration of crude oil to 0.1% (Fig. 4). The higher crude oil concentration caused many small oil droplets on the swarm plate. A faint ring was formed on the oil plate (Fig. 4A). The ring's edge was excised and observed under the microscope, which revealed that many bacterial cells surrounded the oil droplet (Fig. 4B and 4C). Based on the 16S rRNA sequencing analysis, cells surrounding the oil droplet were *P. aeruginosa* 6-1B (100% identity), which demonstrated the existence of chemotactic migration by the 6-1B strain towards crude oil. Similar results have been obtained in the modified agarose plug assay (Fig. 3A and 5A). The maximum cell density was found at the water and oil interface (Fig. 5C); there was a rising trend in cell density as we observed nearer to the interface, which we attributed mainly to a large number of highly motile strain 6-1B that accumulated in the interface around

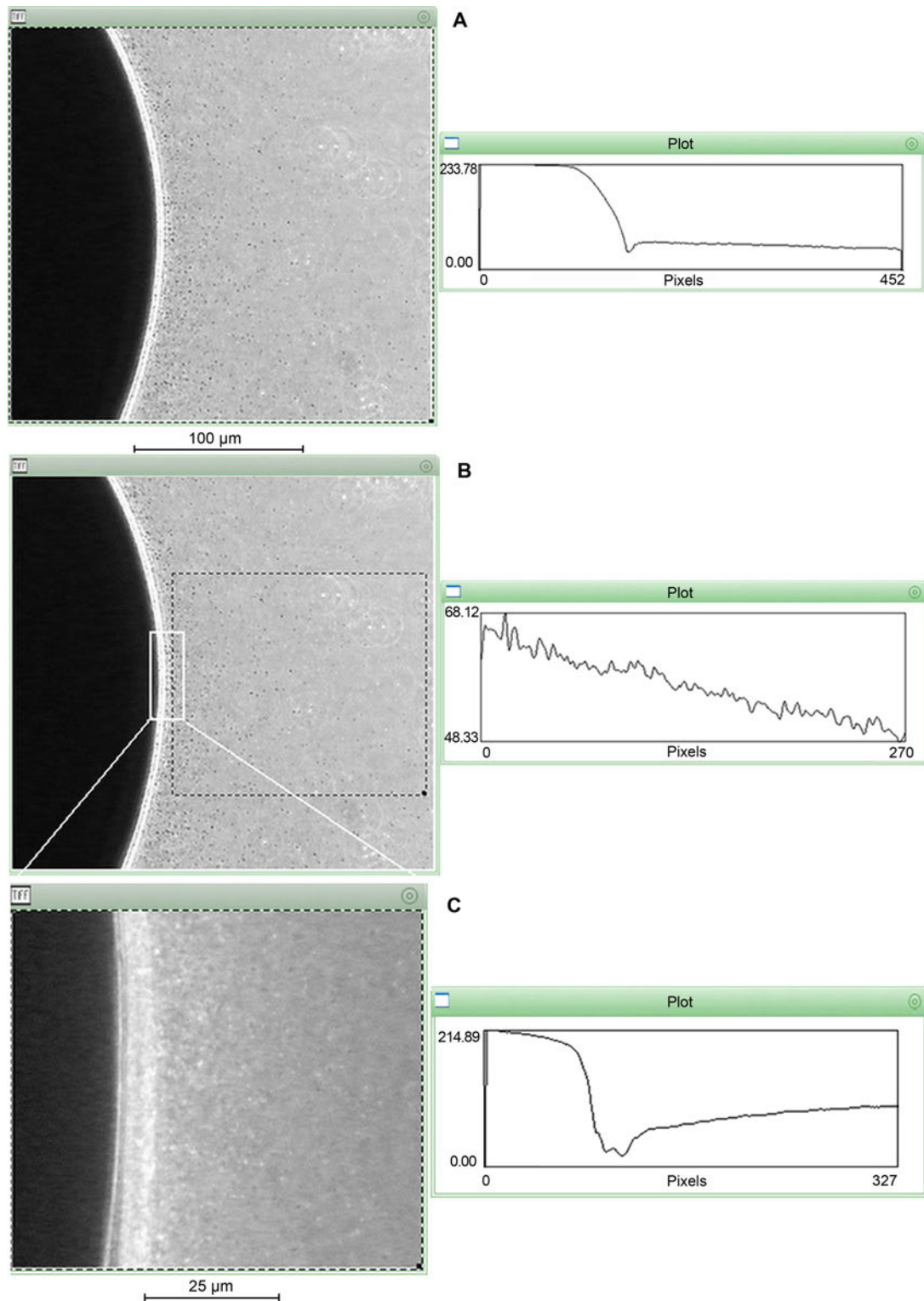


Fig. 5. *P. aeruginosa* 6-1B cells' distribution around the crude oil droplet.

The strain 6-1B movement towards the oil droplets was analyzed under the phase-contrast microscope (Olympus BH2 microscope, Japan) using the Scion Image 3b Software (Scion, Frederick, MD). A) The chemotactic trend of the strain 6-1B toward crude oil (125× magnification); B) the chemotactic trend of the dashed area; C) the chemotactic trend of the strain 6-1B toward crude oil of the area of the white line in Fig. 5B (400× magnification).

the oil droplet when they were observed using negative phase-contrast microscopy.

In contrast, cells of the strain T7-2 were uniformly distributed around the oil droplet and tumbled *in situ*, with no cells moving forward (Fig. 3C). The non-

degrading PAO1 cells also moved randomly, showing no directionality in their movements (Fig. 5C). Based on the evidence listed above, we can conclude that the 6-1B strains present chemotactic migration towards the crude oil.

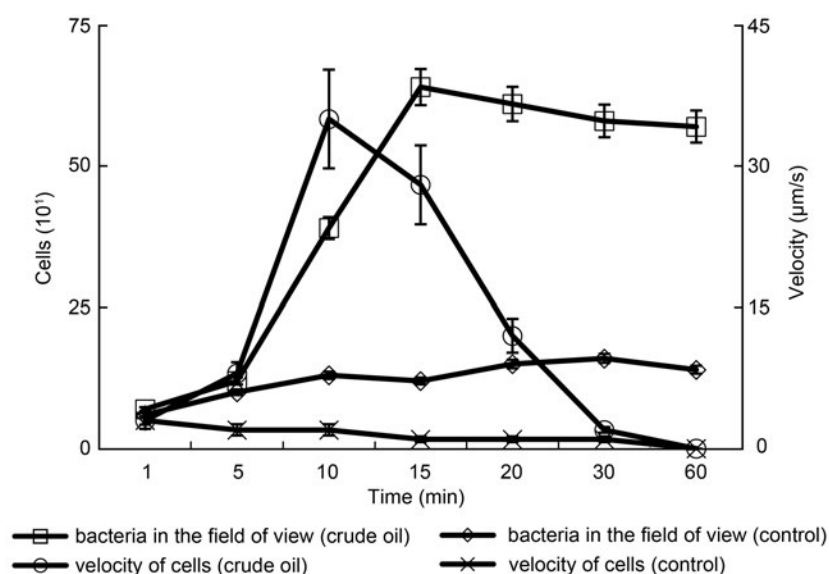


Fig. 6. The number of chemotactic cells (left y-axis) and chemotactic velocity curves (right y-axis) of *P. aeruginosa* 6-1B toward the crude oil.

The control chamber was treated without crude oil, which served as the chemoattractant in the other setups. A chosen $50\ \mu\text{m} \times 50\ \mu\text{m}$ area was magnified 500 times for the determination of cell velocity. The chemotaxis videos were divided into images, and an average velocity was determined from observed cell movements that had relatively straight trajectories. Data represent the averages and the standard deviations of five independent experiments.

Potential chemotactic process of *P. aeruginosa* 6-1B toward the crude oil. Although chemotaxis rings around NAPL-related compounds observed by microscopy had been reported (Vardar et al. 2005), the detailed description of that process was still limited. Here, we characterized the chemotaxis process of the strain 6-1B toward the crude oil (Fig. 6). In the first 5 minutes, most of the cells tumbled *in situ* and did not move at all, while only a few cells moved towards the oil droplet at a low velocity (about $3\text{--}5\ \mu\text{m/s}$). During the following 10 minutes, the cells rapidly swarm toward the crude oil droplet interface, with a velocity reaching up to $35\ \mu\text{m/s}$. The speed changed as time passed, as the number of cells around the oil and near the interface increased. The velocity of the cells declined quickly after 30 minutes. The cells then stopped swimming toward the oil chemoattractant and tumbled *in situ* for several days. According to the above results, the potential chemotaxis process of the strain 6-1B toward crude oil could be summarized in the following steps: searching for the attractant crude oil, moving toward the attractant crude oil, and consuming (degrading) the crude oil. In general, the strain 6-1B can successfully reach the oil-water interface and degrade them by achieving these steps. This chemotactic mechanism may provide the strain 6-1B a greater chance of contacting and utilizing the crude oil as a carbon and energy source.

The chemotactic response to some attractant chemicals is of great advantage for bacterial survival. Bacterial chemotaxis can usually form a dense distribution of cells around the oil quickly, and it is an effective way

to maintain hydrocarbon bioavailability (Pandey and Jain 2002). Chemotaxis provides a more active process to gain proximity to a liquid hydrocarbon source to enhance cell growth and increase the apparent dissolution rate of the hydrocarbon. Contact between a bacterial cell and a target hydrocarbon can significantly increase hydrocarbon diffusion rate into the cell (Meng et al. 2019). To efficiently metabolize the crude oil as a carbon source, the strain 6-1B should migrate closer to the oil and water interface via chemotaxis towards the increased concentrations of crude oil compounds dissolved in the aqueous phase. In this manner, the strain 6-1B can efficiently utilize the hydrocarbons at the oil-water interface, improving their growth. Their ability to produce the rhamnolipid biosurfactant will also increase, improving the crude oil's solubility, decreasing the surface tension and the interfacial tension between oil and water. The biosurfactant was shown to play an essential role in microbial degradation of the crude oil by facilitating the utilization of crude oil dissolved in an aqueous phase (Lee et al. 2018). The rhamnolipids improve the miscibility of hydrocarbons and crude oil in water, contributing to the degradation of crude oil significantly.

Conclusion

Although chemotaxis towards pure hydrocarbons has been demonstrated, the research on bacterial chemotaxis towards crude oil is still limited. In this study,

an oil-degrading strain of *P. aeruginosa*, named 6-1B, has been found to have chemotactic activity towards crude oil and its gradient *n*-alkenes such as dodecane, tridecane, tetradecane, pentadecane, and hexadecane, as demonstrated by the use of two different chemotactic assays. Moreover, according to the different distributions of cells around the crude oil, the potential chemotaxis process of the strain 6-1B toward crude oil is proposed as the following steps: searching, moving and consuming. Thus, it may be assumed that the chemotaxis-dependent movement of the strain 6-1B enhances the chance of bacteria to reach contact with the crude oil, resulting in the improvement of the degradation of crude oil. Subsequently, the produced biosurfactant during degradation could then be used to enhance oil recovery when this process is applied in underground oil wells.

ORCID

Kaiqiang Liang <https://orcid.org/0000-0001-7866-2125>

Acknowledgments

This work was supported by the Demonstration Project of Sino-Australian International Cooperation on CCUS Integration.

Conflict of interest

The authors do not report any financial or personal connections with other persons or organizations, which might negatively affect the contents of this publication and/or claim authorship rights to this publication.

Literature

- Batista SB, Munteer AH, Amorim FR, Tótoia MR.** Isolation and characterization of biosurfactant/bioemulsifier-producing bacteria from petroleum contaminated sites. *Bioresour Technol.* 2006 Apr;97(6):868–875. <https://doi.org/10.1016/j.biortech.2005.04.020>
- Boudko D, Yu HS, Ruiz M, Hou S, Alam M.** A time-lapse capillary assay to study aerotaxis in the archaeon *Halobacterium salinarum*. *J Microbiol Methods.* 2003 Apr;53(1):123–126. [https://doi.org/10.1016/s0167-7012\(02\)00227-0](https://doi.org/10.1016/s0167-7012(02)00227-0)
- Brown LR.** Microbial enhanced oil recovery (MEOR). *Curr Opin Microbiol.* 2010 Jun;13(3):316–320. <https://doi.org/10.1016/j.mib.2010.01.011>
- Bruinsma GM, van der Mei HC, Busscher HJ.** Bacterial adhesion to surface hydrophilic and hydrophobic contact lenses. *Biomaterials.* 2001 Dec;22(24):3217–3224. [https://doi.org/10.1016/s0142-9612\(01\)00159-4](https://doi.org/10.1016/s0142-9612(01)00159-4)
- Dan L, Lei H, Guo-Qiang L, Zhao-Yu L, Ting M, Feng-Lai L, Ru-Lin L.** [Study on the bioemulsifier produced by a hydrocarbon-degrading strain T7-2 and its physic-chemical properties] (In Chinese). *Microbiol China.* 2008;35(5):0653–0660.
- Gandhimathi R, Seghal Kiran G, Hema TA, Selvin J, Rajeetha Raviji T, Shanmughapriya S.** Production and characterization of lipopeptide biosurfactant by a sponge-associated marine actinomycetes *Nocardiopsis alba* MSA10. *Bioprocess Biosyst Eng.* 2009 Oct;32(6):825–835. <https://doi.org/10.1007/s00449-009-0309-x>
- Gomes DLR, Peixoto RS, Barbosa EAB, Napoleão F, Sabbadini PS, Dos Santos KR, Mattos-Guaraldi AL, Hirata R.** Sub-MICs of penicillin and erythromycin enhance biofilm formation and hydrophobicity of *Corynebacterium diphtheriae* strains. *J Med Microbiol.* 2013 May;62(Pt 5):754–760. <https://doi.org/10.1099/jmm.0.052373-0>
- Ha DG, Kuchma SL, O'Toole GA.** Plate-based assay for swarming motility in *Pseudomonas aeruginosa*. *Methods Mol Biol.* 2014; 1149: 67–72. https://doi.org/10.1007/978-1-4939-0473-0_8
- Head IM, Jones DM, Larter SR.** Biological activity in the deep subsurface and the origin of heavy oil. *Nature.* 2003 Nov 20;426(6964):344–352. <https://doi.org/10.1038/nature02134>
- Huang L, Li D, Sun D, Xie YJ, Ma T, Liang FL, Liu RL.** [Isolation and identification of a low temperature hydrocarbon-degrading strain and its degradation characteristics] (In Chinese). *Huan Jing Ke Xue.* 2007 Sep;28(9):2101–2105.
- Kryachko Y.** Novel approaches to microbial enhancement of oil recovery. *J Biotechnol.* 2018 Jan 20;266:118–123. <https://doi.org/10.1016/j.jbiotec.2017.12.019>
- Lanfranchi MP, Alvarez HM, Studdert CA.** A strain isolated from gas oil-contaminated soil displays chemotaxis towards gas oil and hexadecane. *Environ Microbiol.* 2003 Oct;5(10):1002–1008. <https://doi.org/10.1046/j.1462-2920.2003.00507.x>
- Law AM, Aitken MD.** Bacterial chemotaxis to naphthalene desorbing from a nonaqueous liquid. *Appl Environ Microbiol.* 2003 Oct;69(10):5968–5973. <https://doi.org/10.1128/aem.69.10.5968-5973.2003>
- Lee DW, Lee H, Kwon BO, Khim JS, Yim UH, Kim BS, Kim JJ.** Biosurfactant-assisted bioremediation of crude oil by indigenous bacteria isolated from Taean beach sediment. *Environ Pollut.* 2018 Oct;241:254–264. <https://doi.org/10.1016/j.envpol.2018.05.070>
- Liu Y, Yang SF, Li Y, Xu H, Qin L, Tay JH.** The influence of cell and substratum surface hydrophobicities on microbial attachment. *J Biotechnol.* 2004 Jun 10;110(3):251–256. <https://doi.org/10.1016/j.jbiotec.2004.02.012>
- Marx RB, Aitken MD.** Bacterial chemotaxis enhances naphthalene degradation in a heterogeneous aqueous system. *Environ Sci Technol.* 2000 Jul;34(16):3379–3383. <https://doi.org/10.1021/es000904k>
- Meng L, Li W, Bao M, Sun P.** Great correlation: Biodegradation and chemotactic adsorption of *Pseudomonas synxantha* LSH-7⁺ for oil contaminated seawater bioremediation. *Water Res.* 2019 Apr 15;153:160–168. <https://doi.org/10.1016/j.watres.2019.01.021>
- Nakamura S, Minamino T.** Flagella-driven motility of bacteria. *Biomolecules.* 2019 Jul 14;9(7):279. <https://doi.org/10.3390/biom9070279>
- Ni B, Colin R, Link H, Endres RG, Sourjik V.** Growth-rate dependent resource investment in bacterial motile behavior quantitatively follows potential benefit of chemotaxis. *Proc Natl Acad Sci USA.* 2020 Jan 7;117(1):595–601. <https://doi.org/10.1073/pnas.1910849117>
- Pandey G, Jain RK.** Bacterial chemotaxis toward environmental pollutants: role in bioremediation. *Appl Environ Microbiol.* 2002 Dec;68(12):5789–5795. <https://doi.org/10.1128/aem.68.12.5789-5795.2002>
- Parales RE, Harwood CS.** Bacterial chemotaxis to pollutants and plant-derived aromatic molecules. *Curr Opin Microbiol.* 2002 Jun;5(3):266–273. [https://doi.org/10.1016/s1369-5274\(02\)00320-x](https://doi.org/10.1016/s1369-5274(02)00320-x)
- Patowary K, Patowary R, Kalita MC, Deka S.** Characterization of biosurfactant produced during degradation of hydrocarbons using crude oil as sole source of carbon. *Front Microbiol.* 2017 Feb 22;8:279. <https://doi.org/10.3389/fmicb.2017.00279>
- Pedit JA, Marx RB, Miller CT, Aitken MD.** Quantitative analysis of experiments on bacterial chemotaxis to naphthalene. *Biotechnol Bioeng.* 2002 Jun 20;78(6):626–634. <https://doi.org/10.1002/bit.10244>

- Rocha VAL, de Castilho LVA, de Castro RPV, Teixeira DB, Magalhães AV, Gomez JGC, Freire DMG.** Comparison of mono-rhamnolipids and di-rhamnolipids on microbial enhanced oil recovery (MEOR) applications. *Biotechnol Prog.* 2020 Jul;36(4):e2981. <https://doi.org/10.1002/btpr.2981>
- Roggo C, Clerc EE, Hadadi N, Carraro N, Stocker R, van der Meer JR.** Heterologous expression of *Pseudomonas putida* methyl-accepting chemotaxis proteins yields *Escherichia coli* cells chemotactic to aromatic compounds. *Appl Environ Microbiol.* 2018 Aug 31;84(18):e01362-18. <https://doi.org/10.1128/AEM.01362-18>
- Sampedro I, Parales RE, Krell T, Hill JE.** *Pseudomonas* chemotaxis. *FEMS Microbiol Rev.* 2015 Jan;39(1):17–46. <https://doi.org/10.1111/1574-6976.12081>
- Vardar G, Barbieri P, Wood TK.** Chemotaxis of *Pseudomonas stutzeri* OX₁ and *Burkholderia cepacia* G₄ toward chlorinated ethenes. *Appl Microbiol Biotechnol.* 2005 Mar;66(6):696–701. <https://doi.org/10.1007/s00253-004-1685-4>
- Waite AJ, Frankel NW, Emonet T.** Behavioral variability and phenotypic diversity in bacterial chemotaxis. *Annu Rev Biophys.* 2018 May 20;47:595–616. <https://doi.org/10.1146/annurev-biophys-062215-010954>
- Yang J, Chawla R, Rhee KY, Gupta R, Manson MD, Jayaraman A, Lele PP.** Biphasic chemotaxis of *Escherichia coli* to the microbiota metabolite indole. *Proc Natl Acad Sci USA.* 2020 Mar 17;117(11):6114–6120. <https://doi.org/10.1073/pnas.1916974117>
- Zheng M, Wang W, Papadopoulos K.** Direct visualization of oil degradation and biofilm formation for the screening of crude oil-degrading bacteria. *Bioremediat J.* 2020;24(1):60–70. <https://doi.org/10.1080/10889868.2019.1671795>
- Zita A, Hermansson M.** Effects of bacterial cell surface structures and hydrophobicity on attachment to activated sludge flocs. *Appl Environ Microbiol.* 1997 Mar;63(3):1168–70. <https://doi.org/10.1128/AEM.63.3.1168-1170.1997>

Supplementary materials are available on the journal's website.

Spa typing of *Staphylococcus aureus* Isolated from Clinical Specimens from Outpatients in Iraq

KHAIRALLAH A.S. MOHAMMED*, ZAHRAA H. ABDULKAREEM, AYOOB R. ALZAALAN
and AMEL K. YAQOOB

Department of Medical Lab Technology, College of Health and Medical Technology,
Southern Technical University, Basrah, Iraq

Submitted 17 November 2020, revised 18 January 2021, accepted 19 January 2021

Abstract

Methicillin-resistant *Staphylococcus aureus* (MRSA) is notorious as a hospital superbug and a problematic pathogen among communities. The incidence of MRSA has substantially increased over time in Iraq. The aim of this study was to determine the prevalence and *spa* types of MRSA isolates from outpatients or patients upon admission into hospitals. Various biochemical tests identified *S. aureus* isolates, and then this identification was confirmed by PCR using species-specific 16S rRNA primer pairs. Antibiotic susceptibility was determined against methicillin, oxacillin, and vancomycin using the disk diffusion method. Vancomycin MIC was detected by VITEK 2 compact system. All the identified isolates were screened for the presence of *mecA* and *lukS-PV-lukF-PV* genes; 36 of them were subjected to *spa* typing-based PCR. Out of 290 clinical samples, 65 (22.4%) were *S. aureus*, of which 62 (95.4%) strains were resistant to oxacillin and methicillin. Except for two isolates, all MRSA isolates were *mecA* positive. One of the three MSSA isolates was *mecA* positive. Five strains were resistant to vancomycin. Fourteen (21.5%) isolates were positive for the presence of *lukS-PV-lukF-PV* genes. *Spa* typing of 36 *S. aureus* isolates revealed eleven different *spa* types, t304 (30.3%), t307 (19.4%), t346 (8.3%), t044 (8.3%), t15595 (8.3%), t386 (5.5%), t5475 (5.5%), t17928 (2.8%), t14870 (2.8%), t021 (2.8%), and t024 (2.8%). These findings could be useful for assessing the genetic relatedness of strains in the region for epidemiological and monitoring purposes, which would be essential to limiting the spread of MRSA.

Key words: *Staphylococcus aureus*, methicillin resistance, *spa* typing, PCR

Introduction

Staphylococcus aureus is the most common cause of nosocomial and community-acquired infections worldwide (Lakhundi and Zhang 2018; Kourtis et al. 2019). Since the late 1970s, the importance of *S. aureus* increased due to the emergence and spread of their resistance to methicillin and vancomycin (Parker and Hewitt 1970; Bendary et al. 2016; Abd El-Aziz et al. 2018).

Recent studies have shown marked dissemination of methicillin-resistant *S. aureus* in Iraq (Kareem et al. 2015; Kareem et al. 2020). Hence, epidemiological studies of these bacteria are significantly important to determine their source and to control their spread in the community and hospital settings. Different methods such as bacteriophage typing, antibiotyping, genotyping, *spa* typing-based PCR, and DNA sequencing have been used to investigate the hospital and community-

onset *S. aureus* infections (Locatcher-Khorazo and Gutierrez 1960; Fréney et al. 1996; van Leeuwen et al. 1999; Yadav et al. 2018). *Spa* typing is based on the polymorphism of the gene encoding protein A (*spa*). Protein A is an essential virulence factor of *S. aureus* consisting of five IgG binding sites (A, B, C, D, E) and C-terminal cell wall attachment portion. The gene encoding this protein (*spa*) consists of two regions, one encodes the Fc-binding domain, and the other encodes X region (Harmsen et al. 2003). The X region includes the Xr region and the Xc region, which encodes the cell wall attachment sequence. The Xr region consists of a variable number of 24 bp repeats and is located immediately upstream of the region encoding the C-terminal cell wall attachment sequence (Guss et al 1984; Uhlén et al. 1984; Schneewind et al. 1992). The Xr region's diversity may arise from deletion, duplication of the repetitive units, or point mutation (Brigido et al. 1991).

* Corresponding author: K.A.S. Mohammed, Department of Medical Lab Technology, College of Health and Medical Technology, Southern Technical University, Basrah, Iraq; e-mail: dr.kmohammed@stu.edu.iq

© 2021 Khairallah A.S. Mohammed et al.

This work is licensed under the Creative Commons Attribution-NonCommercial-NoDerivatives 4.0 License (<https://creativecommons.org/licenses/by-nc-nd/4.0/>).

Therefore, the *spa* gene is variable in length in various strains of this species because of its X region diversity. *Spa* typing method is based on the number of tandem repeats and the sequence variation in region X of the protein A gene. Numerous studies demonstrated different *spa* gene patterns among MRSA strains isolated from patients in different geographic locations in the world (Furuya et al. 2010). The main advantages of *spa* typing-based PCR and DNA sequencing is the speed, the simplicity of large database establishment and the ease of use as well as the clarity of data. Furthermore, DNA sequencing has demonstrated outstanding type ability and reproducibility for studying the origin and evolution of *S. aureus* strains (Stefani et al. 2012).

In the light of the above, typing of methicillin-resistant *S. aureus* isolates is a useful tool for studying the genetic diversity of the pathogens, clonal relatedness and tracking the spread of MRSA infections. Currently, there is not adequate information about typing of community-associated methicillin-resistant *S. aureus* in Iraq. This study aimed to determine the *spa* types among clinical isolates of *S. aureus* obtained from outpatients in the South of Iraq.

Experimental

Materials and Methods

Bacterial strains and susceptibility test. A total of 65 *S. aureus* strains isolated from 290 clinical specimens were obtained from outpatients or patients upon admission into hospitals in Basrah and Thi-Qar city, South of Iraq. The following patients were excluded: recent admission to hospitals, patients on hemodialysis, recent surgical operation, or an intravenous cannula at the time of swab taking. *S. aureus* isolates were collected from urine samples, tonsil swabs, nasal swabs, wound swabs, burn swabs, blood samples, and sputum (Table I). All strains

were identified as *S. aureus* according to the standard microbiological techniques (Merlino et al. 2000).

Antibiotic susceptibility testing to methicillin (10 µg), oxacillin (1 µg), and vancomycin (30 µg) were carried out on Mueller-Hinton agar (Oxoid Limited, Hampshire, England) using the Kirby-Bauer disk diffusion method, according to the recommendations by the Clinical and Laboratory Standard Institute (CLSI 2019). Vancomycin MIC was detected by VITEK 2 compact system (bioMérieux, Inc., Durham, NC, software version 8.01 and AST-GP580).

DNA isolation and PCR conditions. DNA extraction was carried out with a mercantile DNA isolation kit (Promega, USA) according to the manufacturer's instructions.

Molecular identification of *S. aureus*. PCR was used to amplify 228 bp region of 16S rRNA gene fragment of *S. aureus*, which is highly conserved at a species level, using specific primers F 5'-GTAGGTGGCAAGCGTTATCC-3' and R 5'-CGCACATCAGCGTCAG-3' (Monday and Bohach 1999).

Detection of *mecA* gene. All identified *S. aureus* isolates were tested for the presence of the 310 base pair bp PCR product of the *mecA* gene using the following primers: F 5'-GTAGAAATGACTGAACGTC-CGATAA-3' and (R 5'-CCAATCCACATTGTTTCG-GTCTAA-3' (Geha et al. 1994).

Detection of *lukS-PV-lukF-PV*. All isolates were tested for the presence of the *lukS-PV-lukF-PV* genes, which encode for Pantone-Valentine leucocidin (PVL); in PCR assays using previously described primers and protocols (Lina et al. 1999).

***Spa* typing.** Primers *spa* 1 (F 5'-ATCTGGTG-GCGTAACACCTG-3') and *spa* 2 (R 5'-CGCTGCACCTAACGCTAATG-3') were used to amplify a portion of the *spa* gene (products Variable: 1,150–1,500 bp) of the 65 isolates (Wichelhaus et al. 2001).

PCR mix reaction. The PCR reaction mix had a final volume of 25 µl consisting of 2 µl (50–100 ng)

Table I
Prevalence and characterization of *S. aureus* isolates in different clinical samples.

Sample	Strain No	Vancomycin test		Methicillin and oxacillin test		The <i>mecA</i> gene		The <i>spa</i> gene		The <i>pvl</i> gene
		VSSA	VRSA	MRSA	MSSA	<i>mecA</i> +	<i>mecA</i> -	<i>spa</i> +	<i>spa</i> -	
1 Urine	34	32	2	32	2	31	3	23	11	5
2 Nasal swab	7	4	3	7	0	7	0	7	0	2
3 Wound	9	9	0	9	0	9	0	9	0	3
4 Burn	5	5	0	5	0	5	0	5	0	2
5 Tonsil	6	6	0	6	0	5	1	6	0	2
6 Blood	2	2	0	1	1	2	0	2	0	
7 Sputum/pleural	2	2	0	2	0	2	0	2	0	
Total	65	60	5	62	3	61	4	54	11	14

DNA, 1 µl (20 pmol) of each primer, 12.5 µl of master mix (Taq DNA polymerase, dNTPs, MgCl₂ and reaction buffers; Promega) and 8.5 µl of nuclease-free water, under the following conditions: initial denaturation at 94°C for 4 min; followed by 35 cycles of denaturation at 95°C for 30 s, annealing at 56°C for 30 s, and extension at 72°C for 90 s, followed by a final extension at 72°C for 5 min. The *mecA* and 16S rRNA genes were amplified under similar conditions except that the extension was 1 min. PCR amplification products were separated on 1–2% agarose gels and visualized by staining with ethidium bromide using a UV light transilluminator.

DNA sequencing. According to the Macrogen Company requirement (Seoul, South Korea), 20 µl of *spa* gene PCR products of selected 36 *S. aureus* isolates were sent for DNA sequencing for both strands. The primers used for DNA sequencing of the X region of the *spa* gene were as follows: *spa*-1113f (5'-TAAAGACGATCCTTCGGTGAGC-3') and *spa*-1514r (5'-CAGCAGTAGTGCCGTTTGCTT-3') (Kahl et al. 2005).

DNA sequence analysis. The sequences obtained were analyzed and aligned using the Bio Edit program (Hall 1999). The *spa* typing and evaluation of *spa* types of *S. aureus* strains were performed using the *spa* database <http://spatyper.fortinbras.us/> and (<http://www.ridom.de/spaserver>). The *spa* types' phylogenetic tree was drawn using the Molecular Evolutionary Genetics Analysis (MEGA 7.0) (Kumar et al. 2016).

GenBank accession numbers. The DNA sequences of the partial *spa* gene from the representative isolates have been deposited in the GenBank database under accession numbers LC577038-LC577073 for isolates KAZ1-KAZ37, respectively, and LC586070.1 for KAZ7.1 isolate.

Results

A total of 65 (22.4%) *S. aureus* strains were isolated from 290 clinical specimens. *S. aureus* isolates were identified according to the standard microbiological techniques. All 65 *S. aureus* (100%) samples exhibited positive results for the 16S rRNA gene.

Differentiation was based on sensitivity testing using oxacillin, methicillin, and vancomycin discs, confirmed by detecting the amplified 310 bp *mecA* gene using PCR in MRSA strains.

Among the 65 *S. aureus* isolates, the highest number of isolates were from urine samples (n = 34, 52.3%) followed by wound swabs (n = 9, 13.8%) nasal swabs (n = 7, 10.8%), tonsils (n = 6, 9.2%), burns (n = 5, 7.7%), blood (n = 2, 3.1%) and sputum and tracheal aspirates 2 (3.1%) as shown in Table I.

Antimicrobial susceptibility testing of MRSA isolates. Out of 65 isolates, 62 (95.4%) strains were

resistant to oxacillin and methicillin. The *mecA* gene was detected in 60 (96.8%) MRSA strains, whereas 2 (3.2%) MRSA strains lacked the *mecA* gene (Table I). Out of the four *mecA*-negative *S. aureus*, two strains were resistant to oxacillin and methicillin. On the other hand, a single strain was *mecA*-positive but sensitive to oxacillin and methicillin. Five (7.7%) strains were resistant to vancomycin in addition to resistance to oxacillin and methicillin, as shown in Table I.

The *lukS-PV-lukF-PV* genes detection. All 65 *S. aureus* isolates were screened for the presence of the *lukS-PV-lukF-PV* genes, which encode for Pantone-Valentine leucocidin (PVL). Fourteen (21.5%) isolates were positive for the presence of the *lukS-PV-lukF-PV* genes, these isolates were isolated from burns, tonsil swabs, and urine samples (Table I).

***Spa* typing.** Out of 65 strains, 54 (83.1%) showed the *spa* gene PCR products with different sizes, reflecting the number of 24 bp repeat units within the *spa* gene (Fig. 1, Table I). These PCR products generated two different *spa* types, 52 strains (96.3%) showed a single PCR band, and only two strains (3.7%) showed two PCR bands. The *spa* gene PCR products were not detected in eleven strains, which were all isolated from urine samples (Table I). The absence of the *spa* gene could be due to mutations in the primer-binding region or true deficiency of the *spa* gene in these isolates; however, this finding needs further study to be confirmed. PCR products of the *spa* gene of representative 36 isolates were sequenced and typed.

Spa typing of 36 *S. aureus* isolates revealed eleven different *spa* types, t304 (12 isolates, 30.3%), t307 (7 isolates, 19.4%), t346 (3 isolates, 8.3%), t044 (3 isolates, 8.3%), t15595 (3 isolates, 8.3%), t386 (2 isolates, 5.5%), t5475 (2 isolates, 5.5%), t17928 (1 isolate, 2.8%), t14870 (1 isolate, 2.8%), t021 (1 isolate, 2.8%), and t024 (1 isolate, 2.8%).

Based on phylogenetic relationships, *S. aureus* strains were classified into two main clades (Fig. 2). Except for t14870 and t386, all other *spa* types were included in

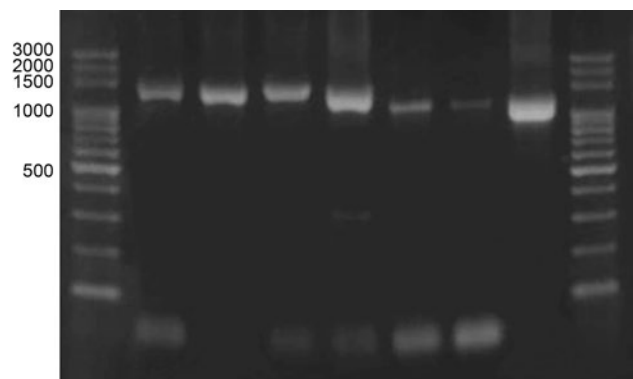


Fig. 1. The variable PCR product of the *spa* gene; lanes 2–8. Lanes 1 and 9, 100-bp DNA ladder.

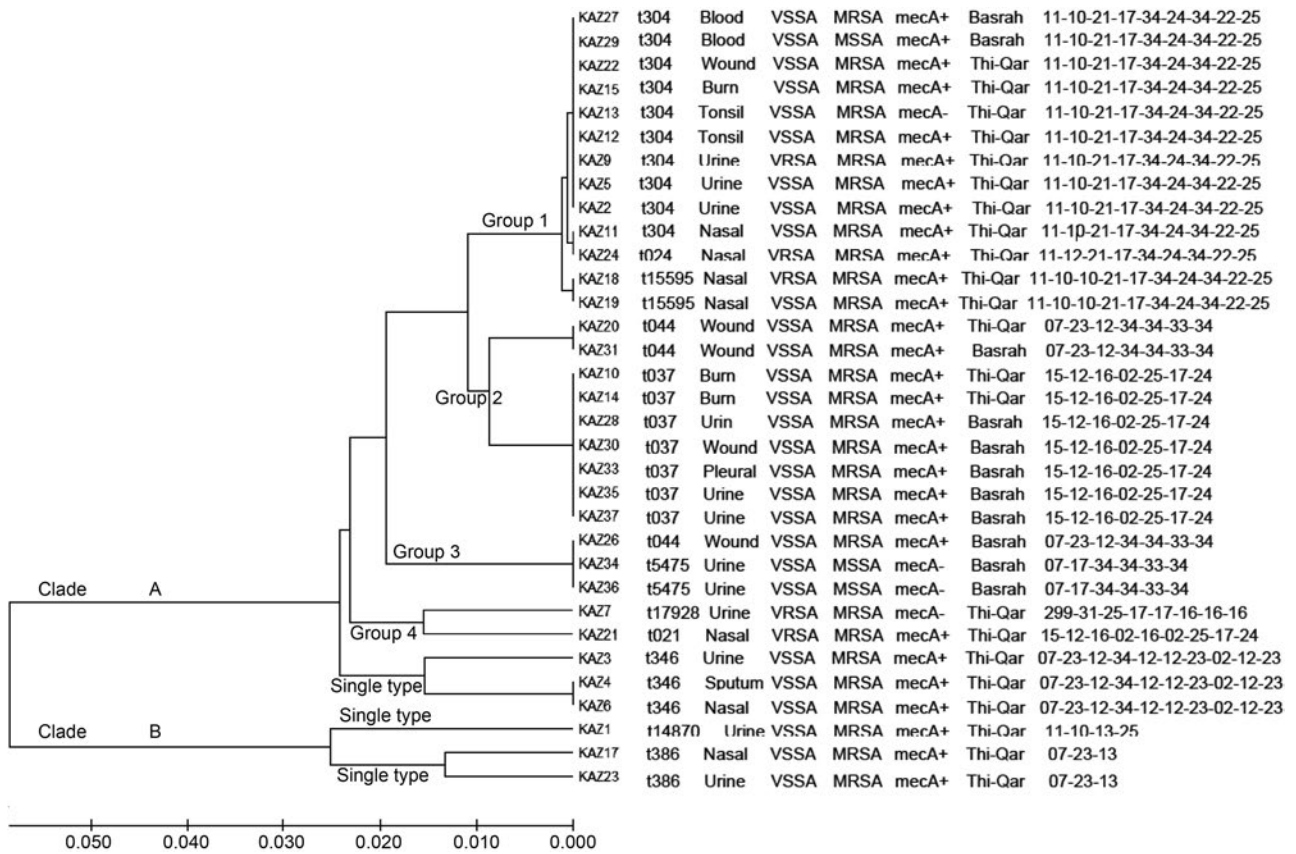


Fig. 2. Phylogenetic tree based on specimens, strain types, *spa* types, vancomycin and methicillin resistance, the *mecA* gene, geographical location, and *spa* repeats.

clade A. Thirty-three (91.7%) isolates were included in clade A, whereas only 3 (8.3%) isolates were included in clade B. Within clade A, the isolates were further clustered into four different groups and three single types based on the variation in tandem repeats of the *spa* gene, methicillin resistance, specimen source, and geographical location (Fig. 2). Cluster 1 consists of 13 out of 36 (36.1%) isolates, including *spa* type 304, t024, and t11595. Cluster 2 consists of nine out of 36 (25%) isolates, including type t044 and t037. Cluster 3 consists of three out of 36 (8.3%) isolates, including t5475 and t044. Cluster 4 consists of two out of 36 (5.5%) isolates, including t17928 and t021. The *spa* types t346, t14870, and t386 showed a single type.

Discussion

The high prevalence of MRSA is becoming a great public health concern. The resistance of *S. aureus* to multiple drugs restricts therapeutic options and causes severe morbidity and mortality in hospitalized patients and among communities (Gajdacs 2019). The rate of methicillin resistance in our study was 95.4%, which is comparable with the findings of previous local studies (Al-kadmy 2013; Ibed and Hamim 2014; Kareem et al.

2015; Kareem et al. 2020) and higher than other studies in different geographic regions of the world (Wang et al. 2012; Cirkovic et al. 2015; Akanbi et al. 2017; Gitau et al. 2018). Many factors could contribute to the variation in the rate of resistance, such as the population studied, type of isolates, and prescription of certain antibiotics in different geographic areas. Two MRSA isolates were negative for the *mecA* gene; this could indicate that these MRSA isolates have a different mechanism for methicillin resistance than through the *mecA* gene (Ba et al. 2014). On the other hand, a single MSSA isolate was *mecA*-positive. It could be due to an effective mutation leading to an inactivate *mecA* gene (Kuwahara-Arai et al. 1996). Our findings show that the presence or absence of the *mecA* gene may not be sufficient for the confirmed characterization of MRSA and MSSA isolates. However, further study is needed to understand the mechanism behind such a phenomenon of these isolates (MRSA *mecA*-negative and MSSA *mecA*-positive).

In Iraq, as indicated in this study and other recent studies (Kareem et al. 2015; Kareem et al. 2020), the prevalence of MRSA has significantly increased. Therefore, rapid and efficient typing of MRSA isolates is essential for epidemiological survey and infection control.

In the present study, *spa* typing based PCR and DNA sequencing were used to determine MRSA types

isolated from clinical samples. A selected number of clinical isolates (33 MRSA and three MSSA) as representative isolates collected from two regions in the south of Iraq were subjected to *spa* typing. Since it has several advantages such as simplicity, high discriminatory power, ease of interpretation, and reproducibility.

Our results revealed 11 different *spa* types, which were clustered into different groups (Fig. 2). This highlights the relationship between *spa* types and the potential application of *spa* typing in assessing phylogenetic and clonal relationships among clinical isolates. For epidemiological purposes, the clinical isolates were classified into two clades (Fig. 2). Out of 36 isolate, 33 strains belonged to t304, t037, t024, t044, t346, t021, t15595, and t5475, t17928 were clustered in clade A, indicating that 91.7% of the tested isolates were clonally related in the south of Iraq. Only three out of 36 strains (8.3%) belonging to two *spa* types (t386, t14700) were included in clade B, which could be explained by patient mobility from a different region in Iraq.

The *spa* types obtained in the present study varied in length between 10 (t346, t15595) and three (t386) repeats. The majority of the tested isolates belonged to t304 (30.3%) followed by t037 (19.4%). To our knowledge, this is the first time that these *spa* types have been found in Iraq. The phylogenetic tree (Fig. 2) showed that t037 is the predominant *spa* type in Basrah province, and all isolates included in this type are methicillin resistance. *Spa* type t037 was widely reported as the second common *spa* type in many Asian countries (Korea, Taiwan, Malaysia, Iran) and African countries (Kim et al. 2011; Asadollahi et al. 2018; Zarizal et al. 2018; Lee et al. 2019). The situation was quite different in Turkey (Güven Gökmen et al. 2018), where t030 was the predominant type, and t037 was detected as a low percentage (8%). Shakeri and Ghaemi (2014) found that the *spa* type t037 was the most predominant and the most common type among MRSA isolates in Iran. The regional clusters of *spa* type t037 found in both countries (Iran and Iraq) could be explained by cross-border patient mobility between Iraq and Iran. Accordingly, the cross-border transfer of patients may have a vital influence on the spreading and prevalence of MRSA in a certain clone (t037).

The present study showed that *spa* type t304 was the predominant type in the Thi-Qar province, and most of the strains of this type were methicillin-resistant. Few strains of this type were isolated from patients in Basrah province. *Spa* type t304 has been reported previously in Oman as the predominant type (Udo et al. 2014) but were not detected in Saudi Arabia (Monecke et al. 2012), Qatar (El-Mahdy et al. 2014), and Kuwait (Udo and Al-Sweih 2013). Generally, *spa* type t304 is rare globally and found only in five countries with a small number (Asadollahi et al. 2018). However,

our results showed a high frequency of t304 (30.6%) as the dominant type.

Other *spa* types identified with lower frequency in this study corresponded to t346, t044, t15595, t386, t5475, t17928, t14870, t021, and t024. All these *spa* types have been recorded for the first time in Iraq. Two strains belonged to t5475, and were isolated from patients in Basra. Both of them are methicillin-sensitive. This type (t5475) is very rare in the world; there are only six isolates with records of *spa* type t5475 in the Ridom SpaServer database (<http://www3.ridom.de/spa-server/>). The first MSSA isolates with *spa* type t5475 was reported from Denmark, but MRSA isolates with the same *spa* type have been reported from Sweden (<http://www3.ridom.de/spa-server/>).

Additionally, the present study showed that only one MRSA strain belonged to *spa* type t17928; noticeably, there is only one MSSA strain with records of this *spa* type that was reported from Sweden (<http://www3.ridom.de/spa-server/>). Furthermore, our results showed three MRSA strains belonged to t044, and one MRSA strain belonged to each of t021 and t024. All of these *spa* types are frequently reported in Europe (Asadollahi et al. 2018).

The present study explored distinct *spa* types recorded for the first time in Iraq and many of these *spa* types were not reported in the local region or neighboring countries. This could be explained by cross-border patient mobility or migrations from or to Iraq during and after the 2003 Iraq invasion. Although these findings provide vital information on the types of MRSA in Iraq, there were some limitations. The sources and the number of clinical samples were not enough to generalize the entire country's conclusions. Further studies are required to investigate more clinical samples, determine the *spa* types of the MRSA isolates, and trace the origin of these isolates.

This study also, revealed that 21.5% of isolates carried genes code for PVL. It was lower than the 44.3% and 54.2% *lukS-PV-lukF-PV*-positive isolates reported in Oman (Udo et al. 2014) and Saudi Arabia (Monecke et al. 2012), respectively but higher than the 14.6% positive rate obtained in Kuwait (AlFouzan et al. 2013) and the 12.7% positive rate obtained in Turkey (Akoğlu et al. 2010). Our results also showed a lower rate of the *lukS-PV-lukF-PV*-positivity than that obtained in Egypt (Abd El-Hamid et al. 2019). On the other hand, the present results are comparable with positive rates obtained in Iran (Fard-Mousavi et al. 2015), indicating the MRSA diversity harbored *lukS-PV-lukF-PV* genes in the region.

The rate of the prevalence of the *lukS-PV-lukF-PV* genes in MRSA isolated from burn specimens and other sites, in this study, suggests that PVL protein is an effective virulence factor of MRSA infections in our

community. Furthermore, no significant association was observed between *lukS-PV-lukF-PV*-positivity and a particular *spa* type, as the presence of the *lukS-lukF-PV* genes were observed among diverse *spa*-types.

In conclusion, our study reported a significant increase in the prevalence of CA-MRSA in Iraq. Based on *spa* typing, eleven different MRSA *spa* types were identified, with *spa* t037 and t304 being the predominant types. The CA-MRSA data could be useful in characterizing MRSA in Iraq and establishing a proper preventive and curative program. Therefore, further studies should focus on identifying MRSA and the incidence of different *S. aureus spa* types.

ORCID

Khairallah A.S. Mohammed <https://orcid.org/0000-0002-1175-0996>

Acknowledgment

The authors thank Mr. Ali N. Alsharefi, for providing part of the clinical specimens.

Conflict of interest

The authors do not report any financial or personal connections with other persons or organizations, which might negatively affect the contents of this publication and/or claim authorship rights to this publication.

Literature

- Abd El-Aziz NK, Abd El-Hamid MI, Bendary MM, El-Azazy AA, Ammar AM. Existence of vancomycin resistance among methicillin resistant *S. aureus* recovered from animal and human sources in Egypt. *Slov. Vet. Res.* 2018;55:221–230.
- Akanbi OE, Njom HA, Fri J, Otigbu AC, Clarke AM. Antimicrobial susceptibility of *Staphylococcus aureus* isolated from recreational waters and beach sand in Eastern Cape Province of South Africa. *Int J Environ Res Public Health.* 2017 Sep 1;14(9):1001. <https://doi.org/10.3390/ijerph14091001>
- Akoğlu, H., P. Zarakolu, B. Altun and S. Ünal. [Epidemiological and molecular characteristics of hospital-acquired methicillin-resistant *Staphylococcus aureus* strains isolated in Hacettepe University Adult Hospital in 2004–2005] (in Turkish). *Mikrobiyol Bul.* 2010 Jul;44(3):343–355.
- AlFouzan W, Al-Haddad A, Udo E, Mathew B, Dhar R. Frequency and clinical association of Pantone-Valentine leukocidin-positive *Staphylococcus aureus* isolates: a study from Kuwait. *Med Princ Pract.* 2013;22(3):245–249. <https://doi.org/10.1159/000343906>
- Al-kadmy IMS. A genetic study to differential HC/AC MRSA isolated from clinical cases in Iraq hospitals. *Mintage J Pharm Med Sci* 2013;2:57–62.
- Asadollahi P, Farahani NN, Mirzaii M, Khoramrooz SS, van Belkum A, Asadollahi K, Dadashi M, Darban-Sarokhalil D. Distribution of the most prevalent *spa* types among clinical isolates of methicillin-resistant and -susceptible *Staphylococcus aureus* around the world: a review. *Front Microbiol.* 2018 Feb 12;9:163. <https://doi.org/10.3389/fmicb.2018.00163>
- Ba X, Harrison EM, Edwards GF, Holden MT, Larsen AR, Petersen A, Skov RL, Peacock SJ, Parkhill J, Paterson GK, et al. Novel mutations in penicillin-binding protein genes in clinical *Staphylococcus aureus* isolates that are methicillin resistant on susceptibility testing, but lack the *mec* gene. *J Antimicrob Chemother.* 2014 Mar;69(3):594–597. <https://doi.org/10.1093/jac/dkt418>
- Bendary MM, Solyman SM, Azab MM, Mahmoud NE, Hanora AM. Characterization of Methicillin Resistant *Staphylococcus aureus* isolated from human and animal samples in Egypt. *Cell Mol Biol (Noisy-le-grand).* 2016 Feb 29;62(2):94–100. <https://doi.org/10.14715/cmb/2016.62.2.16>
- Brigido Mde M, Barardi CR, Bonjardin CA, Santos CL, Junqueira ML, Brentani RR. Nucleotide sequence of a variant protein A of *Staphylococcus aureus* suggests molecular heterogeneity among strains. *J Basic Microbiol.* 1991;31(5):337–45. <https://doi.org/10.1002/jobm.3620310508>
- Cirkovic I, Stepanovic S, Skov R, Trajkovic J, Grgurevic A, Larsen AR. Carriage and genetic diversity of methicillin-resistant *Staphylococcus aureus* among patients and healthcare workers in a Serbian University Hospital. *PLoS One.* 2015 May 20;10(5):e0127347. <https://doi.org/10.1371/journal.pone.0127347>
- CLSI. M100-S29 performance standards for antimicrobial susceptibility testing. Twenty-ninth informational supplement. Wayne (USA): Clinical Laboratory and Standards Institute; 2019.
- El-Mahdy TS, El-Ahmady M, Goering RV. Molecular characterization of MRSA isolated over a two year period in a Qatari hospital from multinational patients. *Clin Microbiol Infect.* 2014 Feb;20(2):169–73. <https://doi.org/10.1111/1469-0691.12240>
- Fard-Mousavi N, Mosayebi G, Amouzandeh-Nobaveh A, Japouni-Nejad A, Ghaznavi-Rad E. The dynamic of *Staphylococcus aureus* nasal carriage in central Iran. *undishapur J Microbiol.* 2015 Jul 25; 8(7):e20760. <https://doi.org/10.5812/jjm.20760v2>
- Frénay HM, Bunschoten AE, Schouls LM, van Leeuwen WJ, Vandembroucke-Grauls CM, Verhoef J, Mooi FR. Molecular typing of methicillin-resistant *Staphylococcus aureus* on the basis of protein A gene polymorphism. *Eur J Clin Microbiol Infect Dis.* 1996 Jan;15(1):60–64. <https://doi.org/10.1007/BF01586186>
- Furuya D, Tsuji N, Kuribayashi K, Tanaka M, Hosono Y, Uehara N, Watanabe N. Evaluation of *spa* typing for the classification of clinical methicillin-resistant *Staphylococcus aureus* isolates. *Jpn J Infect Dis.* 2010 Sep;63(5):364–367.
- Gajdác M. The continuing threat of methicillin-resistant *Staphylococcus aureus*. *Antibiotics (Basel).* 2019 May 2;8(2):52. <https://doi.org/10.3390/antibiotics8020052>
- Geha DJ, Uhl JR, Gustaferro CA, Persing DH. Multiplex PCR for identification of methicillin-resistant staphylococci in the clinical laboratory. *J Clin Microbiol.* 1994 Jul;32(7):1768–1772. <https://doi.org/10.1128/JCM.32.7.1768-1772.1994>
- Gitau W, Masika M, Musyoki M, Museve B, Mutwiri T. Antimicrobial susceptibility pattern of *Staphylococcus aureus* isolates from clinical specimens at Kenyatta National Hospital. *BMC Res Notes.* 2018 Apr 3;11(1):226. <https://doi.org/10.1186/s13104-018-3337-2>
- Guss B, Uhlén M, Nilsson B, Lindberg M, Sjöquist J, Sjö Dahl J. Region X, the cell-wall-attachment part of staphylococcal protein A. *Eur J Biochem.* 1984 Jan 16;138(2):413–420. <https://doi.org/10.1111/j.1432-1033.1984.tb07931.x>
- Güven Gökmen T, Kalayci Y, Yaman A, Köksal F. Molecular characterization of methicillin-resistant *Staphylococcus aureus* strains by *spa* typing and pulsed field gel electrophoresis methods. *BMC Microbiol.* 2018 Oct 24;18(1):155. <https://doi.org/10.1186/s12866-018-1305-6>
- Hall TA. BioEdit: a user-friendly biological sequence alignment editor and analysis program for Windows 95/98/NT. *Nucl Acids Symp Ser.* 1999;41:95–98.
- Harmsen D, Claus H, Witte W, Rothgänger J, Claus H, Turnwald D, Vogel U. Typing of methicillin-resistant *Staphylococcus*

- aureus* in a university hospital setting by using novel software for *spa* repeat determination and database management. *J Clin Microbiol.* 2003 Dec;41(12):5442–5448. <https://doi.org/10.1128/jcm.41.12.5442-5448.2003>
- Ibed AN, Hamim SS.** Molecular detection of methicillin resistant *Staphylococcus aureus* isolated from burns infection in Al-Nasiriyah city. *World J Pharm Pharmaceut Sci* 2014;2:950–954.
- Kahl BC, Mellmann A, Deiwick S, Peters G, Harmsen D.** Variation of the polymorphic region X of the protein A gene during persistent airway infection of cystic fibrosis patients reflects two independent mechanisms of genetic change in *Staphylococcus aureus*. *J Clin Microbiol.* 2005 Jan;43(1):502–505. <https://doi.org/10.1128/JCM.43.1.502-505.2005>
- Kareem SM, Aljubori SS, Ali MR.** Novel determination of *spa* gene diversity and its molecular typing among *Staphylococcus aureus* Iraqi isolates obtained from different clinical samples. *New Microbes New Infect.* 2020 Jan 29;34:100653. <https://doi.org/10.1016/j.nmni.2020.100653>
- Kareem SM, Al-Jubori SS, Ali MR.** Prevalence of *erm* genes among methicillin resistant *Staphylococcus aureus* MRSA Iraqi isolates. *Int J Curr Microbiol Appl Sci* 2015;4(5):575–585.
- Kim T, Yi J, Hong KH, Park JS, Kim EC.** Distribution of virulence genes in *spa* types of methicillin-resistant *Staphylococcus aureus* isolated from patients in intensive care units. *Korean J Lab Med.* 2011 Jan;31(1):30–36. <https://doi.org/10.3343/kjlm.2011.31.1.30>
- Kourtis AP, Hatfield K, Baggs J, Mu Y, See I, Epton E, Nadle J, Kainer MA, Dumyati G, Petit S, et al.; Emerging Infections Program MRSA author group.** Vital Signs: Epidemiology and recent trends in methicillin-resistant and in methicillin-susceptible *Staphylococcus aureus* bloodstream infections – United States. *MMWR Morb Mortal Wkly Rep.* 2019 Mar 8;68(9):214–219. <https://doi.org/10.15585/mmwr.mm6809e1>
- Kumar S, Stecher G, Tamura K.** MEGA7: Molecular Evolutionary Genetics Analysis version 7.0 for bigger datasets. *Mol Biol Evol.* 2016 Jul;33(7):1870–4. <https://doi.org/10.1093/molbev/msw054>
- Kuwahara-Arai K, Kondo N, Hori S, Tateda-Suzuki E, Hiramatsu K.** Suppression of methicillin resistance in a *mecA*-containing pre-methicillin-resistant *Staphylococcus aureus* strain is caused by the *mecI*-mediated repression of PBP 2' production. *Antimicrob Agents Chemother.* 1996 Dec;40(12):2680–2685. <https://doi.org/10.1128/AAC.40.12.2680>
- Lakhundi S, Zhang K.** Methicillin-resistant *Staphylococcus aureus*: molecular characterization, evolution, and epidemiology. *Clin Microbiol Rev.* 2018 Sep 12;31(4):e00020–18. <https://doi.org/10.1128/CMR.00020-18>
- Lee CY, Fang YP, Chang YF, Wu TH, Yang YY, Huang YC.** Comparison of molecular epidemiology of bloodstream methicillin-resistant *Staphylococcus aureus* isolates between a new and an old hospital in central Taiwan. *Int J Infect Dis.* 2019 Feb;79:162–168. <https://doi.org/10.1016/j.ijid.2018.12.002>
- Lina G, Piémont Y, Godail-Gamot F, Bes M, Peter MO, Gauduchon V, Vandenesch F, Etienne J.** Involvement of Pantone-Valentine leukocidin-producing *Staphylococcus aureus* in primary skin infections and pneumonia. *Clin Infect Dis.* 1999 Nov;29(5):1128–1132. <https://doi.org/10.1086/313461>
- Locatcher-Khorazo D, Gutierrez E.** Bacteriophage typing of *Staphylococcus aureus*. A study of normal, infected eyes and environment. *Arch Ophthalmol.* 1960 May;63:774–787. <https://doi.org/10.1001/archophth.1960.00950020776005>
- Merlino J, Leroi M, Bradbury R, Veal D, Harbour C.** New chromogenic identification and detection of *Staphylococcus aureus* and methicillin-resistant *S. aureus*. *J Clin Microbiol.* 2000 Jun;38(6):2378–2380. <https://doi.org/10.1128/jcm.38.6.2378-2380.2000>
- Monday SR, Bohach GA.** Use of multiplex PCR to detect classical and newly described pyrogenic toxin genes in staphylococcal isolates. *J Clin Microbiol.* 1999 Oct;37(10):3411–3414. <https://doi.org/10.1128/JCM.37.10.3411-3414.1999>
- Monecke S, Skakni L, Hasan R, Ruppelt A, Ghazal SS, Hakawi A, Slickers P, Ehrlich R.** Characterisation of MRSA strains isolated from patients in a hospital in Riyadh, Kingdom of Saudi Arabia. *BMC Microbiol.* 2012 Jul 23;12:146. <https://doi.org/10.1186/1471-2180-12-146>
- Parker MT and Hewitt JH.** Methicillin resistance in *Staphylococcus aureus*. *Lancet.* 1970 Apr 18;1(7651):800–804. [https://doi.org/10.1016/s0140-6736\(70\)92408-6](https://doi.org/10.1016/s0140-6736(70)92408-6)
- Schneewind O, Model P, Fischetti VA.** Sorting of protein A to the staphylococcal cell wall. *Cell.* 1992 Jul 24;70(2):267–281. [https://doi.org/10.1016/0092-8674\(92\)90101-h](https://doi.org/10.1016/0092-8674(92)90101-h)
- Shakeri F, Ghaemi EA.** New *spa* types among MRSA and MSSA isolates in north of Iran. *Adv Microb* 2014;4:899–905. <https://doi.org/10.4236/aim.2014.413100>
- Stefani S, Chung DR, Lindsay JA, Friedrich AW, Kearns AM, Westh H, Mackenzie FM.** Methicillin-resistant *Staphylococcus aureus* (MRSA): global epidemiology and harmonisation of typing methods. *Int J Antimicrob Agents.* 2012 Apr;39(4):273–282. <https://doi.org/10.1016/j.ijantimicag.2011.09.030>
- Udo EE, Al-Lawati BA, Al-Muharmi Z, Thukral SS.** Genotyping of methicillin-resistant *Staphylococcus aureus* in the Sultan Qaboos University Hospital, Oman reveals the dominance of Pantone-Valentine leukocidin-negative ST6-IV/t304 clone. *New Microbes New Infect.* 2014 Jul;2(4):100–105. <https://doi.org/10.1002/nmi.2.47>
- Udo EE, Al-Sweih N.** Emergence of methicillin-resistant *Staphylococcus aureus* in the Maternity Hospital, Kuwait. *Med Princ Pract.* 2013;22(6):535–539. <https://doi.org/10.1159/000350526>
- Uhlén M, Guss B, Nilsson B, Gatenbeck S, Philipson L, Lindberg M.** Complete sequence of the staphylococcal gene encoding protein A. A gene evolved through multiple duplications. *J Biol Chem.* 1984 Feb 10;259(3):1695–1702. [https://doi.org/10.1016/S0021-9258\(17\)43463-6](https://doi.org/10.1016/S0021-9258(17)43463-6)
- van Leeuwen W, Verbrugh H, van der Velden J, van Leeuwen N, Heck M, van Belkum A.** Validation of binary typing for *Staphylococcus aureus* strains. *J Clin Microbiol.* 1999 Mar;37(3):664–674. <https://doi.org/10.1128/JCM.37.3.664-674.1999>
- Wang WY, Chiueh TS, Sun JR, Tsao SM, Lu JJ.** Molecular typing and phenotype characterization of methicillin-resistant *Staphylococcus aureus* isolates from blood in Taiwan. *PLoS One.* 2012;7(1):ee30394. <https://doi.org/10.1371/journal.pone.0030394>
- Wichelhaus TA, Hunfeld KP, Böddinghaus B, Kraczy P, Schäfer V, Brade V.** Rapid molecular typing of methicillin-resistant *Staphylococcus aureus* by PCR-RFLP. *Infect Control Hosp Epidemiol.* 2001 May;22(5):294–298. <https://doi.org/10.1086/501903>
- Yadav R, Kumar A, Singh VK, Jayshree, Yadav SK.** Prevalence and antibiotyping of *Staphylococcus aureus* and methicillin-resistant *S. aureus* (MRSA) in domestic animals in India. *J Glob Antimicrob Resist.* 2018 Dec;15:222–225. <https://doi.org/10.1016/j.jgar.2018.08.001>
- Zarizal S, Yeo CC, Faizal GM, Chew CH, Zakaria ZA, Jamil Al-Obaidi MM, Syafinaz Amin N, Mohd Nasir MD.** Nasal colonisation, antimicrobial susceptibility and genotypic pattern of *Staphylococcus aureus* among agricultural biotechnology students in Besut, Terengganu, east coast of Malaysia. *Trop Med Int Health.* 2018 Aug;23(8):905–913. <https://doi.org/10.1111/tmi.13090>

Diversity of Culturable Bacteria Isolated from Highland Barley Cultivation Soil in Qamdo, Tibet Autonomous Region

HU PAN^{1,2}, JIE ZHOU¹, ZHUOMA DAWA², YANNA DAI², YIFAN ZHANG², HUI YANG¹, CHONG WANG¹, HUHUI LIU¹, HUI ZHOU¹, XIANGYANG LU¹ and YUN TIAN^{1*}

¹ College of Bioscience and Biotechnology, Hunan Agricultural University, Changsha, China

² Institute of Agricultural Product Quality Standard and Testing Research, Tibet Academy of Agricultural and Animal Husbandry Sciences, Lhasa, China

Submitted 29 November 2020, revised 17 January 2021, accepted 19 January 2021

Abstract

The soil bacterial communities have been widely investigated. However, there has been little study of the bacteria in Qinghai-Tibet Plateau, especially about the culturable bacteria in highland barley cultivation soil. Here, a total of 830 individual strains were obtained at 4°C and 25°C from a highland barley cultivation soil in Qamdo, Tibet Autonomous Region, using fifteen kinds of media. Seventy-seven species were obtained, which belonged to 42 genera and four phyla; the predominant phylum was Actinobacteria (68.82%), followed by Proteobacteria (15.59%), Firmicutes (14.29%), and Bacteroidetes (1.30%). The predominant genus was *Streptomyces* (22.08%, 17 species), followed by *Bacillus* (6.49%, five species), *Micromonospora* (5.19%, four species), *Microbacterium* (5.19%, four species), and *Kribbella* (3.90%, three species). The most diverse isolates belonged to a high G+C Gram-positive group; in particular, the *Streptomyces* genus is a dominant genus in the high G+C Gram-positive group. There were 62 species and 33 genera bacteria isolated at 25°C (80.52%), 23 species, and 18 genera bacteria isolated at 4°C (29.87%). Meanwhile, only eight species and six genera bacteria could be isolated at 25°C and 4°C. Of the 77 species, six isolates related to six genera might be novel taxa. The results showed abundant bacterial species diversity in the soil sample from the Qamdo, Tibet Autonomous Region.

Key words: Qinghai-Tibet Plateau, *Streptomyces*, 16S rRNA, novel taxa, high-altitude area

Introduction

Bacteria constitute a major proportion of biodiversity in soil ecosystems; they are the main driving force for the conversion and circulation of carbon, nitrogen, and phosphorus, and also the prominent participants in biochemical processes of soil organic matter decomposition and humus formation (Fulthorpe et al. 2008; Řeháková et al. 2015; Malard et al. 2019). Bacterial assemblages are essential components of soils in arid ecosystems, especially in remote high-elevation mountains (Margesin et al. 2009; Yuan et al. 2014). While global surveys of microbial diversity and functional activity have already been conducted (Bodelier 2011; Delgado-Baquerizo et al. 2018), the number of Qinghai-Tibet Plateau samples is restricted, and, therefore bacterial data is still lacking in this area, especially in the most high-altitude area (Zhang et al. 2016).

Highland barley (*Hordeum vulgare* L.) is the fourth most consumed grain worldwide, only ranked after rice, wheat, and maize (Shen et al. 2016; Deng et al. 2020). Highland barley is a hullless barley cultivar and used as the main staple food for the Tibetan people widely grown in Qinghai-Tibet Plateau in China (He et al. 2019; Zhang et al. 2019). Extreme environments such as cold and hypoxia in Tibet have promoted the unique ecological environment and soil bacterial composition (Zhang et al. 2007; 2010a). However, the extreme environments also have led to the decline of soil bacterial activity and the impoverishment of soil for growing highland barley (Yu et al. 2009; Zhao et al. 2014). The research of soil bacteria in the highland barley planting field has important significance for highland barley yield increase, pest control, and soil quality improvement (Bailly and Weisskopf 2012). At present, there were few studies on bacteria in the soil of the highland

* Corresponding author: Y. Tian, College of Bioscience and Biotechnology, Hunan Agricultural University, Changsha, China;
e-mail: tianyun79616@163.com

© 2021 Hu Pan et al.

This work is licensed under the Creative Commons Attribution-NonCommercial-NoDerivatives 4.0 License (<https://creativecommons.org/licenses/by-nc-nd/4.0/>).

barley-planting field (Liu et al. 2019). Significantly, the culturable bacteria isolated from highland barley cultivation soil have not been reported systematically.

The Qamdo region's temperature is between 20°C and 28°C from June to September, a significant growth period for highland barley. While the temperature is below 10°C from November to March, no crops were planted on the land during this period. So the culturable bacteria were isolated from a high-altitude highland barley cultivation soil collected in Qamdo using 15 media at 4°C and 25°C to simulate the temperature conditions over these two periods in this study. The composition of bacterial communities was characterized based on the 16S rRNA gene (Furlong et al. 2002; Li et al. 2019). Our aims were: (1) to reveal the diversity of culturable bacteria isolated from highland barley cultivation soil in the high-altitude area; and (2) to study the effect of different culture temperatures on the species of culturable bacteria in highland barley cultivation soil.

Experimental

Materials and Methods

Study site and samples collection. The sampling site was located in the Zhu Village, Banbar County, Qamdo, Tibet Autonomous Region (30°55'48.9"N, 94°58'13.4"E, Altitude: 4,011 m); the sampling site is the typical high-altitude patches farmland in Qamdo, which is about one-third of Qamdo's farmland. The sample site belongs to the plateau temperate subhumid climate type, the air temperature range is -40–29°C, the annual average air temperature is -1°C, and the yearly frozen period is from September to April. The soil type was sandy loam, and the pH value is 7.6. The previous crop was highland barley, and the yield is about 1,000–1,800 kg/hm² in this area. A highland barley cultivation soil sample was collected from a depth of 5–15 cm using the five-point method and kept in sterilized paper bags in April 2018. Once retrieved, the soil sample was immediately stored at 4°C, and bacteria were isolated in the laboratory in Lhasa in May and June 2018.

Isolation and maintenance of bacteria. The bacteria in highland barley cultivation soil sample were isolated using X1, R, L1, ISP2, GW1, DSM372, F1, F2, M1, M5, M6, M7, M8, HV, and GS media, as shown in Table I. Gram-negative bacteria and Actinobacteria were isolated by using the dilution plating technique as described by Kuklinsky-Sobral et al. (2004) and Zhang et al. (2016), respectively, with some modifications. 0.2 ml of 10⁻², 10⁻³, and 10⁻⁴ soil suspensions were spread onto F1, F2, M1, M5, M6, M7, M8, HV, and GS media to isolate Actinobacteria. While, 0.2 ml of 10⁻⁴, 10⁻⁵, and 10⁻⁶ soil suspension was spread onto X1, R,

L1, ISP2, GW1, and DSM372 media to isolate Gram-negative bacteria. Two sets of plates were incubated at 4°C and 25°C, respectively; the bacterial strains were obtained across 3–60 days. The pure culture isolates were preserved in glycerol suspensions (20%, v/v) at -80°C for further research.

PCR amplification and sequencing of the 16S rRNA gene. According to the manufacturer's protocol, the genomic DNA of bacteria was extracted using a bacterial genomic DNA FastPrep Extraction Kit (TIANGEN DP302). Polymerase chain reaction (PCR) amplification of the partial 16S rRNA gene was performed using the universal primers 27F (5'-AGAGTTTGATCCTGGCTCAG-3') and 1492R (5'-GGTTACCTGTTACGAC TT-3'), PCR was performed using the extracted highly purified genomic DNA as a template under the following conditions: 95°C for 10 min, followed by 94°C for 45 s, 55°C for 45 s, and 72°C for 90 s for 30 cycles with a final 10 min extension at 72°C. The PCR products were detected by agarose gel electrophoresis and then sent to GENEWIZ.lnc for the 16S rRNA gene sequencing. The phylogenetic status of the species was determined by a reaction of 700–750 bp (V1-V4) using the universal primers 27F, if the similarity was less than 98.65% (Kim et al. 2014), then the phylogenetic status of the species was further analyzed by nearly full-length 16S rRNA gene (1,300–1,400 bp).

Phylogenetic analysis. Similarity searches of the 16S rRNA gene sequences were performed in the NCBI and EzBiocloud database for BLAST, then the 16S rRNA gene sequences with the highest homology were obtained for phylogenetic analysis. The sequence alignments were performed using Clustal X, the phylogenetic trees were constructed from evolutionary distances using the neighbor-joining method with a bootstrap of 1,000 repetitions, and the phylogenetic analysis was conducted using the MEGA 7 software (Kumar et al. 2016b).

Nucleotide sequence accession numbers. The full and partial 16S rRNA gene sequences of the strains were submitted to the NCBI GenBank database under the accession numbers (MT611248 -MT611324).

Results

The isolated strains. Bacterial populations were successfully isolated from the highland barley cultivation soil sample using fifteen kinds of media, a total of 830 individual strains were obtained at different culture temperatures (4°C and 25°C) (Fig. 1A). Eighty-three and 747 strains of bacteria were isolated from these media at 4°C and 25°C, respectively. The results showed that X1, R, F1, M1, M5, M8, and GS culture media had a better effect on isolating bacteria at 25°C; however,

Table I
Isolation media.

Media	Composition
X1	peptone 2.0 g, yeast extract 0.5 g, FePO ₄ ·4H ₂ O 0.1 g, MgSO ₄ ·7H ₂ O 0.5 g, CaCO ₃ 0.2 g, NaCl 0.5 g, agar 18.0 g, ddwater 1,000 ml, pH 7.0
R	peptone 10.0 g, yeast extract 5.0 g, maltose extract 5.0 g, casein amino acid 5.0 g, beef extract 2.0 g, glycerol 2.0 g, Tween-80 50.0 mg, MgSO ₄ ·7H ₂ O 1.0 g, agar 18.0 g, ddwater 1,000 ml, pH 7.2–7.6
L1	NaCl 100.0 g, K ₂ HPO ₄ 5.0 g, MgSO ₄ ·7H ₂ O 7.5 g, hydrolyzed casein 1.0 g, yeast extract 5.0 g, Na ₃ C ₆ H ₅ O ₇ ·2H ₂ O 3.0 g, FeSO ₄ ·7H ₂ O 0.1 g, MnCl ₂ ·4H ₂ O 0.1 g, ZnSO ₄ ·7H ₂ O 0.1 g, agar 18.0 g, ddwater 1,000 ml, pH 7.0–8.0
ISP2	NaCl 100.0 g, dextrose 4.0 g, yeast extract 4.0 g, maltose extract 10.0 g, MgSO ₄ ·7H ₂ O 0.5 g, CaCO ₃ 2.0 g, FeSO ₄ 10 mg, agar 18.0 g, ddwater 1,000 ml, pH 7.0–8.0
GW1	NaCl 100.0 g, casein 0.3 g, mannitol 1.0 g, NaHCO ₃ 2.0 g, CaCO ₃ 0.2 g, (NH ₄) ₂ SO ₄ 2.0 g, KNO ₃ 2.0 g, K ₂ HPO ₄ 1.0 g, MgSO ₄ ·7H ₂ O 2.0 g, FeSO ₄ 10.0 mg, Trace-salt 10.0 mg/l, Agar 18.0 g, ddwater 1,000 ml, pH natural
DSM372	NaCl 100.0 g, hydrolyzed casein 5.0 g, yeast extract 5.0 g, Na ₃ C ₆ H ₅ O ₇ ·2H ₂ O 3.0 g, Na ₂ CO ₃ ·10H ₂ O 8.0 g, NaC ₅ H ₈ NO ₄ 1.0 g, KCl 2.0 g, MgSO ₄ ·7H ₂ O 2.0 g, agar 18.0 g, ddwater 1,000 ml, pH natural
F1	glycerol 5.0 g, alanine 3.0 g, arginine 1.0 g, (NH ₄) ₂ SO ₄ 2.64 g, KH ₂ PO ₄ 2.38 g, K ₂ HPO ₄ 5.65 g, MgSO ₄ ·7H ₂ O 1.0 g, CuSO ₄ ·5H ₂ O 0.0064 g, FeSO ₄ ·7H ₂ O 0.0011 g, MnCl ₂ ·4H ₂ O 0.0079 g, ZnSO ₄ ·7H ₂ O 0.0015 g, agar 18.0 g, ddwater 1,000 ml, pH 7.2–7.4 (add 25 µg/ml nalidixic acid and 100 µg/ml nystatin)
F2	MgSO ₄ ·7H ₂ O 0.5 g, CaCO ₃ 0.2 g, FeSO ₄ 10.0 mg, NaCl 0.5 g, MnCl ₂ ·4H ₂ O 1.4 g, Na ₂ MoO ₄ ·2H ₂ O 0.39 g, Co(NO ₃) ₂ ·6H ₂ O 0.025 g, ZnSO ₃ ·7H ₂ O 0.222 g, NaHCO ₃ 2.0 g, NaH ₂ PO ₄ ·2H ₂ O 0.05 g, agar 18.0 g, ddwater 1,000 ml, pH natural (add 25 µg/ml nalidixic acid and 100 µg/ml nystatin)
M1	soluble starch 10.0 g, casein 0.3 g, KNO ₃ 2.0 g, K ₂ HPO ₄ 2.0 g, MgSO ₄ ·7H ₂ O 0.05 g, FeSO ₄ ·7H ₂ O 0.01 g, agar 18.0 g, ddwater 1,000 ml, pH 7.2–7.4 (add 25 µg/ml nalidixic acid and 100 µg/ml nystatin)
M5	yeast extract 4.0 g, soluble starch 15.0 g, K ₂ HPO ₄ 1.0 g, FeSO ₄ ·7H ₂ O 0.01 g, agar 18.0 g, ddwater 1,000 ml, pH 7.2–7.6 (add 25 µg/ml nalidixic acid and 100 µg/ml nystatin)
M6	raffinose 10.0 g, L-histidine 1.0 g, MgSO ₄ ·7H ₂ O 0.5 g, FeSO ₄ ·7H ₂ O 0.01 g, agar 18.0 g, ddwater 1,000 ml, pH 7.2–7.4 (add 25 µg/ml nalidixic acid and 100 µg/ml nystatin)
M7	L-aspartic acid 0.1 g, peptone 2.0 g, sodium propionate 4.0 g, FeSO ₄ ·7H ₂ O 0.01 g, agar 18.0 g, ddwater 1,000 ml, pH 7.2–7.4 (add 25 µg/ml nalidixic acid and 100 µg/ml nystatin)
M8	glycerine 6.0 ml, arginine 1.0 g, MgSO ₄ ·7H ₂ O 0.5 g, agar 18.0 g, ddwater 1,000 ml, pH 7.2–7.4 (add 25 µg/ml nalidixic acid and 100 µg/ml nystatin)
HV	humic acid 1.0g, Na ₂ HPO ₄ 0.5 g, KCl 1.7 g, MgSO ₄ 0.5 g, FeSO ₄ 0.01 g, CaCO ₃ 0.02 g, agar 18.0 g, ddwater 1,000 ml, pH 7.2–7.4 (add 25 µg/ml nalidixic acid and 100 µg/ml nystatin)
GS	soluble starch 20.0 g, NaCl 0.5 g, KNO ₃ 1.0 g, K ₂ HPO ₄ ·3H ₂ O 0.5 g, MgSO ₄ ·7H ₂ O 0.5 g, FeSO ₄ ·7H ₂ O 0.01 g, agar 18.0 g, ddwater 1,000 ml, pH 7.4–7.6 (add 25 µg/ml nalidixic acid and 100 µg/ml nystatin)

X1, R, and M5 culture media had a better effect on isolating bacteria at 4°C, none of the bacteria was isolated from the F2, M7, HV, and GS media at 4°C.

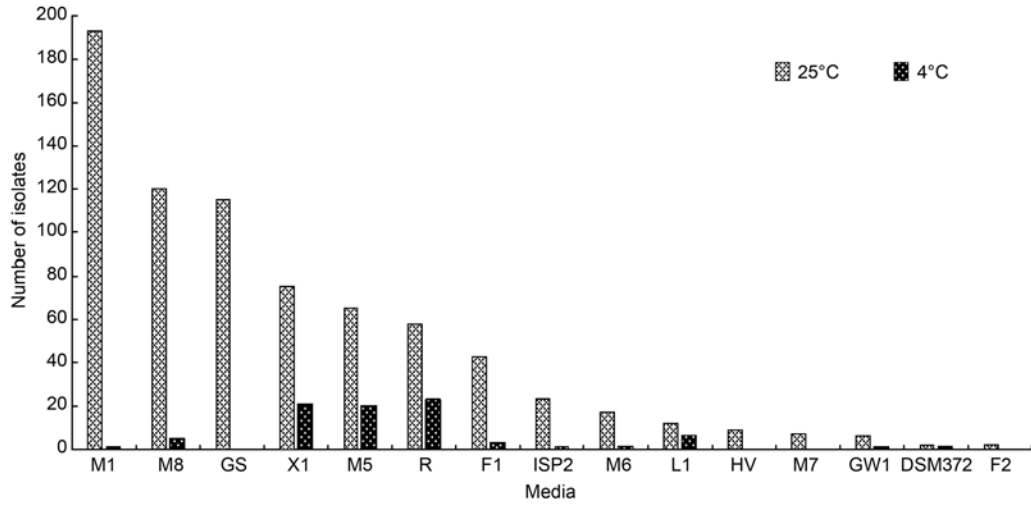
Phylogenetic analysis of culturable strains by the 16S rRNA gene sequence. According to the morphological characteristics of bacteria, 330 strains were screened for the 16S rRNA gene sequence analysis using the universal primers 27F/1492R, and 98.65% of the 16S rRNA gene sequences were used as the species boundary of prokaryotes. After combining more than 98.65% of the 16S rRNA gene sequences with the same species, the sequences of 77 species were obtained, which belonged to 42 genera and four phyla (Actinobacteria, Proteobacteria, Firmicutes, and Bacteroidetes), as shown in Table II. Phylogenetic tree based on the 16S rRNA gene sequences of representative bacteria strains were shown (Fig. 2).

There were 53 species and 25 genera in Actinobacteria, accounting for 68.82% of the species' total num-

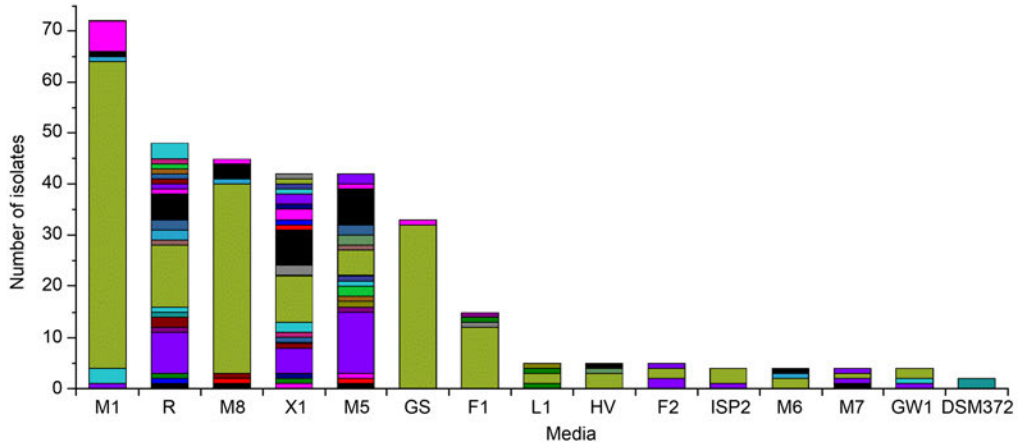
ber. The predominant genus was *Streptomyces* (22.08%, 17 species), followed by *Micromonospora* (5.19%, four species), *Microbacterium* (5.19%, four species), and *Kribbella* (3.90%, three species). Some rare Actinobacteria were also isolated, for example, *Leifsonia*, *Longispora*, *Nocardia*, *Nocardioides*, *Terrabacter*, *Umezawaea*, and *Kribbella*. There were 12 species and ten genera in Proteobacteria, accounting for 15.59% of the total number of species, but no dominant genus was found in Proteobacteria. There were 11 species and six genera in Firmicutes, accounting for 14.29% of the total number of species; the predominant genus was *Bacillus* (6.49%, five species). Only one species was found in Bacteroidetes, classified as *Hymenobacter* (1.30%, one species) (Table III).

Diversity of culturable strains recovered from different culture media. Among the 330 identified bacteria strains, the number of bacterial isolates recovered from M1 was the largest (21.82%, 72 strains), followed

A

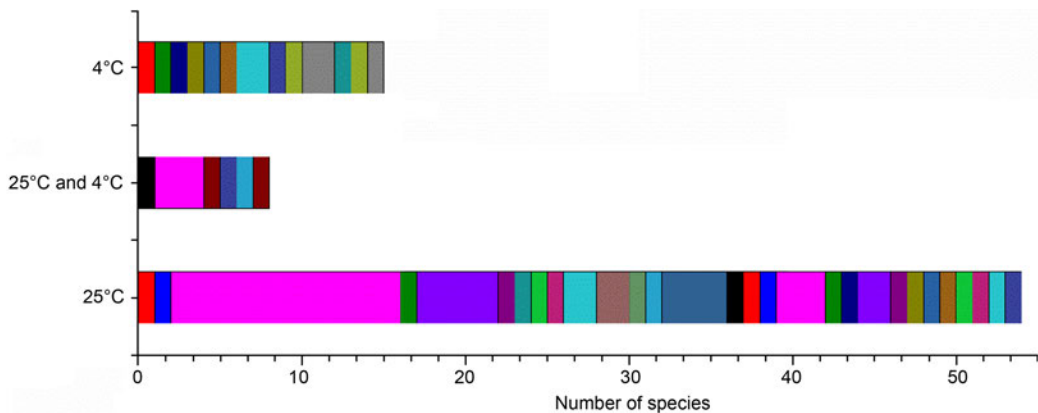


B



- | | | | | | | |
|-----------------|-------------------|--------------------|---------------------|----------------------|------------------------|--------------------------|
| <i>Kocuria</i> | <i>Umezawaea</i> | <i>Longispora</i> | <i>Pseudomonas</i> | <i>Neorhizobium</i> | <i>Aeromicrobium</i> | <i>Exiguobacterium</i> |
| <i>Kaistia</i> | <i>Leifsonia</i> | <i>Kytococcus</i> | <i>Micrococcus</i> | <i>Hymenobacter</i> | <i>Staphylococcus</i> | <i>Yinghuangia</i> |
| <i>Dietzia</i> | <i>Kribbella</i> | <i>Glycomyces</i> | <i>Macrococcus</i> | <i>Arthrobacter</i> | <i>Micromonospora</i> | <i>Paenarthrobacter</i> |
| <i>Nocardia</i> | <i>Agromyces</i> | <i>Terrabacter</i> | <i>Streptomyces</i> | <i>Actinoplanes</i> | <i>Microbacterium</i> | <i>Pseudoxanthomonas</i> |
| <i>Gordonia</i> | <i>Variovorax</i> | <i>Skermanella</i> | <i>Sphingopyxis</i> | <i>Pararhizobium</i> | <i>Peribacillus</i> | <i>Pseudarthrobacter</i> |
| <i>Bacillus</i> | <i>Luteimonas</i> | <i>Rhodococcus</i> | <i>Nocardioides</i> | <i>Paenibacillus</i> | <i>Phyllobacterium</i> | <i>Promicromonospora</i> |

C



- | | | | | |
|----------------------|------------------------|---------------------|--------------------------|--------------------------|
| <i>Kaistia</i> | <i>Leifsonia</i> | <i>Luteimonas</i> | <i>Micrococcus</i> | <i>Aeromicrobium</i> |
| <i>Dietzia</i> | <i>Umezawaea</i> | <i>Longispora</i> | <i>Terrabacter</i> | <i>Staphylococcus</i> |
| <i>Kocuria</i> | <i>Kribbella</i> | <i>Glycomyces</i> | <i>Macrococcus</i> | <i>Micromonospora</i> |
| <i>Nocardia</i> | <i>Agromyces</i> | <i>Pseudomonas</i> | <i>Neorhizobium</i> | <i>Microbacterium</i> |
| <i>Gordonia</i> | <i>Variovorax</i> | <i>Skermanella</i> | <i>Hymenobacter</i> | <i>Peribacillus</i> |
| <i>Bacillus</i> | <i>Kytococcus</i> | <i>Rhodococcus</i> | <i>Streptomyces</i> | <i>Phyllobacterium</i> |
| <i>Sphingopyxis</i> | <i>Exiguobacterium</i> | <i>Yinghuangia</i> | <i>Paenarthrobacter</i> | <i>Pseudoxanthomonas</i> |
| <i>Nocardioides</i> | <i>Actinoplanes</i> | <i>Arthrobacter</i> | <i>Pseudarthrobacter</i> | |
| <i>Pararhizobium</i> | <i>Paenibacillus</i> | | | |

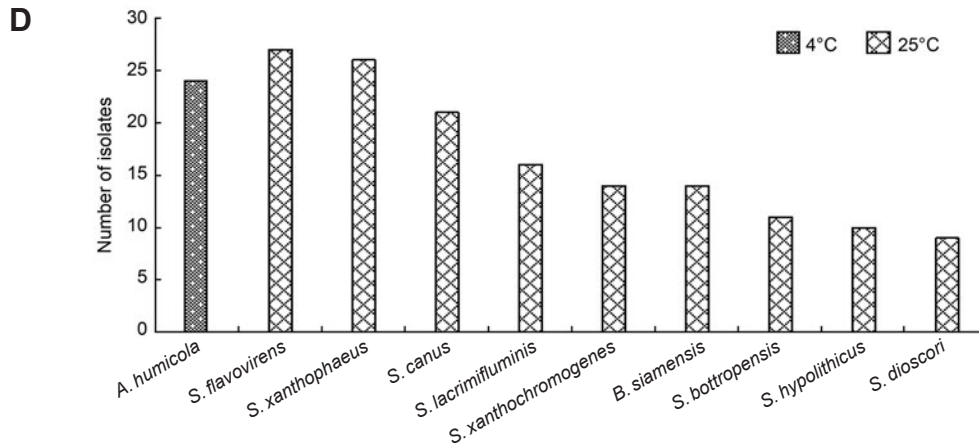


Fig. 1. The number and diversity of bacteria.

A) The numbers of bacteria isolated from different media at 4° and 25°. B) Diversity of bacteria isolated from different culture media. C) Diversity of bacteria isolated from different temperature. D) The numbers of dominant species isolated from 4° and 25°.

by R (14.55%, 48 strains), M8 (13.64%, 45 strains), X1 (12.73%, 42 strains), M5 (12.73%, 42 strains), GS (10.00%, 33 strains), F1 (4.55%, 15 strains), L1 (1.52%, five strains), F2 (1.52%, five strains), HV (1.52%, five strains), ISPT2 (1.21%, four strains), M6 (1.21%, four strains), M7 (1.21%, four strains), GW1 (1.21%, four strains), and DSM372 (0.61%, two strains). The number of bacteria isolated from M1, M8, and GS was larger, while the main genus was only *Streptomyces*. The R, X1, and M5 yielded higher genera diversity (21 genera, 20 genera, and 17 genera, respectively). Meanwhile, media R, X1, and M5 were more useful than other media for isolation of rare genera of bacteria, such as *Nocardioides*, *Leifsonia*, *Terrabacte*, *Umezawaea*, *Variovorax*, *Neorhizobium*, and *Pararhizobium* (Fig. 1B). Here, we presumed that single-nutrition was the main reason, especially when non-monosaccharide was used as the carbon source (Zhang et al. 2010b; Kurm et al.

2019). This study demonstrated that it is necessary to use various isolation media types to increase the number and diversity of bacteria from highland barley cultivation soil samples.

Diversity of culturable strains at different temperature. There were 62 species and 33 genera bacteria isolated at 25°C, accounting for 80.52% of the species' total number. The predominant genus was *Streptomyces* (22.08%, 17 species), followed by *Bacillus* (6.49%, five species), *Micromonospora* (5.19%, four species), *Kribbella* (3.90%, three species), and *Paenarthrobacter* (3.90%, three species). There were 23 species and 18 genera bacteria isolated at 4°C, accounting for 29.87% of the total species, but no dominant genus was found. Meanwhile, only eight species and six genera of bacteria could be isolated at 25°C and 4°C (Fig. 1C). Most common bacteria could be isolated at 25°C, but some rare bacteria could be isolated at 4°C without

Table II
Genera distributed in each of the four phyla.

Actinobacteria		Proteobacteria	Firmicutes	Bacteroidetes
<i>Actinoplanes</i>	<i>Micrococcus</i>	<i>Kaistia</i>	<i>Bacillus</i>	<i>Hymenobacter</i>
<i>Aeromicrobium</i>	<i>Micromonospora</i>	<i>Luteimonas</i>	<i>Exiguobacterium</i>	
<i>Agromyces</i>	<i>Nocardia</i>	<i>Neorhizobium</i>	<i>Macrococcus</i>	
<i>Arthrobacter</i>	<i>Nocardioides</i>	<i>Pararhizobium</i>	<i>Paenibacillus</i>	
<i>Dietzia</i>	<i>Paenarthrobacter</i>	<i>Phyllobacterium</i>	<i>Peribacillus</i>	
<i>Glycomyces</i>	<i>Promicromonospora</i>	<i>Pseudomonas</i>	<i>Staphylococcus</i>	
<i>Gordonia</i>	<i>Pseudarthrobacter</i>	<i>Pseudoxanthomonas</i>		
<i>Kocuria</i>	<i>Rhodococcus</i>	<i>Skermanella</i>		
<i>Kribbella</i>	<i>Streptomyces</i>	<i>Sphingopyxis</i>		
<i>Kytococcus</i>	<i>Terrabacter</i>	<i>Variovorax</i>		
<i>Leifsonia</i>	<i>Umezawaea</i>			
<i>Longispora</i>	<i>Yinghuangia</i>			
<i>Microbacterium</i>				

Table III
BLAST results based on 16S rRNA gene sequences of 77 bacterial species.

Strain number	Name of strain having the highest 16S rRNA gene similarity	The highest similarity (%)	Strain number	Name of strain having the highest 16S rRNA gene similarity	The highest similarity (%)
T74*	<i>Actinoplanes digitatis</i> IFO 12512	98.82	T608	<i>Paenarthrobacter aurescens</i> NBRC 12136	99.07
T203	<i>Aeromicrobium ginsengisoli</i> Gsoil 098	99.82	T236	<i>Paenarthrobacter nitroguajacolicus</i> G2-1	100
T96*	<i>Agromyces binzhouensis</i> OAct353	98.62	T808*	<i>Pararhizobium herbae</i> CCBAU 83011	98.79
T229*	<i>Agromyces humatus</i> CD5	98.74	T209	<i>Peribacillus simplex</i> NBRC 15720	100
T805	<i>Arthrobacter crystallopoietes</i> DSM 20117	99.85	T811	<i>Phyllobacterium ifriqiyense</i> STM 370	100
T763	<i>Arthrobacter humicola</i> KV-653	100	T274*	<i>Phyllobacterium zundukense</i> Tri-48	98.57
T65	<i>Bacillus siamensis</i> KCTC 13613	100	T63	<i>Promicromonospora alba</i> 1C-HV12	100
T94	<i>Bacillus cereus</i> ATCC 14579	100	T193*	<i>Pseudarthrobacter siccitolerans</i> 4J27	99.34
T228*	<i>Bacillus drentensis</i> LMG 21831	99.34	T755	<i>Pseudomonas laurylsulfatorans</i> AP3_22	99.73
T59	<i>Bacillus pumilus</i> ATCC 7061	100	T776	<i>Pseudomonas lini</i> CFBP 5737	100
T115	<i>Bacillus selenatarsenatis</i> SF-1	99.6	T174*	<i>Pseudoxanthomonas sacheonensis</i> BD-c54	99.34
T822	<i>Dietzia kunjamensis</i> subsp DSM 44907	99.86	T127*	<i>Rhodococcus jostii</i> DSM 44719	99.32
T230	<i>Exiguobacterium mexicanum</i> 8NT	100	T788	<i>Rhodococcus qingshengii</i> JCM 15477	100
T183*	<i>Glycomyces algeriensis</i> NRRL B-16327	98.9	T185*	<i>Skermanella aerolata</i> 5416T-32	98.86
T64	<i>Gordonia otitidis</i> NBRC 100426	100	T93	<i>Sphingopyxis fribergensis</i> Kp5.2	99.87
T830*	<i>Hymenobacter humi</i> DG31A	98.60	T45	<i>Staphylococcus caprae</i> ATCC 35538	100
T769*	<i>Kaistia defluvii</i> B6-12	99.72	T61	<i>Staphylococcus cohnii</i> subsp ATCC 49330	100
T144	<i>Kocuria sediminis</i> FCS-11	99.43	T666	<i>Streptomyces albogriseolus</i> NRRL B-1305	100
T145	<i>Kribbella albertanoniae</i> BC640	100	T313	<i>Streptomyces atroolivaceus</i> NRRL ISP-5137	100
T214*	<i>Kribbella catacumbae</i> DSM 19601	99.6	T234	<i>Streptomyces bottropensis</i> ATCC 25435	99.87
T422	<i>Kribbella karoonensis</i> Q41	99.87	T130	<i>Streptomyces caniferus</i> NBRC 15389	99.87
T823	<i>Kytococcus schroeteri</i> DSM 13884	99.73	T235	<i>Streptomyces canus</i> DSM 40017	99.73
T781	<i>Leifsonia flava</i> SYP-B2174	99.73	T690	<i>Streptomyces dioscori</i> A217	99.47
T146	<i>Longispora urticae</i> NEAU-PCY-3	99.88	T532	<i>Streptomyces flavovirens</i> NBRC 3716	99.85
T181*	<i>Luteimonas composti</i> CC-YY255	98.9	T674*	<i>Streptomyces humidus</i> NBRC 12877	98.8
T156	<i>Macrococcus canis</i> KM 45013	99.86	T296	<i>Streptomyces hydrogenans</i> NBRC 13475	99.46
T489	<i>Microbacterium maritypicum</i> DSM 12512	99.55	T219	<i>Streptomyces hypolithicus</i> HSM10	99.46
T773	<i>Microbacterium natoriense</i> TNJL143-2	99.87	T426	<i>Streptomyces kurssanovii</i> NBRC 13192	99.6
T804	<i>Microbacterium phyllosphaerae</i> DSM 13468	99.73	T569	<i>Streptomyces lunaelactis</i> MM109	99.2
T133	<i>Microbacterium thalassium</i> IFO 16060	98.93	T348	<i>Streptomyces niveus</i> NRRL 2466	99.46
T226	<i>Micrococcus luteus</i> NCTC 2665	99.63	T84	<i>Streptomyces phaeoluteigriseus</i> DSM 41896	99.6
T47	<i>Micromonospora cremea</i> DSM 45599	99.87	T581	<i>Streptomyces turgidiscabies</i> ATCC 700248	100
T206	<i>Micromonospora luteifusca</i> GUI2	99.87	T110*	<i>Streptomyces xanthochromogenes</i> NRRL B-5410	98.97
T197*	<i>Micromonospora palomenae</i> NEAU-CX1	98.74	T100	<i>Streptomyces xanthophaeus</i> NRRL B-5414	99.71
T92	<i>Micromonospora saelicesensis</i> Lupac 09	100	T111*	<i>Terrabacter ginsengisoli</i> Gsoil 653	99.19
T786*	<i>Neorhizobium vignae</i> CCBAU 05176	98.70	T160	<i>Umezawaea tangerina</i> NRRL B-24463	99.18
T62	<i>Nocardia salmonicida</i> subsp R89	99.47	T812	<i>Variovorax boronicumulans</i> BAM-48	99.47
T105*	<i>Nocardioides caeni</i> MN8	98.01	T134*	<i>Yinghuangia seranimata</i> YIM 45720	98.73
T218	<i>Paenibacillus odorifer</i> DSM 15391	99.63			

* – shown that the full length 16S rRNA gene of this bacterium was sequenced

the inhibitory effect of dominant species, promoting the diversity of bacteria (Margesin 2012; Collins and Margesin 2019). The numbers of dominant species mainly isolated at 4°C were *Arthrobacter humicola* (7.25%, 24 strains), while the numbers of dominant

species mainly isolated at 25°C were *Streptomyces flavovirens* (8.19%, 27 strains), *Streptomyces xanthophaeus* (7.58%, 25 strains), *Streptomyces canus* (6.36%, 21 strains), and *Bacillus siamensis* (4.24%, 14 strains) (Fig. 1D). The species of culturable bacteria and the

Table IV

The sequence analyses based on almost full-length of the 16S rRNA gene of six potential new species.

Strain number	Name of strain having the highest 16S rRNA gene similarity	Separation medium	The highest similarity (%)	Separation temperature (°C)
T96	<i>Agromyces binzhouensis</i> OAct353 ^T	98.62	M5	25
T105	<i>Nocardioides caeni</i> MN8 ^T	98.01	M5	25
T274	<i>Phyllobacterium zundukense</i> Tri-48 ^T	98.57	M8	25
T786	<i>Neorhizobium vignae</i> CCBAU 05176 ^T	98.70	R	4
T808	<i>Pararhizobium herbae</i> CCBAU 83011 ^T	98.79	M5	4
T830	<i>Hymenobacter humi</i> DG31A ^T	98.60	F1	4

numbers of dominant species were significantly different at 4°C and 25°C in this study.

Potential new species information. Among the 77 species, four bacterial strains exhibited low 16S rRNA gene sequence similarities (< 98.65 %) with validly described species based on the results of the BLAST search in EzBioCloud (Table IV), which indicated that these isolates could represent novel taxa. *Neorhizobium* gen. nov. was a new genus of rhizobia established by Mousavi et al. (2014); so far, only five species had been published. The T786 strain had 98.70%, 98.47%, 98.24%, 98.16%, 97.79%, and 96.55% sequence similarity with *Neorhizobium vignae* CCBAU 05176^T (GU128881), *Neorhizobium alkalisoli* CCBAU01393^T (EU074168), *Neorhizobium tomejilense* T17_20^T (PVBG01000052), *Neorhizobium huautlense* S02^T (AF025852), *Neorhizobium galegae* ATCC43677^T(D11343), and *Neorhizobium lilium* 24NR^T (MK386721), respectively (Fig. 3). Further data analysis suggested that the dDDH and ANI values between strain T786 and *N. vignae* CCBAU 05176^T, *N. alkalisoli* CCBAU 01393^T, *N. tomejilense* T17_20^T, *N. huautlense* S02^T, and *N. galegae* ATCC 43677^T were 20.20–20.50% and 76.64–80.01%, respectively, which were lower than the threshold values of 70% and 95–96% for species discrimination (unpublished). *Pararhizobium* gen. nov. was a new genus of rhizobia also established by Mousavi et al. (2015); so far, only seven species had been published. The T808 strain had high similarity with *Pararhizobium herbae* CCBAU83011^T (GU565534) (98.79%), *Pararhizobium polonicum* F5.1^T (LGLV01000030) (98.65%), and *Pararhizobium giardinii* H152^T (ARBG01000149) (98.50%). The 16S rRNA sequence of strain T808 had about 40 more bases in the V1-V2 region than the seven validly published species of *Pararhizobium*, while the NCBI database showed that T808 had 98.54–99.15% similarity with Uncultured bacterium clone barrow_FF_26 (JX668750.1), *Rhizobium* sp.Ia8 (KF444807), and Rhizobiaceae bacterium strain FW305-C-27(MN067584), all of which were uncultured bacteria without lacking the 40 bases in V1-V2 region (Fig. 4). Based on the above analysis, T808 might be a poten-

tially new species of *Pararhizobium*. *Neorhizobium* and *Pararhizobium* were important non-symbiotic species of rhizobia with poor nodulation or nitrogen fixation genes, which have the important microbial niche value (Shen et al. 2018; Soenens et al. 2019).

Three potential new species were isolated from media M5, and one species was isolated from media M8, R, and F1, respectively. Half of six potential new species were cultured at 4°C, while others were cultured at 25°C. The culture medium and temperature have a significant influence on the separation of new species. All six potential new species will be further identified with a polyphasic approach (including chemotaxonomic properties, DNA-DNA hybridization analysis) to determine their taxonomic positions.

Discussion

Together with the incubation of the highland barley cultivation soil sample using fifteen kinds of media at 25°C and 4°C, a total of 830 individual strains were purified. The 16S rRNA gene sequence analysis results are consistent with a previous report, in which Actinobacteria, Proteobacteria, Firmicutes were found to be dominant phyla in the arctic-alpine area, especially in the Qinghai-Tibet plateau (Jiang et al. 2006; Kumar et al. 2016a; Tang et al. 2016). The predominant genus was *Streptomyces*, followed by *Bacillus*, *Micromonospora*, and *Microbacterium*. The most diverse isolates belonged to high the G+C Gram-positive group; in particular, the *Streptomyces* genus is a dominant genus in the high G+C Gram-positive group. The bacteria in arctic-alpine areas are mainly the spore producing, stress-resistant, and thick cell walls microorganisms (Zhang et al. 2010b; Rao et al. 2016).

The Actinobacteria are widely dispersed throughout the highland barley cultivation soil, while few studies are on it. The bacteria in highland barley cultivation soil in Lhasa analyzed by high-throughput sequencing technology showed that the main actinomycetes were *Gaiiella*, *Arthrobacter*, and *Nocardioides* (Liu et al.

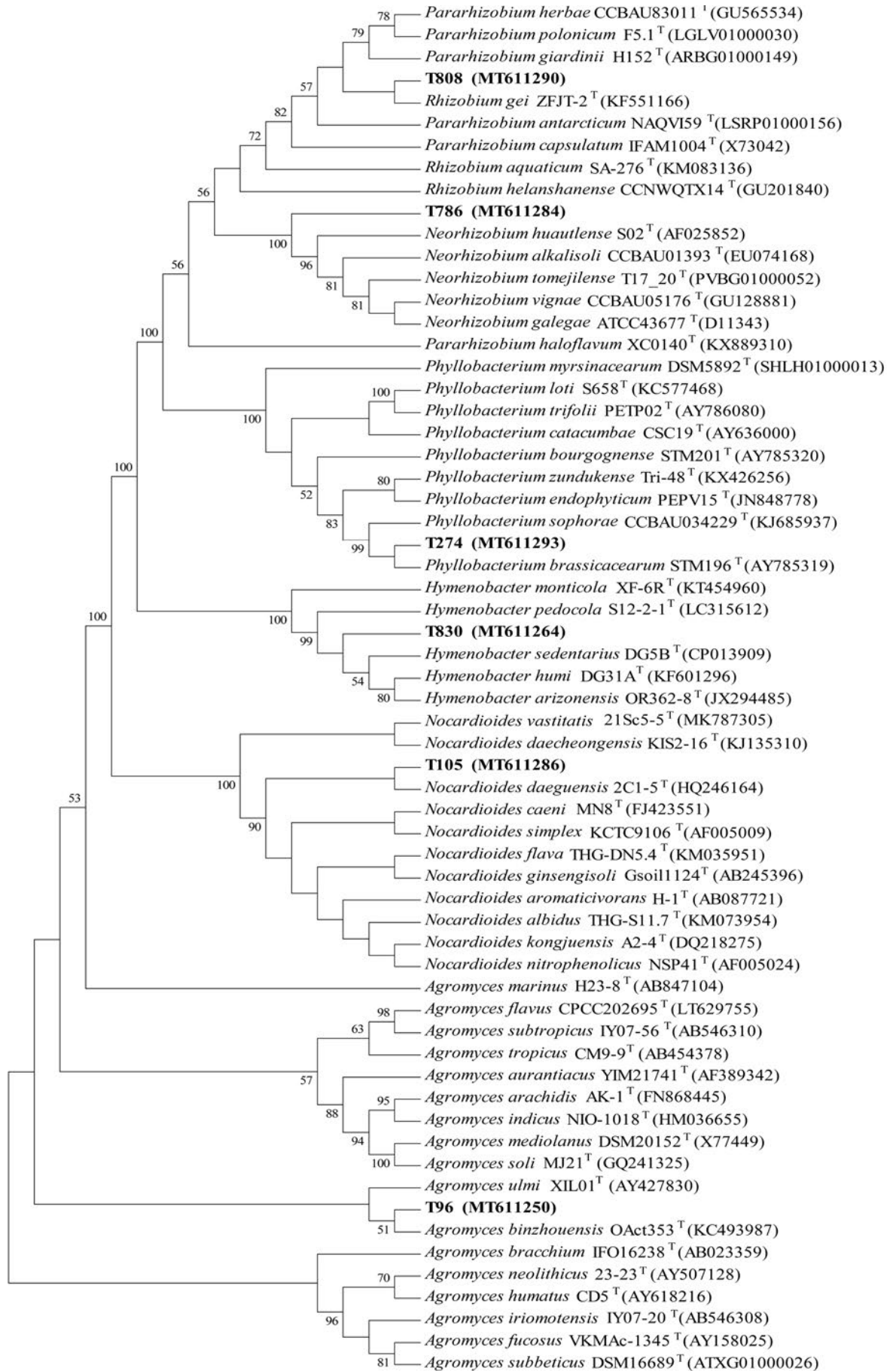


Fig. 3. Phylogenetic tree based on the 16S rRNA gene sequences of new candidates and related species.

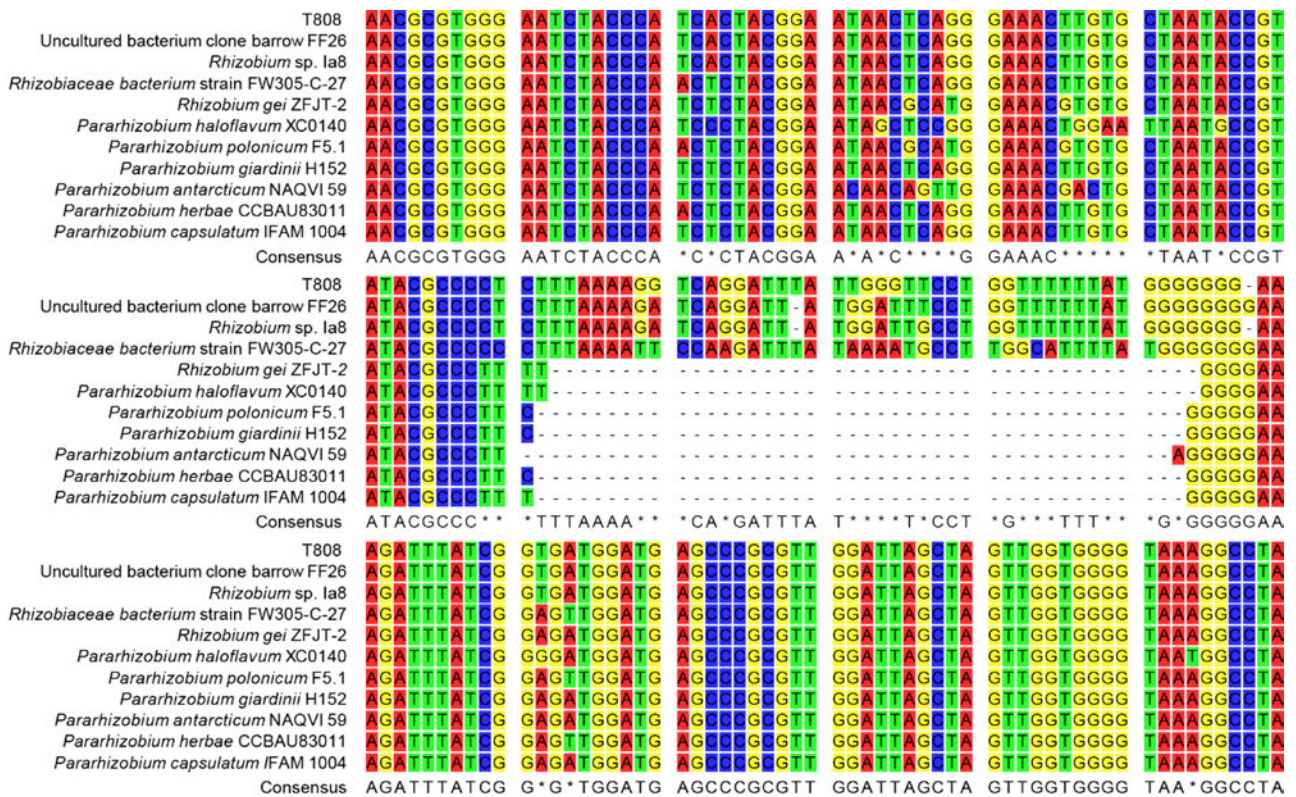


Fig. 4. The Clustal X analysis of strain T808.

2020), which was quite different from our study using the culturable technique. In other previous reports, the main genus in the highland barley cultivation soil was *Streptomyces*, *Arthrobacter*, and *Nocardioidea*. Most Actinomycetes had a wide spectrum of inhibitory activity against pathogenic bacteria, highly IAA production, and phosphate solubilization, which were in similarity with our study (Qi et al. 2017; Yin et al. 2017; Gao et al. 2019). As the most well-known genus in Actinobacteria, *Streptomyces* contains 960 species (<http://www.bacterio.net/streptomyces>) and 4227 genome assemblies available (<https://www.ncbi.nlm.nih.gov/genome/streptomyces>) at the time of writing. Members of the genus *Streptomyces* are well known as the primary sources of antibiotics with diverse biological activities and chemical structures (Jones and Elliot 2017; Li et al. 2018). In this study, 17 species of *Streptomyces* were found in the highland barley cultivation soil, the larger numbers of dominant species of *Streptomyces* were *Streptomyces flavovirens*, *Streptomyces xanthophaeus* and *Streptomyces canus*, which were mainly isolated at 25°C. The Qamdo region's temperature is between 20°C and 28°C from June to September, which is also a critical growth period for highland barley. We believe that these *Streptomyces* that can produce many biological activities have an essential role in the growth of highland barley in this period. The other dominant isolates in highland barley cultivation soil were *Arthrobacter humicola* and *Bacillus siamensis*,

which are important plant growth-promoting rhizobacteria (PGPR) (Bai et al. 2015).

Meanwhile, *Arthrobacter humicola* was mainly isolated at 4°C, producing cold lipase and biopolymeric flocculant (Agunbiade et al. 2017). The low-temperature adaptation and ecological function of *A. humicola* in highland barley cultivation soil need to be studied in-depth. Some rare Actinobacteria were also isolated from the soil sample, for example, *Leifsonia*, *Longispora*, *Nocardia*, *Nocardioidea*, *Terrabacter*, *Umezawaea*, and *Kribbella*. Rare Actinobacteria are also important sources in discovering novel antibiotics and have been seldom studied (Cai et al. 2018; Bundale et al. 2019).

In summary, this study has demonstrated a rich diversity of bacteria (especially Actinobacteria) and some undiscovered bacteria species in the highland barley cultivation soil of Qinghai-Tibet plateau it suggests that these strains might represent a valuable source of new taxa for further microbial development and utilization. Additionally, this study indicates that cultivating Actinobacteria in highland barley cultivation soil of Qinghai-Tibet plateau could be interesting for further study.

Acknowledgments

National Natural Science Foundation of China (32060025), the Special Financial Item of Tibet Autonomous Region (XZNKY-2018-C-026) and the "Double First-Class" construction project of Hunan Agricultural University (SYL201802002) funded this work.

Conflict of interest

The authors do not report any financial or personal connections with other persons or organizations, which might negatively affect the contents of this publication and/or claim authorship rights to this publication

Literature

- Agunbiade MO, Van Heerden E, Pohl CH, Ashafa AT. Flocculating performance of a bioflocculant produced by *Arthrobacter humicola* in sewage waste water treatment. BMC Biotechnol. 2017 Dec;17(1):51. <https://doi.org/10.1186/s12896-017-0375-0>
- Bai Y, Müller DB, Srinivas G, Garrido-Oter R, Potthoff E, Rott M, Dombrowski N, Münch PC, Spaepen S, Remus-Emsermann M, et al. Functional overlap of the *Arabidopsis* leaf and root microbiota. Nature. 2015 Dec;528(7582):364–369. <https://doi.org/10.1038/nature16192>
- Bailly A, Weisskopf L. The modulating effect of bacterial volatiles on plant growth: current knowledge and future challenges. Plant Signal Behav. 2012 Jan;7(1):79–85. <https://doi.org/10.4161/psb.7.1.18418>
- Bodelier PLE. Toward understanding, managing, and protecting microbial ecosystems. Front Microbiol. 2011;2:80. <https://doi.org/10.3389/fmicb.2011.00080>
- Bundale S, Singh J, Begde D, Nashikkar N, Upadhyay A. Rare actinobacteria: a potential source of bioactive polyketides and peptides. World J Microbiol Biotechnol. 2019 Jun;35(6):92. <https://doi.org/10.1007/s11274-019-2668-z>
- Cai Y, Tao WZ, Ma YJ, Cheng J, Zhang MY, Zhang YX. *Leifsonia flava* sp. nov., a novel actinobacterium isolated from the rhizosphere of *Aquilegia viridiflora*. J Microbiol. 2018 Aug;56(8):549–555. <https://doi.org/10.1007/s12275-018-8061-z>
- Collins T, Margesin R. Psychrophilic lifestyles: mechanisms of adaptation and biotechnological tools. Appl Microbiol Biotechnol. 2019 Apr;103(7):2857–2871. <https://doi.org/10.1007/s00253-019-09659-5>
- Delgado-Baquerizo M, Oliverio AM, Brewer TE, Benavent-González A, Eldridge DJ, Bardgett RD, Maestre FT, Singh BK, Fierer N. A global atlas of the dominant bacteria found in soil. Science. 2018 Jan 19;359(6373):320–325. <https://doi.org/10.1126/science.aap9516>
- Deng N, Zheng B, Li T, Liu RH. Assessment of the phenolic profiles, hypoglycemic activity, and molecular mechanism of different highland barley (*Hordeum vulgare* L.) varieties. Int J Mol Sci. 2020 Feb 11;21(4):1175. <https://doi.org/10.3390/ijms21041175>
- Fulthorpe RR, Roesch LFW, Riva A, Triplett EW. Distantly sampled soils carry few species in common. ISME J. 2008 Sep;2(9):901–910. <https://doi.org/10.1038/ismej.2008.55>
- Furlong MA, Singleton DR, Coleman DC, Whitman WB. Molecular and culture-based analyses of prokaryotic communities from an agricultural soil and the burrows and casts of the earthworm *Lumbricus rubellus*. Appl Environ Microbiol. 2002 Mar;68(3):1265–1279. <https://doi.org/10.1128/AEM.68.3.1265-1279.2002>
- Gao X, Gu YF, Nyima T, Liu GY, Liu T, Liu Y, Pubu G. Analysis of the genetic diversity and promoting functions of the culturable Actinomycetes in the rhizosphere of highland barley in Tibet. Sichuan Nongye Daxue Xuebao. 2019;37(6):777–784.
- He Q, Wang X, He L, Yang L, Wang S, Bi Y. Alternative respiration pathway is involved in the response of highland barley to salt stress. Plant Cell Rep. 2019 Mar;38(3):295–309. <https://doi.org/10.1007/s00299-018-2366-6>
- Jiang H, Dong H, Zhang G, Yu B, Chapman LR, Fields MW. Microbial diversity in water and sediment of Lake Chaka, an athalasoaline lake in northwestern China. Appl Environ Microbiol. 2006 Jun;72(6):3832–3845. <https://doi.org/10.1128/AEM.02869-05>
- Jones SE, Elliot MA. *Streptomyces* exploration: competition, volatile communication and new bacterial behaviours. Trends Microbiol. 2017 Jul;25(7):522–531. <https://doi.org/10.1016/j.tim.2017.02.001>
- Kim M, Oh HS, Park SC, Chun J. Towards a taxonomic coherence between average nucleotide identity and 16S rRNA gene sequence similarity for species demarcation of prokaryotes. Int J Syst Evol Microbiol. 2014 Feb 01;64(Pt_2):346–351. <https://doi.org/10.1099/ijs.0.059774-0>
- Kuklinsky-Sobral J, Araújo WL, Mendes R, Geraldi IO, Pizzirani-Kleiner AA, Azevedo JL. Isolation and characterization of soybean-associated bacteria and their potential for plant growth promotion. Environ Microbiol. 2004 Dec;6(12):1244–1251. <https://doi.org/10.1111/j.1462-2920.2004.00658.x>
- Kumar M, Männistö MK, van Elsas JD, Nissinen RM. Plants impact structure and function of bacterial communities in Arctic soils. Plant Soil. 2016a Feb;399(1–2):319–332. <https://doi.org/10.1007/s11104-015-2702-3>
- Kumar S, Stecher G, Tamura K. MEGA7: Molecular Evolutionary Genetics Analysis Version 7.0 for Bigger Datasets. Mol Biol Evol. 2016b Jul;33(7):1870–1874. <https://doi.org/10.1093/molbev/msw054>
- Kurm V, van der Putten WH, Hol WHG. Cultivation-success of rare soil bacteria is not influenced by incubation time and growth medium. PLoS One. 2019 Jan 10;14(1):e0210073. <https://doi.org/10.1371/journal.pone.0210073>
- Li F, Liu S, Lu Q, Zheng H, Osterman IA, Lukyanov DA, Sergiev PV, Dontsova OA, Liu S, Ye J, et al. Studies on antibacterial activity and diversity of cultivable actinobacteria isolated from mangrove soil in Futian and Maowei Hai of China. Evid Based Complement Alternat Med. 2019 Jun 09;2019:1–11. <https://doi.org/10.1155/2019/3476567>
- Li L, Wei K, Zheng G, Liu X, Chen S, Jiang W, Lu Y. CRISPR-Cpf1-assisted multiplex genome editing and transcriptional repression in *Streptomyces*. Appl Environ Microbiol. 2018 Jul 06;84(18):e00827–18. <https://doi.org/10.1128/AEM.00827-18>
- Liu GH, Narsing Rao MP, Dong ZY, Wang JP, Chen Z, Liu B, Li WJ. Two novel alkaliphiles, *Bacillus alkalisolis* sp. nov., and *Bacillus solitudinis* sp. nov., isolated from saline-alkali soil. Extremophiles. 2019 Nov;23(6):759–764. <https://doi.org/10.1007/s00792-019-01127-2>
- Liu QH, Pan H, Da WZM, Tian Y, Liu HH, Wang C, Lu XY, Bai JP. [High-throughput analysis of bacterial diversity in highland barley cultivation soil in Lhasa] (in Chinese). J Biol. 2020;37(2):46–51.
- Malard LA, Anwar MZ, Jacobsen CS, Pearce DA. Biogeographical patterns in soil bacterial communities across the Arctic region. FEMS Microbiol Ecol. 2019 Sep 01;95(9):fiz128. <https://doi.org/10.1093/femsec/fiz128>
- Margesin R, Jud M, Tschirko D, Schinner F. Microbial communities and activities in alpine and subalpine soils. FEMS Microbiol Ecol. 2009 Feb;67(2):208–218. <https://doi.org/10.1111/j.1574-6941.2008.00620.x>
- Margesin R. Psychrophilic microorganisms in alpine soils. In: Lütz C, editor. Plants in Alpine regions. Vienna (Austria): Springer; 2012. p. 187–198.
- Mousavi SA, Österman J, Wahlberg N, Nesme X, Lavire C, Vial L, Paulin L, de Lajudie P, Lindström K. Phylogeny of the *Rhizobium-Allorhizobium-Agrobacterium* clade supports the delineation of *Neorhizobium* gen. nov. Syst Appl Microbiol. 2014 May;37(3):208–215. <https://doi.org/10.1016/j.syapm.2013.12.007>
- Mousavi SA, Willems A, Nesme X, de Lajudie P, Lindström K. Revised phylogeny of *Rhizobiaceae*: proposal of the delineation of *Pararhizobium* gen. nov., and 13 new species combinations. Syst Appl Microbiol. 2015 Mar;38(2):84–90. <https://doi.org/10.1016/j.syapm.2014.12.003>

- Qi SS, Zhou LH, Hu JP, Liu M, Zhao H, Xiong Y. [Isolation, identification and diversity of soil bacteria in multiple regions from Tibetan Plateau] (in Chinese). *Xi Nan Nong Ye Xue Bao*. 2017; 30(7):1629–1635.
- Rao S, Chan OW, Lacap-Bugler DC, Pointing SB. Radiation-tolerant bacteria isolated from high altitude soil in Tibet. *Indian J Microbiol*. 2016 Dec;56(4):508–512. <https://doi.org/10.1007/s12088-016-0604-6>
- Řeháková K, Chroňáková A, Křišťůfek V, Kuchtová B, Čapková K, Scharfen J, Čapek P, Doležal J. Bacterial community of cushion plant *Thylacospermum caespitosum* on elevational gradient in the Himalayan cold desert. *Front Microbiol*. 2015 Apr 16;6:304. <https://doi.org/10.3389/fmicb.2015.00304>
- Shen X, Li Y, Zhao Z, Han YF, Zhang WW, Yu XY, Zhang CY, Sun C, Wu M. Polyphasic taxonomic characterisation of a novel strain as *Pararhizobium haloflavum* sp. nov., isolated from soil samples near a sewage treatment tank. *Antonie van Leeuwenhoek*. 2018 Apr;111(4):485–491. <https://doi.org/10.1007/s10482-017-0969-5>
- Shen Y, Zhang H, Cheng L, Wang L, Qian H, Qi X. *In vitro* and *in vivo* antioxidant activity of polyphenols extracted from black highland barley. *Food Chem*. 2016 Mar;194:1003–1012. <https://doi.org/10.1016/j.foodchem.2015.08.083>
- Soenens A, Gomila M, Imperial J. *Neorhizobium tomejilense* sp. nov., first non-symbiotic *Neorhizobium* species isolated from a dryland agricultural soil in southern Spain. *Syst Appl Microbiol*. 2019 Mar;42(2):128–134. <https://doi.org/10.1016/j.syapm.2018.09.001>
- Tang JY, Ma J, Li XD, Li YH. Illumina sequencing-based community analysis of bacteria associated with different bryophytes collected from Tibet, China. *BMC Microbiol*. 2016 Dec;16(1):276. <https://doi.org/10.1186/s12866-016-0892-3>
- Yin MY, He JQ, Zhang GJ. [Biological activity and diversity of psychrophilic Actinomycetes in Tibet] (in Chinese). *J Northwest Agric Forest Univer (Nat Sci Ed)*. 2017;45(6):221–234.
- Yu Y, Guo Z, Wu H, Kahmann JA, Oldfield F. Spatial changes in soil organic carbon density and storage of cultivated soils in China from 1980 to 2000. *Global Biogeochem Cy*. 2009;23: GB2021. <https://doi.org/10.1029/2008GB003428>
- Yuan Y, Si G, Wang J, Luo T, Zhang G. Bacterial community in alpine grasslands along an altitudinal gradient on the Tibetan Plateau. *FEMS Microbiol Ecol*. 2014 Jan;87(1):121–132. <https://doi.org/10.1111/1574-6941.12197>
- Zhang G, Niu F, Ma X, Liu W, Dong M, Feng H, An L, Cheng G. Phylogenetic diversity of bacteria isolates from the Qinghai-Tibet Plateau permafrost region. *Can J Microbiol*. 2007 Aug;53(8): 1000–1010. <https://doi.org/10.1139/W07-031>
- Zhang K, Yang J, Qiao Z, Cao X, Luo Q, Zhao J, Wang F, Zhang W. Assessment of β -glucans, phenols, flavor and volatile profiles of hull-less barley wine originating from highland areas of China. *Food Chem*. 2019 Sep;293:32–40. <https://doi.org/10.1016/j.foodchem.2019.04.053>
- Zhang S, Yang G, Wang Y, Hou S. Abundance and community of snow bacteria from three glaciers in the Tibetan Plateau. *J Environ Sci (China)*. 2010a Sep;22(9):1418–1424. [https://doi.org/10.1016/S1001-0742\(09\)60269-2](https://doi.org/10.1016/S1001-0742(09)60269-2)
- Zhang Y, Dong S, Gao Q, Liu S, Zhou H, Ganjurjav H, Wang X. Climate change and human activities altered the diversity and composition of soil microbial community in alpine grasslands of the Qinghai-Tibetan Plateau. *Sci Total Environ*. 2016 Aug;562:353–363. <https://doi.org/10.1016/j.scitotenv.2016.03.221>
- Zhang YQ, Liu HY, Chen J, Yuan LJ, Sun W, Zhang LX, Zhang YQ, Yu LY, Li WJ. Diversity of culturable actinobacteria from Qinghai-Tibet plateau, China. *Antonie van Leeuwenhoek*. 2010b Aug;98(2): 213–223. <https://doi.org/10.1007/s10482-010-9434-4>
- Zhao NN, Guggenberger G, Shibistova O, Thao DT, Shi WJ, Li XG. Aspect-vegetation complex effects on biochemical characteristics and decomposability of soil organic carbon on the eastern Qinghai-Tibetan Plateau. *Plant Soil*. 2014 Nov;384(1–2):289–301. <https://doi.org/10.1007/s11104-014-2210-x>

Campylobacter fetus Induced Proinflammatory Response in Bovine Endometrial Epithelial Cells

LIZETH GUADALUPE CAMPOS-MÚZQUIZ^{1*}, ESTELA TERESITA MÉNDEZ-OLVERA^{2#},
MONIKA PALACIOS MARTÍNEZ² and DANIEL MARTÍNEZ-GÓMEZ^{3*}

¹Doctorado en Ciencias Agropecuarias, Universidad Autónoma Metropolitana Xochimilco, México

²Laboratorio de Biología Molecular, Departamento de Producción Agrícola y Animal,
Universidad Autónoma Metropolitana Xochimilco, México

³Laboratorio de Microbiología Agropecuaria, Departamento de Producción Agrícola y Animal,
Universidad Autónoma Metropolitana Xochimilco, México

Submitted 1 November 2020, revised 26 January 2021, accepted 26 January 2021

Abstract

Campylobacter fetus subsp. *fetus* is the causal agent of sporadic abortion in bovines and infertility that produces economic losses in livestock. In many infectious diseases, the immune response has an important role in limiting the invasion and proliferation of bacterial pathogens. Innate immune sensing of microorganisms is mediated by pattern-recognition receptors (PRRs) that identify pathogen-associated molecular patterns (PAMPs) and induces the secretion of several proinflammatory cytokines, like IL-1 β , TNF- α , and IL-8. In this study, the expression of IL-1 β , TNF- α , IL-8, and IFN- γ in bovine endometrial epithelial cells infected with *C. fetus* and *Salmonella* Typhimurium (a bacterial invasion control) was analyzed. The results showed that expression levels of IL-1 β and IL-8 were high at the beginning of the infection and decreased throughout the intracellular period. Unlike in this same assay, the expression levels of IFN- γ increased through time and reached the highest peak at 4 hours post infection. In cells infected with *S. Typhimurium*, the results showed that IL8 expression levels were highly induced by infection but not IFN- γ . In cells infected with *S. Typhimurium* or *C. fetus* subsp. *fetus*, the results showed that TNF- α expression did not show any change during infection. A cytoskeleton inhibition assay was performed to determine if cytokine expression was modified by *C. fetus* subsp. *fetus* intracellular invasion. IL-1 β and IL-8 expression were downregulated when an intracellular invasion was avoided. The results obtained in this study suggest that bovine endometrial epithelial cells could recognize *C. fetus* subsp. *fetus* resulting in early proinflammatory response.

Key words: bacterial infection, pathogenicity, virulence, pathogen-host interaction (MesH)

Introduction

The innate immune system senses microbial infections and triggers an immediate response to control pathogens' invasion. Microbial sensing is mediated by pattern-recognition receptors (PRRs), which include Toll-like receptors (TLR), Nucleotide-binding Oligomerization Domain (NOD), Leucine-rich repeat-containing receptors (NLRs), C-Type Lectin-Like Receptors, and Cytoplasmic Nucleic Acid Sensors. These receptors are important in innate and adaptive immune response because they identify Pathogen Associated Molecular Patterns (PAMPs) and determine the type of immune response required (Bryant et al. 2015). The innate immune response includes proinflammatory

cytokines secretion, which recruits and activates phagocytic cells to eliminate the pathogenic microorganisms (Iwasaki and Medzhitov 2015).

The female reproductive tract's mucosal surface forms a physical and immunological barrier that can interact with sexually transmitted pathogens and spermatozoa. Therefore, innate immune mechanisms have an important role in maintaining its integrity (Amjadi et al. 2014). The cells in mucosal epithelia recognize pathogens and stimulate the underlying immune cells like macrophages, inducing an inflammatory reaction via cytokines' production, resulting in adaptive immunity activation. They also produce antimicrobial peptides that eliminate several bacterial and viral agents (Turner et al. 2014).

Lizeth Guadalupe Campos-Múzquiz and Estela Teresita Méndez-Olvera contribute equally to this work and are co-first authors.

* Corresponding author: D. Martínez-Gómez, Laboratorio de Microbiología Agropecuaria, Departamento de Producción Agrícola y Animal, Universidad Autónoma Metropolitana Xochimilco, México; e-mail: dmartinez@correo.xoc.uam.mx

© 2021 Lizeth Guadalupe Campos-Múzquiz et al.

This work is licensed under the Creative Commons Attribution-NonCommercial-NoDerivatives 4.0 License (<https://creativecommons.org/licenses/by-nc-nd/4.0/>).

Campylobacter fetus subsp. *fetus* is frequently isolated from the intestinal tract of asymptomatic cattle, goats, and sheep. In animals, *C. fetus* subsp. *fetus* exhibits a tropism for placental and reproductive tract tissues and is one of the major causes of sporadic and epidemic septic abortions (Viejo et al. 2001; Iraola et al. 2012). *C. fetus* subsp. *fetus* can attach in an irreversible way to bull spermatozoa and affect sperm quality (Cagnoli et al. 2020). The diseases produced by *C. fetus* subsp. *fetus* generate considerable economic losses, representing a significant problem in animal production (Mshelia et al. 2010). Heifers infected with *C. fetus* showed a light inflammatory reaction with few mononuclear and polymorphonuclear cells distributed diffusely beneath the epithelia of vagina and cervix, and moderate endometritis and salpingitis (Cipolla et al. 1994). Such light inflammation reaction can be due to the composition of the external membrane of microorganisms. *C. fetus* possesses lipooligosaccharides (LOS) instead of lipopolysaccharide (LPS) (Preston and Penner 1987; Moran et al. 2002). Also, it has a protein surface layer known as S-layer, which protects *C. fetus* against complement and opsonization-phagocytosis response; it also prevents recognition by host innate immune system (Blaser et al. 1987; Fogg et al. 1990; Blaser et al. 1993).

We have previously demonstrated the ability of *C. fetus* subsp. *fetus* to invade bovine endometrial cells (Campos-Múzquiz et al. 2019). This phenomenon was dependent on the viability of *C. fetus*, since dead bacteria could not invade this type of cells (in press). The ability of *C. fetus* subsp. *fetus* to invade endometrial cells raises new questions about the pathogen's mechanisms to infect these surfaces and induce reproductive diseases. The inflammatory response induced by *C. fetus* in bovine endometrium has not yet been entirely described; meanwhile, for other *Campylobacter* species, the induction of proinflammatory cytokines in epithelial cells has been described along with the benefits that this represents for tissue invasion (Al-Salloom et al. 2003; Zheng et al. 2008; Eucker et al. 2014). Hence in this study, the cytokine expression patterns induced in bovine endometrial epithelial cells by infection with *C. fetus* subsp. *fetus* were evaluated, to establish the role of inflammation in diseases produced by this species in the bovine reproductive tract.

Experimental

Materials and Methods

Bacterial strains and growth conditions. *C. fetus* subsp. *fetus* ATCC 27374 (Salama et al. 1995) was grown at 37°C for 48 h under microaerophilic atmosphere (85% N₂, 10% CO₂ and 5% O₂) on *Campylobacter*

selective agar supplemented with 5% sheep blood. *Salmonella enterica* subsp. *enterica* serovar Typhimurium ATCC 14028 was also grown on hyperosmolar Luria Bertani broth at 37°C for 12 h.

Endometrial epithelial cell culture. Epithelial cells from the endometrium were recovered using Skarzynski protocol (Skarzynski et al. 2015) with some modifications. The uterus was removed from three sacrificed cows 15 min after exsanguination at a slaughterhouse. Tissue was washed with Hank's solution supplemented with 1.6 mg/ml of gentamicin and transported to the laboratory in the same buffer solution on ice. The endometrium was cut and washed three times with phosphate-buffered saline solution pH 7.2 (PBS, NaH₂PO₄ 1.9 mM, Na₂HPO₄ 8.1 mM, NaCl 154 mM). Tissue pieces were treated with digestion solution (0.5 mg/ml collagenase type I from *Clostridium histolyticum*, 0.1 mg/ml DNase, 100 µg/ml gentamicin, Dulbecco's Modified Eagle Medium supplemented with 10% fetal bovine serum) at 37°C for 2 h. A tissue debris-free supernatant was recovered and centrifuged at 4,000 × g for 10 min. The pellet was suspended in 5 ml of DMEM supplemented with 10% fetal bovine serum and filtered with a 40-µm strainer. Cells were placed on cell culture flasks with HEPES (25 mM) and antibiotic/antifungal solutions (penicillin G 10,000 U, streptomycin 5,000 µg, amphotericin B 12.5 µg). For fibroblast depuration, one-minute of trypsinization was performed daily for three consecutive days. Cell type was confirmed by immunofluorescence and RT-PCR (Campos-Múzquiz et al. 2019).

Invasion assays. Gentamicin protection assays were performed with *C. fetus* (multiplicity of infection – MOI – 100:1) and *S. Typhimurium* (MOI 50:1). An amount of 200,000 endometrial epithelial cells were cultured in a 25 cm² culture flask. Bacteria inoculum was diluted in DMEM, added to cultures, and incubated 2 hrs at 37°C. Following the incubation, the cell monolayers were washed three times with PBS and incubated with DMEM/gentamicin (10% fetal bovine serum, 25 mM HEPES, 30 µg/ml gentamicin) at 37°C. Cell lysates were recovered at 0, 2, and 4 h post-infection by adding 500 µl of Triton X100 (1%). Cell lysates (50 µl) of each infection hour was placed on *Campylobacter* selective agar supplemented with 5% sheep blood at 37°C for 72 h in an anaerobic chamber under low oxygen conditions (Oxoid Campy Gen, England). Cell lysates were treated with TRIzol (Invitrogen, USA) following the manufacturer's indication to recover cell and bacteria RNA. Three independent assays with three replications of each time were performed. For cytoskeleton inhibition, before the invasion assays, cell cultures were treated with cytochalasin D (3 mM) (Sigma-Aldrich, USA) for 30 min at 37°C. Then the invasion assays were made as described previously.

Intracellular survival evaluation by reverse transcription qPCR. Quantitative reverse transcription PCR using random primers and a commercial kit to synthesize complementary DNA (ProtoScript® First Strand cDNA Synthesis Kit, New England Biolabs) were used to evaluate the intracellular survival ability of *C. fetus* subsp. *fetus*. The cDNA was employed to quantify mRNA copies (RC) of *C. fetus* subsp. *fetus* and *Salmonella* Typhimurium (Power SYBR green, Fermentas). The primer sequences used in these assays for *C. fetus* subsp. *fetus* were: 5'-GGCAATATCATAGAAATCCGTTATC-3' and 5'-TCCTGCTCTTTCATTTGCTT-3' these primers amplified a 161 bp fragment from fumarate reductase gene (*frdA*). The primers used for *S. Typhimurium* amplified a 110 bp segment of the *rpoD* gene (Botteldoorn et al. 2006). A standard curve was built with 1 ng, 100 pg, 10 pg, 1 pg and 100 fg RNA of *C. fetus* subsp. *fetus* ATCC 27374 or *Salmonella* Typhimurium ATCC 14028. The specificity of the PCR product was confirmed by high resolution melting curve.

Gene expression analysis of proinflammatory cytokines. RNA recuperated from invasion assays was used to synthesize cDNA using commercial kit and Oligo dT primers (ProtoScript® First Strand cDNA Synthesis Kit, New England Biolabs). A quantitative PCR (Maxima SYBR green, Thermo Fisher) was performed using the primers: TAF2 (5'-CATCTCCTGGAACCCAGAAA-3', 5'-GGCTGTTCTCCTCAATCTGC-3', 98 bp), β -actin (5'-AAATCGTGCGTGACATTAAG-3', 5'-GAGTACTTGCGCTCAGGAG-3', 341 bp) and GPDH (5'-GCCATCACCATCTTCCAGG-3', 5'-GGTAGTGAGACCCCAGTGG-3', 115 bp), as reference genes; and IL-1 β (5'-GAAAGAGACAACAAGATTCCTGTGG-3', 5'-GGTCTACTTCCAGCTGCA-3', 108 bp), TNF- α (5'-CATCTACTCRCAGGTCCTCTT-3', 5'-GCAATGCGGCTGATGGT-3', 82 bp), IL-8 (5'-AGTACAGAACTTCGATGCCAATG-3', 5'-GTAAGCTTAACAATTTCTGAATTTTC-3', 127 bp), IFN- γ (5'-GGGTTTTTCTGGTTCTTATG-GC-3', 5'-GTCACTTTCATCTTCCAATTCTT-3', 144 bp) as inflammatory genes. The specificity of the PCR product was confirmed by high resolution melting curve. The amplification efficiency (E) of each gene was calculated from the standard curves using the equation $E = (-1 + 10^{-1/\text{slope}}) \times 100$ (Livak and Schmittgen 2001). For gene normalization, we obtained a geometric average of the three reference genes (Vandesompele et al. 2002). The cytokine expression analysis was realized with treated cells with cytochalasin D to determine if the inhibitors could induce cytokine expression.

Statistical analysis. To analyze differences between gene expression and intracellular microorganisms, an F test was performed to establish the equality of variance of the data. A comparative CT method ($2^{-\Delta\Delta C_T}$) was used to calculate from each gene using the geometric average

of the reference genes (Schmittgen and Livak 2008), and a Student's *t*-test was used to determine the difference between CT of treatment versus CT of control.

Results

Endometrial epithelial cell culture. The results obtained in primary cell cultures showed that the endometrial epithelial cells presented an epithelial-like appearance in the second week of incubation. In primary cell culture, the expression of Keratin 8 was confirmed by RT-PCR and immunofluorescence. A PCR product of 215 pb corresponding to a segment of the gene encoding for keratin 8 was obtained from RNA recuperated from cell cultures, and more than 90% of cells in the monolayer showed positive results to cytokeratin 18 (data not shown).

Invasion assays. In the intracellular survival assays, the results showed that viable *C. fetus* subsp. *fetus* decreased in number over time. At 0 h post-infection (p.i.) the average (\sim) colony-forming unit (CFU) were 22,408 CFU. At a second time (2 h p.i.), it decreased to \sim 1,316 CFU and 4 h p.i. there were \sim 233 CFU (Fig. 1); these results confirm that there was an intracellular bacterial cells reduction through the time ($p = 2.2e^{-16}$). In cells infected with *Salmonella* Typhimurium, the CFU increased at the end of the assay, indicating intracellular replication of bacteria ($p = 1.49e^{-10}$). At 0 h p.i., the average number of intracellular bacteria was \sim 42,150 CFU, 2 h p.i., CFU decreased to \sim 37,125 CFU, and 4 h p.i. bacteria proliferated, and their number increased to 72,925 CFU (Fig. 1).

To confirm *C. fetus* subsp. *fetus* intracellular survival ability, a bacterial mRNA quantification assay was

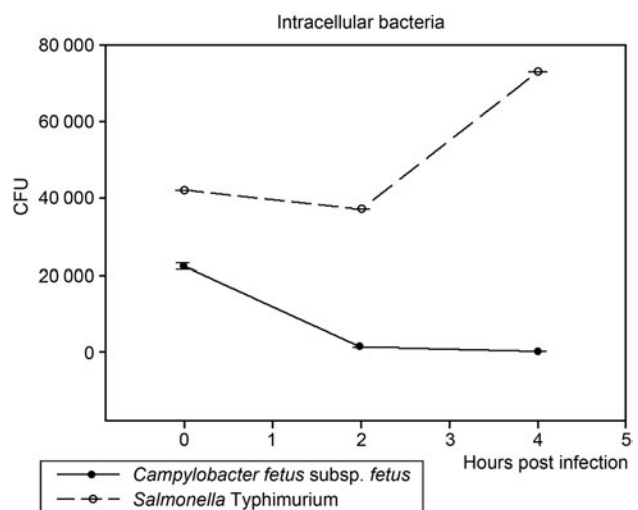


Fig. 1. *Salmonella* Typhimurium and *Campylobacter fetus* subsp. *fetus* invasion assays in endometrial cells. A gentamicin protection assay was performed to demonstrate that *C. fetus* subsp. *fetus* invades bovine endometrial epithelial cells but does not survive.

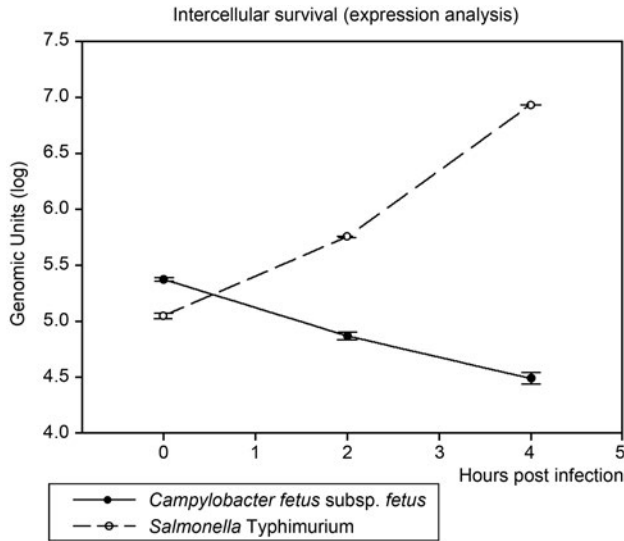


Fig. 2. Intracellular survival expression analysis of *Campylobacter fetus* subsp. *fetus* and *Salmonella* Typhimurium in bovine endometrial epithelial cells. An invasion assay was performed, and RNA was extracted from cells. The cDNA was synthesized using random primers, and a quantitative PCR was performed.

performed. For *C. fetus* subsp. *fetus*, *frdA* analysis (the constitutive gene) showed that the number of mRNA copies (genomic copies, GC) decreased significantly during invasion assays ($p=0.002$). At 0 h p.i., the number of GC were ~ 5.3767 log, 2 h p.i., this value decreased to ~ 4.8724 log, and 4 h p.i., the value was ~ 4.4922 log (Fig. 2). The *rpoD* analysis in cells infected with *S. Typhimurium* showed that the number of GC of this

constitutive gene increased through time ($p=1.586e^{-06}$). At 0 h p.i., the number of GC was ~ 5.0526 log, 2 h p.i., it increased to ~ 5.7581 log, and 4 h p.i., it increased to 6.9379 log (Fig. 2).

Cytokine expression analysis. A gene expression assay was carried out to evaluate the expression of proinflammatory cytokines in endometrial cells infected with *C. fetus* subsp. *fetus*. Cells invaded by *C. fetus* subsp. *fetus* showed an early IL-1 β high expression level (4.65-fold change at 0 h p.i.). Unlike cells invaded by *S. Typhimurium*, the IL-1 β highest expression level was reached at 4 h p.i. (3.56-fold change). The cells infected with *C. fetus* subsp. *fetus* had the highest level of IL-1 β (1.09 fold change, $p=6.645e^{-05}$). The expression level of IL-1 β decreased over time ($p=7.492e^{-05}$) in cells infected with *C. fetus* subsp. *fetus*. At 0 h p.i., the fold change was 4.65, and it decreased to 3.78 2 h p.i., and this tendency was continued until 4 h p.i., where the fold change in expression was 1.09-fold. In cells infected with *S. Typhimurium*, the IL-1 β expression levels showed an increment in time ($p=0.0007$), at 0 h p.i., there was a 4-fold change value and increased to 3.56 at 4 h p.i. (Fig. 3).

The expression levels of IL-8 showed the same pattern in cells infected with *C. fetus* subsp. *fetus* and *S. Typhimurium* throughout the time. In both cases, IL-8 expression levels were high at the beginning of the infection and decreased through time ($p=0.031$, $p=5.127e^{-05}$, respectively). At 0 h p.i., the expression level of IL-8 in cells infected with *C. fetus* subsp. *fetus* there was a 3.41-fold change and 6.14-fold for cells infected with

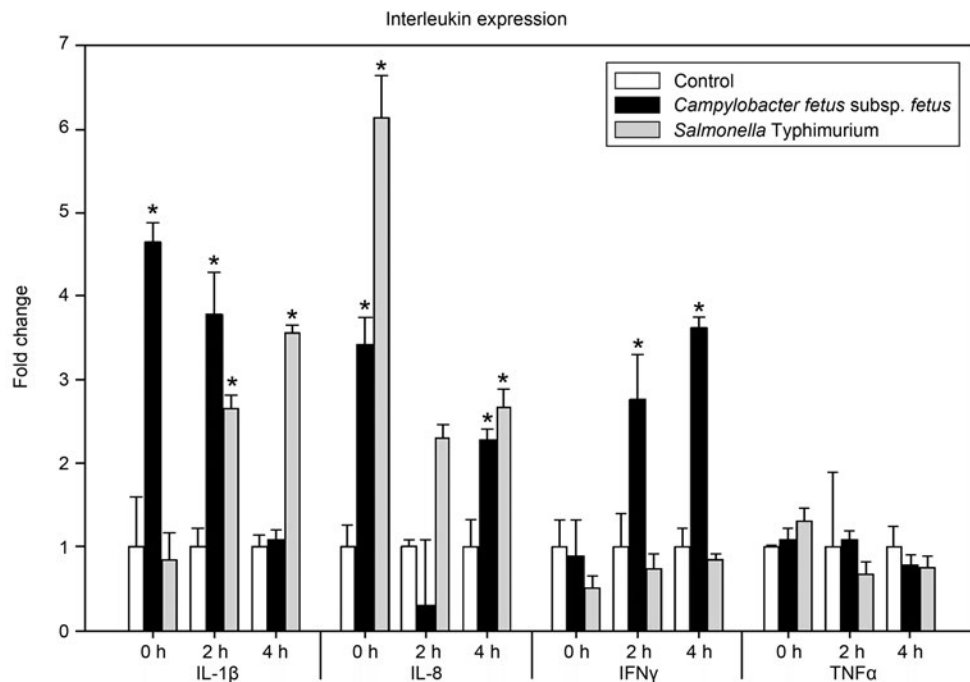


Fig. 3. Interleukin expression in bovine endometrial epithelial cells challenged with *Campylobacter fetus* subsp. *fetus* or *Salmonella* Typhimurium. Expression was analyzed with a $2^{-\Delta\Delta CT}$ and compared to control cells (no infected). A student *t*-test was performed to ΔCT (CT gene of interest – geometric media CT housekeeping genes) compared against non-treated cells; * $p < 0.05$.

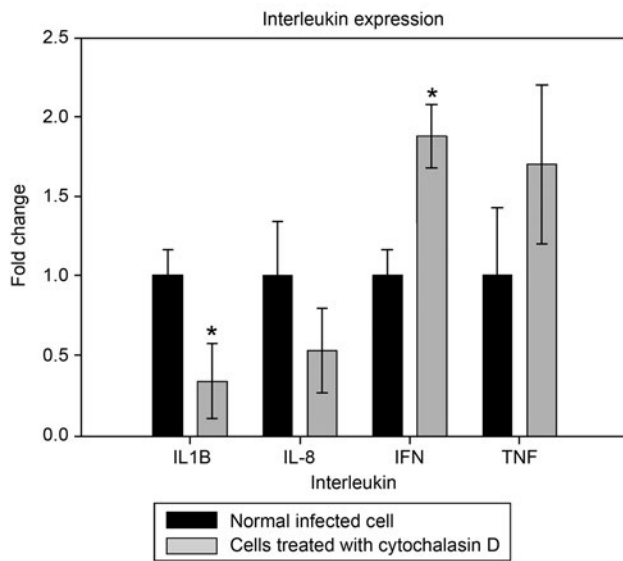


Fig. 4. Interleukin expression in bovine endometrial epithelial cells treated with cytochalasin D and challenged with *Campylobacter fetus* subsp. *fetus*. Expression was analyzed with a $2^{-\Delta\Delta CT}$ and compared to control cells (non-cytochalasin D-treated cells). A student *t*-test was performed to the ΔCT (CT gene of interest – geometric media CT housekeeping genes) comparing against non-cytochalasin D-treated cells; * $p < 0.05$.

S. Typhimurium. Simultaneously, the expression levels of IL-8 were highest in cells infected with *S. Typhimurium* compared to cells infected with *C. fetus* subsp. *fetus* ($p = 0.015$). At 4 h p.i., for the expression level of IL-8 in cells infected with *C. fetus* subsp. *fetus*, there was a 2.28-fold change. For cells infected with *S. Typhimurium*, there was a 2.68-fold change (Fig. 3), so there was no difference in the expression levels between both treatments at this time (p -value = 0.4401) (Fig. 3).

The expression levels of IFN- γ in cells infected with *C. fetus* subsp. *fetus* showed a different pattern in comparison with IL-1 β and IL-8. In this case, the expression level of IFN- γ increased through time ($p = 0.002$). At 0 h p.i., the expression level increased 0.89-folds, at 2 h p.i., it increased 2.77-fold, and at 4 h p.i., it reached a 3.62-fold increase (Fig. 3). In cells infected with *S. Typhimurium*, the expression levels of IFN- γ did not change throughout the time ($p = 0.367$). At 0 h p.i., the expression level was two times lower, 2 h p.i. it changed by 0.74, and 0.85 4 h p.i. Finally, the expression levels of TNF- α did not change either in cells infected with *C. fetus* subsp. *fetus* or *S. Typhimurium*, and there were no differences when compared to the control (uninfected cells) at any time during the assay.

To determine if *C. fetus* subsp. *fetus* intracellular invasion was necessary for the induction of IL-1 β , IL-8, and IFN- γ , a cytoskeleton inhibition assay was performed, and cytokines expression was evaluated. In cells treated and infected with *C. fetus* subsp. *fetus*, the expression level of IL-1 β was reduced by 0.34 compared with non-

treated cells ($p = 0.005$). A similar result was observed, with IL-8 expression (0.53-fold change). Nonetheless, the difference was non-significant ($p = 0.105$). Finally, the expression levels of IFN- γ in cells treated with cytochalasin D and infected with *C. fetus* subsp. *fetus* showed an increment (1.90-fold change) in comparison with non-treated cells ($p = 0.021$) (Fig. 4).

Discussion

Pathogen-associated molecular patterns by PRRs upregulate the transcription of proinflammatory cytokines like IL-1 β , TNF- α , and IL8 (Takeuchi and Akira 2010). In this study, endometrial epithelial cells showed a high expression of IL-1 β and IL8 due to the infection with *C. fetus* subsp. *fetus*, suggesting that these cells could recognize some molecular patterns in this pathogen through their PRRs. These results agree with other studies that show the induction of proinflammatory cytokines by *Campylobacter* spp. infection (Wang et al. 2000; Arce et al. 2010b; Man et al. 2010; Yu et al. 2016). In the abovementioned studies, the authors used other types of cells as Caco-2, HEp-2, and HT-29 in their experiments. In this study, primary cell culture of endometrial cells was used, and the same phenomenon was observed during the infection. The early high IL-1 β expression in cells infected with *C. fetus* subsp. *fetus* (4.65-fold change at 0 h p.i.) suggests an immediate immune recognition that might induce an acute inflammatory response. It could be used by *C. fetus* subsp. *fetus* to invade tissues. An invasion study in human trophoblast cells showed that in *C. rectus* there was a correlation between invasion and cytokine production (Man et al. 2010).

The IL-1 β up-expression in bovine endometrial epithelial cells infected with *C. fetus* subsp. *fetus* was earlier than in *S. Typhimurium* (0 h p.i vs 4 h p.i respectively), and it decreased through time. Previously, a similar phenomenon was observed in a 4-week old chicken challenged with *S. Typhimurium* and *Campylobacter jejuni*. The peak of IL-1 β expression in *C. jejuni*-infected chicks was at 20 h p.i., and in the *Salmonella*-infected chicks, it was at 48 h p.i. (Shaughnessy et al. 2009). A possible explanation for this could be that in the *C. fetus* genome, there are not virulence factors associated with immune suppression as in *S. Typhimurium*. Therefore, the induction of cytokines could be faster in *C. fetus* subsp. *fetus* in comparison with *S. Typhimurium*, which can modify the immune response (Kienesberger et al. 2014; Hu et al. 2017). Analysis of the present results also showed that the expression of pro-inflammatory cytokines in endometrial cells infected with *S. Typhimurium* took longer to reach the higher peak of expression, in comparison with cells infected with *C. fetus* subsp. *fetus*. Rolhion

et al. (2016) shown that *Salmonella* Typhi uses SpvD, an effector protein secreted through the type III secretion system, to avoid nuclear translocation of NF- κ B transcriptional factor. Therefore, infected cells reduce proinflammatory cytokines secretion.

C. fetus subsp. *fetus* did not survive in endometrial cells in comparison with *S. Typhimurium*. In intracellular survival assays, the number of intracellular *C. fetus* subsp. *fetus* showed a reduction over time. This result was confirmed by two different methods, quantification of the number of transcripts (mRNA copies of constitutive genes) and CFUs. Considering that each method has different criteria to establish the number of viable microorganisms (gene expression and growth in specific media), we could say that reduction in the CFU number of *C. fetus* subsp. *fetus* was not due to the formation of viable non-culturable microorganisms but to the elimination of the pathogen. In the case of *S. Typhimurium*, the results showed a different pattern, indicating that the bacterium could survive and replicate inside the cells. This phenomenon has been previously reported (Campos-Múzquiz et al. 2019). These could be explained by *Salmonella* capability adaptation to intracellular niche (Larock et al. 2015) or by an immune stimulation that results in bacteria elimination. Furthermore, when *C. fetus* subsp. *fetus* internalization was inhibited, the IL-1 β expression was halved. These results showed that *C. fetus* has been recognized intracellularly and that this recognition was required to induce higher inflammation and cellular mechanisms to eliminate the intracellular bacteria.

The results obtained in this study show a decrease in IL-1 β expression through time. Stephenson et al. (2014) showed that *C. jejuni* flagellum binds to Siglec-10 of dendritic cells and increases IL-10 expression. This molecule has been described in human uterine cells (Sammar et al. 2016) but not in bovine endometrial cells. More studies are necessary to evaluate if the reduction of IL-1 β was mediated by this molecule or only by infection control in the endometrial cells.

The pattern expression of IL-8 was like that of IL-1 β , suggesting that *C. fetus* subsp. *fetus* infection promotes early neutrophil recruitment (Foley et al. 2012). In epithelial cell lines IPEC-J2 and IPI-2I, a high IL-8 expression was shown in response to *S. Typhimurium* LPS (Arce et al. 2010a), suggesting a prompt recognition by cells. The decrease of IL-8 also is due to an IL-10 increase described for IL-1 β (Méndez-Samperio et al. 2002) or IFN- γ upregulation since it represses genes involved in leukocyte recruitment (Hoeksema et al. 2015). Moreover, when *C. fetus* subsp. *fetus* internalization was inhibited, the expression of IL-8 was not altered, indicating that the external sensing and not the bacteria's internalization induce polymorphonuclear recruitment (Takeuchi and Akira 2010).

Unlike our observation on IL-1 β and IL-8 expression, IFN- γ showed an inverse pattern that increased over time in *C. fetus* subsp. *fetus* infected cells. These results are related to the studies observed in INT-407 cells infected with *C. jejuni* in which IFN- γ peak was recorded at 12 hours post stimulation (Al-Amri et al. 2008). IFN- γ alters epithelial barrier function during inflammation by disrupting tight cell junctions and increasing permeability in polarized epithelial cells, which leads to cytosolic translocation of occludins and claudins (Bruewer et al. 2005). The increment of IFN- γ expression could be used by *C. fetus* subsp. *fetus* to invade submucosae.

In the presence of IFN- γ , *C. jejuni* was able to translocate across the monolayer more efficiently than in the absence of IFN- γ . This IFN- γ expression suggests also that epithelial cells from the endometrium might be associated with macrophage and adaptive immunity activation in campylobacteriosis (Hoeksema et al. 2015).

On the other hand, IFN- γ expression showed a slight increase when cells were treated with cytochalasin D. This could be due to a synergistic effect of *C. fetus* subsp. *fetus* sensing and *Campylobacter* toxins, for example, cytolethal distending toxin, which alters DNA (Rees et al. 2008). It has been reported before that cytochalasin D activates the p53 transcriptional factor, which controls DNA damage stress signaling (Rubtsova et al. 1998); however, more research is necessary to describe this phenomenon. The expression of IFN- γ in the cells infected with *S. enterica* subsp. *enterica* serovar Pullorum was non-significant. These results are not surprising since *Salmonella* possesses an immune response modulator IpaJ that decreases IFN- γ expression in macrophage cell line HD11 (Yin et al. 2018). Also, the principal sources of IFN- γ during *Salmonella* spp. infection are the neutrophils and NK cells (Pham and McSorley 2015).

In the cells infected with *S. Typhimurium* or *C. fetus* subsp. *fetus*, TNF- α expression did not change. A similar phenomenon was reported by Cronin et al. (2012) in bovine endometrial epithelial cells challenged with lipopolysaccharide. The same result was observed in bovine endometrial epithelial cells challenged with the danger-associated molecular patterns (DAMPs) (Healy et al. 2014). The TNF- α expression in these cells was possibly due to different conditions since the endometrium's primary function is blastocyst implantation (Kaneko et al. 2013).

In conclusion, the present study examined the proinflammatory response to *C. fetus* subsp. *fetus* in bovine endometrial epithelial cells. These bovine endometrial epithelial cells were able to recognize *C. fetus* subsp. *fetus* resulting in early proinflammatory response. Additionally, the internalization of the bacteria was necessary to induce IL-1 β expression but not IL-8, suggesting the

importance of intracellular *C. fetus* subsp. *fetus* recognition. Their inability to survive inside of epithelial cells, the early induction of cytokines, and the upregulation of IFN- γ imply that the principal pathogenesis mechanism of *C. fetus* subsp. *fetus* in the uterine cavity is only to pass through the epithelium. This movement induces an inflammatory response that alters the tight junctions, as demonstrated in human HT-29/B6 and Caco-2 cells (Baker et al. 2010, Bückner et al. 2017).

ORCID

Lizeth Guadalupe Campos-Múzquiz

<https://orcid.org/0000-0002-7507-0885>

Estela Teresita Méndez-Olvera

<https://orcid.org/0000-0003-4490-0863>

Monika Palacios Martínez

<https://orcid.org/0000-0001-6777-9918>

Daniel Martínez-Gomez <https://orcid.org/0000-0001-8051-8210>

Acknowledgments

We are grateful with Doctorado en Ciencias Agropecuarias and Temamantla slaughterhouse for providing facilities. This work was supported by Universidad Autónoma Metropolitana, Unidad Xochimilco and by Consejo Nacional de Ciencia y Tecnología, México (CONACYT- becario 469811).

Conflict of interest

The authors do not report any financial or personal connections with other persons or organizations, which might negatively affect the contents of this publication and/or claim authorship rights to this publication.

Literature

- Al-Amri AI, Botta GA, Tabbara KS, Ismael AY, Al-Mahmeed AE, Qareeballa AY, Bin Dayna KM, Bakhiet MO. *Campylobacter jejuni* induces diverse kinetics and profiles of cytokine genes in INT-407 cells. Saudi Med J. 2008 Apr;29(4):514–519.
- Al-Salloom FS, Al Mahmeed A, Ismael A, Botta GA, Bakhiet M. *Campylobacter*-stimulated INT407 cells produce dissociated cytokine profiles. J Infect. 2003 Oct;47(3):217–224. [https://doi.org/10.1016/S0163-4453\(03\)00076-8](https://doi.org/10.1016/S0163-4453(03)00076-8)
- Amjadi F, Salehi E, Mehdizadeh M, Aflatoonian R. Role of the innate immunity in female reproductive tract. Adv Biomed Res. 2014 Jan 9;3:1. <https://doi.org/10.4103/2277-9175.124626>
- Arce C, Ramírez-Boo M, Lucena C, Garrido JJ. Innate immune activation of swine intestinal epithelial cell lines (IPEC-J2 and IPI-2I) in response to LPS from *Salmonella typhimurium*. Comp Immunol Microbiol Infect Dis. 2010a Mar;33(2):161–174. <https://doi.org/10.1016/j.cimid.2008.08.003>
- Arce RM, Diaz PI, Barros SP, Galloway P, Bobetsis Y, Threadgill D, Offenbacher S. Characterization of the invasive and inflammatory traits of oral *Campylobacter rectus* in a murine model of fetoplacental growth restriction and in trophoblast cultures. J Reprod Immunol. 2010b Mar;84(2):145–153 <https://doi.org/10.1016/j.jri.2009.11.003>
- Baker NT, Graham LL. *Campylobacter fetus* translocation across Caco-2 cell monolayers. Microb Pathog. 2010 Nov;49(5):260–272. <https://doi.org/10.1016/j.micpath.2010.06.008>
- Blaser MJ, Smith PF, Hopkins JA, Heinzer I, Bryner JH, Wang WL. Pathogenesis of *Campylobacter fetus* infections: serum resistance associated with high-molecular-weight surface proteins. J Infect Dis. 1987 Apr;155(4):696–706. <https://doi.org/10.1093/infdis/155.4.696>
- Blaser MJ. Role of the S-layer proteins of *Campylobacter fetus* in serum-resistance and antigenic variation: a model of bacterial pathogenesis. Am J Med Sci. 1993 Nov;306(5):325–329. <https://doi.org/10.1097/00000441-199311000-00011>
- Botteldoorn N, Van Coillie E, Grijspeerd K, Werbrouck H, Haesebrouck F, Donné E, D'Haese E, Heyndrickx M, Pasmans F, Herman L. Real-time reverse transcription PCR for the quantification of the *mntH* expression of *Salmonella enterica* as a function of growth phase and phagosome-like conditions. J Microbiol Methods. 2006 Jul;66(1):125–135. <https://doi.org/10.1016/j.mimet.2005.11.003>
- Bruwer M, Utech M, Ivanov AI, Hopkins AM, Parkos CA, Nusrat A. Interferon-gamma induces internalization of epithelial tight junction proteins via a macropinocytosis-like process. FASEB J. 2005 Jun;19(8):923–933. <https://doi.org/10.1096/fj.04-3260com>
- Bryant CE, Orr S, Ferguson B, Symmons MF, Boyle JP, Monie TP. International Union of Basic and Clinical Pharmacology. XCVI. Pattern recognition receptors in health and disease. Pharmacol Rev. 2015;67(2):462–504. <https://doi.org/10.1124/pr.114.009928>
- Bückner R, Krug SM, Fromm A, Nielsen HL, Fromm M, Nielsen H, Schulzke JD. *Campylobacter fetus* impairs barrier function in HT-29/B6 cells through focal tight junction alterations and leaks. Ann N Y Acad Sci. 2017 Oct;1405(1):189–201. <https://doi.org/10.1111/nyas.13406>
- Cagnoli CI, Chiapparrone ML, Cacciato CS, Rodríguez MG, Aller JF, Catena MDC. Effects of *Campylobacter fetus* on bull sperm quality. Microb Pathog. 2020 Dec;149:104486. <https://doi.org/10.1016/j.micpath.2020.104486>
- Campos-Múzquiz LG, Méndez-Olvera ET, Arellano-Reynoso B, Martínez-Gómez D. *Campylobacter fetus* is internalized by bovine endometrial epithelial cells. Pol J Microbiol. 2019;68(2):217–224. <https://doi.org/10.33073/pjm-2019-022>
- Cipolla AL, Casaro AP, Terzolo HR, Estela ES, Brooks BW, Garcia MM. Persistence of *Campylobacter fetus* subspecies venerealis in experimentally infected heifers. Vet Rec. 1994 Jun 11;134(24):628. <https://doi.org/10.1136/vr.134.24.628>
- Cronin JG, Turner ML, Goetze L, Bryant CE, Sheldon IM. Toll-like receptor 4 and MYD88-dependent signaling mechanisms of the innate immune system are essential for the response to lipopolysaccharide by epithelial and stromal cells of the bovine endometrium. Biol Reprod. 2012 Feb 29;86(2):1–9. <https://doi.org/10.1095/biolreprod.111.092718>
- Eucker TP, Samuelson DR, Hunzicker-Dunn M, Konkel ME. The focal complex of epithelial cells provides a signalling platform for interleukin-8 induction in response to bacterial pathogens. Cell Microbiol. 2014 Sep;16(9):1441–1455. <https://doi.org/10.1111/cmi.12305>
- Fogg GC, Yang LY, Wang E, Blaser MJ. Surface array proteins of *Campylobacter fetus* block lectin-mediated binding to type A lipopolysaccharide. Infect Immun. 1990 Sep;58(9):2738–2744. <https://doi.org/10.1128/IAI.58.9.2738-2744.1990>
- Foley C, Chapwanya A, Creevey CJ, Narciandi F, Morris D, Kenny EM, Cormican P, Callanan JJ, O'Farrelly C, Meade KG. Global endometrial transcriptomic profiling: transient immune activation precedes tissue proliferation and repair in healthy beef cows. BMC Genomics. 2012 Sep 18;13:489. <https://doi.org/10.1186/1471-2164-13-489>
- Healy LL, Cronin JG, Sheldon IM. Endometrial cells sense and react to tissue damage during infection of the bovine endometrium via interleukin 1. Sci Rep. 2014 Nov 14;4:7060. <https://doi.org/10.1038/srep07060>
- Hoeksema MA, Scicluna BP, Boshuizen MC, van der Velden S, Neele AE, Van den Bossche J, Matlung HL, van den Berg TK, Goossens P, de Winther MP. IFN- γ priming of macrophages represses a part of the inflammatory program and attenuates neutrophil recruitment. J Immunol. 2015 Apr 15;194(8):3909–3916. <https://doi.org/10.4049/jimmunol.1402077>

- Hu GQ, Song PX, Chen W, Qi S, Yu SX, Du CT, Deng XM, Ouyang HS, Yang YJ. Critical role for *Salmonella* effector SopB in regulating inflammasome activation. *Mol Immunol*. 2017 Oct;90:280–286. <https://doi.org/10.1016/j.molimm.2017.07.011>
- Iraola G, Hernández M, Calleros L, Paolicchi F, Silveyra S, Velilla A, Carretto L, Rodríguez E, Pérez R. Application of a multiplex PCR assay for *Campylobacter fetus* detection and subspecies differentiation in uncultured samples of aborted bovine fetuses. *J Vet Sci*. 2012 Dec;13(4):371–376. <https://doi.org/10.4142/jvs.2012.13.4.371>
- Iwasaki A, Medzhitov R. Control of adaptive immunity by the innate immune system. *Nat Immunol*. 2015 Apr;16(4):343–353. <https://doi.org/10.1038/ni.3123>
- Kaneko Y, Day ML, Murphy CR. Uterine epithelial cells: Serving two masters. *Int J Biochem Cell Biol*. 2013 Feb;45(2):359–363. <https://doi.org/10.1016/j.biocel.2012.10.012>
- Kienesberger S, Sprenger H, Wolgruber S, Halwachs B, Thalinger GG, Perez-Perez GI, Blaser MJ, Zechner EL, Gorkiewicz G. Comparative genome analysis of *Campylobacter fetus* subspecies revealed horizontally acquired genetic elements important for virulence and niche specificity. *PLoS One*. 2014 Jan 9;9(1):e85491. <https://doi.org/10.1371/journal.pone.0085491>
- LaRock DL, Chaudhary A, Miller SI. Salmonellae interactions with host processes. *Nat Rev Microbiol*. 2015 Apr;13(4):191–205. <https://doi.org/10.1038/nrmicro3420>
- Livak KJ, Schmittgen TD. Analysis of relative gene expression data using real-time quantitative PCR and the $2^{-\Delta\Delta C_T}$ method. *Methods*. 2001;25(4):402–408. <https://doi.org/10.1006/meth.2001.1262>
- Man SM, Kaakoush NO, Leach ST, Nahidi L, Lu HK, Norman J, Day AS, Zhang L, Mitchell HM. Host attachment, invasion, and stimulation of proinflammatory cytokines by *Campylobacter concisus* and other non-*Campylobacter jejuni* *Campylobacter* species. *J Infect Dis*. 2010 Dec 15;202(12):1855–1865. <https://doi.org/10.1086/657316>
- Méndez-Samperio P, García E, Vázquez A, Palma J. Regulation of interleukin-8 by interleukin-10 and transforming growth factor beta in human monocytes infected with *Mycobacterium bovis*. *Clin Diagn Lab Immunol*. 2002 Jul;9(4):802–807. <https://doi.org/10.1128/cdli.9.4.802-807.2002>
- Moran AP, Penner JL, Aspinall GO. *Campylobacter* lipopolysaccharides. In: Nachamkin I, Blaser M, editors. *Campylobacter*. 2nd ed. Washington DC (USA): ASM Press; 2002.
- Mshelia GD, Amin JD, Woldehiwet Z, Murray RD, Egwu GO. Epidemiology of bovine venereal campylobacteriosis: geographic distribution and recent advances in molecular diagnostic techniques. *Reprod Domest Anim*. 2010 Oct;45(5):e221–e230. <https://doi.org/10.1111/j.1439-0531.2009.01546.x>
- Pham OH, McSorley SJ. Protective host immune responses to *Salmonella* infection. *Future Microbiol*. 2015;10(1):101–110. <https://doi.org/10.2217/fmb.14.98>
- Preston MA, Penner JL. Structural and antigenic properties of lipopolysaccharides from serotype reference strains of *Campylobacter jejuni*. *Infect Immun*. 1987 Aug;55(8):1806–1812. <https://doi.org/10.1128/IAI.55.8.1806-1812.1987>
- Rees LE, Cogan TA, Dodson AL, Birchall MA, Bailey M, Humphrey TJ. *Campylobacter* and IFN γ interact to cause a rapid loss of epithelial barrier integrity. *Inflamm Bowel Dis*. 2008 Mar;14(3):303–309. <https://doi.org/10.1002/ibd.20325>
- Rolhion N, Furniss RC, Grabe G, Ryan A, Liu M, Matthews SA, Holden DW. Inhibition of nuclear transport of NF- κ B p65 by the *Salmonella* Type III secretion system effector SpvD. *PLoS Pathog*. 2016 May 27;12(5):e1005653. <https://doi.org/10.1371/journal.ppat.1005653>
- Rubtsova SN, Kondratov RV, Kopnin PB, Chumakov PM, Kopnin BP, Vasiliev JM. Disruption of actin microfilaments by cytochalasin D leads to activation of p53. *FEBS Lett*. 1998 Jul 3;430(3):353–357. [https://doi.org/10.1016/s0014-5793\(98\)00692-9](https://doi.org/10.1016/s0014-5793(98)00692-9)
- Salama SM, Newnham E, Chang N, Taylor DE. Genome map of *Campylobacter fetus* subsp. *fetus* ATCC 27374. *FEMS Microbiol Lett*. 1995 Oct 15;132(3):239–245. [https://doi.org/10.1016/0378-1097\(95\)00316-w](https://doi.org/10.1016/0378-1097(95)00316-w)
- Sammar M, Siwetz M, Meiri H, Fleming V, Altevogt P, Hupertz B. Expression of CD24 and Siglec-10 in first trimester placenta: implications for immune tolerance at the fetal-maternal interface. *Histochem Cell Biol*. 2017 May;147(5):565–574. <https://doi.org/10.1007/s00418-016-1531-7>
- Schmittgen TD, Livak KJ. Analyzing real-time PCR data by the comparative C(T) method. *Nat Protoc*. 2008;3(6):1101–1108. <https://doi.org/10.1038/nprot.2008.73>
- Shaughnessy RG, Meade KG, Cahalane S, Allan B, Reiman C, Callanan JJ, O'Farrelly C. Innate immune gene expression differentiates the early avian intestinal response between *Salmonella* and *Campylobacter*. *Vet Immunol Immunopathol*. 2009 Dec 15;132(2–4):191–198. <https://doi.org/10.1016/j.vetimm.2009.06.007>
- Skarzynski DJ, Miyamoto Y, Okuda K. Production of prostaglandin F $_{2\alpha}$ by cultured bovine endometrial cells in response to tumor necrosis factor α : cell type specificity and intracellular mechanisms. *Biol Reprod*. 2000 May;62(5):1116–1120. <https://doi.org/10.1095/biolreprod62.5.1116>
- Stephenson HN, Mills DC, Jones H, Milioris E, Copland A, Dorrell N, Wren BW, Crocker PR, Escors D, Bajaj-Elliott M. Pseudaminic acid on *Campylobacter jejuni* flagella modulates dendritic cell IL-10 expression via Siglec-10 receptor: a novel flagellin-host interaction. *J Infect Dis*. 2014 Nov 1;210(9):1487–1498. <https://doi.org/10.1093/infdis/jiu287>
- Takeuchi O, Akira S. Pattern recognition receptors and inflammation. *Cell*. 2010 Mar 19;140(6):805–820. <https://doi.org/10.1016/j.cell.2010.01.022>
- Turner ML, Cronin JG, Healey GD, Sheldon IM. Epithelial and stromal cells of bovine endometrium have roles in innate immunity and initiate inflammatory responses to bacterial lipopeptides *in vitro* via Toll-like receptors TLR2, TLR1, and TLR6. *Endocrinology*. 2014 Apr;155(4):1453–1465. <https://doi.org/10.1210/en.2013-1822>
- Vandesompele J, De Preter K, Pattyn F, Poppe B, Van Roy N, De Paepe A, Speleman F. Accurate normalization of real-time quantitative RT-PCR data by geometric averaging of multiple internal control genes. *Genome Biol*. 2002 Jun 18;3(7):research0034. <https://doi.org/10.1186/gb-2002-3-7-research0034>
- Viejo G, Gomez B, De Miguel D, Del Valle A, Otero I, De La Iglesia P. *Campylobacter fetus* subspecies *fetus* bacteremia associated with chorioamnionitis and intact fetal membranes. *Scand J Infect Dis*. 2001;33(2):126–127. <https://doi.org/10.1080/003655401750065517>
- Wang B, Kraig E, Kolodrubetz D. Use of defined mutants to assess the role of the *Campylobacter rectus* S-layer in bacterium-epithelial cell interactions. *Infect Immun*. 2000 Mar;68(3):1465–1473. <https://doi.org/10.1128/iai.68.3.1465-1473.2000>
- Yin C, Xu L, Li Y, Liu Z, Gu D, Li Q, Jiao X. Construction of pSPI12-cured *Salmonella enterica* serovar Pullorum and identification of IpaJ as an immune response modulator. *Avian Pathol*. 2018 Aug;47(4):410–417. <https://doi.org/10.1080/03079457.2018.1471195>
- Yu ZT, Nanthakumar NN, Newburg DS. The human milk oligosaccharide 2'-fucosyllactose quenches *Campylobacter jejuni*-induced inflammation in human epithelial cells HEp-2 and HT-29 and in mouse intestinal mucosa. *J Nutr*. 2016 Oct;146(10):1980–1990. <https://doi.org/10.3945/jn.116.230706>
- Zheng J, Meng J, Zhao S, Singh R, Song W. *Campylobacter*-induced interleukin-8 secretion in polarized human intestinal epithelial cells requires *Campylobacter*-secreted cytolethal distending toxin- and Toll-like receptor-mediated activation of NF- κ B. *Infect Immun*. 2008 Oct;76(10):4498–4508. <https://doi.org/10.1128/IAI.01317-07>

Clonal Dissemination of KPC-2, VIM-1, OXA-48-Producing *Klebsiella pneumoniae* ST147 in Katowice, Poland

DOROTA OCHOŃSKA¹, HANNA KLAMIŃSKA-CEBULA², ANNA DOBRUT¹, MAŁGORZATA BULANDA¹
and MONIKA BRZYCHCZY-WŁOCH^{1*} 

¹Department of Molecular Medical Microbiology, Chair of Microbiology, Faculty of Medicine,
Jagiellonian University Medical College, Krakow, Poland

²Department of Bacteriology, Leszek Giec Upper-Silesian Medical Centre of the Silesian
Medical University in Katowice, Katowice, Poland

Submitted 27 October 2020, revised 4 February 2021, accepted 8 February 2021

Abstract

Carbapenem-resistant *Klebsiella pneumoniae* (CRKP) is an important bacterium of nosocomial infections. In this study, CRKP strains, which were mainly isolated from fecal samples of 14 patients in three wards of the hospital in the Silesia Voivodship, rapidly increased from February to August 2018. Therefore, we conducted microbiological and molecular studies of the CRKP isolates analyzed. Colonized patients had critical underlying diseases and comorbidities; one developed bloodstream infection, and five died (33.3%). Antibiotic susceptibilities were determined by the E-test method. A disc synergy test confirmed carbapenemase production. CTX-Mplex PCR evaluated the presence of resistance genes *bla*_{CTX-M-type}, *bla*_{CTX-M-1}, *bla*_{CTX-M-9}, and the genes *bla*_{SHV}, *bla*_{TEM}, *bla*_{KPC-2}, *bla*_{NDM-1}, *bla*_{OXA-48}, *bla*_{IMP}, and *bla*_{VIM-1} was detected with the PCR method. Clonality was evaluated by Multi Locus Sequence Typing (MLST) and Pulsed Field Gel Electrophoresis (PFGE). Six (40%) strains were of XDR (Extensively Drug-Resistant) phenotype, and nine (60%) of the isolates exhibited MDR (Multidrug-Resistant) phenotype. The range of carbapenem minimal inhibitory concentrations (MICs, µg/mL) was as follows doripenem (16 to >32), ertapenem (>32), imipenem (4 to >32), and meropenem (>32). PCR and sequencing confirmed the *bla*_{CTX-M-15}, *bla*_{KPC-2}, *bla*_{OXA-48}, and *bla*_{VIM-1} genes in all strains. The isolates formed one large PFGE cluster (clone A). MLST assigned them to the emerging high-risk clone of ST147 (CC147) pandemic lineage harboring the *bla*_{OXA-48} gene. This study showed that the *K. pneumoniae* isolates detected in the multi-profile medical centre in Katowice represented a single strain of the microorganism spreading in the hospital environment.

Key words: clonal dissemination, carbapenem-resistant *Klebsiella pneumoniae*, hospital, PFGE, MLST

Introduction

Klebsiella pneumoniae is a critical multidrug-resistant (MDR) bacterium in humans responsible for numerous hospital infections linked to high morbidity and mortality since treatment options are limited (Navon-Venezia et al. 2017). *K. pneumoniae* from the family *Enterobacteriaceae*, occurs in the human and animal gastrointestinal tract microbiome. It is a commonly found opportunistic pathogen associated with the hospital environment and, overall, accountable for approximately a third of all Gram-negative infections. It has a role in extraintestinal infections, such as urinary tract infections, pneumonia, surgical site infections, cystitis, and life-threatening infections, including endo-

carditis and septicemia. It is also a significant cause of severe community-onset infections, such as necrotizing pneumonia, endogenous endophthalmitis, and pyogenic liver abscesses (Podschun and Ullmann 1998).

With the ever-growing antibiotic resistance, *K. pneumoniae* is a pathogen recognized for its antibiotic resistance; hence, it is categorized as an ESKAPE organism, besides other essential MDR pathogens (Boucher et al. 2009). The accumulation of ARGs by *K. pneumoniae*, by de novo mutations, is continuous under antibiotic selective pressure, and through the acquisition of plasmids and transferable genetic elements, it stimulates extensively drug-resistant (XDR) strains harboring a 'super resistome'. In the past twenty years, many high-risk (HiR) MDR and XDR *K. pneumoniae* sequence

* Corresponding author: M. Brzychczy-Włoch, Department of Molecular Medical Microbiology, Chair of Microbiology, Faculty of Medicine, Jagiellonian University Medical College, Krakow, Poland; e-mail: mbrzych@cm-uj.krakow.pl

© 2021 Dorota Ochońska et al.

This work is licensed under the Creative Commons Attribution-NonCommercial-NoDerivatives 4.0 License (<https://creativecommons.org/licenses/by-nc-nd/4.0/>).

types have appeared that exhibit great capacity of causing multicontinental outbreaks and continued global dissemination (Navon-Venezia et al. 2017).

Currently, the spread of carbapenem-resistant *K. pneumoniae* (CRKP) has become a severe problem in the molecular epidemiology of hospital infections.

Frequently, carbapenems serve as the last resort in the effective treatment of serious infections caused by multidrug-resistant bacteria. Enzymes that hydrolyze carbapenems, called carbapenemases, are the major cause of carbapenem resistance (Matsumura et al. 2017). The molecular classes A, B, and D carbapenemases are rapidly disseminated worldwide, challenging the treatment of Gram-negative infections (Nordmann and Poirel 2014). Recent reports have demonstrated that various carbapenem-hydrolyzing enzymes are disseminated worldwide in CRKP isolates. The fast evolution of carbapenem resistance quickly evolved in *Enterobacteriaceae* in the past decade and became a developing global threat. The majority of studies on antibiotic-resistant *K. pneumoniae* focus on characterizing carbapenemase producers (KPC, NDM, VIM, and OXA-48), various clonal groups or complexes (e.g., CG15, CG17, CG258, or CC147), and epidemic plasmids (IncA/C, IncFII, IncL/M, and IncN) that have been suggested to participate in their global expansion (Nordmann and Poirel 2014). Carbapenemase co-producers have been reported in distinct geographic locations: European countries (France, Germany, Greece, Italy, and Poland), Israel, the United States, China, and West Asia (Turkey) (Baraniak et al. 2011; Nordmann and Poirel 2014; Baraniak et al. 2015; Guo et al. 2016; Lee et al. 2016; Zautner et al. 2017; Bukavaz et al. 2018).

The majority of KPC-producing microorganisms also express β -lactamases and possess genes conferring resistance to other antimicrobials, i.e. aminoglycosides, fluoroquinolones, or co-trimoxazole (Nordmann and Poirel 2014). The resistance rates vary significantly across countries; MDR *K. pneumoniae* is endemic in Mediterranean countries, and Eastern and South-Western Europe. It stems from ES β L production in more than 50–60% strains, and non-susceptibility to third-generation cephalosporins, fluoroquinolones, and aminoglycosides (Navon-Venezia et al. 2017).

In 2011, the National Reference Center for Susceptibility Testing (NRCTS) and the KPC-PL Study Group published the first report from Poland that presented the molecular characteristics of *K. pneumoniae* producing KPC carbapenemases (Baraniak et al. 2011). Between 2011 and 2015, the bacteria caused 1,067 infection outbreaks; among them, 123 were caused by *K. pneumoniae*, and a higher number of outbreaks were reported from Masovian and Silesian voivodships (Baraniak et al. 2011). Poland belongs to the countries of the highest rate of *K. pneumoniae*

isolates' resistance to all groups of drugs subjected to monitoring, and these rates are twice as high as elsewhere in the European Union (EU)/European Economic Area (EEA). In these countries, resistant *K. pneumoniae* isolates consist on average 20.5% of all MDR multidrug-resistant strains (Bukavaz et al. 2018).

Given the abovementioned data and the increased frequency of isolation of CRKP strains from the hospital environment, we conducted a microbiological and molecular characterization of carbapenem-resistant *K. pneumoniae* isolates with emphasis on the antibiotic resistance profile, identification of ES β L genes, detection of carbapenemase genes, and the isolates' genetic relationship.

Experimental

Materials and Methods

Hospital settings and sample collection. The study was performed in the Upper-Silesian Medical Centre of the Silesian Medical University in Katowice (GCM), one of the largest multi-profile medical centres, and one of the largest hospitals in Poland. The hospital consists of 24 departments and treats over 160 thousand patients per year. Between February and August 2018, 15 non-duplicate CRKP isolates were collected from fecal samples of 14 patients admitted to three hospital wards characterized below. The Department of Neurology with the Stroke Sub-department (NR) receives 1,750 admissions per year and has 14 rooms with 44 beds; the Department of Internal Medicine and Rheumatology (REU) receives 1,935 admissions per year and has 12 rooms with 37 beds, and the Department of Anaesthesia and Intensive Care (OAIT) receives 1,750 admissions per year and has five rooms with ten beds (Table I). A total of 505 *Enterobacteriaceae* isolates were obtained from the patients in these wards over one-year.

Bacterial identification, antimicrobial susceptibility testing and phenotypic screening. Bacterial identification and preliminary susceptibility testing were performed using the automated VITEK[®] 2 Compact System (bioMérieux, France). The MICs of the 23 antimicrobial agents were evaluated with E-test strips (AB BIODISK, bioMérieux, France). MIC value results were interpreted according to the EUCAST breakpoints (EUCAST 2019). All isolates were screened phenotypically for the presence of KPC-, OXA-48-, and metallo- β -lactamases (MBL). Double-disc synergy tests (DDST) were carried out to confirm ES β L production (CLSI 2018) and to detect MBL production, as published previously (Matsumura et al. 2017). The phenotypic detection of KPC-producing isolates was assessed

Table I
Demographic data and characteristics of the fourteen patients with *K. pneumoniae* co-producing KPC-2, OXA-48, VIM-1 and CTX-M-15 during the outbreak

Patient ID/ Isolate no.	Age (years) /sex	Hospital ward(s)	Date of isolation	Type of specimen	Status (type) of colonization/infection	Duration of hospitalization (days)	Underlying conditions	Antimicrobial used prior to isolation of carbapenemase producer(s)	Antimicrobial used as treatment for infections	Outcome Alive/Dead
3	74/M	OAIT	08/03/2018	Rectal swab	Colonization	03/01–14/04/2018 (102 days)	Abdominal Aortic Aneurysm (AAA)	Ciprofloxacin + Gentamycin + Itraconazole	Metronidazole	Dead
6965	60/F	OAIT	28/02/2018	Rectal swab	Colonization	08/02–01/04/2018 (53 days)	Tuberculosis, Chronic Obstructive Pulmonary Disease (COPD)	Colistin + Voriconazole	–	Dead
6976/1 6976/2	45/M	OAIT	01/03/2018 12/03/2018	Rectal swab Blood	Colonization Bacteremia	21/02–29/03/2018 (37 days)	Guillain–Barré Syndrome (GBS)	Colistin + Linezolid	Ampicillin/sulbactam + Amikacin	Alive
1	67/F	OAIT	07/03/2018	Rectal swab	Colonization	02/03–29/06/2018 (112 days)	COPD, diabetes, hypertension	Ceftriaxone + Levofloxacin	–	Dead
6968 (index case)	63/M	NR	28/02/2018	Rectal swab	Colonization	16/02–31/03/2018 (44 days)	Hypertension, atherosclerosis	Ceftriaxone + Metronidazole	–	Alive
2	69/M	NR	07/03/2018	Rectal swab	Colonization	23/02–28/03/2018 (34 days)	Post-stroke conditions	–	–	Alive
4	43/M	NR	08/03/2018	Rectal swab	Colonization	26/02–12/03/2018 (15 days)	Hypertension	Ceftriaxone + Metronidazole	–	Dead
154/25428	61/M	NR	30/07/2018	Rectal swab	Colonization	04/07–06/08/2018 (34 days)	Stroke	–	–	Dead
7/25804	70/M	NR	04/08/2018	Rectal swab	Colonization	25/07–02/08/2018 (9 days)	Stroke	Amoxicillin/clavulanic acid	–	Alive
11/25808	50/F	NR	04/08/2018	Rectal swab	Colonization	23/07–03/08/2018 (12 days)	Stroke	–	–	Alive
13/25810	77/M	NR	04/08/2018	Rectal swab	Colonization	22/07–09/08/2018 (19 days)	Hypertension, ischemic heart disease	Amoxicillin/clavulanic acid	–	Alive
6	70/F	REU	09/03/2018	Rectal swab	Colonization	26/02–14/03/2018 (17 days)	Diabetes, metastatic lung cancer	–	–	Alive
7	78/F	REU	09/03/2018	Rectal swab	Colonization	27/02–16/03/2018 (18 days)	Rheumatoid Arthritis (RA), hemorrhagic diathesis, coronary disease, peptic ulcer disease, hypertension, atherosclerosis, gout	Imipenem	Vancomycin	Alive
5	90/F	REU	08/03/2018	Rectal swab	Colonization	03.03–17.03.2018 (14 days)	Atherosclerosis, acute arterial thrombosis of the lower extremity	Meropenem + Amikacin	–	Alive

F – Female; M – male; NR – Department of Neurology with the Stroke Subdepartment; OAIT – Department of Anaesthesiology and Intensive Care; REU – Department of Internal Medicine and Rheumatology

by an available protocol (Doi et al. 2008). According to the protocol, the boronic acid combined-disk tests using meropenem (10 µg) as the antibiotic substrate and 3-aminophenylboronic acid (3-APBA) (300 g, Sigma-Aldrich) as the inhibitor of KPC production was used. The detection of OXA-48 was performed in line with the EUCAST guidelines (Shaker et al. 2018). MDR and XDR were defined according to a standardized international document (Magiorakos et al. 2012).

Extended-spectrum β-lactamase genes (ESβLs) identification. Polymerase chain reaction (PCR), as described by Caltagirone et al. (2017) was used to determine bla_{SHV} and bla_{TEM} . CTX-Mplex PCR was used to detect $bla_{CTX-M-type}$, $bla_{CTX-M-1}$, and $bla_{CTX-M-9}$ (Xu et al. 2005).

Carbapenemase genes detection. The existence of carbapenemase encoding genes (bla_{KPC-2} , bla_{NDM-1} , bla_{OXA-48} , bla_{IMP} and bla_{VIM-1}) was confirmed using the PCR method (Bukavaz et al. 2018).

PFGE. The genetic relatedness of isolates was investigated using the Pulsed Field Gel Electrophoresis (PFGE) method, following genomic DNA extraction and digestion with *Xba*I endonuclease (Fermentas, Lithuania), as described previously (Han et al. 2013). *Salmonella enterica* subsp. *enterica* serovar Braenderup strain H9812 (ATCC® BAA664™) and *K. pneumoniae* ATCC® BAA-1705™ were used as reference markers. PFGE banding patterns were compared using BioNumerics v.6.5 (Applied Maths, Belgium) software. The relatedness was determined by the unweighted pair group method using the average linkages (UPGMA), and the similarity of bands was calculated using the Dice coefficient.

MLST. Multilocus Sequence Typing (MLST) was conducted with the use of seven conserved housekeeping genes (*gapA*, *infB*, *mdh*, *pgi*, *phoE*, *rpoB*, and *tonB*) (Guo

et al. 2016). A complete protocol of the MLST procedure, including the allelic profile and sequence type (ST) assignment techniques, is available in MLST databases.

Results

Patients' characteristics. Patients' characteristics is presented in Table I. During seven months, the 15 *K. pneumoniae* isolates were collected from fourteen patients aged 65.5 years on average. The average duration of hospitalization was 37 days. All patients were found to be colonized by similar CRKP isolates. One patient developed a bloodstream infection (only blood isolate available) and was successfully treated with linezolid and colistin. Two of the improved patients were treated with carbapenem. Five patients died; their deaths were not associated with any particular etiology, though. CRKP strains were isolated at various stages of patients' hospital stay. An average time from patient admission to the microorganism isolation was 16 days; in patient no. 3 the corresponding period was 64 days, while in patients nos. 1 and 5 – the period was only five days. None of the patients had traveled abroad shortly before their hospital admissions, so any travel experience could explain the colonization.

Epidemiologic investigation. The studied *K. pneumoniae* isolates' epidemic curve exhibited a bimodal distribution of cases with two peaks separated by 148 days (Fig. 1). It could indicate double discrete periods (February-March 2018 and July-August 2018) with unobserved cases in January, April, May, and June. The NR ward was involved in these distinct periods. Following the index case, four new cases were registered in the OAIT, six cases in the NR, and three in the REU (Table I).

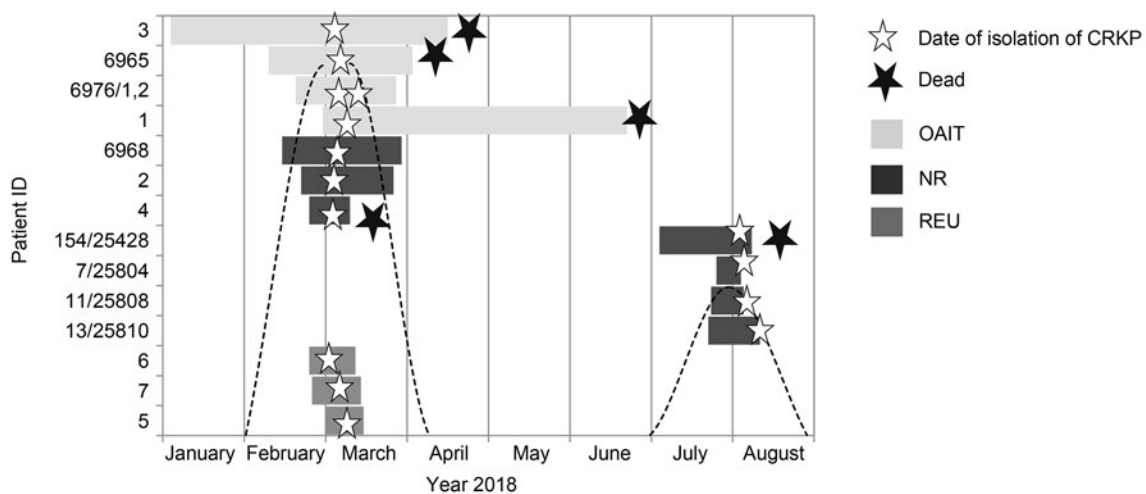


Fig. 1. Gantt diagram depicting a timeline of patients' admissions in relationship with the three wards and the length of stay in each ward. Epidemic curve based on the number of *K. pneumoniae* isolated in the time frame of the study.

Abbreviations: OAIT-Department of Anaesthesia and Intensive Care, NR-Department of Neurology with the Stroke Subdepartment, REU-Department of Internal Medicine and Rheumatology.

Antimicrobial resistance. The antimicrobial resistance profiles for the isolates are listed in Table II. We have classified nine (60%) strains as MDR and six (40%) as XDR. All isolates showed resistance to penicillins, cephalosporins, carbapenems (doripenem, ertapenem, meropenem), quinolone (ciprofloxacin), aminoglycosides (amikacin, gentamycin, netilmycin, tobramycin), and other antibiotics (aztreonam, trimethoprim/sulfamethoxazole, fosfomicin). Eleven isolates (73.3%) were sensitive to amikacin, two isolates (13.3%) were in the intermediate range with the MIC values equal to 12 µg/ml, and two isolates (13.3%) were resistant. Moreover, seven strains (42.8%) were resistant to tigecycline, five (35.7%) were in the intermediate range with the MIC values above 2 µg/ml. Interestingly, two isolates (13.3%) showed susceptibility to imipenem, and the resistance of one isolate (6.7%) to imipenem was within the intermediate range.

Phenotypic screening of carbapenemases and associated β-lactamases. In all *K. pneumoniae* isolates (n = 15, 100%), the ESβL mechanism was not found in phenotypic tests. Also, MBL production was not phenotypically detected in these isolates. However, all strains were positive for *K. pneumoniae* carbapenemase (KPC) production by the modified Hodge test (n = 15, 100%). In addition, phenotyping detection of carbapenem-resistant class D using the carbapenemase detection set with temocillin disc (30 µg) revealed that all isolates were positive for OXA-48 (n = 15, 100%).

β-lactamase genes detection. PCR amplification and sequencing analysis confirmed the presence of

*bla*_{KPC-2}, *bla*_{OXA-48}, *bla*_{VIM-1} in all 15 of the *K. pneumoniae* isolates. In addition, the only identified *bla*_{CTX-M} variant in all 15 strains was *bla*_{CTX-M-15}. The results are presented in Fig. 2. No isolate was found to be positive for *bla*_{SHV}, *bla*_{TEM}, *bla*_{NDM-1}, and *bla*_{IMP}.

Molecular epidemiology. Out of fifteen isolates concerned, all belonged to a single PFGE cluster (clone A) (Fig. 2).

Moreover, an MLST analysis allowed us to classify all isolates as the sequence type ST147 (allelic profile: 3-4-6-1-7-4-38) belonging to the CC147 clonal complex. It confirmed clonal relationships between the isolates.

Discussion

The presented work stems from the problem of clonal dissemination of KPC-2, VIM-1, and OXA-48-producing *K. pneumoniae* ST147 noticed in one hospital in Katowice, the Silesian Voivodeship, Poland.

K. pneumoniae belongs to Gram-negative bacteria of the family *Enterobacteriaceae*. The pathogens can easily cause hazardous epidemic outbreaks and spread globally in the form of clones with increased virulence and epidemicity. These features are associated with the widespread presence of *Enterobacteriaceae* in humans (gastrointestinal carriage) and their great importance as frequent infection etiologic agent in facilities that carry out inpatient and outpatient treatment (Navon-Venezia et al. 2017). Studies that focus on *K. pneumoniae* are therefore desired, as they provide vital scientific

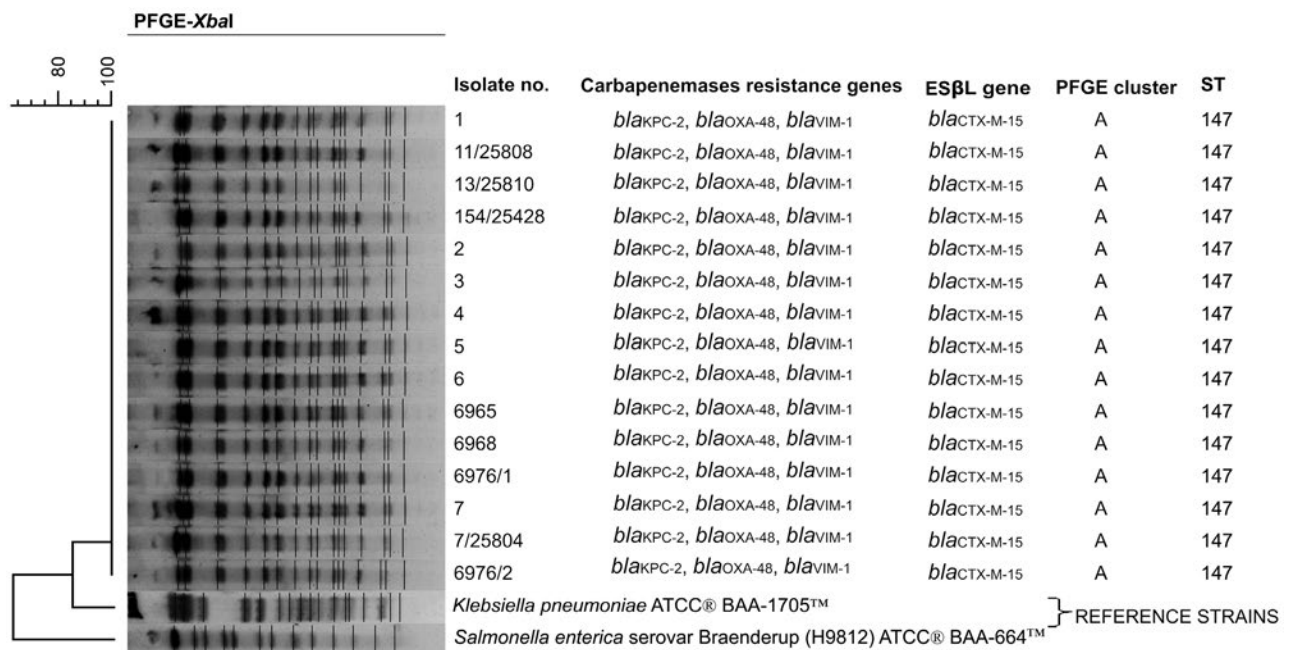


Fig. 2. Dendrogram of *Xba*I-digested genomic DNA from carbapenemase-co-producing *K. pneumoniae* isolates, additionally presenting the results of PCRs for genes encoding carbapenemases and other β-lactamase. PFGE settings: similarity coefficient, Dice; optimization, 1%; tolerance, 1%; clustering method, UPGMA.

Table II
Antimicrobial resistance profiles of the studied *K. pneumoniae* isolates.

Antibiotics:	Patient ID/Isolate no.		3		6965		6976/1		6976/2		1		6968		2		4		154/25428		7/25804		111/25808		13/25810		6		7		5	
	R/I/S	MIC (µg/ml)	R/I/S	MIC (µg/ml)	R/I/S	MIC (µg/ml)	R/I/S	MIC (µg/ml)	R/I/S	MIC (µg/ml)	R/I/S	MIC (µg/ml)	R/I/S	MIC (µg/ml)	R/I/S	MIC (µg/ml)	R/I/S	MIC (µg/ml)	R/I/S	MIC (µg/ml)	R/I/S	MIC (µg/ml)	R/I/S	MIC (µg/ml)	R/I/S	MIC (µg/ml)	R/I/S	MIC (µg/ml)	R/I/S	MIC (µg/ml)		
Penicillins		>256	R	>256	R	>256	R	>256	R	>256	R	>256	R	>256	R	>256	R	>256	R	>256	R	>256	R	>256	R	>256	R	>256	R	>256	R	
	Amoxicillin/Clavulanic acid	>256	R	>256	R	>256	R	>256	R	>256	R	>256	R	>256	R	>256	R	>256	R	>256	R	>256	R	>256	R	>256	R	>256	R	>256	R	
	Ampicillin	>256	R	>256	R	>256	R	>256	R	>256	R	>256	R	>256	R	>256	R	>256	R	>256	R	>256	R	>256	R	>256	R	>256	R	>256	R	
Cephalosporins	Cefaclor	>256	R	>256	R	>256	R	>256	R	>256	R	>256	R	>256	R	>256	R	>256	R	>256	R	>256	R	>256	R	>256	R	>256	R	>256	R	
	Cefuroxime	>256	R	>256	R	>256	R	>256	R	>256	R	>256	R	>256	R	>256	R	>256	R	>256	R	>256	R	>256	R	>256	R	>256	R	>256	R	
	Cefotaxime	>256	R	>256	R	>256	R	>256	R	>256	R	>256	R	>256	R	>256	R	>256	R	>256	R	>256	R	>256	R	>256	R	>256	R	>256	R	
	Cefotaxime/Cefotaxime + clavulanic acid	>16/>1	R	>16/>1	R	>16/>1	R	>16/>1	R	>16/>1	R	>16/>1	R	>16/>1	R	>16/>1	R	>16/>1	R	>16/>1	R	>16/>1	R	>16/>1	R	>16/>1	R	>16/>1	R	>16/>1	R	
	Ceftazidime	>256	R	>256	R	>256	R	>256	R	>256	R	>256	R	>256	R	>256	R	>256	R	>256	R	>256	R	>256	R	>256	R	>256	R	>256	R	
Carbapenems	Ceftazidime/Ceftazidime + clavulanic acid	>34/>4	R	>34/>4	R	>34/>4	R	>34/>4	R	>34/>4	R	>34/>4	R	>34/>4	R	>34/>4	R	>34/>4	R	>34/>4	R	>34/>4	R	>34/>4	R	>34/>4	R	>34/>4	R	>34/>4	R	
	Cefepime	>256	R	>256	R	>256	R	>256	R	>256	R	>256	R	>256	R	>256	R	>256	R	>256	R	>256	R	>256	R	>256	R	>256	R	>256	R	
	Doripenem	>32	R	>32	R	>32	R	>32	R	>32	R	>32	R	>32	R	>32	R	>32	R	>32	R	>32	R	>32	R	>32	R	>32	R	>32	R	
	Ertapenem	>32	R	>32	R	>32	R	>32	R	>32	R	>32	R	>32	R	>32	R	>32	R	>32	R	>32	R	>32	R	>32	R	>32	R	>32	R	
	Imipenem	>32	R	>32	R	>32	R	>32	R	>32	R	>32	R	>32	R	>32	R	>32	R	>32	R	>32	R	>32	R	>32	R	>32	R	>32	R	
Quinolone	Meropenem	>32	R	>32	R	>32	R	>32	R	>32	R	>32	R	>32	R	>32	R	>32	R	>32	R	>32	R	>32	R	>32	R	>32	R	>32	R	
	Ciprofloxacin	>32	R	>32	R	>32	R	>32	R	>32	R	>32	R	>32	R	>32	R	>32	R	>32	R	>32	R	>32	R	>32	R	>32	R	>32	R	
Aminoglycosides	Amikacin	4	S	8	S	12	R	8	S	4	S	4	S	8	S	8	S	8	S	8	S	8	S	8	S	8	S	8	S	8	S	
	Gentamycin	64	R	64	R	64	R	64	R	64	R	64	R	64	R	64	R	64	R	64	R	64	R	64	R	64	R	64	R	64	R	
	Netilmycin	128	R	4	I	64	R	64	R	128	R	16	R	16	R	16	R	16	R	16	R	16	R	16	R	16	R	16	R	16	R	
	Tobramycin	64	R	64	R	64	R	32	R	64	R	64	R	64	R	64	R	64	R	64	R	64	R	64	R	64	R	64	R	64	R	
Other	Aztreonam	>256	R	>256	R	>256	R	>256	R	>256	R	>256	R	>256	R	>256	R	>256	R	>256	R	>256	R	>256	R	>256	R	>256	R	>256	R	
	Colistin	0.50	S	0.75	S	0.125	S	0.125	S	0.50	S	0.50	S	0.50	S	0.50	S	0.50	S	0.50	S	0.75	S	0.50	S	0.50	S	0.50	S	0.50	S	
	Tetracycline	32	R	128	R	8	R	8	R	32	R	8	R	32	R	8	R	8	R	8	R	8	R	8	R	8	R	8	R	128	R	
	Tigecycline	2	R	8	R	4	R	4	R	2	R	4	R	2	R	4	R	4	R	4	R	4	R	4	R	4	R	4	R	4	R	
	Trimethoprim/Sulfamethoxazole	>32	R	>32	R	>32	R	>32	R	>32	R	>32	R	>32	R	>32	R	>32	R	>32	R	>32	R	>32	R	>32	R	>32	R	>32	R	
Fosfomycin	>256	R	>256	R	>256	R	>256	R	>256	R	>256	R	>256	R	>256	R	>256	R	>256	R	>256	R	>256	R	>256	R	>256	R	>256	R		

MIC – Minimum Inhibitory Concentration; R – Resistant; I – Susceptible, increased exposure; S – Susceptible

grounds for the relevant action to be taken in the field of public health in respect of molecular epidemiology.

This study's subject was a particular group of microorganisms classified as bacterial alarm agents (BCA) of particular virulence or resistance, i.e., carbapenemase-producing *K. pneumoniae* strains belonging to the order *Enterobacteriales*. All *K. pneumoniae* isolates were derived from intestinal colonization cases in the patients studied. This work elaborated epidemiological opinions on the BCA epidemic threat occurrence in the multi-profile medical center in Katowice. It was also based on suspicion of an epidemic outbreak since we noticed clonal dissemination of several CRKP isolates and one case of symptomatic hospital infection with a blood CRKP strain. This strain was isolated in a given department 48 hours after the patient's admission. The colonization of fourteen consecutive hospitalized patients with the same strain of the CRKP was also reported. CRKP isolates had unique properties such as the accumulation of numerous antibiotic resistance mechanisms and the capability to persist in a hospital environment. It resulted in special attention being paid to CRKP strains' health care risk (Navon-Venezia et al. 2017). The genes encoding KPC, MBL, and OXA-48 are located on the so-called mobile genetic elements (plasmids, transposons) that allow effective spreading within bacterial populations. The genes encoding KPC carbapenemases (bla_{KPC}) are located on the Tn4401 transposon located on plasmids with different types of replicons (IncF, IncL/M, ColE1, IncR, and IncX3). These plasmids show the ability to conjugate and propagate the bla_{KPC} genes to new bacterial populations (Baraniak et al. 2011).

On the other hand, the most important families of the MBL acquired are the enzymes IMP and VIM occurring both in non-fermenting and intestinal bacilli. The bla_{IMP} and bla_{VIM} genes always exist as cassettes inserted into integrons. In turn, integrons can be located on transposons and move with them between DNA molecules (Izdebski et al. 2018b). ES β L enzymes exist mainly as acquired, plasmid-encoded β -lactamases. ES β L-encoding genes are often located on conjugation plasmids (IncFII, IncI), including those with a broad host range (IncA/C, IncL/M). It allows them to spread rapidly, also between strains belonging to different species. Frequently noted are encoded by bla_{CTX-M} genes ES β L enzymes, active against cefotaxime CTX-M and localized on plasmids in *Enterobacteriales* (Izdebski et al. 2018a; 2018b).

The isolates' antibiotic susceptibility testing confirmed the β -lactamase antibiotics resistance profile typical for carbapenemase producers, as presented elsewhere (Zacharczuk et al. 2011; Guo et al. 2016; Izdebski et al. 2018a). All strains expressed high-level resistance to doripenem, ertapenem, meropenem, although they showed varying levels of resistance to imipenem. Ertapenem is the carbapenem that has been suggested as

most suitable for detecting the presence of bla_{KPC} , which was confirmed by high MIC values for ertapenem (> 32 μ g/ml) in the present study. The presence of KPC does not always result in expression of *in vitro* resistance to imipenem or meropenem, as this carbapenemase shows limited efficiency of β -lactam ring hydrolysis in carbapenem particles. In this study, E-test showed resistance to ertapenem of 7/25804, 11/25808, 13/25810 strains, and susceptibility or medium susceptibility to imipenem (MICs 4–8 μ g/ml), while PCR confirmed the presence of the bla_{KPC-2} gene in all three isolates. Imipenem and meropenem resistance of other strains might have resulted from decreased outer membrane permeability or other β -lactamases providing a synergistic effect with KPC (Protonotariou et al. 2018). The strains' resistance to third-generation cephalosporins confirmed this hypothesis similarly to the various β -lactamases production by *K. pneumoniae*. The variability in CRKP strains' carbapenem susceptibility illustrates the difficulties encountered while trying to identify strains producing carbapenemases only with the E-testing of resistance profiles. To reliably identify such strains, additional and more specific techniques should be applied (Xu et al. 2005; Magiorakos et al. 2012; Han et al. 2013; Caltagirone et al. 2017; Bukavaz et al. 2018).

The bla_{KPC-2} , bla_{OXA-48} , and bla_{VIM-1} carbapenemase encoding genes and an additional $bla_{CTX-M-15}$ cefotaxime encoding genes have been found to coexist in all the strains concerned. Lee et al. (2016) found that *K. pneumoniae* can carry multiple β -lactamase genes in the same strain, which could be partly responsible for the pathogen's selective success. All types of the bla genes were reported in combinations for this species (Lee et al. 2016). So far, *K. pneumoniae* that produce KPC-2 and KPC-3 carbapenemases have been frequently found in Europe, including Poland (Baraniak et al. 2011; Zacharczuk et al. 2011; Baraniak et al. 2015; Grundmann et al. 2017). On the other hand, Matsumura et al. (2017) presented the global dissemination of *Enterobacteriaceae* strains carrying the bla_{VIM} genes. The VIM-producing *Enterobacteriaceae* are generally present in Europe, particularly in Greece, Spain, Hungary, and Italy (Matsumura et al. 2017). Significantly, an increasing problem with VIM-producing *K. pneumoniae* has been recorded in Greece, where the strains have accounted for the deaths of 48% of patients over the last two years (Protonotariou et al. 2018). In Poland, Izdebski et al. (2018b), collected one hundred and nineteen cases of VIM/IMP-positive *Enterobacteriaceae* in the period from 2006 to 2012, and showed many specific or entirely new features of these microorganisms, undoubtedly related to the properties of pathogens isolated in the abovementioned central-southern countries Europe, including several likely imported from abroad (e.g., from Greece) (Izdebski et al. 2018b).

The strains containing OXA-48 β -lactamases provide another example of rapid immigration of harmful microorganisms to Europe from their endemic regions, mostly eastern and southern Mediterranean countries (Egypt, Morocco, and Turkey). OXA-48-like-positive strains cause hospital outbreaks of epidemics in Belgium, France, Netherlands, Germany, Spain, and other countries (Nordmann and Poirel 2014; Grundmann et al. 2017). In the most recent report developed by OXA-48-PL Study Group monitoring the *Enterobacteriaceae* OXA-48-positive strains' spread, the authors demonstrate that these strains have been isolated relatively rarely in Poland (Izdebski et al. 2018a). It was confirmed by other European and international research teams (Nordmann and Poirel 2014; Grundmann et al. 2017). Conjugative transfer of a specific plasmid group is regarded to be the central mechanism in the spread of OXA-48 among the *Enterobacteriaceae* populations (Nordmann and Poirel 2014).

The high MIC values ($>256 \mu\text{g/ml}$) for cefotaxime may suggest that the strains produced CTX-M β -lactamases. Multiplex PCR and sequencing have confirmed $bla_{\text{CTX-M-15}}$ presence in all isolates. The presence of various CTX-M β -lactamases in *K. pneumoniae* in Poland has been confirmed by other research teams (Baraniak et al. 2011; Izdebski et al. 2018a; 2018b). No bla_{SHV} or bla_{TEM} have been identified among the isolates. These results are in line with the persisting trend of diminished prevalence of hospital-associated *K. pneumoniae* strains producing SHV or TEM β -lactamases, which has also been noted by other scientists (Rodrigues et al. 2014). The type of ES β Ls present in *K. pneumoniae* shifted in the 2000s, which caused outbreaks in hospitals due to the acquisition of plasmids and transposons encoding $bla_{\text{CTX-M-type}}$ ES β Ls, consequently resulting in the predominance of CTX-M-producing strains (Calbo and Garau 2015).

Among non- β -lactam antibiotics, colistin has shown the highest activity towards the strains concerned. Similar results have been published by other authors (Zacharczuk et al. 2011). Among aminoglycosides, amikacin showed the highest activity. The vast majority of strains (92.8%) were susceptible to amikacin, unlike in China, where total *K. pneumoniae* resistance to amikacin was demonstrated (Guo et al. 2016). The other aminoglycosides (gentamicin, netilmicin, and tobramycin) were nonreactive to the CRKP isolates concerned, in line with data reported by other authors (Zacharczuk et al. 2011; Guo et al. 2016). On the other hand, Bukavaz et al. (2018) presented other aminoglycoside susceptibility profiles in CRKP strains. These discrepancies are most likely due to different quantities or origins of the strains concerned, though they might as well be related to particular hospitals' or ward's antibiotic policies.

The present analysis has shown a relatively high percentage of isolates resistant to tigecycline (42.8%), a synthetic minocycline analogue with a broad spectrum of activity. The antibiotic is successfully applied to treat infections caused by multi-resistant bacterial strains, including *K. pneumoniae*. During tigecycline treatment, *Enterobacteriaceae* representatives, including CRKP strains, may become resistant to the antibiotic, as evidenced by Pfarrell et al. (2018). They demonstrated cross-resistance between tigecycline and minocycline in resistant *Enterobacteriaceae* strains due to the MDR pumps, which remove drugs from cells. The distribution of acquired tigecycline resistance can vary depending on the geographic location or time; therefore, it is recommended to concern data on local resistance, particularly while treating severe infections (Pfarrell et al. 2018).

Genetic similarity of CRKP isolates was determined by comparing PFGE profiles (Han et al. 2013). This method has been widely used by European and non-European research teams that study epidemic outbreaks of *K. pneumoniae* and evidence global spread of this species' epidemic clones (Guo et al. 2016; Bukavaz et al. 2018; Protonotariou et al. 2018). All *K. pneumoniae* strains analyzed in this study belonged to ST147 (CC147). Navon-Venezia et al. (2017) reported that ST147 *K. pneumoniae* clone spread globally. The involvement of this pandemic clone in the spread of CTX-M-15 and other carbapenemases in European, Asian, and Middle East countries was confirmed by others (Rodrigues et al. 2014; Guo et al. 2016; Zautner et al. 2017). The data found in the literature on *K. pneumoniae* clonal organization has been confirmed by research focused on the molecular epidemiology of infections due to antibiotic-resistant *Enterobacteriaceae* (Guo et al. 2016; Protonotariou et al. 2018).

Because of the clonal nature of the isolates studied, the clinical data about their origin was reviewed to examine whether the same clonal type was circulating in the three various hospital wards. The study focused mainly on stroke patients or patients suffering from cardiovascular complications who were transferred to multiple-bed hospital rooms in Stroke Recovery Units, which were the only places where they were in touch. Moreover, it is plausible that the neurology ward played a major role in disseminating the bacteria throughout the hospital. The spread of the pathogen isolates across three different hospital wards could imply that the personnel who can access all hospital wards freely, unlike the patients and their relatives, might have transmitted the infections. Scientific literature emphasizes the role of hospitalization (and its duration) in the process of bacterial colonization. The frequency of gastrointestinal colonization with *K. pneumoniae* strains in hospitalized patients was high in our study. Gastrointestinal

colonization with CRKP is an important risk factor for infections with strains of the same phenotype due to the easy transfer of the genes and strains' persistence in hospital environments, which hinders their eradication. This research evidences *K. pneumoniae* adaptation typical of endemic hospital strains, which are corroborated by the accumulation of locally spreading resistance mechanisms to the antibiotics most commonly used for therapeutic purposes.

ORCID

Monika Brzywczy-Włoch <https://orcid.org/0000-0002-7415-0154>

Ethics approval

The study was approved by the Bioethics Committee of the Jagiellonian University in Krakow, Poland (KBET/1072.6120.264.2019).

Authors' contributions

DO collected the data, performed the molecular analysis and drafted the manuscript; HK-C collected the isolates with clinical data, performed the hospital laboratory analysis and coordinated the microbiological analysis; MB consulted the cases and edited the manuscript; MBW supervised the research and analysis, coordinated and edited the manuscript.

Funding

The present work was financially supported by Jagiellonian University Medical College in Krakow (Poland), Grant No: K/ZDS/007829.

Acknowledgments

The authors are thankful to Karolina Winiewicz and Renata Wrona-Moczurad, the employees of the Department of Bacteriology of the GCM for their cooperation and assistance in conducting the study.

Conflict of interest

The authors do not report any financial or personal connections with other persons or organizations, which might negatively affect the contents of this publication and/or claim authorship rights to this publication.

Literature

- Baraniak A, Grabowska A, Izdebski R, Fiett J, Herda M, Bojarska K, Żabicka D, Kania-Pudło M, Młynarczyk G, Żak-Puławska Z, et al.; KPC-PL Study Group. Molecular characteristics of KPC-producing *Enterobacteriaceae* at the early stage of their dissemination in Poland, 2008–2009. *Antimicrob Agents Chemother*. 2011 Dec;55(12):5493–5499 <https://doi.org/10.1128/AAC.05118-11>
- Baraniak A, Izdebski R, Fiett J, Herda M, Derde LP, Bonten MJ, Adler A, Carmeli Y, Goossens H, Hryniewicz W, et al.; MOSAR WP2, WP3, and WP5 Study Groups. KPC-Like Carbapenemase-Producing *Enterobacteriaceae* Colonizing Patients in Europe and Israel. *Antimicrob Agents Chemother*. 2015 Dec 28;60(3):1912–1917. <https://doi.org/10.1128/AAC.02756-15>
- Boucher HW, Talbot GH, Bradley JS, Edwards JE, Gilbert D, Rice LB, Scheld M, Spellberg B, Bartlett J. Bad bugs, no drugs: no ESCAPE! An update from the Infectious Diseases Society of America. *Clin Infect Dis*. 2009 Jan 1;48(1):1–12. <https://doi.org/10.1086/595011>
- Bukavaz S, Budak M, and Celik AD. *bla*_{KPC-2} and *bla*_{OXA-48} producing *Klebsiella pneumoniae* found in a Turkish hospital in the Balkans. *Afr J Microbiol Res*. 2018;12(16):370–379. <https://doi.org/10.5897/AJMR2018.8841>
- Calbo E, Garau J. The changing epidemiology of hospital outbreaks due to ESBL-producing *Klebsiella pneumoniae*: the CTX-M-15 type consolidation. *Future Microbiol*. 2015;10(6):1063–1075. <https://doi.org/10.2217/fmb.15.22>
- Caltagirone M, Nucleo E, Spalla M, Zara F, Novazzi F, Marchetti VM, Piazza A, Bitar I, De Cicco M, Paolucci S, et al. Occurrence of extended spectrum β -lactamases, KPC-type, and MCR-1.2-producing *Enterobacteriaceae* from wells, river water, and wastewater treatment plants in Oltrepò Pavese area, Northern Italy. *Front Microbiol*. 2017 Nov 10;8:2232. <https://doi.org/10.3389/fmicb.2017.02232>
- CLSI. Performance standards for antimicrobial susceptibility testing. CLSI supplement M100: 282. Wayne (USA): Clinical and Laboratory Standards Institute; 2018.
- Doi Y, Potoski BA, Adams-Haduch JM, Sidjabat HE, Pasculle AW, Paterson DL. Simple disk-based method for detection of *Klebsiella pneumoniae* carbapenemase-type β -lactamase by use of a boronic acid compound. *J Clin Microbiol*. 2008 Dec;46(12):4083–4086. <https://doi.org/10.1128/JCM.01408-08>
- EUCAST. The European Committee on Antimicrobial Susceptibility Testing. Breakpoint tables for interpretation of MICs and zone diameters. Version 9.0. Basel (Switzerland): The European Committee on Antimicrobial Susceptibility Testing; 2019.
- Grundmann H, Glasner C, Albiger B, Aanensen DM, Tomlinson CT, Andrasević AT, Cantón R, Carmeli Y, Friedrich AW, Giske et al.; European Survey of Carbapenemase-Producing *Enterobacteriaceae* (EuSCAPE) Working Group. Occurrence of carbapenemase-producing *Klebsiella pneumoniae* and *Escherichia coli* in the European survey of carbapenemase-producing *Enterobacteriaceae* (EuSCAPE): a prospective, multinational study. *Lancet Infect Dis*. 2017 Feb;17(2):153–163. [https://doi.org/10.1016/S1473-3099\(16\)30257-2](https://doi.org/10.1016/S1473-3099(16)30257-2)
- Guo L, An J, Ma Y, Ye L, Luo Y, Tao C, Yang J. Nosocomial outbreak of OXA-48-producing *Klebsiella pneumoniae* in a Chinese hospital: clonal transmission of ST147 and ST383. *PLoS One*. 2016 Aug 4; 11(8):e0160754. <https://doi.org/10.1371/journal.pone.0160754>
- Han H, Zhou H, Li H, Gao Y, Lu Z, Hu K, Xu B. Optimization of pulse-field gel electrophoresis for subtyping of *Klebsiella pneumoniae*. *Int J Environ Res Public Health*. 2013 Jul 1;10(7):2720–2731. <https://doi.org/10.3390/ijerph10072720>
- Izdebski R, Baraniak A, Zabicka D, Machulska M, Urbanowicz P, Fiett J, Literacka E, Bojarska K, Kozinska A, Zieniuk B, et al.; OXA-48-PL Study Group. *Enterobacteriaceae* producing OXA-48-like carbapenemases in Poland, 2013–January 2017. *J Antimicrob Chemother*. 2018a Mar 1;73(3): 620–625. <https://doi.org/10.1093/jac/dkx457>
- Izdebski R, Baraniak A, Zabicka D, Sekowska A, Gospodarek-Komkowska E, Hryniewicz W, Gniadkowski M. VIM/IMP carbapenemase-producing *Enterobacteriaceae* in Poland: epidemic *Enterobacter hormaechei* and *Klebsiella oxytoca* lineages. *J Antimicrob Chemother*. 2018b Oct 1;73(10):2675–2681. <https://doi.org/10.1093/jac/dky257>
- Lee CR, Lee JH, Park KS, Kim YB, Jeong BC, Lee SH. Global dissemination of carbapenemase-producing *Klebsiella pneumoniae*: epidemiology, genetic context, treatment options, and detection methods. *Front Microbiol*. 2016 Jun 13;7:895. Available from: <https://doi.org/10.3389/fmicb.2016.00895>
- Magiorakos AP, Srinivasan A, Carey RB, Carmeli Y, Falagas ME, Giske CG, Harbarth S, Hindler JF, Kahlmeter G, Olsson-Liljequist B, et al. Multidrug-resistant, extensively drug-resistant and pandrug-resistant bacteria: an international expert proposal for

- interim standard definitions for acquired resistance. *Clin Microbiol Infect.* 2012 Mar;18(3):268–281.
<https://doi.org/10.1111/j.1469-0691.2011.03570.x>
- Matsumura Y, Peirano G, Devlin R, Bradford PA, Motyl MR, Adams MD, Chen L, Kreiswirth B, Pitout JDD.** Genomic epidemiology of global VIM-producing Enterobacteriaceae. *J Antimicrob Chemother.* 2017 Aug 1;72(8):2249–2258.
<https://doi.org/10.1093/jac/dkx148>
- Navon-Venezia S, Kondratyeva K, Carattoli A.** *Klebsiella pneumoniae*: a major worldwide source and shuttle for antibiotic resistance. *FEMS Microbiol Rev.* 2017 May 1;41(3):252–275.
<https://doi.org/10.1093/femsre/fux013>
- Nordmann P, Poirel L.** The difficult-to-control spread of carbapenemase producers among *Enterobacteriaceae* worldwide. *Clin Microbiol Infect.* 2014 Sep;20(9):821–830.
<https://doi.org/10.1111/1469-0691.12719>
- Pfaller MA, Huband MD, Streit JM, Flamm RK, Sader HS.** Surveillance of tigecycline activity tested against clinical isolates from a global (North America, Europe, Latin America, and Asia-Pacific). *Int J Antimicrob Agents.* 2018 Jun;51(6):848–853.
<https://doi.org/10.1016/j.ijantimicag.2018.01.006>
- Podschun R, Ullmann U.** *Klebsiella* spp. as nosocomial pathogens: epidemiology, taxonomy, typing methods, and pathogenicity factors. *Clin Microbiol Rev.* 1998 Oct;11(4):589–603.
<https://doi.org/10.1128/CMR.11.4.589>
- Protonotariou E, Poulou A, Politi L, Sgouropoulos I, Metallidis S, Kachrimanidou M, Pournaras S, Tsakris A, Skoura L.** Hospital outbreak due to a *Klebsiella pneumoniae* ST147 clonal strain co-producing KPC-2 and VIM-1 carbapenemases in a tertiary teaching hospital in Northern Greece. *Int J Antimicrob Agents.* 2018 Sep; 52(3):331–337. <https://doi.org/10.1016/j.ijantimicag.2018.04.004>
- Rodrigues C, Machado E, Ramos H, Peixe L, Novais Â.** Expansion of ESBL-producing *Klebsiella pneumoniae* in hospitalized patients: a successful story of international clones (ST15, ST147, ST336) and epidemic plasmids (IncR, IncFII_K). *Int J Med Microbiol.* 2014 Nov;304(8):1100–1108.
<https://doi.org/10.1016/j.ijmm.2014.08.003>
- Shaker OA, Gomaa HE, ElMasry SA, Halim RMA, Abdelrahman AH, Kamal JS.** Evaluation of combined use of temocillin disk and mastdisks inhibitor combination set against polymerase chain reaction for detection of carbapenem-resistant *Enterobacteriaceae*. *Open Access Maced J Med Sci.* 2018 Feb 1;6(2):242–247.
<https://doi.org/10.3889/oamjms.2018.090>
- Xu L, Ensor V, Gossain S, Nye K, Hawkey P.** Rapid and simple detection of *bla*_{CTX-M} genes by multiplex PCR assay. *J Med Microbiol.* 2005 Dec;54(Pt 12):1183–1187.
<https://doi.org/10.1099/jmm.0.46160-0>
- Zacharczuk K, Piekarska K, Szych J, Zawidzka E, Sulikowska A, Wardak S, Jagielski M, Gierczynski R.** Emergence of *Klebsiella pneumoniae* coproducing KPC-2 and 16S rRNA methylase ArmA in Poland. *Antimicrob Agents Chemother.* 2011 Jan;55(1):443–446.
<https://doi.org/10.1128/AAC.00386-10>
- Zautner AE, Bunk B, Pfeifer Y, Spröer C, Reichard U, Eiffert H, Scheithauer S, Groß U, Overmann J, Bohne W.** Monitoring microevolution of OXA-48-producing *Klebsiella pneumoniae* ST147 in a hospital setting by SMRT sequencing. *J Antimicrob Chemother.* 2017 Oct 1;72(10):2737–2744.
<https://doi.org/10.1093/jac/dkx216>

A Clinical Trial to Evaluate the Efficacy of α -Viniferin in *Staphylococcus aureus* – Specific Decolonization without Depleting the Normal Microbiota of Nares

MD ABDUR RAHIM^{1,2*}, HOONHEE SEO^{2*}, SUKYUNG KIM², YOON KYOUNG JEONG²,
HANIEH TAJDOZIAN^{1,2}, MIJUNG KIM², SAEBIM LEE² and HO-YEON SONG^{1,2*}

¹ Department of Microbiology and Immunology, School of Medicine, Soonchunhyang University, Cheonan, Republic of Korea

² Probiotics Microbiome Convergence Center, Asan, Republic of Korea

Submitted 28 December 2020, revised 3 February 2021, accepted 8 February 2021

Abstract

Staphylococcus aureus is currently a significant multidrug-resistant bacterium, causing severe healthcare-associated and community-acquired infections worldwide. The current antibiotic regimen against this pathogen is becoming ineffective due to resistance, in addition, they disrupt the normal microbiota. It highlights the urgent need for a pathogen-specific drug with high antibacterial efficacy against *S. aureus*. α -Viniferin, a bioactive phytochemical compound, has been reported to have excellent anti-*Staphylococcus* efficacy as a topical agent. However, so far, there were no clinical trials that have been conducted to elucidate its efficacy. The present study aimed to investigate the antibacterial efficacy of α -viniferin against *S. aureus* in a ten-day clinical trial. Based on the results, α -viniferin showed 50% minimum inhibitory concentrations (MIC₅₀ values) of 7.8 μ g/ml in culture broth medium. α -Viniferin was administered in the nares three times a day for ten days using a sterile cotton swab stick. Nasal swab specimens were collected before (0 days) and after finishing the trial (10th day), and then analyzed. In the culture and RT-PCR-based analysis, *S. aureus* was reduced significantly: 0.01. In addition, 16S ribosomal RNA-based amplicon sequencing analysis showed that *S. aureus* reduced from 51.03% to 23.99% at the genus level. RNA-seq analysis was also done to gain insights into molecular mechanisms of α -viniferin against *S. aureus*, which revealed that some gene groups were reduced in 5-fold FC cutoff at two times MIC conditions. The study results demonstrate α -viniferin as a potential *S. aureus*-specific drug candidate.

Key words: α -viniferin, clinical trial, MRSA, PCR, 16S rRNA amplicon sequencing analysis

Introduction

Staphylococcus aureus is one of the most common opportunistic pathogens carried by approximately 30–50% of humans and continues to be a leading cause of infection-related deaths, ranging from 6–40% around the globe (Frank et al. 2010; Islam et al. 2020). Although the axilla, throat, and perineum are essential reservoirs, the anterior nares are the primary niche for *S. aureus* and serve as a reservoir for the pathogen's spread (Lowy 1998). *S. aureus* nasal colonization causes a range of mild infections to life-threatening conditions, including fatal endocarditis, pneumonia, bacteremia, or chronic osteomyelitis. Additionally, it is a risk factor for life-threatening surgical site infections and infections in

dialysis (Mitchell and Howden 2005). So far, antibiotic therapy has been the best option for treating *S. aureus*. However, *S. aureus* infections have become a serious global challenge because of resistance to a wide range of clinically significant antibiotics and a limited number of new antibiotics. Previous studies showed that the rate of discovery of new antibiotics is slowing, while the occurrence of antibiotic-resistant infections is increasing sharply, therefore, the rate of antibiotic withdrawal from the healthcare system is higher than that of approvals (Kinch et al. 2014). In addition, the current antibiotic regimen reduces and changes the skin's microbial composition and supports pathogen overgrowth (Chambers and Deleo 2009; Song et al. 2018), highlighting the need to develop new drugs that

Md Abdur Rahim and Hoonhee Seo contribute equally to this work and are co-first authors.

* Corresponding author: H.-Y. Song, Department of Microbiology and Immunology, School of Medicine, Soonchunhyang University, Cheonan, Republic of Korea; Probiotics Microbiome Convergence Center, Asan, Republic of Korea; e-mail: songmic@sch.ac.kr

© 2021 Md Abdur Rahim et al.

This work is licensed under the Creative Commons Attribution-NonCommercial-NoDerivatives 4.0 License (<https://creativecommons.org/licenses/by-nc-nd/4.0/>).

not only serve as effective alternatives to the current drug regimen but also preserve skin microbiota.

Natural products and secondary metabolites produced by living systems, mostly plants, have a wide range of pharmacological properties, including antimicrobial and anti-inflammatory ones, and a high potential for treating human diseases, such as coronary heart diseases, cancer, diabetes, and infectious diseases (Chabán et al. 2019). According to the World Health Organization, 65–80% of the world's population depends on traditional medicine to treat many diseases (Chew et al. 2011). α -Viniferin is a phytochemical compound extracted from *Carex humilis*, a medicinal plant that grows in eastern Asian countries, such as Japan, China, and Korea (Seo et al. 2017). It was also identified from *Iris clarkei*, *Caragana Sinica*, and *Caragana chamlagu* (Chung et al. 2003). α -Viniferin isolated and identified as a stilbene oligomer has various biological activities, including antioxidant, anti-tumor, anti-cancer, and anti-arthritis. It has also been reported to inhibit cyclooxygenase, acetylcholinesterase, and prostaglandin H-2 synthase (Sim et al. 2014; Seo et al. 2017). Additionally, α -viniferin shows antibacterial activity against drug-susceptible and drug-resistant strains of *Mycobacterium tuberculosis* and excellent anti-*Staphylococcus* activity against three *Staphylococcus* species, including methicillin-susceptible *S. aureus* (MSSA), methicillin-resistant *S. aureus* (MRSA), and methicillin-resistant *Staphylococcus epidermidis* (MRSE) (Seo et al. 2017). Previous studies using animal models have demonstrated that α -viniferin improves general health in mammals and is rapidly absorbed in the blood stream (Baur et al. 2006; Fan et al. 2020). Although α -viniferin is assumed to be a potential *S. aureus*-specific drug, there were no clinical studies on its effects on *S. aureus* to the best of our knowledge. In this study, we investigated α -viniferin clinical efficacy in eradicating *S. aureus* from the nasal carriage. Additionally, we looked over the effectiveness of α -viniferin against nasal MRSA.

Experimental

Materials and Methods

α -Viniferin and its antimicrobial inhibition. We purchased the α -viniferin, pale brown powder (Cat No.: CFN97068) from Chem Faces (Wuhan, Hubei, China) and confirmed its specific toxicity against 20 bacterial strains obtained from the National Culture Collection for Pathogens (NCCP) (Chungbuk, Korea). The minimal inhibitory concentration (MIC) of α -viniferin against each bacterial strain was determined using cation-adjusted Mueller-Hinton broth according to the Clinical and Laboratory Standards Institute (CLSI).

Each well of a 96-well plate was inoculated with 200 μ l of the inoculum suspension (1×10^5 to 1×10^6 CFU/ml) and the plates were incubated for 24 h. The MIC values were determined as the lowest drug concentrations that showed complete inhibition of visible growth. The bacterial strains were as follows: *Escherichia coli* NCCP 14762, *Proteus vulgaris* NCCP 14765, *Shigella boydii* NCCP 14745, *Shigella flexneri* NCCP 14744, *Shigella dysenteriae* NCCP 14746, *Staphylococcus aureus* NCCP 14780, *Staphylococcus epidermidis* NCCP 14768, *Staphylococcus aureus* MRSA NCCP 14769, *Corynebacterium diphtheriae* NCCP 10353, *Salmonella enteritidis* NCCP 14771, *Acinetobacter baumannii* NCCP 14782, *Streptococcus sanguinis* NCCP 14775, *Streptococcus pyogenes* NCCP 14783, *Streptococcus pneumoniae* NCCP 14774, *Serratia marcescens* NCCP 14770, *Citrobacter freundii* NCCP 14766, *Enterobacter aerogenes* NCCP 14761, *Proteus mirabilis* NCCP 14763, *Klebsiella pneumoniae* NCCP 14764, and *Escherichia coli* O157 NCCP 14541.

Study design and subjects. Our study enrolled 20 Korean adult females aged between 20 and 60 years following inclusion and exclusion criteria. The inclusion criteria comprised health and physical fitness, age > 18 years, and the willingness to avoid topical agent applied to the nares during the entire trial. The characteristics of the subjects are shown in Table SI. The Institutional Review Board approved this study of the Korea Dermatology Research Institute (IRB Number: KDRI-IRB-20231, Study Code: KDRI-2020-231). We obtained written informed consent from all participants before conducting the study. The study was carried out according to the 1964 declaration of Helsinki.

Clinical experiment. Following the randomization sequence, we sequentially numbered containers with the study drug, α -viniferin, and provided it to the numerical order participants. Nare's specimens were collected on day 0 and at day ten by a professional. During the trial, each participant's skin moisture content was measured on days 0, 4, and 8 using a corneometer CM 825 (Courage and Khazaka, Germany). Each time, the corneometer measurement was done five times at constant temperature and humidity (20–24°C, 40–60% RH), at the same site, in the same way, and the average value was recorded as an immediate value. The recorded value was then analyzed to observe our study drug's moisturizing power because moisture content plays a key role in maintaining an intact skin barrier (Mojumdar et al. 2017). During and immediately after the test, a dermatologist examined the skin for irritation or allergic symptoms.

Skin irritation test. Before the clinical trials, a skin irritation test for three concentrations of α -viniferin (10 μ g/ml, 100 μ g/ml, 1,000 μ g/ml) was done on 32 Korean adult females in a different place to rule

out the possibility of skin irritation of the test drug. The characteristics of the participants are shown in Table SII. The drug solution was loaded into a clear patch chamber, and then the patches were applied onto the participants' backs. All participants were advised to avoid water, heavy exercise, and scratching. The patch chambers were removed after 48 hours. After thirty minutes of patch removal (total 48 hours test), the reaction site was observed and observed again after 24 hours (total 72 hours of the test). The reactions were graded according to the recommendation of the International Contact Dermatitis Research Group (ICDRG), and Frosch and Kligman (Frosch and Kligman 1979; Lachapelle and Maibach 2020). This study was approved by the Institutional Review Board of the COREDERM Skin Research Center (IRB Number: CDIRB-QR-20-025, Study Code: CDS-2000-005-14). We obtained written informed consent from all participants before conducting this study.

Preparation and application of α -viniferin. We prepared α -viniferin suspension by mixing the powder with sterile distilled water at 100 mg/l. A sterile cotton swab (BD Difco, USA) was used to treat the nares; the swab was moistened with the drug suspension and then gently rubbed the anterior nares while rotating it for 15 seconds. The drug was applied three times daily for ten days in right and left nares. The participants themselves made the application of the drug solution.

Sample collection. An expert did the collection of nasal specimens at day zero (0) and the end of the trial (at day 10), by swabbing the anterior nares with sterile foam-tipped swabs moistened with a mixed solution of 0.15 M NaCl and 0.1% Tween 20 solution (Sigma-Aldrich, France) (You et al. 2019). Each region was swabbed for 15 seconds while rotating the swab and exerting gentle pressure. Each swab was then placed into the swab container without touching any objects and transported to the laboratory in a dry-ice bag container within two hours of collection.

Culture of microorganisms. Upon receiving the lab samples, we added 2 ml 0.15 M NaCl solution into the swab container, vortexed it enough, and transferred it into a fresh microcentrifuge tube. After doing a 10-fold serial dilution four times (10^{-1} to 10^{-4}) in 0.15 M NaCl solution, we placed a 10- μ l sample from each of the dilution-tube in duplicate onto the nutrient agar, a staphylococcus agar medium (BD Difco, USA), and a second staphylococcus agar medium containing methicillin antibiotic (50 μ g/ml) for the culture-based quantification of nasal microbiota, *S. aureus*, and MRSA, respectively, using a spread plate method. After 48 hours of incubation at 37°C, plates were inspected for the growth of colonies with morphology characteristic of *S. aureus*. We distinguished *S. aureus* from other *Staphylococcus* species by its round and golden-yellow colonies. For

each dilution, the average of the two duplicate plates was calculated. When two successive dilutions yielded 30 to 300 colonies, the average count of both dilutions was calculated. We stored the rest of the samples at -80°C for further molecular analysis.

DNA extraction. We extracted DNA for real-time quantitative PCR (qRT-PCR) and next-generation sequencing (NGS)-based 16S rRNA profiling by thawing samples and transferring them to Lysing Matrix B tubes aseptically (MP, Biomedicals, USA), followed by mechanical lysis through bead beating. After centrifuging enough, we collected supernatant without any visible particles. Next, we checked the quality of extracted DNA by agarose gel electrophoresis and visualized it using ethidium bromide (Bio-Rad, ChemiDoc, USA). We also quantified the isolated DNA by a Qubit Fluorometer using a dsDNA HS Assay kit (Invitrogen, USA). We used a 0.15 M NaCl solution as a negative control to ensure no DNA contamination occurred during the whole process (Rainer et al. 2020).

qRT-PCR. We did qRT-PCR (C1000 Thermal Cycler) to test for the presence and quantification of *S. aureus* and MRSA in the nasal swab samples separately, targeting organism-specific genes is a significant correlation between PCR cycle threshold (Ct) value and bacterial load (Dionne et al. 2013; Davies et al. 2018). We used the following primers in this study: SA1 (5'-AATCT-TTGTCGGTACACGATATTCTTCACG-3') and SA2 (5'-CGTAATGAGATTTTCAGTAGATAATACAACA-3') specific for *S. aureus* (Pereira et al. 2010); and MRS1 (5'-TAGAAATGACTGAAC GTCCG-3') and MRS2 (5'-TTGCGATCAATGTTACC GTAG-3') specific for MRSA (Del Vecchio et al. 1995). We also used 16S rRNA universal primers to quantify resident nasal microbiota. We did the assay in a final volume of 20 μ l consisting of a 5- μ l extracted template DNA and 15 μ l reaction mixtures: 4 μ l nuclease-free water, 10 μ l iQ SYBR Green Supermix (Bio-Rad Laboratories, USA), and 0.5 μ l each of the forward and reverse primer (10 pmol/ μ l). We did amplification as follows: an initial DNA denaturation and enzyme activation at 95°C for 3 min, followed by 49 cycles of a 10-s denaturation step at 95°C, a 10-s annealing step at 55°C, and a 30-s extension step at 72°C.

Absolute quantification. To make a qRT-PCR standard curve (threshold cycle versus the number of CFU/ml curve), we cultivated an *S. aureus* stock culture (0.1% inoculation) in Mueller-Hinton broth (BD Difco, USA) for 6–8 hours at 37°C using a shaker incubator (BioFree, Korea). We then checked the optical density (OD at 600 nm) using a spectrophotometer (DR 1900, Hach, USA); it was 0.8 to 1.0. Next, we centrifuged the broth culture to get the bacterial pellet at 1,811.16 \times g for 10 mins employing a Hanil combi R515 (Hanil Scientific Inc., Korea) serially diluted the pellet 10-fold eight times

using sterile distilled water. After that, we extracted DNA through mechanical lysis as described in the DNA Extraction section, amplified it by qRT-PCR, and used the data to create the standard curve in which each target CFU is plotted against the resulting C_t value.

16S rRNA-based amplicon sequencing. Following the DNA extraction, we amplified the V4 hyper-variable region of the 16S ribosomal RNA gene. We used the V4 region-specific primers with a locus-specific overhang sequence: 515F-5' – TCGTCGGCAGCGTCAGATGTGTATAAGAGACAG- GTGCCAGCMGCCGCGGTAA and 806R – 5'-GTCTCGTGGGCTCGGAGATGTGTATAAGAGACAG-GGACTACHVGGGTWTCTAAT (overhang sequence-locus specific-sequence). We attached indexes and Illumina sequencing adapters through index PCR using a Nextera XT Index kit v2 (Illumina, USA). We used Agencourt AMPure XP (Beckman Coulter, USA) beads after every PCR step to purify the PCR products and quantified them using the Qubit dsDNA HS Assay kit (Invitrogen, USA). We then normalized the samples, pooled, mixed them with PhiX Control v3 (Illumina), and sequenced them using Illumina iSeq 100 platform (Illumina). Finally, we analyzed the sequence data using Ezcloud software that exhibits the entire microbial profile within the sample tested.

Gene expression profiling. Drug treatment, RNA extraction, and analysis. To understand how α -viniferin downregulate *S. aureus* gene expression, we treated an *S. aureus* broth culture with α -viniferin, extracted RNA, and sent it for the RNA sequencing. We cultivated *S. aureus* culture and measured optical density as described in the absolute quantification section. Then, we distributed the broth culture into three tubes; each tube contained 30 ml of broth. Afterward, we added a specific volume of α -viniferin stock solution to the tubes separately to make the drug concentration $1 \times$ the MIC value (10 $\mu\text{g/ml}$) and $2 \times$ the MIC value (20 $\mu\text{g/ml}$). We also used drug-free 0.15 M NaCl solution in one of the tubes as a negative control. We then incubated the drug-treated and drug-free culture at 37°C for 6–8 hours on a shaker incubator. After the incubation, we extracted total RNA from the broth cultures of *S. aureus* using the RNA Protect Bacterial Reagent and RNeasy Mini kit (QIAGEN, Germany), according to the manufacturer's instructions (RNeasy Mini Handbook). We also used an RNase-free DNase set (QIAGEN) for the degradation of the existing DNA. We assessed the quality of the isolated total RNA through 2% agarose gel electrophoresis since high-quality RNA is a prerequisite for ensuring all expressed genes' representation. We sent RNA samples for RNA sequencing, which has become a standard tool for analyzing gene expression in bacterial infections (Saliba et al. 2017). We did an RNA sequencing assay using a commercial RNA sequencing service (Ebiogen, Seoul, Korea).

Library preparation, sequencing, and data analysis. We used a QuantSeq 3'mRNA-Seq Library Prep Kit (Lexogen, Inc., Austria) to construct an RNA library following the manufacturer's instructions. In brief, we hybridized 500 ng of the total RNA with an oligo-dT primer containing an Illumina-compatible sequence at the 5' end, followed by reverse transcription. We initiated the second-strand synthesis using a random primer containing an Illumina-compatible linker sequence at its 5' end after the degradation of the RNA template. We used magnetic beads to remove all the reaction components and purify the double-stranded library. We then amplified the library to add the entire adapter sequences essential for cluster generation. Finally, we purified the complete library from PCR components, did a high throughput sequencing as single-end 75 sequencing using NextSeq 500 (Illumina). After the sequencing, we used Bowtie2 to align the QuantSeq 3'mRNA-Seq reads. We created Bowtie2 indices from either a representative transcript sequence or a genome assembly sequence for aligning with genome and transcriptome. We used alignment files for assembling transcripts, estimating their abundances, and detecting different expressions of genes. We used Bedtool coverage to find the differentially expressed genes based on counts from unique and multiple alignments. We processed the RT (Read Count) data based on Quantile normalization using EdgeR within R using Bioconductor. We based gene classification on searches done in the DAVID (<http://david.abcc.ncifcrf.gov/>) and Medline databases (<http://www.ncbi.nlm.nih.gov/>).

Statistical analysis. We analyzed the corneometer value, CFU, and qRT-PCR data using Prism 7.0 (Graph-Pad Software, Inc., La Jolla, USA). We used a two-tailed Student's *t*-test to evaluate the statistical significance of the results of three independent experiments done in triplicate. In the graph, data are represented as mean \pm standard deviation (SD). Means were considered to be significant at $p < 0.05$ ($*p < 0.05$, $**p < 0.01$, $***p < 0.001$, $****p < 0.0001$). We analyzed NGS-based 16S rRNA sequencing data using Ezcloud software. We also used the hypergeometric distribution to analyze the RNA sequencing data.

Results

Antimicrobial inhibition. Antibacterial inhibition of α -viniferin was tested against 20 bacterial isolates. The antibacterial activities of α -viniferin and two references antibiotics VAN and MET, expressed as MICs, are shown in Fig. 1, where MICs values were expressed up to 100 $\mu\text{g/ml}$. However, in this study, α -viniferin showed excellent anti-*staphylococcus* efficacy with the MIC value of 7.8 $\mu\text{g/ml}$ against three *Staphylococcus*

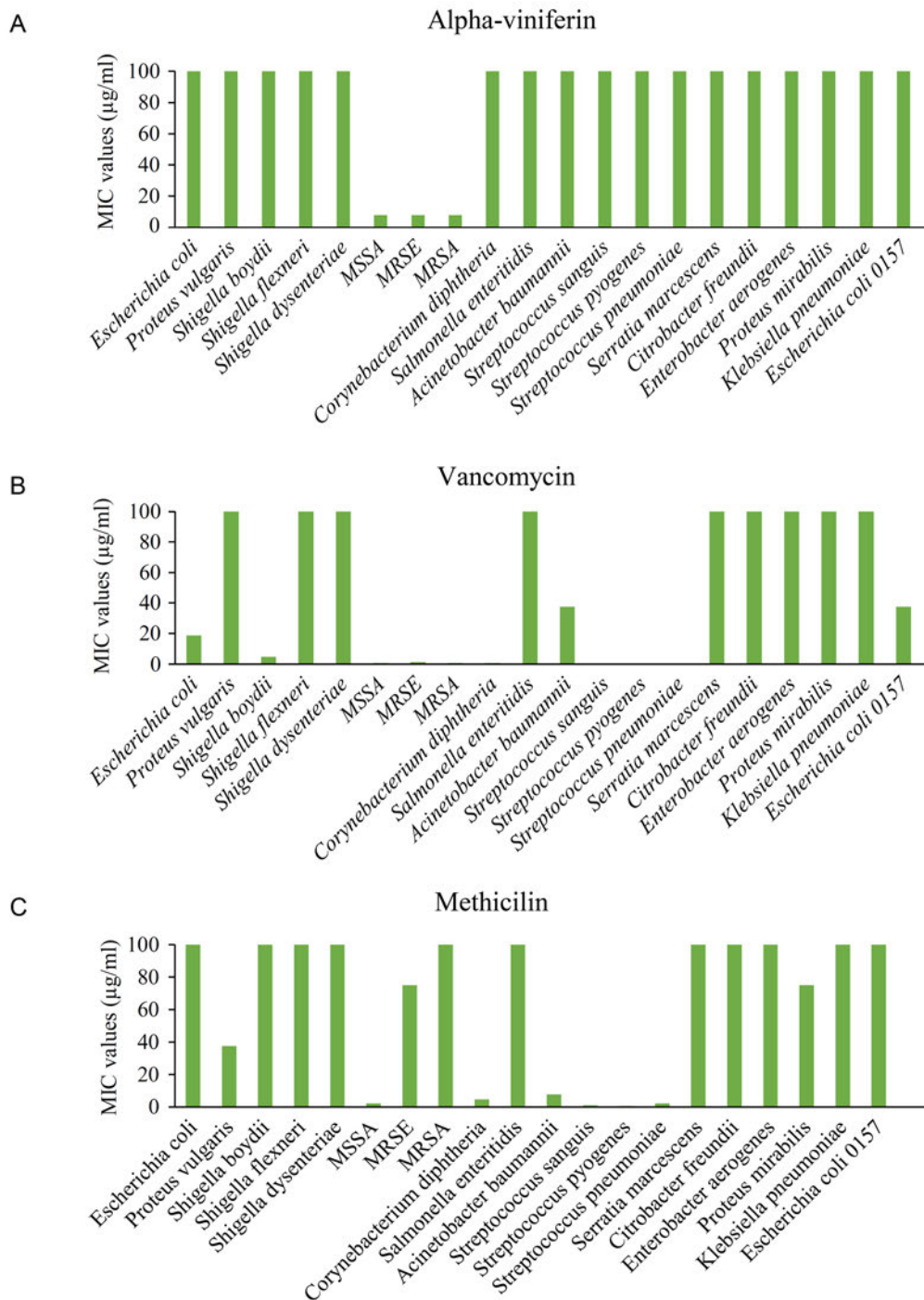


Fig. 1. Antimicrobial inhibition. Antibacterial activities, expressed as MIC₅₀, of α -viniferin (A), Vancomycin (B) and Methicillin (C) against 20 bacterial isolates. Bacterial suspensions (1×10^5 to 1×10^6 CFU/ml) were incubated with varying concentrations of α -viniferin, Vancomycin, Methicillin in Mueller Hinton Broth in a 96 well plate for 24 h at 37°C. *In vitro* MICs were determined by the broth dilution procedures described by the Clinical and Laboratory Standards Institute (CLSI).

species including methicillin-susceptible *S. aureus* (MSSA), methicillin-resistant *S. aureus* (MRSA), and methicillin-resistant *S. epidermidis* (MRSE) with no toxicity to other bacterial strains (Fig. 1A). The reference drug VAN was also active against three *Staphylococcus* species, but it also showed toxicity against other bacterial strains (Fig. 1B), and MET was also tested as a second reference drug (Fig. 1C). These results indicate

α -viniferin as a potential antibacterial agent with specific toxicity against *Staphylococcus* group.

Clinical experiment. We performed a 10-day clinical trial to investigate the antimicrobial efficiency of α -viniferin, in which 20 healthy Korean adult females participated. The drug was applied in the right and left anterior nares three times daily. We collected the nasal swab samples before (day 0) and after conducting

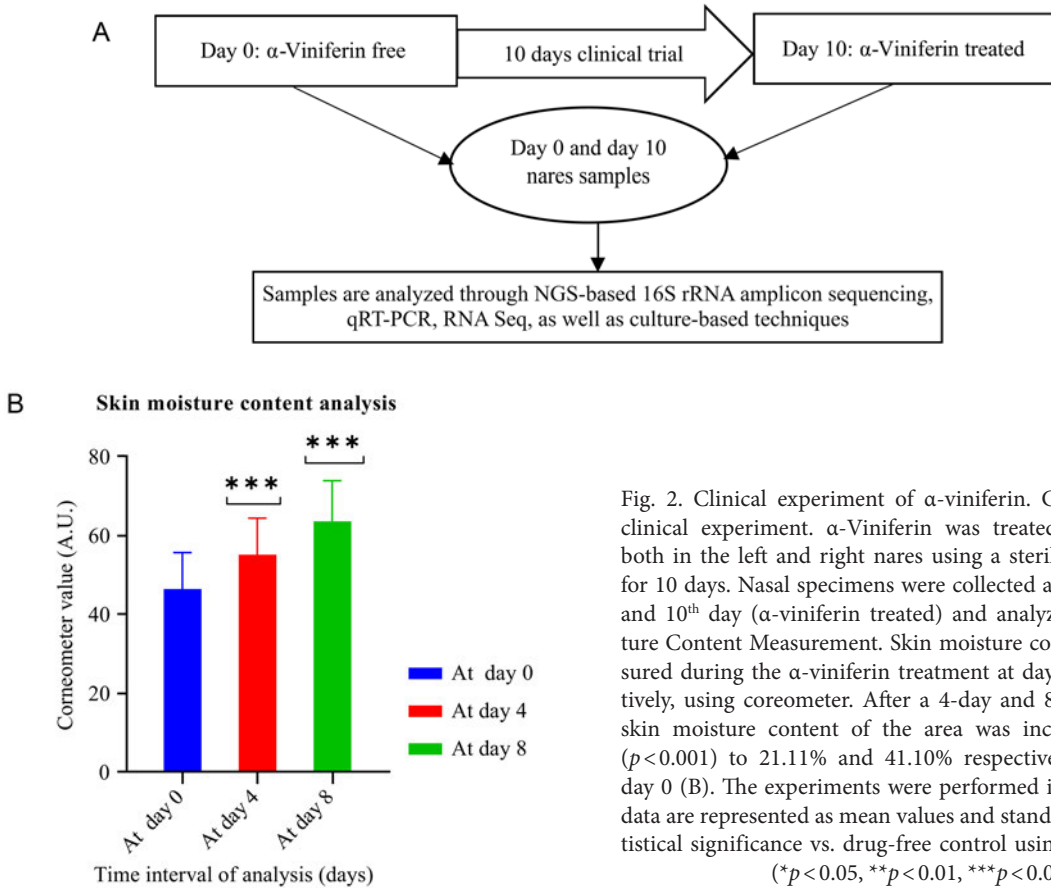


Fig. 2. Clinical experiment of α -viniferin. General overview of clinical experiment. α -Viniferin was treated three times daily both in the left and right nares using a sterile cotton swab stick for 10 days. Nasal specimens were collected at 0th day (drug-free) and 10th day (α -viniferin treated) and analyzed (A). Skin Moisture Content Measurement. Skin moisture content was also measured during the α -viniferin treatment at day 0, 4, and 8 respectively, using coreometer. After a 4-day and 8-day treatment, the skin moisture content of the area was increased dramatically ($p < 0.001$) to 21.11% and 41.10% respectively, compared to at day 0 (B). The experiments were performed in triplicate, and the data are represented as mean values and standard deviations. *Statistical significance vs. drug-free control using one-way ANOVA (* $p < 0.05$, ** $p < 0.01$, *** $p < 0.001$).

the clinical trial (day 10), and we analyzed them through culture-based and molecular-based techniques (Fig. 2A). We also measured each participant's skin surface's hydration level using a corneometer at day 0, fourth, and eighth, respectively, and then the corneometer value, A.U, was analyzed. We observed that skin moisture content increased to a statistically significant level ($p < 0.001$) at day 4 (21.11%) and at day 8 (41.10%), compared to day 0, demonstrating the moisturizing power of α -viniferin (Fig. 2B).

Skin irritation test. A skin irritation test of α -viniferin was done in 32 healthy females in different loca-

tions before performing the clinical trial; with all participants, after the patch was attached for 48 hours, α -viniferin did not show skin irritation or allergic reactions at 30 mins and 24 hours after patch removal. The mean values with three different α -viniferin concentrations in both cases were 0.00 and were classified as having a low range (0.00–0.87) irritation potential according to the classification criteria (Table I). These results ensure the safety profile of α -viniferin as a topical agent.

Culture-based quantification. To enumerate the culturable bacteria, *S. aureus*, and MRSA in the drug-free and α -viniferin-treated samples, we collected nasal

Table I
Skin irritation test result.

Material's name	No. responder	30 min. after patch removal (48 hrs.)						24 hrs. after patch removal (72 hrs.)						Mean ^a
		0.5+	1+	2+	3+	4+	mean	0.5+	1+	2+	3+	4+	mean	
1. α -viniferin 10	0	- ^b	-	-	-	-	0.00	-	-	-	-	-	0.00	0.00
2. α -viniferin 100	0	-	-	-	-	-	0.00	-	-	-	-	-	0.00	0.00
3. α -viniferin 1,000	0	-	-	-	-	-	0.00	-	-	-	-	-	0.00	0.00
4. Negative control	0	-	-	-	-	-	0.00	-	-	-	-	-	0.00	0.00

^a - Mean: (mean value of skin reaction at 48 hrs. + mean value of skin reaction at 72 hrs.)/2. (Mean score: 0.00–0.87, low; 0.88–2.42, mild; 2.43–3.44, moderate; 3.45–4.00, severe)

^b - "-": No reaction. (Reaction score: 0, -, no reaction; 0.5, ±, Barely perceptible erythema, Doubtful or questionable reaction; 1, +, Slight erythema, either spotty or diffuse; 2, ++, Moderate uniform erythema; 3, +++, Intense redness with edema; 4, +++++, Intense redness with edema and vesicles).

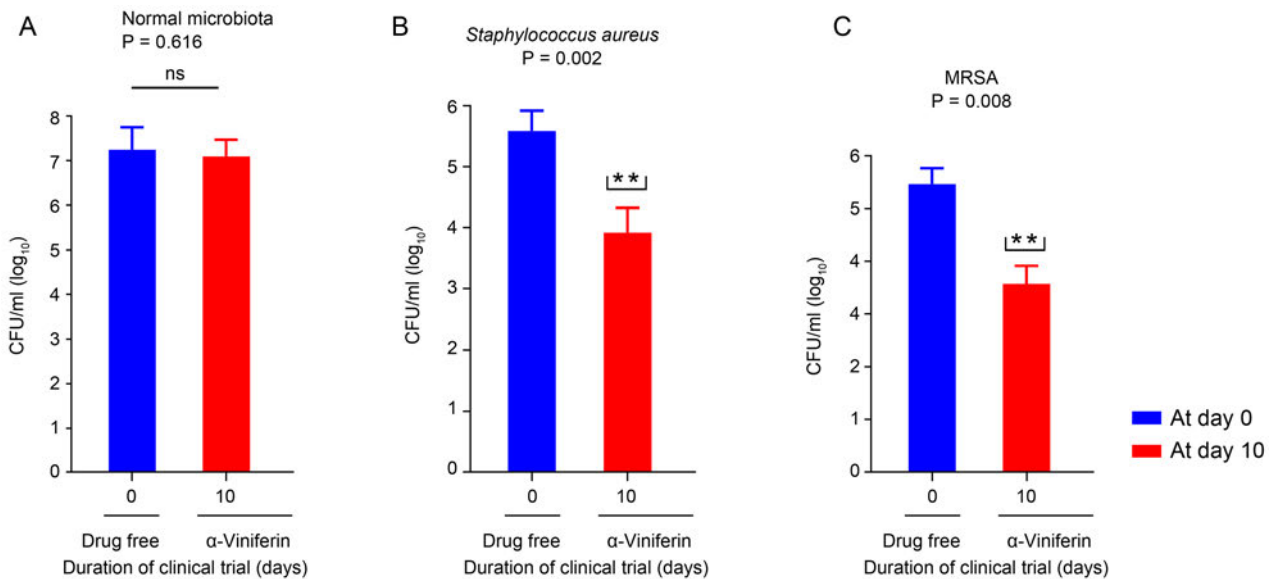


Fig. 3. Culture-based quantification. Nasal swab samples of 0 and 10th days were collected and incubated in nutrient agar, staphylococcus agar media 110, and staphylococcus agar media 110 containing methicillin antibiotic for 48 hours at 37°C by using spread plate technique. After this period, antimicrobial activity was determined by the colony forming unit (CFU) method against normal flora (A), *S. aureus* (B), and MRSA (C), respectively. The experiments were performed in triplicate, and the data are represented as mean values and standard deviations. *Statistical significance vs. drug-free control using unpaired two-tailed Student's *t*-test (* $p < 0.05$, ** $p < 0.01$, *** $p < 0.001$).

specimens on day 0 and tenth. We assayed them on the nutrient agar, staphylococcus agar medium, and a staphylococcus agar medium containing methicillin (50 µg/ml) through spread-plate techniques. After incubation, we analyzed the resulting CFU data, which revealed that the samples' bacterial content remained almost constant throughout the clinical trial period. The average number of commensal bacteria before and after the treatment was 1.7×10^7 CFU/ml and 1.2×10^7 CFU/ml, respectively, and the p was 0.616 ($p > 0.05$) (Fig. 3A), indicating lack of significant change in bacterial content after α -viniferin treatment. On the other hand, the average number of *S. aureus* before and after the treatment was 3.8×10^5 CFU/ml and 8.3×10^3 CFU/ml, respectively, and the p was 0.002 ($p < 0.01$) (Fig. 3B). The MRSA number was 7.8×10^4 CFU/ml and 2.9×10^3 CFU/ml, respectively, and the p was 0.008 (Fig. 3C), indicating a significant reduction in the number of *S. aureus* and MRSA during the clinical trial. Overall, the culture-based quantification results demonstrate α -viniferin as an antibacterial agent with specific activity against the *staphylococcus* group, including MRSA without affecting the nares' resident normal microbiota.

qRT-PCR-based quantification. We did qRT-PCR using *S. aureus*- and MRSA-specific primers to evaluate and quantify these organisms in the nares samples. We then analyzed the resulting C_t value and found that the C_t values for *S. aureus* and MRSA increased, which indicated the reduction of the organism populations. It is also noteworthy that there was no noticeable change in the C_t value of normal microbiota ($p > 0.05$) (Fig. 43).

In Fig. 4B, the difference of the C_t value between the columns is four, which indicates that the *S. aureus* number was reduced 16-fold while the MRSA number decreased 32-fold (Fig. 4C). Since we know that in each amplification cycle, the target doubles exponentially, and the C_t value is inversely related to the content of starting material. To calculate the reduction of bacterial numbers in the samples, we generated a qRT-PCR standard curve (Fig. 4D). Comparing the analyzed data with this curve, the initial and final average C_t value of *S. aureus* was 31 and 35 ($p < 0.01$), which corresponded to 1.6×10^4 CFU/ml and 1×10^3 CFU/ml, respectively. Furthermore, MRSA's initial and final average C_t value was 32 and 37 ($p < 0.001$), which corresponded to 1×10^4 CFU/ml and 3.2×10^2 CFU/ml, respectively. Based on the C_t values in this study, we can conclude that α -viniferin treatment did not significantly change the microbiota, but the prevalence of *S. aureus*, including MRSA, changed significantly. These findings demonstrated the specific antimicrobial effectiveness of α -viniferin against *S. aureus* and MRSA.

NGS-based 16s rRNA profiling. To determine the whole bacterial composition throughout the α -viniferin-treatment period, we did 16S rRNA amplicon sequencing. Based on the results, the *Staphylococcaceae* family and *Staphylococcus* genus were the most abundant in the nares, covering 51.04% and 51.03% of the whole microbial community. After α -viniferin treatment, we observed that the organisms decreased from 51.04% to 23.99% at the family level and 51.03% to 23.99% at the genus level (Fig. 5).

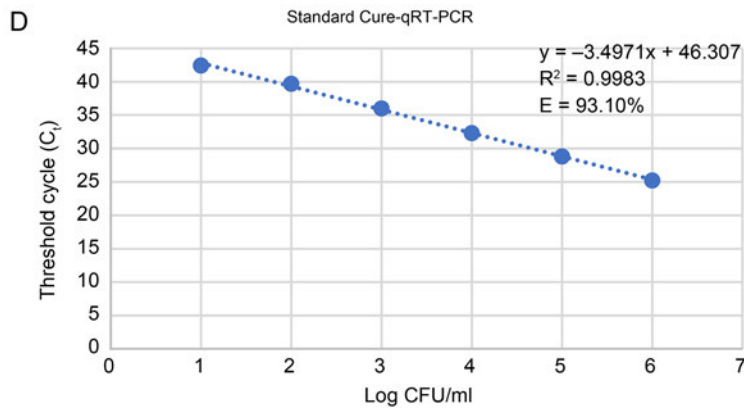
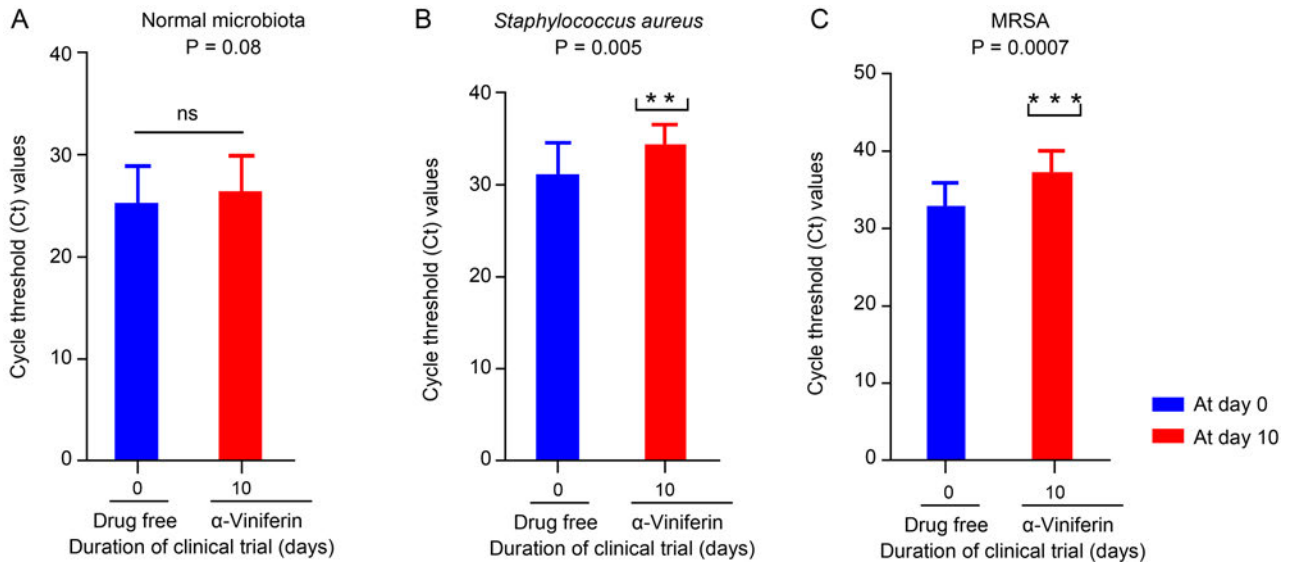


Fig. 4. qRT-PCR-based quantification. Nares swab samples of 0 and 10th days were collected, following by DNA extraction and qRT-PCR was performed. Antimicrobial activity of α-viniferin (A, B, C) was determined by comparing the resulting C_t value with the standard curve (D) against normal flora, *S. aureus*, and MRSA, respectively. The experiments were carried out 3 times, and the data are given as mean values and standard deviations. * Statistical significance vs. drug-free control using unpaired two-tailed Students' *t*-test (**p* < 0.05, ***p* < 0.01, ****p* < 0.001).

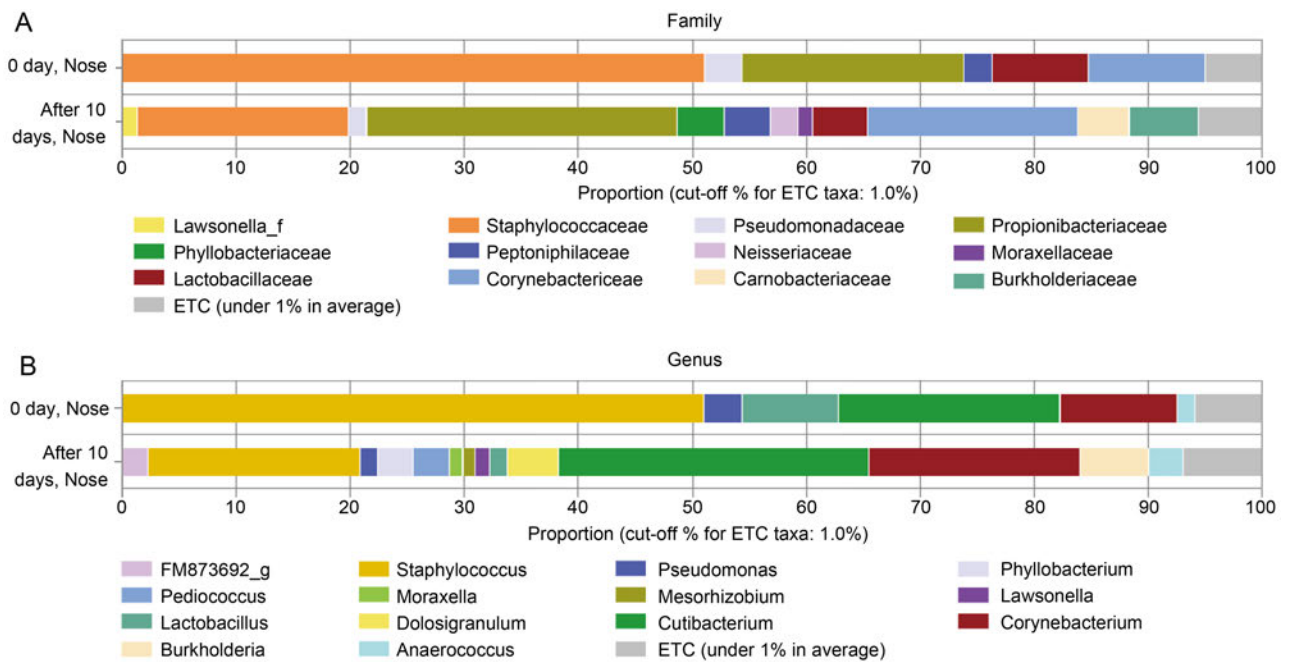


Fig. 5. NGS-based 16S rRNA profiling. To know the whole bacterial composition throughout the α-viniferin treatment, we conducted 16S rRNA amplicon sequencing with 0th (α-viniferin-free) and 10th days (α-viniferin treated) nasal swab samples, and the resulting data was analyzed by Ezcloud software. *Staphylococcaceae* is the most dominant family, which decreased from 51.04% to 23.99% (A), and *Staphylococcus* is the most abundant among the genus level group that reduced from 51.03% to 23.99% (B) after the α-viniferin treatment.

Table II
Number of genes (FC cutoff > 2 and 5) regulated in *S. aureus* by 1× and 2× MIC α-viniferin treatment for 8 hours at 37°C, according to functional class.

Functional classification	Total number of genes	2-fold				5-fold			
		1 × MIC		2 × MIC		1 × MIC		2 × MIC	
		up	down	up	down	up	down	up	down
1 DNA metabolism	92	9	2	20	11	2	0	2	0
2 Energy metabolism	126	10	17	22	31	1	5	5	11
3 Protein synthesis	85	5	4 ^a	12	15	0	0	1	1
4 Transport and binding proteins	195	29 ^b	32 ^b	42 ^a	48 ^b	4	4	16 ^b	19
5 Protein fate	77	5	4 ^a	13	10	2	1	6	1
6 Amino acid biosynthesis	62	13 ^b	5	25	5 ^a	3 ^a	2	11	2
7 Signal transduction	13	0	3	0	3	0	0	0	2
8 Purines, pyrimidines, nucleosides, and nucleotides	37	1	5	2	7	1	0	1	2
9 Regulatory functions; Signal transduction	9	0	2	1	4	0	1	0	1
10 Cellular processes	90	9	11	15	21	0	5	5	8
11 Biosynthesis of cofactors, prosthetic groups, and carriers; Transport and binding proteins	3	0	2	0	2	0	1	0	1
12 Central intermediary metabolism	21	1	4	6	7	0	2	1	3
13 Regulatory functions	55	3	8	6	11	1	1	1	3
14 DNA metabolism; Regulatory functions; Cellular processes	1	0	0	0	0	0	0	0	0
15 Cell envelope	50	4	4	8	11	0	0	1	1
16 Cellular processes; Transport and binding proteins	13	5 ^b	2	5	1	2 ^a	0	3 ^a	0
17 Energy metabolism; Purines, pyrimidines, nucleosides, and nucleotides	2	0	0	0	1	0	0	0	0
18 Transcription	22	1	2	3	3	0	0	0	1
19 Biosynthesis of cofactors, prosthetic groups, and carriers	99	8	7 ^a	25 ^a	13 ^a	1	3	6	2
20 Protein fate; Energy metabolism	4	0	1	1	1	0	0	0	1
21 Fatty acid and phospholipid metabolism	24	0	2	3	3	0	0	0	0
22 Transport and binding proteins; Signal transduction	10	0	2	2	3	0	0	0	1
23 Hypothetical proteins	26	3	3	5	4	1	1	3	3
24 Cell envelope; Central intermediary metabolism	1	0	0	0	0	0	0	0	0
25 DNA metabolism; Mobile and extrachromosomal element functions	3	1	0	1	0	0	0	1	0
26 Cellular processes; DNA metabolism	8	0	2	1	4 ^a	0	0	0	0
27 Protein fate; Transport and binding proteins	1	0	0	0	0	0	0	0	0
28 Regulatory functions; Purines, pyrimidines, nucleosides, and nucleotides	1	0	0	0	0	0	0	0	0
29 Protein fate; Cellular processes	6	1	0	1	0	0	0	0	0
30 Energy metabolism; Central intermediary metabolism	1	0	0	0	0	0	0	0	0
31 Regulatory functions; Cellular processes	2	0	1	0	1	0	0	0	0
32 Signal transduction; Regulatory functions	1	0	0	0	0	0	0	0	0
33 DNA metabolism; Cellular processes	3	0	1	1	1	0	0	0	0
34 Biosynthesis of cofactors, prosthetic groups, and carriers; Central intermediary metabolism	1	0	0	1	0	0	0	0	0
35 Mobile and extrachromosomal element functions	32	1	1	5	1	0	0	0	0
36 Protein synthesis; Cellular processes; Regulatory functions	1	0	0	0	0	0	0	0	0
37 Cellular processes; Cell envelope	2	0	0	0	0	0	0	0	0
38 Transport and binding proteins; Cellular processes	2	0	0	0	0	0	0	0	0
39 Protein fate; Cell envelope	3	0	1	1	0	0	0	0	0

Table II, Continued

Functional classification	Total number of genes	2-fold				5-fold			
		1 × MIC		2 × MIC		1 × MIC		2 × MIC	
		up	down	up	down	up	down	up	down
40 Cell envelope; Cellular processes	4	0	0	1	1	0	0	0	0
41 Cell envelope; Transport and binding proteins	4	1	0	1	0	0	0	0	0
42 Regulatory functions; Transport and binding proteins	2	0	0	0	1	0	0	0	0
43 DNA metabolism; Regulatory functions	3	0	0	0	0	0	0	0	0
44 Cellular processes; Protein fate	4	0	0	0	1	0	0	0	0
45 Mobile and extrachromosomal element functions; Regulatory functions	3	0	1	0	1	0	0	0	1
46 Mobile and extrachromosomal element functions; Hypothetical proteins	2	0	0	0	0	0	0	0	0
47 Protein fate; Signal transduction	3	0	1	1	1	0	0	0	0
48 Regulatory functions; Amino acid biosynthesis	2	0	1	0	0	0	0	0	0
49 Purines, pyrimidines, nucleosides, and nucleotides; Central intermediary metabolism	1	0	0	0	0	0	0	0	0
50 Protein synthesis; Biosynthesis of cofactors, prosthetic groups, and carriers	1	0	0	0	0	0	0	0	0
51 Regulatory functions; Central intermediary metabolism	2	0	1	0	1	0	0	0	0
52 Protein fate; Regulatory functions	3	0	0	2	0	0	0	0	0
53 Regulatory functions; Energy metabolism	1	0	1	0	0	0	0	0	0
54 Mobile and extrachromosomal element functions; Protein fate	1	0	0	1	0	0	0	0	0
55 Regulatory functions; Central intermediary metabolism; Signal transduction	1	0	1	0	1	0	1	0	1
56 Central intermediary metabolism; Cell envelope	1	0	0	0	0	0	0	0	0
57 Cellular processes; Mobile and extrachromosomal element functions	4	0	0	0	0	0	0	0	0
58 Protein fate; Purines, pyrimidines, nucleosides, and nucleotides	1	0	1	0	1	0	0	0	1

^a - $p < 0.05$; ^b - $p < 0.01$; ^c - $p < 0.001$

Exploring α -viniferin-induced gene expression in *S. aureus*. We verified the integrity of extracted total RNA by the sharpness of the ribosomal RNA bands visualized on the 2% agarose gel using ethidium bromide. We observed distinct 23S and 16S rRNA bands without degradation in all samples tested (Fig. S1). Then, we did transcriptional profiling of *S. aureus* using 2,842 whole-genome RNA sequencing to measure the effects of α -viniferin relative to a sample of logarithmically growing *S. aureus*. Compared with the drug-free control group, 583 (1 × MIC, 8 h) and 1,057 (2 × MIC, 8 h) genes had expression levels altered 2-fold. When the FC cutoff was raised to 5-fold, we found that 94 (1 × MIC, 8 h) and 256 (2 × MIC, 8 h) genes had altered expression levels in the α -viniferin-treated group (Table II). To better understand the transcriptional response of *S. aureus* to α -viniferin, we adopted more specific functional classifications. We used a hypergeometric distribution to determine whether the enrichment of genes within a particular functional category in

response to α -viniferin-treatment was significant. We observed that protein synthesis, transport, and binding proteins, protein fate, amino acid biosynthesis, cellular processes; transport and binding proteins, biosynthesis of cofactors, prosthetic group, and carriers, cellular processes, and DNA metabolism functional groups were significantly reduced five-fold when the bacteria were treated with a drug at a concentration equal to 2 × MIC (Table III). These results demonstrated how α -viniferin inhibited the growth of the *Staphylococcus* group.

Discussion

In a 10-day clinical trial, we investigated the decolonization efficiency of α -viniferin as an *S. aureus*-specific drug candidate. Before the clinical trial, we checked the specific toxicity of α -viniferin and two other reference drugs against 20 bacterial isolates. α -Viniferin showed excellent antibacterial effectiveness against the

Table III

Number of (FC cutoff > 2 and 5) specific regulated gene groups in *S. aureus* by 1 × and 2 × MIC α-viniferin treatment for 8 hours at 37°C, according to functional classification.

Functional classification	Total number of genes	2-fold				5-fold			
		1 × MIC		2 × MIC		1 × MIC		2 × MIC	
		up	down	up	down	up	down	up	down
3 Protein synthesis									
a tRNA aminoacylation	12	1	1	1	4	0	0	1	1
b Ribosomal proteins: synthesis and modification	25	2	3	5	4	0	0	0	0
c tRNA and rRNA base modification	37	2	0	6	4	0	0	0	0
d Other	85	9	8	16	18	2	0	6	2
e Translation factors	7	0	0	0	2	0	0	0	0
4 Transport and binding proteins									
a Amino acids, peptides and, amines	32	5	2	7	4	0	1	4a	1
b Cations and iron carrying compounds	72	8	9	12	10	1	0	2	3
c Carbohydrates, organic alcohols, and acids	27	4	6	7	8	1	1	3	5b
d Anions	18	4	2	5	10	0	1	2	5
e Anions; Other	1	1	0	1	0	0	0	1a	0
f Other	85	9	8	16	18	2	0	6	2
g Nucleosides, purines and, pyrimidines	6	0	3	0	5b	0	1	0	3b
h Unknown substrate	20	3	6	6	6	0	0	1	2
i Cations and iron carrying compounds; Anions	3	0	1	0	2	0	0	0	0
5 Protein fate									
a Protein and peptide secretion and trafficking	27	2	2	3	5	0	0	2	0
b Degradation of proteins, peptides, and glycopeptides	18	1	0	5	0	0	0	2	0
c Protein modification and repair	20	0	0	0	3	0	0	0	0
d Protein folding and stabilization	4	2a	1	2	1	2b	1	2a	1
e Degradation of proteins, peptides, and glycopeptides; Protein folding and stabilization	6	0	0	3	0	0	0	0	0
f Degradation of proteins, peptides, and glycopeptides; Protein modification and repair	1	0	0	0	0	0	0	0	0
g Protein and peptide secretion and trafficking; Protein modification and repair	1	0	1	0	1	0	0	0	0
6 Amino acid biosynthesis									
a Aspartate family	15	3	1	8b	0	1	0	3a	0
b Serine family	11	3	0	4	2	0	0	1	0
c Glutamate family	7	0	3a	0	2	0	1	0	1
d Pyruvate family	12	5b	1	8	1	0	1	5	1
e Histidine family	8	0	0	2	0	0	0	0	0
f Aromatic amino acid family	9	2	0	3	0	2b	0	2	0
16 Cellular processes; Transport and binding proteins									
a Toxin production and resistance; Other	13	3	1	4	1	2a	0	3a	0
b Toxin production and resistance; Unknown substrate	3	2a	1	1	0	0	0	0	0
c Detoxification; Other	1	0	0	0	0	0	0	0	0
19 Biosynthesis of cofactors, prosthetic groups, and carriers									
a Glutathione and analogs	4	0	0	1	1	0	0	0	0
b Menaquinone and ubiquinone	17	0	0	3	1	0	0	0	0
c Other	85	9	8	16	18	2	0	6	2
d Heme, porphyrin, and cobalamin	19	3	2	7a	2	0	1	2	1
e Folic acid	6	0	0	0	0	0	0	0	0
f Pyridoxine	2	0	2 ^a	0	2 ^a	0	2	0	0

Table III. Continued

Functional classification	Total number of genes	2-fold				5-fold			
		1 × MIC		2 × MIC		1 × MIC		2 × MIC	
		up	down	up	down	up	down	up	down
g Riboflavin, FMN, and FAD	6	0	0	2	0	0	0	0	0
h Thiamine	7	0	0	0	2	0	0	0	0
i Lipoate	1	0	0	0	0	0	0	0	0
j Other; Thiamine; Pyridoxine	2	0	0	0	0	0	0	0	0
k Pantothenate and coenzyme A	6	0	1	1	1	0	0	0	0
l Biotin	6	2	0	4 ^a	0	1	0	2 ^a	0
m Pyridine nucleotides	2	0	0	0	0	0	0	0	0
n Molybdopterin	4	1	0	2	0	0	0	0	0
26 Cellular processes; DNA metabolism									
a Cell division; Chromosome-associated proteins	8	0	2	1	4 ^a	0	0	0	0

^a - $p < 0.05$; ^b - $p < 0.01$; ^c - $p < 0.001$

Staphylococcus group. On the other hand, several reports showed VAN resulted in rapid depletion of intestinal microflora and significantly promoted the growth of vancomycin-resistant bacteria (Edlund et al. 1997; Isaac et al. 2016) highlighting the drawbacks of VAN even though it was the most effective anti-*Staphylococcus* reference drug in the present MIC study. We have also tested MET as another reference drug.

In this study, we analyzed the nasal swab samples through culture-based techniques to investigate the antimicrobial effectiveness of α -viniferin against the nares normal microflora, *S. aureus*, and MRSA. α -Viniferin was active against *S. aureus* and MRSA but showed no activity against nasal microflora. To further confirm this, we did qRT-PCR using *S. aureus*- and MRSA-specific primers since precise detection and quantification are achievable by using this technique. Expectedly, α -viniferin was active against *S. aureus* and MRSA while preserving the resident nasal microflora. Moreover, α -viniferin improved the skin moisture content, which is essential in maintaining skin plasticity and barrier integrity without toxicity.

In addition, we used NGS-based 16S rRNA profiling to investigate further the clinical efficiency of α -viniferin against the *Staphylococcus* group. We also evaluated the effect of α -viniferin against normal nasal microflora using NGS, where NGS upgrades DNA sequencing methodology to the next level through parallel sequencing processes that enable the simultaneous sequencing of different DNA fragments while providing precise identification results (Abayasekara et al. 2017). The NGS results demonstrated *Staphylococcus* as the most dominant group in the anterior nares, supporting similar published findings (Hogan et al. 2016; Warnke et al. 2016; Lu et al. 2018). α -Viniferin drastically reduced the number of *Staphylococcus* in

the anterior nares, while the decrease in the number of other bacteria groups was statistically insignificant. The important thing is that α -viniferin significantly decreased the *Staphylococcus* group. This molecular approach provides evidence of the antimicrobial specificity of α -viniferin as a pathogen-specific potential drug, and the results were consistent with the culture and qRT-PCR-based findings. The results were also in agreement with a previous study finding that demonstrated the *in vitro* activity of α -viniferin against MRSA (Seo et al. 2017).

RNA sequencing technology is a powerful tool for studying the molecular basis of genetic interactions; it makes it possible to examine the relatively unbiased measurements of expression levels across the entire length of a transcript using high-throughput sequencing platforms (Pickrell et al. 2010). In the present study we did RNA sequencing to understand α -viniferin-induced gene expression in *S. aureus*. Our results showed that α -viniferin inhibits the growth of *S. aureus*, which may be attributed to its effects on some of the gene groups mentioned. Further research is required to elucidate this finding. In conclusion, we demonstrated the clinical efficiency of α -viniferin as a potential *S. aureus*-specific drug candidate for the first time through a clinical trial.

Acknowledgments

This research was financially supported by the Minister of SMEs (Small and Medium-sized Enterprises) and Startups (MSS), Korea, under the "SME Technology Innovation Development Project" (reference number S2612483) supervised by the Korea Technology and Information Promotion Agency for SMEs (TIPA). This study was also supported by Soonchunhyang University Research Fund.

We want to thank all the staff members and our subjects for their interest and willingness to participate in the project and efforts towards this study.

Conflict of interest

The authors do not report any financial or personal connections with other persons or organizations, which might negatively affect the contents of this publication and/or claim authorship rights to this publication.

Literature

- Abayasekara LM, Perera J, Chandrasekharan V, Gnanam VS, Udunuwara NA, Liyanage DS, Bulathsinhala NE, Adikary S, Aluthmuhandiram JVS, Thanaseelan CS, et al. Detection of bacterial pathogens from clinical specimens using conventional microbial pathway and 16S metagenomics: A comparative study. *BMC Infect Dis.* 2017 Sep 19;17(1):631. <https://doi.org/10.1186/s12879-017-2727-8>
- Baur JA, Pearson KJ, Price NL, Jamieson HA, Lerin C, Kalra A, Prabhu VV, Allard JS, Lopez-Lluch G, Lewis K, et al. Resveratrol improves health and survival of mice on a high-calorie diet. *Nature.* 2006 Nov 16;444(7117):337–342. <https://doi.org/10.1038/nature05354>
- Chabán MF, Karagianni C, Joray MB, Toumpa D, Sola C, Crespo MI, Palacios SM, Athanassopoulos CM, Carpinella MC. Antibacterial effects of extracts obtained from plants of Argentina: Bioguided isolation of compounds from the anti-infectious medicinal plant *Lepechinia meyenii*. *J Ethnopharmacol.* 2019 Jul 15; 239:111930. <https://doi.org/10.1016/j.jep.2019.111930>
- Chambers HF, Deleo FR. Waves of resistance: *Staphylococcus aureus* in the antibiotic era. *Nat Rev Microbiol.* 2009 Sep;7(9):629–641. <https://doi.org/10.1038/nrmicro2200>
- Chew YL, Chan EW, Tan PL, Lim YY, Stanslas J, Goh JK. Assessment of phytochemical content, polyphenolic composition, antioxidant and antibacterial activities of Leguminosae medicinal plants in Peninsular Malaysia. *BMC Complement Altern Med.* 2011 Feb 10;11:12. <https://doi.org/10.1186/1472-6882-11-12>
- Chung EY, Kim BH, Lee MK, Yun YP, Lee SH, Min KR, Kim Y. Anti-inflammatory effect of the oligomeric stilbene α -viniferin and its mode of the action through inhibition of cyclooxygenase-2 and inducible nitric oxide synthase. *Planta Med.* 2003 Aug;69(8):710–714. <https://doi.org/10.1055/s-2003-42787>
- Davies KA, Planche T, Wilcox MH. The predictive value of quantitative nucleic acid amplification detection of *Clostridium difficile* toxin gene for faecal sample toxin status and patient outcome. *PLoS One.* 2018 Dec 5;13(12):e0205941. <https://doi.org/10.1371/journal.pone.0205941>
- Del Vecchio VG, Petroziello JM, Gress MJ, McCleskey FK, Melcher GP, Crouch HK, Lupski JR. Molecular genotyping of methicillin-resistant *Staphylococcus aureus* via fluorophore-enhanced repetitive-sequence PCR. *J Clin Microbiol.* 1995 Aug;33(8):2141–2144. <https://doi.org/10.1128/JCM.33.8.2141-2144.1995>
- Dionne LL, Raymond F, Corbeil J, Longtin J, Gervais P, Longtin Y. Correlation between *Clostridium difficile* bacterial load, commercial real-time PCR cycle thresholds, and results of diagnostic tests based on enzyme immunoassay and cell culture cytotoxicity assay. *J Clin Microbiol.* 2013 Nov;51(11):3624–3630. <https://doi.org/10.1128/JCM.01444-13>
- Edlund C, Barkholt L, Olsson-Liljequist B, Nord CE. Effect of vancomycin on intestinal flora of patients who previously received antimicrobial therapy. *Clin Infect Dis.* 1997 Sep;25(3):729–732. <https://doi.org/10.1086/513755>
- Fan Y, Zhao L, Huang X, Jia Q, Wang W, Gao M, Jia X, Chang Y, Ouyang H, He J. Pharmacokinetic and bioavailability studies of α -viniferin after intravenous and oral administration to rats. *J Pharm Biomed Anal.* 2020 Sep 5;188:113376. <https://doi.org/10.1016/j.jpba.2020.113376>
- Frank DN, Feazel LM, Bessesen MT, Price CS, Janoff EN, Pace NR. The human nasal microbiota and *Staphylococcus aureus* carriage. *PLoS One.* 2010 May 17;5(5):e10598. <https://doi.org/10.1371/journal.pone.0010598>
- Frosch PJ, Kligman AM. The soap chamber test. A new method for assessing the irritancy of soaps. *J Am Acad Dermatol.* 1979 Jul;1(1): 35–41. [https://doi.org/10.1016/s0190-9622\(79\)70001-6](https://doi.org/10.1016/s0190-9622(79)70001-6)
- Hogan B, Rakotozandrindrainy R, Al-Emran H, Dekker D, Hahn A, Jaeger A, Poppert S, Frickmann H, Hagen RM, Mischeel V et al. Prevalence of nasal colonisation by methicillin-sensitive and methicillin-resistant *Staphylococcus aureus* among healthcare workers and students in Madagascar. *BMC Infect Dis.* 2016 Aug 15; 16(1):420. <https://doi.org/10.1186/s12879-016-1733-6>
- Isaac S, Scher JU, Djukovic A, Jiménez N, Littman DR, Abramson SB, Pamer EG, Ubeda C. Short- and long-term effects of oral vancomycin on the human intestinal microbiota. *J Antimicrob Chemother.* 2017 Jan;72(1):128–136. <https://doi.org/10.1093/jac/dkw383>
- Islam MZ, Johannesen TB, Lilje B, Urth TR, Larsen AR, Angen Ø, Larsen J. Investigation of the human nasal microbiome in persons with long- and short-term exposure to methicillin-resistant *Staphylococcus aureus* and other bacteria from the pig farm environment. *PLoS One.* 2020 Apr 30;15(4):e0232456. <https://doi.org/10.1371/journal.pone.0232456>
- Kinch MS, Patridge E, Plummer M, Hoyer D. An analysis of FDA-approved drugs for infectious disease: antibacterial agents. *Drug Discov Today.* 2014 Sep;19(9):1283–1287. <https://doi.org/10.1016/j.drudis.2014.07.005>
- Lachapelle J-M, Maibach HI. Patch testing and prick testing: A practical guide official publication of the ICDRG. Cham (Switzerland): Springer Nature; 2020. <https://doi.org/10.1007/978-3-030-27099-5>
- Lowy FD. *Staphylococcus aureus* infections. *N Engl J Med.* 1998 Aug 20;339(8):520–532. <https://doi.org/10.1056/NEJM199808203390806>
- Lu YJ, Sasaki T, Kuwahara-Arai K, Uehara Y, Hiramatsu K. Development of a new application for comprehensive viability analysis based on microbiome analysis by next-generation sequencing: Insights into staphylococcal carriage in human nasal cavities. *Appl Environ Microbiol.* 2018 May 17;84(11):e00517–18. <https://doi.org/10.1128/AEM.00517-18>
- Mitchell DH, Howden BP. Diagnosis and management of *Staphylococcus aureus* bacteraemia. *Intern Med J.* 2005 Dec;35 Suppl 2:S17–24. <https://doi.org/10.1111/j.1444-0903.2005.00977.x>
- Mojumdar EH, Pham QD, Topgaard D, Sparr E. Skin hydration: interplay between molecular dynamics, structure and water uptake in the stratum corneum. *Sci Rep.* 2017 Nov 16;7(1):15712. <https://doi.org/10.1038/s41598-017-15921-5>
- Pereira EM, Schuenck RP, Malvar KL, Iorio NL, Matos PD, Olendzki AN, Oelemann WM, dos Santos KR. *Staphylococcus aureus*, *Staphylococcus epidermidis* and *Staphylococcus haemolyticus*: Methicillin-resistant isolates are detected directly in blood cultures by multiplex PCR. *Microbiol Res.* 2010 Mar 31;165(3):243–249. <https://doi.org/10.1016/j.micres.2009.03.003>
- Pickrell JK, Marioni JC, Pai AA, Degner JF, Engelhardt BE, Nkadori E, Veyrieras JB, Stephens M, Gilad Y, Pritchard JK. Understanding mechanisms underlying human gene expression variation with RNA sequencing. *Nature.* 2010 Apr 1;464(7289):768–772. <https://doi.org/10.1038/nature08872>
- Rainer BM, Thompson KG, Antonescu C, Florea L, Mongodin EF, Bui J, Fischer AH, Pasioka HB, Garza LA, Kang S, et al. Characterization and analysis of the skin microbiota in rosacea: A case-control study. *Am J Clin Dermatol.* 2020 Feb;21(1):139–147. <https://doi.org/10.1007/s40257-019-00471-5>
- Saliba AE, C Santos S, Vogel J. New RNA-seq approaches for the study of bacterial pathogens. *Curr Opin Microbiol.* 2017 Feb;35:78–87. <https://doi.org/10.1016/j.mib.2017.01.001>

Seo H, Kim M, Kim S, Mahmud HA, Islam MI, Nam KW, Cho ML, Kwon HS, Song HY. In vitro activity of alpha-viniferin isolated from the roots of *Carex humilis* against *Mycobacterium tuberculosis*. *Pulm Pharmacol Ther.* 2017 Oct;46:41–47.

<https://doi.org/10.1016/j.pupt.2017.08.003>

Sim J, Jang HW, Song M, Kim JH, Lee SH, Lee S. Potent inhibitory effect of alpha-viniferin on human cytochrome P450. *Food Chem Toxicol.* 2014 Jul;69:276–280.

<https://doi.org/10.1016/j.fct.2014.04.023>

Song M, Zeng Q, Xiang Y, Gao L, Huang J, Huang J, Wu K, Lu J. The antibacterial effect of topical ozone on the treatment of MRSA skin infection. *Mol Med Rep.* 2018 Feb;17(2):2449–2455.

<https://doi.org/10.3892/mmr.2017.8148>

Warnke P, Devidé A, Weise M, Frickmann H, Schwarz NG, Schäffler H, Ottl P, Podbielski A. Utilizing moist or dry swabs for the sampling of nasal MRSA carriers? An *in vivo* and *in vitro* study. *PLoS One.* 2016 Sep 14;11(9):e0163073.

<https://doi.org/10.1371/journal.pone.0163073>

You HS, Lee SH, Ok YJ, Kang HG, Sung HJ, Lee JY, Kang SS, Hyun SH. Influence of swabbing solution and swab type on DNA recovery from rigid environmental surfaces. *J Microbiol Methods.* 2019 Jun;161:12–17.

<https://doi.org/10.1016/j.mimet.2019.04.011>

Supplementary materials are available on the journal's website.

Growth Inhibition of Phytopathogenic Fungi and Oomycetes by Basidiomycete *Irpex lacteus* and Identification of its Antimicrobial Extracellular Metabolites

DAISY PINEDA-SUAZO¹ , JOSAPHAT MIGUEL MONTERO-VARGAS² , JOSÉ JUAN ORDAZ-ORTIZ² 
and GERARDO VÁZQUEZ-MARRUFO^{1*} 

¹ Centro Multidisciplinario de Estudios en Biotecnología, Facultad de Medicina Veterinaria y Zootecnia,
Universidad Michoacana de San Nicolás de Hidalgo, Morelia, Michoacán, Mexico

² Unidad de Genómica Avanzada, CINVESTAV-IPN, Irapuato, Guanajuato, Mexico

Submitted 18 December 2020, revised 17 February 2021, accepted 23 February 2021

Abstract

In dual culture confrontation assays, basidiomycete *Irpex lacteus* efficiently antagonized *Fusarium* spp., *Colletotrichum* spp., and *Phytophthora* spp. phytopathogenic strains, with growth inhibition percentages between 16.7–46.3%. Antibiosis assays evaluating the inhibitory effect of soluble extracellular metabolites indicated *I. lacteus* strain inhibited phytopathogens growth between 32.0–86.7%. Metabolites in the extracellular broth filtrate, identified by UPLC-QTOF mass spectrometer, included nine terpenes, two aldehydes, and derivatives of a polyketide, a quinazoline, and a xanthone, several of which had antifungal activity. *I. lacteus* strain and its extracellular metabolites might be valuable tools for phytopathogenic fungi and oomycete biocontrol of agricultural relevance.

Key words: antagonism, antifungal, extracellular metabolites, mycelium, terpenes

Phytopathogenic fungi and oomycetes have caused significant losses in several crop production around the world (Dean et al. 2012; Kamoun et al. 2015). Disease control caused by these pathogens depends to a large extent on agrochemicals, which use has increased worldwide (Carvalho 2017); however, they have accumulated in the trophic chains, affecting wildlife and livestock and causing public health problems (Bourguet and Guillemaud 2016). On the other hand, phytopathogenic microorganisms have increased their resistance to several agrochemicals used to fight them (Sparks and Lorschbach 2017), so they have become less effective. Therefore, the use of alternative plant protection biocontrol methods has been intensively explored during the last decades. Biocontrol methods include both preparations containing living microorganisms and bioactive metabolites obtained from organic or aqueous extracts of different taxa, which may be specific to those that need to be controlled and have low toxicity to wild and human life (Loiseleur 2017).

Previous studies have documented efficient *in vitro* antagonism of basidiomycete species against phytopathogenic microorganisms, through the use of more than one mechanism (White and Traquair 2006; Gholami et al. 2019). A wide variety of extracts and metabolites obtained from basidiomycete fungi have shown antimicrobial activity, sufficient for growth inhibition of pathogenic microorganisms of medical and agricultural relevance (Shen et al. 2017). Due to the intrinsic ecophysiological role, metabolite production with antimicrobial activity by vegetative mycelium is relevant for species competition; hence, not only antimicrobial activity of biomass extracts but also extracellular filtrates obtained from liquid cultures of vegetative mycelium has been evaluated (Shen et al. 2017). Here we analyzed a wild *I. lacteus* strain antagonist activity against worldwide relevant phytopathogenic fungi and oomycete species. We also conducted a chemical characterization of extracellular filtrates of such strain aiming to identify putative metabolites with antifungal/antimicrobial activity. The

* Corresponding author: G. Vázquez-Marrufo, Centro Multidisciplinario de Estudios en Biotecnología, Facultad de Medicina Veterinaria y Zootecnia, Universidad Michoacana de San Nicolás de Hidalgo, Morelia, Tarímbaro, Michoacán, Mexico;

e-mail: gvazquez@umich.mx

© 2021 Daisy Pineda-Suazo et al.

This work is licensed under the Creative Commons Attribution-NonCommercial-NoDerivatives 4.0 License (<https://creativecommons.org/licenses/by-nc-nd/4.0/>).

I. lacteus strain CMU-8413 was isolated from basidiocarps collected in September 2013 from the community of Atécuaro, Michoacán, Mexico. Both data on collection and phylogenetic identification of the strain have been previously reported (Damián-Robles et al. 2017). The strain has been deposited in the Laboratorio de Conservación Microbiana y Biotecnología del Centro Multidisciplinario de Estudios en Biotecnología de la Facultad de Medicina Veterinaria y Zootecnia, de la Universidad Michoacana de San Nicolás de Hidalgo, and it may be available for research purposes upon request. The phytopathogenic strains tested correspond to fungi *Fusarium pseudocircinatum*, *Fusarium mexicanum*, *Colletotrichum coccodes*, *Colletotrichum gloeosporioides*, and oomycetes *Phytophthora capsici* and *Phytophthora cinnamomi*. All these phytopathogens have been isolated from crop fields in Michoacán, and they have been properly identified and kindly provided by Dr. Sylvia P. Fernández-Pavía, of the Universidad Michoacana.

Antagonism in dual culture and antibiosis assays were studied according to Steyaert et al. (2016) in three independent replicas for each phytopathogen. The incubation time was adjusted as described below, and incubation temperature to 28°C. The inoculum of *I. lacteus* and phytopathogens for these assays consisted of a 6 mm plug obtained from the edge of an actively growing colony in PDA at 28°C. For antagonism assays, phytopathogens were inoculated at one extreme of a 90 mm Petri plate containing potato dextrose agar (PDA) medium, and they were incubated until the colony reached a 2 cm radius. At this stage, the PDA Petri plate opposite extreme was inoculated in the same way with the *I. lacteus* strain, and then incubation was resumed. The fungi colony diameter was measured every 24 h. A respective control of axenic cultures for each phytopathogenic strain was incubated in the same condition. For antibiosis assays, Petri plates containing PDA were covered with sterilized cellophane sheets, and they were inoculated with *I. lacteus* strain in the center. After a 4-day incubation, the cellophane sheets with the mycelium were aseptically removed. This same PDA plate, on which the *I. lacteus* strain previously grew, was used for phytopathogens inoculation and incubation in independent assays, and colony diameter was measured every 24 h. Each phytopathogenic strain was inoculated in a fresh PDA medium and was incubated under the same conditions as a control.

For antagonism and antibiosis, assays were finished when the mycelium of each phytopathogen in the control plate had covered 2/3 of the surface area; then, the colony diameter was measured expressing the growth inhibition percentage according to the formula:

$$\% \text{ inhibition} = [(D1 - D2)/D1 \times 100]$$

where D1 = the phytopathogen colony diameter growing in PDA (fresh/axenic), and D2 = the phytopatho-

gen colony diameter growing in dual culture or in the medium that contained *I. lacteus* which had been previously incubated.

In antagonism in dual culture assays, *I. lacteus* showed significant growth inhibition against *F. pseudocircinatum* (46.3%), *F. mexicanum* (16.7%), *C. coccodes* (22.8%), *P. cinnamomi* (35.0%) and *P. capsici* (22.9%) (Fig. 1), and it was not able to antagonize *C. gloeosporioides*. Using the same test, White and Traquair (2006) found that *I. lacteus* showed efficient growth inhibition of *Botrytis cinerea*, and this previous work is the only antagonism study between *I. lacteus* and phytopathogenic fungi, in addition to results reported here. Antibiosis assays showed even better *I. lacteus* growth inhibitory activity against the six phytopathogenic strains tested, with growth inhibition percentages fluctuating between 32.0 and 86.7%. *C. coccodes* was the most susceptible species (Fig. 1). The antibiosis assay is used to determine if a fungal strain produces non-volatile metabolites that diffuse into the medium and affect phytopathogenic fungi growth (Steyaert et al. 2016). As far as we could document, there has been no previously published work on antibiosis assays that used basidiomycetes to test their *in vitro* activity against phytopathogenic fungi/oomycetes.

Antifungal activity of aqueous and organic extracts from basidiocarp and vegetative mycelium of *I. lacteus* (Shen et al. 2017) had been documented. However, reports evaluating the antifungal activity of extracellular broth filtrates from *I. lacteus* are scarce; consequently, in this work, it was of particular interest to assess such effect and identifying metabolites secreted by studied strain. The studied strain growth kinetic was conducted in 250 ml Erlenmeyer flasks with 50 ml of potato dextrose broth (PDB) medium, inoculated with six inocula obtained as previously described. The inoculated flasks were incubated at 125 rpm of orbital shaking and 28°C for 14 days. The mycelium dry weight was determined every 24 hours, and the CMU-8413 strain reached the stationary phase after a seven-day incubation (data not shown). Extracellular filtrates were recovered three days after the studied strain reached the stationary phase at the end of 10 days of incubation. Broth culture at the stationary phase was filtered through Whatman No. 1 paper. The filtrate broth was recovered and concentrated by evaporation to dryness in a rotary evaporator at 70°C, without adding any solvent. Concentrates obtained were stored for no more than one week in 1 ml vials at -4°C until biological assays were carried out. Compounds identification in culture filtrate of independent samples for each assay was performed by UPLC (Acquity™ Class I, Waters Corporation) coupled to an orthogonal QTOF mass spectrometer (Synapt™ G1, Waters Corporation), as described elsewhere (Varela-Rodríguez et al. 2019). MS data were



Fig 1. Phytopathogens growth inhibition in dual culture antagonism and antibiosis assays by *I. lacteus* (CMU-8413). In dual culture antagonism assays, *I. lacteus* was inoculated at the left. Tested phytopathogens were *Fusarium pseudocircinatum*, *Fusarium mexicanum*, *Colletotrichum coccodes*, *Colletotrichum gloeosporioides*, *Phytophthora capsici*, and *Phytophthora cinnamomi*. Assays were conducted in potato dextrose agar (PDA) medium at 28°C. Growth inhibition percentages are the mean of three independent assays and standard deviation (S.D.) is shown in parenthesis. Statistically significant ($p < 0.01$) growth inhibition values when compared with their respective control are indicated with an asterisk. Significance was determined by Student's *t*-tests, independent by groups, and they were carried out using STATISTICA data analysis software system (StatSoft, Inc. 2007, version 7. <http://www.statsoft.com>).

continuously acquired and processed with MassLynx® (version 4.1, Waters Corporation), and metabolites were putatively identified with Progenesis® QI for small molecules (Nonlinear Dynamics version 2.3, Waters Corporation) using Chemspider and Progenesis MetaScope as identification methods. The Progenesis QI software for small molecules considers precursor mass accuracy < than 5 ppm, fragmentation pattern, and isotopic similarities, each accounting for 20%. The maximum score is 60% (20 + 20 + 20), pre-identified metabolites have at least 50% of the total score.

A total of 14 extracellular metabolites (Table I) belonging to five chemical groups were found in the *I. lacteus* broth filtrate. The largest chemical group found was terpenes with nine metabolites, followed by aldehydes with two metabolites. The remaining metabolites found belong to polyketides, quinazolines, and xanone derivatives, with one metabolite each. All metabolites found in *I. lacteus* extracellular broths were previously described in other basidiomycete or ascomycete species (Table II). Eight have been described as extracellular in broth media, like here. Terpenes produced by

I. lacteus showed antifungal activity against *Nigrospora oryzae*, *C. gloeosporioides*, and *Didymella glomerata* (Wu et al. 2019). It has been previously documented among aldehydes that *I. lacteus* produces 5-pentenyl-2-furaldehyde, a potent antifungal volatile compound tested against the phytopathogens *Fusarium oxysporum* f. sp. *lycopersici*, *Colletotrichum fragariae*, and *B. cinerea* (Koitabashi et al. 2004). Also, a frequentin identified here in the *I. lacteus* broth is an aldehyde derivative that has been previously described as antifungal efficiently inhibiting spore germination in *Botrytis allii*, *Penicillium gladioli*, *Stachybotrys atra*, and *Mucor mucedo* (Curtis et al. 1951). Finally, microdiplodiasol is a xanone derivative inhibiting the growth of fungal species *Microbotryum violaceum* (Siddiqui et al. 2011). Both, previous studies and extracellular metabolites secreted to the broth by the CMU-8413 *I. lacteus* strain allowed us to anticipate its efficient antagonism and growth inhibition of phytopathogenic fungi and oomycetes.

Phytopathogens growth inhibition assays conducted in solid PDA medium were used as indicative of extracellular inhibitory metabolites by CMU-8413

Table I
Extracellular metabolites produced by *Irpex lacteus* (strain CMU-8413) at stationary phase.

Compound name	Molecular formula	Observed m/z	Adduct	Main fragment ions m/z	Compound class
Apotrichodiol	C ₁₅ H ₂₄ O ₃	251.1652	M-H	233.1547	Sesquiterpene
Apotrichothecene	C ₁₅ H ₂₄ O ₂	201.1637	M+H-2H ₂ O	157.1481, 186.1403, 173.1348, 159.1185, 145.1029, 128.0639, 115.0558, 105.0711	Sesquiterpenoid epoxide
Blennin D	C ₁₅ H ₂₂ O ₄	265.1436	M-H	237.1386, 221.1418, 205.1473, 191.1441, 187.1406, 175.1412	Sesquiterpene
Collybial	C ₁₅ H ₂₀ O ₂	215.1424	M+H-H ₂ O/ M+H	187.1512, 173.1325, 159.0804, 157.1008, 142.0792, 128.0869, 115.0534	Sesquiterpene
Cyclocalopin A	C ₁₅ H ₂₀ O ₆	295.1168	M-H	251.1160, 233.1149, 221.1123, 215.0924, 203.1027, 189.1142, 173.0818, 167.0634, 157.0526	Sesquiterpene
Dehydrooreadone	C ₁₄ H ₁₈ O ₃	279.1218	M+FA-H	261.0987, 233.1046, 219.0902, 201.0804, 189.1178, 185.0502, 183.0663, 173.0874	Sesquiterpene
Dictyoquinazol A	C ₁₇ H ₁₆ N ₂ O ₄	311.1090	M-H	267.1079, 237.0366, 205.1134, 193.1114, 187.1005, 175.1036, 159.0740, 151.0638, 149.0482	Quinazoline
Dihydromarasmone	C ₁₅ H ₂₀ O ₅	279.1216	M-H	235.0976, 219.1390, 217.1131, 207.1277, 191.1342, 173.1250, 163.0871	Sesquiterpene
Frequentin	C ₁₄ H ₂₀ O ₄	233.1181	M-H ₂ O-H	205.1234, 196.8934, 189.1195, 173.0864	Cyclohexanecarbaldehyde
Ganodermic acid Jb	C ₃₀ H ₄₆ O ₄	453.3436	M+H-H ₂ O	322.2571, 208.3768, 119.0945	Triterpene
Geosmin	C ₁₂ H ₂₂ O	203.1431	M+Na-2H	201.1177, 188.1100, 187.1010, 175.1426, 147.0792	Sesquiterpene
Microdiplodiasol	C ₁₅ H ₁₈ O ₇	309.0948	M-H	265.0858, 203.0963, 193.1139, 187.0612, 175.1035	Xanthone derivative
Pandangolide 1	C ₁₂ H ₂₀ O ₅	243.1242	M-H	203.6930, 181.1234	Polyketide
Piperdial	C ₁₅ H ₂₂ O ₃	251.1617	M+H	233.1537, 215.1455, 205.1587, 191.1067, 187.1503, 177.0810, 159.1189, 145.1029	Unsaturated dialdehyde

Table II
The previous reports on extracellular metabolites produced by *Irpex lacteus* (strain CMU-8413) at stationary phase.

Metabolite	Fungal species	Source ^a	Bioactivity/Comment ^a	Reference
Apotrichodiol	<i>Fusarium</i> spp.	EM	mycotoxin	(Lebrun et al. 2015)
Apotrichothecene	<i>Fusarium</i> spp.	EM	mycotoxin	(Lebrun et al. 2015)
Blennin D	<i>Lentinellus cochleatus</i>	BE	inhibitor of leukotriene biosynthesis	(Wunder et al. 1996)
Collybial	<i>Collybia confluens</i>	EM	antibacterial, antiviral	(Simon et al. 1995)
Cyclocalopin A	<i>Caloboletus radicans</i>	BE	antioxidant, antibacterial	(Tareq et al. 2018)
Dehydrooreadone	<i>Marasmius oreades</i>	EM	NT	(Ayer and Craw 1989)
Dictyoquinazol A	<i>Dictyophora indusiata</i> /other basidiomycetes	BE	neuroprotective	(Lee et al. 2002)
Dihydromarasmone	<i>Marasmius oreades</i>	EM	antimicrobial	(Ayer and Craw 1989)
Frequentin	<i>Penicillium frequentans</i> / <i>Penicillium</i> spp.	EM	antifungal, antibacterial	(Curtis et al. 1951)
Ganodermic acid Jb	<i>Ganoderma lucidum</i>	ME	NT	(Shiao et al. 1988)
Geosmin	<i>Cortinarius herculeus</i> / <i>Cystoderma</i> spp.	BE	musty-earthly odor	(Breheret et al. 1999)
Microdiplodiasol	<i>Microdiplodia</i> sp.	EM	antifungal antibacterial	(Siddiqui et al. 2011)
Pandangolide 1	<i>Cladosporium marine</i>	EM	NA	(Gesner et al. 2005)
Piperdial	<i>Lactarius</i> spp./ <i>Russula queletii</i>	BE	produced by damage	(Sterner et al. 1985)

BE – basidiocarp extract;

EM – extracellular metabolite produced by mycelium growing in broth;

ME – mycelium extract; NT – not tested as far as we know;

NA – not biological activity detected in conducted assays

I. lacteus strain. Based on such results, the identification of the extracellular metabolites was conducted in broth culture to ensure metabolites production in sufficient quantity to be identified by MS. However, it should be noted that the antagonistic and antibiosis assays performed in a solid medium might induce specific metabolite production, which was not produced in broth. In this regard, it has been previously documented that *I. lacteus* produces the antifungal terpenes conocanol B, 5-demethyl conocanol C, irpenigirin B, as well as 4-(4-dihydroxymethylphenoxy)benzaldehyde only by fermentation in the solid substrate but not in broth culture (Wu et al. 2019). Furthermore, while *I. lacteus* only produced the first compound in co-culture with the phytopathogen *N. oryzae*, the remaining three metabolites were produced both in axenic culture and in co-culture. Therefore, extracellular metabolites identified here were not necessarily the same as induced by antagonism in dual culture and antibiosis assays. Co-culture induction of specific metabolites may explain high percentages of fungal/oomycete growth inhibition found here in antagonism/antibiosis assays; however, these findings require further study. Hence, extracellular metabolites produced by the CMU-8413 strain described in this investigation may be considered basal, given that no induction conditions to increase its secretion were evaluated. Based on culture conditions described here, it may be suggested that gene clusters responsible for the synthesis of the identified extracellular metabolites were constitutively expressed or they were not subject to carbon catabolite repression (CCR). CCR and transcription factors associated with secondary metabolism were molecular and metabolic issues scarcely studied in basidiomycetes (Adnan et al. 2018; García-Estrada et al. 2018). Necessary physiological and metabolic studies, like those conducted here, could help to know what kind of metabolites may not be subject to this metabolic control.

It should be noted that extracellular metabolites produced by the CMU-8413 strain have a wide variety of pharmacological activities, besides antimicrobials previously described (Table II). For instance, apotrichodiol and apotrichothecene are neurotoxic mycotoxins (Lebrun et al. 2015), whereas dictyoquinazol A has been described as neuroprotective (Lee et al. 2002) and blennins are inhibitors of leukotriene biosynthesis (Wunder et al. 1996). So, it will be necessary to select favorable culture conditions to develop an enrichment protocol or use heterologous expression systems (Qiao et al. 2019) to obtain the desirable metabolites and avoid toxic molecules' synthesis. Further studies incubating the CMU-8413 strain in different induction conditions could show its potential to secrete a chemical diversity of metabolites useful for agriculture or other biotechnological applications.

ORCID

Daisy Pineda-Suazo <https://orcid.org/0000-0002-8939-0687>
 Josaphat Miguel Montero-Vargas
<https://orcid.org/0000-0002-7471-9152>
 José Juan Ordaz-Ortiz <https://orcid.org/0000-0001-7738-7184>
 Gerardo Vázquez-Marrufo
<https://orcid.org/0000-0003-4683-699X>

Conflict of interest

The authors do not report any financial or personal connections with other persons or organizations, which might negatively affect the contents of this publication and/or claim authorship rights to this publication.

Literature

- Adnan M, Zheng W, Islam W, Arif M, Abubakar YS, Wang Z, Lu G. Carbon catabolite repression in filamentous fungi. *Int J Mol Sci*. 2018 Dec 24;19(1):48. <https://doi.org/10.3390/ijms19010048>
- Ayer WA, Craw P. Metabolites of the fairy ring fungus, *Marasmius oreades*. Part 2. Norsesquiterpenes, further sesquiterpenes, and agrocycin. *Can J Chem*. 1989 Sep 01;67(9):1371–1380. <https://doi.org/10.1139/v89-210>
- Bourguet D, Guillemaud T. The hidden and external costs of pesticide use. In: Lichtfouse E, editor. *Sustainable agriculture reviews* (Vol 19). Cham (Switzerland): Springer International Publishing Switzerland; 2016. p. 35–120.
- Breheret S, Talou T, Rapior S, Bessière JM. Geosmin, a sesquiterpenoid compound responsible for the musty-earthly odor of *Cortinarius herculeus*, *Cystoderma amianthinum*, and *Cy. carcharias*. *Mycologia*. 1999 Jan 01;91:117–120. <https://doi.org/10.1080/00275514.1999.12060999>
- Carvalho FP. Pesticides, environment, and food safety. *Food Energy Secur*. 2017 June 09;6(2):48–60. <https://doi.org/10.1002/fes3.108>
- Curtis PJ, Hemming HG, Smith WK. Frequentin: an antibiotic produced by some strains of *Penicillium frequentans* westling. *Nature*. 1951 Apr 07;167(4249):557–558. <https://doi.org/10.1038/167557a0>
- Damián-Robles RM, Castro-Montoya AJ, Saucedo-Luna J, Vázquez-Garcidueñas MS, Arredondo-Santoyo M, Vázquez-Marrufo G. Characterization of ligninolytic enzyme production in white-rot wild fungi strains suitable for kraft pulp bleaching. *3Biotech*. 2017 Sept 15; 7(5):319. <https://doi.org/10.1007/s13205-017-0968-2>
- Dean R, Van Kan JA, Pretorius ZA, Hammond-Kosack KE, Di Pietro A, Spanu PD, Rudd JJ, Dickman M, Kahmann R, Ellis J, et al. The Top 10 fungal pathogens in molecular plant pathology. *Mol Plant Pathol*. 2012 Apr 04;13(4):414–430. <https://doi.org/10.1111/j.1364-3703.2011.00783.x>
- García-Estrada C, Domínguez-Santos R, Kosalková K, Martín JF. Transcription factors controlling primary and secondary metabolism in filamentous fungi: the β -lactam paradigm. *Fermentation*. 2018 June 19;4(2):47. <https://doi.org/10.3390/fermentation4020047>
- Gesner S, Cohen N, Ilan M, Yarden O, Carmeli S. Pandangolide 1a, a metabolite of the sponge-associated fungus *Cladosporium* sp., and the absolute stereochemistry of pandangolide 1 and *iso*-cladospolide B. *J Nat Prod*. 2005 Aug 18;68:1350–1353. <https://doi.org/10.1021/np0501583>
- Gholami M, Amini J, Abdollahzadeh J, Ashengroph M. Basidiomycetes fungi as biocontrol agents against take-all disease of wheat. *Biol Control*. 2019 Mar;130:34–43. <https://doi.org/10.1016/j.biocontrol.2018.12.012>

- Kamoun S, Furzer O, Jones JD, Judelson HS, Ali GS, Dalio RJ, Roy SG, Kamoun S, Furzer O, Jones JD, Judelson HS, Ali GS, Dalio RJ, Roy SG, Schena L, Zambounis A, Panabières F, et al. The Top 10 oomycete pathogens in molecular plant pathology. *Mol Plant Pathol*. 2015 Sept 01;16(4):413–434. <https://doi.org/10.1111/mpp.12190>
- Koitabashi M, Kajitani Y, Hirashima K. Antifungal substances produced by fungal strain Kyu-W63 from wheat leaf and its taxonomic position. *J Gen Plant Pathol*. 2004 Apr;70(2):124–130. <https://doi.org/10.1007/s10327-003-0095-2>
- Lebrun B, Tardivel C, Félix B, Abysique A, Troadec JD, Gaigé S, Dallaporta M. Dysregulation of energy balance by trichothecene mycotoxins: Mechanisms and prospects. *Neurotoxicology*. 2015 July 01;49:15–27. <https://doi.org/10.1016/j.neuro.2015.04.009>
- Lee IK, Yun BS, Han G, Cho DH, Kim YH, Yoo ID. Dictyoquinazols A, B, and C, new neuroprotective compounds from the mushroom *Dictyophora indusiata*. *J Nat Prod*. 2002 Dec 01;65(12):1769–1772. <https://doi.org/10.1021/np020163w>
- Loiseleur O. Natural products in the discovery of agrochemicals. *CHIMIA*. 2017 Dec 01;71(12):810–822. <https://doi.org/10.2533/chimia.2017.810>
- Qiao YM, Yu RL, Zhu P. Advances in targeting and heterologous expression of genes involved in the synthesis of fungal secondary metabolites. *RSC Adv*. 2019 Oct 30;9(60):35124–35134. <https://doi.org/10.1039/C9RA06908A>
- Shen HS, Shao S, Chen JC, Zhou T. Antimicrobials from mushrooms for assuring food safety. *Compr Rev Food Sci Food Saf*. 2017 Feb 09;16(2):316–329. <https://doi.org/10.1111/1541-4337.12255>
- Shiao MS, Lin LJ, Yeh SF. Triterpenes in *Ganoderma lucidum*. *Phytochemistry*. 1988 27(7):873–875. [https://doi.org/10.1016/0031-9422\(88\)84110-4](https://doi.org/10.1016/0031-9422(88)84110-4)
- Siddiqui IN, Zahoor A, Hussain H, Ahmed I, Ahmad VU, Padula D, Draeger S, Schulz B, Meier K, Steinert M, et al. Diversenol and blennolide derivatives from the endophytic fungus *Microdiplodia* sp.: Absolute configuration of diversenol. *J Nat Prod*. 2011 Jan 18;74(3):365–373. <https://doi.org/10.1021/np100730b>
- Simon B, Anke T, Andersb U, Neuhaus M, Hansske F. Collybial, a new antibiotic sesquiterpenoid from *Collybia confluens* (Basidiomycetes). *Z Naturforsch C*. 1995 Mar-Apr;50(3–4):173–180. <https://doi.org/10.1515/znc-1995-3-403>
- Sparks TC, Lorsbach BA. Perspectives on the agrochemical industry and agrochemical discovery. *Pest Manag Sci*. 2017 Apr;73(4):672–677. <https://doi.org/10.1002/ps.4457>
- Sterner O, Bergman R, Franzén C, Wickberg B. New sesquiterpenes in a proposed russulaceae chemical defense system. *Tetrahedron Lett*. 1985 26(26):3163–3166. [https://doi.org/10.1016/S0040-4039\(00\)98646-5](https://doi.org/10.1016/S0040-4039(00)98646-5)
- Steyaert J, Hicks E, Kandula J, Kandul D, Alizadeh H, Braithwaite M, Yardley J, Mendoza-Mendoza A. Methods for the evaluation of the bioactivity and biocontrol potential of species of *Trichoderma*. In: Glare TR, Moran-Diez ME, editors. *Microbial-based biopesticides: methods and protocols*. Methods in molecular biology, vol. 1477. New York (USA): Springer Science+Business Media; 2016. p. 23–35. <https://doi.org/10.1007/978-1-4939-6367-63>
- Tareq FS, Hasan CM, Rahman MM, Hanafi MMM, Colombi Ciacchi L, Michaelis M, Harder T, Tebben J, Islam MT, Spitteller P. Anti-staphylococcal calopins from fruiting bodies of *Caloboletus radicans*. *J Nat Prod*. 2018 Feb 23;81(2):400–404. <https://doi.org/10.1021/acs.jnatprod.7b00525>
- Varela-Rodríguez L, Sánchez-Ramírez B, Rodríguez-Reyna IS, Ordaz-Ortiz JJ, Chávez-Flores D, Salas-Muñoz E, Osorio-Trujillo JC, Ramos-Martínez E, Talamás-Rohana P. Biological and toxicological evaluation of *Rhus trilobata* Nutt. (*Anacardiaceae*) used traditionally in Mexico against cancer. *BMC Complement Altern Med*. 2019 July 1;19(1):153. <https://doi.org/10.1186/s12906-019-2566-9>
- White GJ, Traquair JA. Necrotrophic mycoparasitism of *Botrytis cinerea* by cellulolytic and ligninocellulolytic Basidiomycetes. *Can J Microbiol*. 2006 June 01;52(6):508–518. <https://doi.org/10.1139/w05-141>
- Wu YM, Zhou QY, Yang XQ, Luo YJ, Qian JJ, Liu SX, Yang YB, Ding ZT. Induction of anti-phytopathogenic metabolite and squalene production and phytotoxin elimination by adjustment of the mode of fermentation in cocultures of phytopathogenic *Nigrospora oryzae* and *Irpex lacteus*. *J Agric Food Chem*. 2019 Oct 30;67(43):11877–11882. <https://doi.org/10.1021/acs.jafc.9b04209>
- Wunder A, Anke T, Klostermeyer D, Steglich W. Lactarane type sesquiterpenoids as inhibitors of leukotriene biosynthesis and other, new metabolites from submerged cultures of *Lentinellus cochleatus* (Pers. ex Fr.) Karst. *Zeitschrift für Naturforschung C*. 1996. 51(7–8):493–499. <https://doi.org/10.1515/znc-1996-7-807>



INFORMACJE Z POLSKIEGO TOWARZYSTWA MIKROBIOLOGÓW

Od ostatniej informacji o działalności Zarządu Głównego Polskiego Towarzystwa Mikrobiologów, zamieszczonej w zeszytach nr 4 z 2020 r. kwartalników *Advancements of Microbiology – Postępy Mikrobiologii* i *Polish Journal of Microbiology*, ZG PTM zajmował się następującymi sprawami:

1. Na dzień 01.01 2021 r. około 1/3 członków PTM nie opłaciło składki członkowskiej za 2020 r. Oddziały Terenowe PTM przypominały poszczególnym osobom o tym obowiązku. Na początku marca 2021 r. sekretariat ZG PTM wysłał ponad 150 e-maili i 40 listów (brak adresów e-mailowych) do osób, które nadal nie uregulowały składek za 2020 r. W przypadku ich nieuregulowania do 15.03.2021 r. ZG PTM podejmie uchwałę o usunięciu z listy PTM członków z nieopłaconą składką roczną za 2020 r.
2. Na jesieni 2020 r. zwrócono się do PTM z prośbą o opłacenie składki dotyczącej przynależności Polski do European Union of Medical Specialists, Section of Medical Microbiology (<https://uems-smm.eu/uems-smm/>). Prezydium ZG PTM stoi na stanowisku, że PTM mogłoby zapłacić część, ale nie całość składki do UEMS. Inicjatywa udziału Polski w UEMS wyszła od Naczelnej Izby Lekarskiej i uważamy, że ona powinna płacić część składki. Przez 12 lat kontakt z UEMS miało Towarzystwo Mikrobiologii Klinicznej i uważamy, że ono również powinno płacić część składki. PTM zrzeszające mikrobiologów pracujących w różnych obszarach mikrobiologii, o sprawie UEMS dowiedziało się dopiero w 2020 r., gdy pojawiła się kwestia opłacania składki. Nie mamy wiedzy, aby wcześniej NIL czy TMK sygnalizowały PTM powyższą sprawę. Nie proponowano wyboru przedstawiciela PTM do UEMS. Jednakże ze względu na fakt, że część zrzeszonych osób to lekarze zajmujący się mikrobiologią kliniczną deklarujemy gotowość wniesienia 1/3 opłaty. Uważamy, że Pani Prof. dr hab. Katarzyna Dzierżanowska-Fangrat jest delegatem PTM do UEMS.
3. Podpisaliśmy umowę z Panem Dawidem Ceculą dyrektorem firmy Exeley Co, wydającym czasopisma PTM on-line dotyczącą przedłużenia umowy wydawniczej obejmującej *Polish Journal of Microbiology*, na lata 2021 i 2022.
4. Bardzo dobrze rozwija się nasze czasopismo *Polish Journal of Microbiology*. Okazało się, jednak że do codziennej pracy redaktorskiej nad zeszytami *Polish Journal of Microbiology* nie wystarczy darmowy Dropbox (pojemność 2 Gb), w Dropbox przechowywane są wszystkie wersje manuskryptu, formalne dokumenty, odpowiedzi dla recenzentów, itp. Takie są wymogi międzynarodowe dla czasopism w PubMed. W związku z tym zakupiono płatny Dropbox (5 Tb),
5. Po raz pierwszy w historii PTM, w 2020 r. przychody *Polish Journal of Microbiology* były wyższe od poniesionych kosztów. Zysk ten był na tyle wysoki, że pokrył straty wydawnicze czasopisma *Postępy Mikrobiologii – Advancements of Microbiology* w 2020 r. Tym samym realizuje się długofalowa polityka władz PTM, aby czasopisma PTM przynosiły zysk Towarzystwu, a nie straty.
6. Władze Warszawskiego Uniwersytetu Medycznego wyraziły zgodę na przedłużenie do 31.12.2021 r. umowy WUM-PTM dotyczącej użyczenia pokoju dla potrzeb ZG PTM na dotychczasowych warunkach finansowych.
7. PTM objęło patronatem konferencję on-line „III Ogólnopolskie Spotkanie Mikrobiologów i Epidemiologów” organizowaną w dniu 01.03.2021 r. przez Konsultanta Wojewódzkiego w dziedzinie Mikrobiologia Lekarska Panią prof. dr hab. Ewę Augustynowicz-Kopeć. <https://www.webinar-med.pl/osme/>.
8. W bieżącym roku podjęto **Uchwałę 1-2021** o honorariach dla członków redakcji *Polish Journal of Microbiology* w 2021 r., **Uchwałę 2-2021** o honorariach dla członków redakcji *Advancements of Microbiology* w 2021 r. oraz **Uchwałę 3-2021** o kontynuacji współpracy z Zakładem Wydawniczym Letter Quality reprezentowanym przez Panią Romę Walendzewicz, dotyczącej sporządzania składu i druku cyfrowego oraz dystrybucji papierowych zeszytów czasopism PJM i PM.
9. Na bieżąco uaktualniamy stronę internetową PTM, zamieszczając na niej informacje m.in. o stypendiach i spotkaniach on-line.
10. Zostały zapłacone składki członkostwa PTM w FEMS i IUMS za 2021 r.
11. Sprawozdanie finansowe PTM za rok 2020 przygotowane przez naszą Panią księgową wykazało, że Towarzystwo osiągnęło niewielki zysk finansowy w ocenianym okresie, niewątpliwie dzięki przychodom z wydawania PJM.
12. Przygotowujemy doroczne zebranie Zarządu Głównego PTM, które odbędzie się on-line w dniu 22.03.2021 r. Zostaną podjęte ustalenia dotyczące organizacji Ogólnopolskiego XXIX Zjazdu PTM oraz Walnego Zjazdu Delegatów PTM w 2021 r.

Warszawa, 10.03.2021 r.

SEKRETARZ
Polskiego Towarzystwa Mikrobiologów
A. Laudy
dr hab. n. farm. Agnieszka E. Laudy

PREZES
Polskiego Towarzystwa Mikrobiologów
prof. dr hab. Stefan Tyski



XXIX OGÓLNOPOLSKI ZJAZD
POLSKIEGO TOWARZYSTWA
MIKROBIOLOGÓW
14-17 WRZEŚNIA 2021,
WARSZAWA



XXIX OGÓLNOPOLSKI ZJAZD POLSKIEGO TOWARZYSTWA MIKROBIOLOGÓW

14-17 WRZEŚNIA 2021,
WARSZAWA



Miejsce Zjazdu:

Sangate Hotel Airport
Warszawa, ul. Komitetu Obrony Robotników 32
(dawniej 17 Stycznia, róg ul. Żwirki i Wigury)

Główny Organizator Zjazdu:

Polskie Towarzystwo Mikrobiologów
ul. Stefana Banacha 1b, 02-097 Warszawa
ptm.zmf@wum.edu.pl, www.microbiology.pl

CZŁONKOWIE WSPIERAJĄCY PTM

**Członek Wspierający PTM – Złoty
od 27.03.2017 r.**



HCS Europe – Hygiene & Cleaning Solutions
ul. Warszawska 9a, 32-086 Węgrzce k. Krakowa
tel. (12) 414 00 60, 506 184 673, fax (12) 414 00 66
www.hcseurope.pl

Firma projektuje profesjonalne systemy utrzymania czystości i higieny dla klientów o szczególnych wymaganiach higienicznych, m.in. kompleksowe systemy mycia, dezynfekcji, osuszania rąk dla pracowników służby zdrowia, preparaty do dezynfekcji powierzchni dla służby zdrowia, systemy sterylizacji narzędzi.

**Członek Wspierający PTM – Srebrny
od 12.09.2017 r.**



Firma Ecolab Sp. z o.o. zapewnia: najlepszą ochronę środowiska pracy przed patogenami powodującymi zakażenia podczas leczenia pacjentów, bezpieczeństwo i wygodę personelu, funkcjonalność posiadanego sprzętu i urządzeń. Firma jest partnerem dla przemysłów farmaceutycznego, biotechnologicznego i kosmetycznego.

**Członek Wspierający PTM – Zwyczajny
od 12.09.2017 r.**



Merck Sp. z o.o. jest częścią międzynarodowej grupy Merck KGaA z siedzibą w Darmstadt, Niemcy i dostarcza na rynek polski od roku 1992 wysokiej jakości produkty farmaceutyczne i chemiczne, w tym podłoża mikrobiologiczne

**Członek Wspierający PTM – Zwyczajny
od 06.06.2019 r.**



BART Spółka z o.o. Sp. K
ul. Norwida 4, 05-250 Słupno
NIP: 1180741884, KRS: 0000573068
<https://bart.pl/>, email: info@bart.pl

Firma BART jest producentem i dystrybutorem surowców oraz dodatków dla przemysłu spożywczego i farmaceutycznego. Specjalizujemy się w probiotykach oraz surowcach uzyskiwanych metodami biotechnologicznymi.
Współpracujemy z renomowanymi producentami: Probiotal, Gnosis, Lesaffre